



American Concrete Institute

Always advancing

440.2R-17

Document ID:



Automatically sign me into this document in the future.

(Do not select this when using a public computer)

ACI 440.2R-17

Guide for the Design and Construction of Externally Bonded FRP Systems for Strengthening Concrete Structures

Reported by ACI Committee 440



American Concrete Institute
Always advancing



American Concrete Institute
Always advancing

First Printing
May 2017
ISBN: 978-1-945487-59-0

Guide for the Design and Construction of Externally Bonded FRP Systems for Strengthening Concrete Structures

Copyright by the American Concrete Institute, Farmington Hills, MI. All rights reserved. This material may not be reproduced or copied, in whole or part, in any printed, mechanical, electronic, film, or other distribution and storage media, without the written consent of ACI.

The technical committees responsible for ACI committee reports and standards strive to avoid ambiguities, omissions, and errors in these documents. In spite of these efforts, the users of ACI documents occasionally find information or requirements that may be subject to more than one interpretation or may be incomplete or incorrect. Users who have suggestions for the improvement of ACI documents are requested to contact ACI via the errata website at <http://concrete.org/Publications/DocumentErrata.aspx>. Proper use of this document includes periodically checking for errata for the most up-to-date revisions.

ACI committee documents are intended for the use of individuals who are competent to evaluate the significance and limitations of its content and recommendations and who will accept responsibility for the application of the material it contains. Individuals who use this publication in any way assume all risk and accept total responsibility for the application and use of this information.

All information in this publication is provided “as is” without warranty of any kind, either express or implied, including but not limited to, the implied warranties of merchantability, fitness for a particular purpose or non-infringement.

ACI and its members disclaim liability for damages of any kind, including any special, indirect, incidental, or consequential damages, including without limitation, lost revenues or lost profits, which may result from the use of this publication.

It is the responsibility of the user of this document to establish health and safety practices appropriate to the specific circumstances involved with its use. ACI does not make any representations with regard to health and safety issues and the use of this document. The user must determine the applicability of all regulatory limitations before applying the document and must comply with all applicable laws and regulations, including but not limited to, United States Occupational Safety and Health Administration (OSHA) health and safety standards.

Participation by governmental representatives in the work of the American Concrete Institute and in the development of Institute standards does not constitute governmental endorsement of ACI or the standards that it develops.

Order information: ACI documents are available in print, by download, on CD-ROM, through electronic subscription, or reprint and may be obtained by contacting ACI.

Most ACI standards and committee reports are gathered together in the annually revised ACI Manual of Concrete Practice (MCP).

American Concrete Institute
38800 Country Club Drive
Farmington Hills, MI 48331
Phone: +1.248.848.3700
Fax: +1.248.848.3701

www.concrete.org

Guide for the Design and Construction of Externally Bonded FRP Systems for Strengthening Concrete Structures

Reported by ACI Committee 440

Carol K. Shield, Chair

William J. Gold, Secretary

Tarek Alkhrdaji
Charles E. Bakis
Lawrence C. Bank
Abdeldjelil Belarbi
Brahim Benmokrane
Luke A. Bisby
Gregg J. Blaszak
Hakim Bouadi
Timothy E. Bradberry
Vicki L. Brown
John Busel
Raafat El-Hacha
Garth J. Fallis

Amir Z. Fam
Russell Gentry
Nabil F. Grace
Mark F. Green
Zareh B. Gregorian
Doug D. Gremel
Shawn P. Gross
H. R. Trey Hamilton III
Issam E. Harik
Kent A. Harries*
Mark P. Henderson
Ravindra Kanitkar
Yail Jimmy Kim

Michael W. Lee
Maria Lopez de Murphy
Ibrahim M. Mahfouz
Amir Mirmiran
John J. Myers
Antonio Nanni
Ayman M. Okeil
Carlos E. Ospina
Renato Parretti
Maria A. Polak
Max L. Porter
Andrea Prota
Hayder A. Rasheed

Sami H. Rizkalla
Rajan Sen
Rudolf Seracino
Venkatesh Seshappa
Pedro F. Silva
Samuel A. Steere, III
Jennifer E. Tanner
Jay Thomas
Houssam A. Toutanji
J. Gustavo Tumialan
Milan Vatovec
David White
Sarah E. Witt*

*Co-chairs of the subcommittee that prepared this document.

Consulting Members

P. N. Balaguru
Craig A. Ballinger
Harald G. F. Budelmann
C. J. Burgoyne
Rami M. Elhassan
David M. Gale

Srinivasa L. Iyer
Koichi Kishitani
Howard S. Klinger
Kyuichi Maruyama
Antoine E. Naaman
Hajime Okamura

Mark A. Postma
Ferdinand S. Rostasy
Mohsen Shahawy
Surendra P. Shah
Yasuhisa Sonobe
Minoru Sugita

Luc R. Taerwe
Ralejs Tefpers
Taketo Uomoto
Paul Zia

Fiber-reinforced polymer (FRP) systems for strengthening concrete structures are an alternative to traditional strengthening techniques such as steel plate bonding, section enlargement, and external post-tensioning. FRP strengthening systems use FRP composite materials as supplemental externally-bonded or near-surface-mounted reinforcement. FRP systems offer advantages over traditional strengthening techniques: they are lightweight, relatively

easy to install, and noncorroding. Due to the characteristics of FRP materials as well as the behavior of members strengthened with FRP, specific guidance on the use of these systems is needed. This guide offers general information on the history and use of FRP strengthening systems; a description of the material properties of FRP; and recommendations on the engineering, construction, and inspection of FRP systems used to strengthen concrete structures. This guide is based on the knowledge gained from experimental research, analytical work, and field applications of FRP systems used to strengthen concrete structures.

ACI Committee Reports, Guides, and Commentaries are intended for guidance in planning, designing, executing, and inspecting construction. This document is intended for the use of individuals who are competent to evaluate the significance and limitations of its content and recommendations and who will accept responsibility for the application of the material it contains. The American Concrete Institute disclaims any and all responsibility for the stated principles. The Institute shall not be liable for any loss or damage arising therefrom.

Reference to this document shall not be made in contract documents. If items found in this document are desired by the Architect/Engineer to be a part of the contract documents, they shall be restated in mandatory language for incorporation by the Architect/Engineer.

Keywords: aramid fibers; bridges; buildings; carbon fibers; corrosion; cracking; development length; earthquake resistance; fiber-reinforced polymers; structural design.

ACI 440.2R-17 supersedes ACI 440.2R-08 and was adopted and published May 2017. Copyright © 2017, American Concrete Institute

All rights reserved including rights of reproduction and use in any form or by any means, including the making of copies by any photo process, or by electronic or mechanical device, printed, written, or oral, or recording for sound or visual reproduction or for use in any knowledge or retrieval system or device, unless permission in writing is obtained from the copyright proprietors.

CONTENTS

CHAPTER 1—INTRODUCTION AND SCOPE, p. 3

- 1.1—Introduction, p. 3
- 1.2—Scope, p. 4

CHAPTER 2—NOTATION AND DEFINITIONS, p. 6

- 2.1—Notation, p. 6
- 2.2—Definitions, p. 9

CHAPTER 3—BACKGROUND INFORMATION, p. 10

- 3.1—Historical development, p. 10
- 3.2—Commercially available externally bonded FRP systems, p. 10

CHAPTER 4—CONSTITUENT MATERIALS AND PROPERTIES, p. 11

- 4.1—Constituent materials, p. 11
- 4.2—Physical properties, p. 12
- 4.3—Mechanical properties, p. 12
- 4.4—Time-dependent behavior, p. 13
- 4.5—Durability, p. 14
- 4.6—FRP systems qualification, p. 14

CHAPTER 5—SHIPPING, STORAGE, AND HANDLING, p. 15

- 5.1—Shipping, p. 15
- 5.2—Storage, p. 15
- 5.3—Handling, p. 15

CHAPTER 6—INSTALLATION, p. 15

- 6.1—Contractor competency, p. 16
- 6.2—Temperature, humidity, and moisture considerations, p. 16
- 6.3—Equipment, p. 16
- 6.4—Substrate repair and surface preparation, p. 16
- 6.5—Mixing of resins, p. 17
- 6.6—Application of FRP systems, p. 17
- 6.7—Alignment of FRP materials, p. 18
- 6.8—Multiple plies and lap splices, p. 18
- 6.9—Curing of resins, p. 18
- 6.10—Temporary protection, p. 19

CHAPTER 7—INSPECTION, EVALUATION, AND ACCEPTANCE, p. 19

- 7.1—Inspection, p. 19
- 7.2—Evaluation and acceptance, p. 19

CHAPTER 8—MAINTENANCE AND REPAIR, p. 20

- 8.1—General, p. 20
- 8.2—Inspection and assessment, p. 20
- 8.3—Repair of strengthening system, p. 21
- 8.4—Repair of surface coating, p. 21

CHAPTER 9—GENERAL DESIGN CONSIDERATIONS, p. 21

- 9.1—Design philosophy, p. 21
- 9.2—Strengthening limits, p. 21

- 9.3—Selection of FRP systems, p. 22
- 9.4—Design material properties, p. 23

CHAPTER 10—FLEXURAL STRENGTHENING, p. 24

- 10.1—Nominal strength, p. 24
- 10.2—Reinforced concrete members, p. 24
- 10.3—Prestressed concrete members, p. 29
- 10.4—Moment redistribution, p. 31

CHAPTER 11—SHEAR STRENGTHENING, p. 31

- 11.1—General considerations, p. 32
- 11.2—Wrapping schemes, p. 32
- 11.3—Nominal shear strength, p. 32

CHAPTER 12—STRENGTHENING OF MEMBERS SUBJECTED TO AXIAL FORCE OR COMBINED AXIAL AND BENDING FORCES, p. 34

- 12.1—Pure axial compression, p. 34
- 12.2—Combined axial compression and bending, p. 36
- 12.3—Ductility enhancement, p. 36
- 12.4—Pure axial tension, p. 37

CHAPTER 13—SEISMIC STRENGTHENING, p. 37

- 13.1—Background, p. 38
- 13.2—FRP properties for seismic design, p. 38
- 13.3—Confinement with FRP, p. 38
- 13.4—Flexural strengthening, p. 40
- 13.5—Shear strengthening, p. 41
- 13.6—Beam-column joints, p. 41
- 13.7—Strengthening reinforced concrete shear walls, p. 41

CHAPTER 14—FIBER-REINFORCED POLYMER REINFORCEMENT DETAILS, p. 43

- 14.1—Bond and delamination, p. 43
- 14.2—Detailing of laps and splices, p. 44
- 14.3—Bond of near-surface-mounted systems, p. 45

CHAPTER 15—DRAWINGS, SPECIFICATIONS, AND SUBMITTALS, p. 46

- 15.1—Engineering requirements, p. 46
- 15.2—Drawings and specifications, p. 46
- 15.3—Submittals, p. 46

CHAPTER 16—DESIGN EXAMPLES, p. 47

- 16.1—Calculation of FRP system tensile properties, p. 47
- 16.3—Flexural strengthening of an interior reinforced concrete beam with FRP laminates, p. 50
- 16.4—Flexural strengthening of an interior reinforced concrete beam with near-surface-mounted FRP bars, p. 56
- 16.5—Flexural strengthening of an interior prestressed concrete beam with FRP laminates, p. 62
- 16.6—Shear strengthening of an interior T-beam, p. 68
- 16.7—Shear strengthening of an exterior column, p. 71
- 16.8—Strengthening of a noncircular concrete column for axial load increase, p. 73
- 16.9—Strengthening of a noncircular concrete column for increase in axial and bending forces, p. 76

16.11—Lap-splice clamping for seismic strengthening, p. 86

16.12—Seismic shear strengthening, p. 88

16.13—Flexural and shear seismic strengthening of shear walls, p. 91

CHAPTER 17—REFERENCES, p. 97

Authored documents, p. 98

APPENDIX A—MATERIAL PROPERTIES OF CARBON, GLASS, AND ARAMID FIBERS, p. 105

APPENDIX B—SUMMARY OF STANDARD TEST METHODS, p. 107

APPENDIX C—AREAS OF FUTURE RESEARCH, p. 108

APPENDIX D—METHODOLOGY FOR COMPUTATION OF SIMPLIFIED P-M INTERACTION DIAGRAM FOR NONCIRCULAR COLUMNS, p. 109

CHAPTER 1—INTRODUCTION AND SCOPE

1.1—Introduction

The strengthening or retrofitting of existing concrete structures to resist higher design loads, correct strength loss due to deterioration, correct design or construction deficiencies, or increase ductility has historically been accomplished using conventional materials and construction techniques. Externally bonded steel plates, steel or concrete jackets, and external post-tensioning are some of the many traditional techniques available.

Composite materials made of fibers in a polymeric resin, also known as fiber-reinforced polymers (FRPs), have emerged as a viable option for repair and rehabilitation. For the purposes of this guide, an FRP system is defined as the fibers and resins used to create the composite laminate, all applicable resins used to bond it to the concrete substrate, and all applied coatings used to protect the constituent materials. Coatings used exclusively for aesthetic reasons are not considered part of an FRP system.

FRP materials are lightweight, noncorroding, and exhibit high tensile strength. These materials are readily available in several forms, ranging from factory-produced pultruded laminates to dry fiber sheets that can be wrapped to conform to the geometry of a structure before adding the polymer resin. The relatively thin profiles of cured FRP systems are often desirable in applications where aesthetics or access is a concern. FRP systems can also be used in areas with limited access where traditional techniques would be difficult to implement.

The basis for this document is the knowledge gained from a comprehensive review of experimental research, analytical work, and field applications of FRP strengthening systems. Areas where further research is needed are highlighted in this document and compiled in [Appendix C](#).

1.1.1 Use of FRP systems—This document refers to commercially available FRP systems consisting of fibers

and resins combined in a specific manner and installed by a specific method. These systems have been developed through material characterization and structural testing. Untested combinations of fibers and resins could result in an unexpected range of properties as well as potential material incompatibilities. Any FRP system considered for use should have sufficient test data to demonstrate adequate performance of the entire system in similar applications, including its method of installation. [ACI 440.8](#) provides a specification for unidirectional carbon and glass FRP materials made using the wet layup process.

The use of FRP systems developed through material characterization and structural testing, including well-documented proprietary systems, is recommended. The use of untested combinations of fibers and resins should be avoided. A comprehensive set of test standards and guides for FRP systems has been developed by several organizations, including ASTM, ACI, ICRI, and ICC.

1.1.2 Sustainability—Sustainability of FRP materials may be evaluated considering environmental, economic, and social goals. These should be considered not only throughout the construction phase, but also through the service life of the structure in terms of maintenance and preservation, and for the end-of-life phase. This represents the basis for a life-cycle approach to sustainability ([Menna et al. 2013](#)). Life cycle assessment (LCA) takes into account the environmental impact of a product, starting with raw material extraction, followed by production, distribution, transportation, installation, use, and end of life. LCA for FRP composites depends on the product and market application, and results vary. FRP composite materials used to strengthen concrete elements can use both carbon fiber and glass fiber, which are derived from fossil fuels or minerals, respectively, and therefore have impacts related to raw material extraction. Although carbon and glass fibers have high embodied energies associated with production, on the order of 86,000 Btu/lb and 8600 Btu/lb (200 and 20 mJ/kg), respectively ([Howarth et al. 2014](#)), the overall weight produced and used is orders of magnitude lower than steel (having embodied energy of 5600 Btu/lb [13 mJ/kg]), concrete (430 Btu/lb [1 mJ/kg]), and reinforcing steel (3870 Btu/lb [9 mJ/kg]) ([Griffin and Hsu 2010](#)). The embodied energy and potential environmental impact of resin and adhesive systems are less studied, although the volume used is also small in comparison with conventional construction materials. In distribution and transportation, FRP composites' lower weight leads to less impact from transportation, and easier material handling allows smaller equipment during installation. For installation and use, FRP composites are characterized as having a longer service life because they are more durable and require less maintenance than conventional materials. The end-of-life options for FRP composites are more complex.

Although less than 1 percent of FRP composites are currently recycled, composites can be recycled in many ways, including mechanical grinding, incineration, and chemical separation ([Howarth et al. 2014](#)). It is difficult, however, to separate the materials, fibers, and resins without some degradation of the resulting recycled materials. The

market for recycled composite materials is small, although aircraft manufacturers in particular are considering methods and programs to recycle and repurpose composite materials at the end of an aircraft's life cycle.

Apart from the FRP materials and systems, their use in the repair and retrofit of structures that may otherwise be decommissioned or demolished is inherently sustainable. In many cases, FRP composites permit extending the life or enhancing the safety or performance of existing infrastructure at a monetary and environmental cost of only a fraction of replacement. Additionally, due to the high specific strength and stiffness of FRP composites, an FRP-based repair of an existing concrete structure will often represent a less energy-intensive option than a cementitious or metallic-based repair.

Within this framework of sustainability, FRP retrofit of existing structures may lead to benefits, contributing to the longevity and safety of retrofitted structures. Thus, FRP retrofit can be regarded as a viable method for sustainable design for strengthening and rehabilitation of existing structures. The environmental advantages of FRP, as evaluated by LCA investigations, have been enumerated by [Napolano et al. \(2015\)](#), [Moliner Santistevé et al. \(2013\)](#), [Zhang et al. \(2012\)](#), and [Das \(2011\)](#).

1.2—Scope

This document provides guidance for the selection, design, and installation of FRP systems for externally strengthening concrete structures. Information on material properties, design, installation, quality control, and maintenance of FRP systems used as external reinforcement is presented. This information can be used to select an FRP system for increasing the strength, stiffness, or both, of reinforced concrete beams or the ductility of columns and other applications.

A significant body of research serves as the basis for this guide. This research, conducted since the 1980s, includes analytical studies, experimental work, and monitored field applications of FRP strengthening systems. Based on the available research, the design procedures outlined herein are considered conservative.

The durability and long-term performance of FRP materials has been the subject of much research; however, this research remains ongoing. The design guidelines in this guide account for environmental degradation and long-term durability by providing reduction factors for various environments. Long-term fatigue and creep are also addressed by stress limitations indicated in this document. These factors and limitations are considered conservative. As more research becomes available, however, these factors may be modified, and the specific environmental conditions and loading conditions to which they should apply will be better defined. Additionally, the coupling effect of environmental conditions and loading conditions requires further study. Caution is advised in applications where the FRP system is subjected simultaneously to extreme environmental and stress conditions. The factors associated with the long-term

durability of the FRP system may also affect the tensile modulus of elasticity of the material used for design.

Many issues regarding bond of the FRP system to the substrate remain the focus of a great deal of research. For both flexural and shear strengthening, there are many different modes of debonding failure that can govern the strength of an FRP-strengthened member. While most of the debonding modes have been identified by researchers, more accurate methods of predicting debonding are still needed. Throughout the design procedures, significant limitations on the strain achieved in the FRP material (and thus, the stress achieved) are imposed to conservatively account for debonding failure modes. Future development of these design procedures should include more thorough methods of predicting debonding.

This document gives guidance on proper detailing and installation of FRP systems to prevent many types of debonding failure modes. Steps related to the surface preparation and proper termination of the FRP system are vital in achieving the levels of strength predicted by the procedures in this document. Research has been conducted on various methods of anchoring FRP strengthening systems, such as U-wraps, mechanical fasteners, fiber anchors, and U-anchors. Because no anchorage design guidelines are currently available, the performance of any anchorage system should be substantiated through representative physical testing that includes the specific anchorage system, installation procedure, surface preparation, and expected environmental conditions.

The design equations given in this document are the result of research primarily conducted on moderately sized and proportioned members fabricated of normalweight concrete. Caution should be given to applications involving strengthening of very large or lightweight concrete members or strengthening in disturbed regions (D-regions) of structural members such as deep beams, corbels, and dapped beam ends. When warranted, specific limitations on the size of members and the state of stress are given herein.

This guide applies only to FRP strengthening systems used as additional tensile reinforcement. These systems should not be used as compressive reinforcement. While FRP materials can support compressive stresses, there are numerous issues surrounding the use of FRP for compression. Microbuckling of fibers can occur if any resin voids are present in the laminate. Laminates themselves can buckle if not properly adhered or anchored to the substrate, and highly unreliable compressive strengths result from misaligning fibers in the field. This document does not address the construction, quality control, and maintenance issues that would be involved with the use of the material for this purpose, nor does it address the design concerns surrounding such applications.

This document does not specifically address masonry (concrete masonry units, brick, or clay tile) construction, including masonry walls. Information on the repair of unreinforced masonry using FRP can be found in [ACI 440.7R](#).

1.2.1 Applications and use—FRP systems can be used to rehabilitate or restore the strength of a deteriorated structural

member, retrofit or strengthen a sound structural member to resist increased loads due to changes in use of the structure, or address design or construction errors. The licensed design professional should determine if an FRP system is a suitable strengthening technique before selecting the type of FRP system.

To assess the suitability of an FRP system for a particular application, the licensed design professional should perform a condition assessment of the existing structure that includes establishing its existing load-carrying capacity, identifying deficiencies and their causes, and determining the condition of the concrete substrate. The overall evaluation should include a thorough field inspection, a review of existing design or as-built documents, and a structural analysis in accordance with ACI 364.1R. Existing construction documents for the structure should be reviewed, including the design drawings, project specifications, as-built information, field test reports, past repair documentation, and maintenance history documentation. The licensed design professional should conduct a thorough field investigation of the existing structure in accordance with ACI 437R, ACI 562, ACI 369R, and other applicable ACI documents. As a minimum, the field investigation should determine the following:

- a) Existing dimensions of the structural members
- b) Location, size, and cause of cracks and spalls
- c) Quantity and location of existing reinforcing steel
- d) Location and extent of corrosion of reinforcing steel
- e) Presence of active corrosion
- f) In-place compressive strength of concrete
- g) Soundness of the concrete, especially the concrete cover, in all areas where the FRP system is to be bonded to the concrete

The tensile strength of the concrete on surfaces where the FRP system may be installed should be determined by conducting a pull-off adhesion test in accordance with ASTM C1583/C1583M. The in-place compressive strength of concrete should be determined using cores in accordance with ACI 562 requirements. The load-carrying capacity of the existing structure should be based on the information gathered in the field investigation, the review of design calculations and drawings, and as determined by analytical methods. Load tests or other methods can be incorporated into the overall evaluation process if deemed appropriate.

FRP systems used to increase the strength of an existing member should be designed in accordance with Chapters 9 through 15, which include a comprehensive discussion of load limitations, rational load paths, effects of temperature and environment on FRP systems, loading considerations, and effects of reinforcing steel corrosion on FRP system integrity.

1.2.1.1 Strengthening limits—In general, to prevent sudden failure of the member in case the FRP system is damaged, strengthening limits are imposed such that the increase in the load-carrying capacity of a member strengthened with an FRP system is limited. The philosophy is that a loss of FRP reinforcement should not cause member failure. Specific guidance, including load combinations for assessing

member integrity after loss of the FRP system, is provided in Chapter 9.

1.2.1.2 Fire and life safety—FRP-strengthened structures should comply with applicable building and fire codes. Smoke generation and flame spread ratings in accordance with ASTM E84 should be satisfied for the installation according to applicable building codes, depending on the classification of the building. Coatings (Apicella and Imbrogno 1999) and insulation systems (Williams et al. 2006) can be used to limit smoke and flame spread.

Because of the degradation of most FRP materials at high temperature, the strength of externally bonded FRP systems is assumed to be lost completely in a fire, unless it can be demonstrated that the FRP will remain effective for the required duration of the fire. The fire resistance of FRP-strengthened concrete members may be improved through the use of certain resins, coatings, insulation systems, or other methods of fire protection (Bisby et al. 2005b). Specific guidance, including load combinations and a rational approach to calculating structural fire resistance, is given in 9.2.1.

1.2.1.3 Maximum service temperature—The physical and mechanical properties of the resin components of FRP systems are influenced by temperature and degrade at temperatures close to or above their glass-transition temperature T_g (Bisby et al. 2005b). The T_g for commercially available, ambient temperature-cured FRP systems typically ranges from 140 to 180°F (60 to 82°C). The T_g for a particular FRP system can be obtained from the system manufacturer or through testing by dynamic mechanical analysis (DMA) according to ASTM E1640. Reported T_g values should be accompanied by descriptions of the test configuration; sample preparation; curing conditions (time, temperature, and humidity); and size, heating rate, and frequency used. The T_g defined by this method represents the extrapolated onset temperature for the sigmoidal change in the storage modulus observed in going from a hard and brittle state to a soft and rubbery state of the material under test. This transition occurs over a temperature range of approximately 54°F (30°C) centered on the T_g . This change in state will adversely affect the mechanical and bond properties of the cured laminates. For a dry environment, it is generally recommended that the anticipated service temperature of an FRP system not exceed $T_g - 27^\circ\text{F}$ ($T_g - 15^\circ\text{C}$) (Xian and Karbhari 2007), where T_g is taken as the lowest T_g of the components of the system comprising the load path. This recommendation is for elevated service temperatures such as those found in hot regions or certain industrial environments. In cases where the FRP will be exposed to a moist environment, the wet glass-transition temperature T_{gw} should be used (Luo and Wong 2002). Testing may be required to determine the critical service temperature for FRP in other environments. The specific case of fire is described in more detail in 9.2.1.

1.2.1.4 Minimum concrete substrate strength—FRP systems need to be bonded to a sound concrete substrate and should not be considered for applications on structural members containing corroded reinforcing steel or deteriorated concrete unless the substrate is repaired using

the recommendations in 6.4. Concrete distress, deterioration, and corrosion of existing reinforcing steel should be evaluated and addressed before the application of the FRP system. Concrete deterioration concerns include, but are not limited to, alkali-silica reactions, delayed ettringite formation, carbonation, longitudinal cracking around corroded reinforcing steel, and laminar cracking at the location of the steel reinforcement.

The strength of the existing concrete substrate is an important parameter for bond-critical applications, including flexure or shear strengthening. The substrate should possess the necessary strength to develop the design stresses of the FRP system through bond. The substrate, including all bond surfaces between repaired areas and the original concrete, should have sufficient direct tensile and shear strength to transfer force to the FRP system. For bond-critical applications, the tensile strength should be at least 200 psi (1.4 MPa), determined by using a pull-off type adhesion test per **ICRI 210.3R** or **ASTM C1583/C1583M**. FRP systems should not be used when the concrete substrate has a compressive strength f'_c less than 2500 psi (17 MPa). Contact-critical applications, such as column wrapping for confinement that rely only on intimate contact between the FRP system and the concrete, are not governed by these minimum values. Design stresses in the FRP system are developed by deformation or dilation of the concrete section in contact-critical applications.

The application of FRP systems will not stop the ongoing corrosion of existing reinforcing steel (**El-Maaddawy et al. 2006**). If steel corrosion is evident or is degrading the concrete substrate, placement of FRP reinforcement is not recommended without arresting the ongoing corrosion and repairing any degradation of the substrate.

CHAPTER 2—NOTATION AND DEFINITIONS

2.1—Notation

- A_c = cross-sectional area of concrete in compression member, in.² (mm²)
- A_{cw} = area of concrete section of individual vertical wall, in.² (mm²)
- A_e = cross-sectional area of effectively confined concrete section, in.² (mm²)
- A_f = area of FRP external reinforcement, in.² (mm²)
- $A_{fanchor}$ = area of transverse FRP U-wrap for anchorage of flexural FRP reinforcement, in.² (mm²)
- A_{fv} = area of FRP shear reinforcement with spacing s , in.² (mm²)
- A_g = gross area of concrete section, in.² (mm²)
- A_p = area of prestressed reinforcement in tension zone, in.² (mm²)
- A_s = area of nonprestressed steel reinforcement, in.² (mm²)
- A_{sc} = area of the longitudinal reinforcement within a distance of w_f in the compression region, in.² (mm²)
- A_{si} = area of i -th layer of longitudinal steel reinforcement, in.² (mm²)
- A_{st} = total area of longitudinal reinforcement, in.² (mm²)

- A_{sw} = area of longitudinal reinforcement in the central area of the wall, in.² (mm²)
- a = depth of the equivalent concrete compression block, in. (mm)
- a_b = smaller cross-sectional dimension for rectangular FRP bars, in. (mm)
- b = width of compression face of member, in. (mm)
= short side dimension of compression member of prismatic cross section, in. (mm)
- b_b = larger cross-sectional dimension for rectangular FRP bars, in. (mm)
- b_w = web width or diameter of circular section, in. (mm)
- C_E = environmental reduction factor
- C_{sc} = compressive force in A_{sc} , lb (N)
- c = distance from extreme compression fiber to the neutral axis, in. (mm)
- c_y = distance from extreme compression fiber to the neutral axis at steel yielding, in. (mm)
- D = diameter of compression member for circular cross sections or diagonal distance equal to $\sqrt{b^2 + h^2}$ for prismatic cross section (diameter of equivalent circular column), in. (mm)
- d = distance from extreme compression fiber to centroid of tension reinforcement, in. (mm)
- d' = distance from the extreme compression fiber to the center of A_{sc} , in. (mm)
- d'' = distance from the extreme tension fiber to the center of A_{st} , in. (mm)
- d_{bt} = diameter of longitudinal steel in confined plastic hinge, in. (mm)
- d_f = effective depth of FRP flexural reinforcement, in. (mm)
- d_{fv} = effective depth of FRP shear reinforcement, in. (mm)
- d_i = distance from centroid of i -th layer of longitudinal steel reinforcement to geometric centroid of cross section, in. (mm)
- d_p = distance from extreme compression fiber to centroid of prestressed reinforcement, in. (mm)
- E_2 = slope of linear portion of stress-strain model for FRP-confined concrete, psi (MPa)
- E_c = modulus of elasticity of concrete, psi (MPa)
- E_f = tensile modulus of elasticity of FRP, psi (MPa)
- E_{ps} = modulus of elasticity of prestressing steel, psi (MPa)
- E_s = modulus of elasticity of steel, psi (MPa)
- e_s = eccentricity of prestressing steel with respect to centroidal axis of member at support, in. (mm)
- e_m = eccentricity of prestressing steel with respect to centroidal axis of member at midspan, in. (mm)
- f_c = compressive stress in concrete, psi (MPa)
- f'_c = specified compressive strength of concrete, psi (MPa)
- f'_{cc} = compressive strength of confined concrete, psi (MPa)
- f'_{co} = compressive strength of unconfined concrete; also equal to $0.85f'_c$, psi (MPa)
- $f_{c,s}$ = compressive stress in concrete at service condition, psi (MPa)
- f_f = stress in FRP reinforcement, psi (MPa)



f_{fd} = design stress of externally bonded FRP reinforcement, psi (MPa)	$\ell_{d,E}$ = length over which the FRP anchorage wraps are provided, in. (mm)
f_{fe} = effective stress in the FRP; stress attained at section failure, psi (MPa)	ℓ_{df} = development length of FRP system, in. (mm)
f_{fs} = stress in FRP caused by a moment within elastic range of member, psi (MPa)	ℓ_o = length, measured along the member axis from the face of the joint, over which special transverse reinforcement must be provided, in. (mm)
f_{fu} = design ultimate tensile strength of FRP, psi (MPa)	ℓ_{prov} = length of steel lap splice, in. (mm)
f_{fu}^* = ultimate tensile strength of the FRP material as reported by the manufacturer, psi (MPa)	M_{cr} = cracking moment, in.-lb (N-mm)
f_l = maximum confining pressure due to FRP jacket, psi (MPa)	M_n = nominal flexural strength, in.-lb (N-mm)
f_{ps} = stress in prestressed reinforcement at nominal strength, psi (MPa)	M_{nf} = contribution of FRP reinforcement to nominal flexural strength, lb-in. (N-mm)
$f_{ps,s}$ = stress in prestressed reinforcement at service load, psi (MPa)	M_{np} = contribution of prestressing reinforcement to nominal flexural strength, lb-in. (N-mm)
f_{pu} = specified tensile strength of prestressing tendons, psi (MPa)	M_{ns} = contribution of steel reinforcement to nominal flexural strength, lb-in. (N-mm)
f_s = stress in nonprestressed steel reinforcement, psi (MPa)	M_s = service moment at section, in.-lb (N-mm)
f_{sc} = stress in the longitudinal reinforcement corresponding to A_{sc} , psi (MPa)	M_{snet} = service moment at section beyond decompression, in.-lb (N-mm)
f_{si} = stress in the i -th layer of longitudinal steel reinforcement, psi (MPa)	M_u = factored moment at a section, in.-lb (N-mm)
$f_{s,s}$ = stress in nonprestressed steel reinforcement at service loads, psi (MPa)	N = number of plies of FRP reinforcement
f_{st} = stress in the longitudinal reinforcement corresponding to A_{st} , psi (MPa)	n_f = modular ratio of elasticity between FRP and concrete = E_f/E_c
f_{sw} = stress in the longitudinal reinforcement corresponding to A_{sw} , psi (MPa)	n_s = modular ratio of elasticity between steel and concrete = E_s/E_c
f_y = specified yield strength of nonprestressed steel reinforcement, psi (MPa)	P_e = effective force in prestressing reinforcement (after allowance for all prestress losses), lb (N)
g = clear gap between the FRP jacket and adjacent members, in. (mm)	P_n = nominal axial compressive strength of a concrete section, lb (N)
h = overall thickness or height of a member, in. (mm)	$\frac{P_u}{P_{fu}}$ = factored axial load, lb (N)
= long side cross-sectional dimension of rectangular compression member, in. (mm)	p_{fu} = mean tensile strength per unit width per ply of FRP reinforcement, lb/in. (N/mm)
h_f = member flange thickness, in. (mm)	p_{fu}^* = ultimate tensile strength per unit width per ply of FRP reinforcement, lb/in. (N/mm); $p_{fu}^* = f_{fu}^* t_f$
h_w = height of entire wall from base to top, or clear height of wall segment or wall pier considered, in. (mm)	R_n = nominal strength of a member
I_{cr} = moment of inertia of cracked section transformed to concrete, in. ⁴ (mm ⁴)	$R_{n\phi}$ = nominal strength of a member subjected to elevated temperatures associated with a fire
I_{tr} = moment of inertia of uncracked section transformed to concrete, in. ⁴ (mm ⁴)	R = radius of gyration of a section, in. (mm)
K = ratio of depth of neutral axis to reinforcement depth measured from extreme compression fiber	r_c = radius of edges of a prismatic cross section confined with FRP, in. (mm)
k_1 = modification factor applied to κ_v to account for concrete strength	S_{DL} = dead load effects
k_2 = modification factor applied to κ_v to account for wrapping scheme	S_{LL} = live load effects
k_f = stiffness per unit width per ply of the FRP reinforcement, lb/in. (N/mm); $k_f = E_f t_f$	s_f = center-to-center spacing of FRP strips, in. (mm)
L_e = active bond length of FRP laminate, in. (mm)	T_f = tensile force in FRP, lb (N)
L_p = plastic hinge length, in. (mm)	T_g = glass-transition temperature, °F (°C)
L_w = length of the shear wall, in. (mm)	T_{gw} = wet glass-transition temperature, °F (°C)
ℓ_{db} = development length of near-surface-mounted FRP bar, in. (mm)	T_{ps} = tensile force in prestressing steel, lb (N)
	T_{st} = tensile force in A_{st} , lb (N)
	T_{sw} = tensile force in A_{sw} , lb (N)
	t_f = nominal thickness of one ply of FRP reinforcement, in. (mm)
	t_w = thickness of the existing concrete shear wall, in. (mm)
	V_c = nominal shear strength provided by concrete with steel flexural reinforcement, lb (N)
	V_e = design shear force for load combinations including earthquake effects, lb (N)
	V_f = nominal shear strength provided by FRP stirrups, lb (N)

V_n = nominal shear strength, lb (N)	ϵ_{pe} = effective strain in prestressing steel after losses, in./in. (mm/mm)
V_n^* = shear strength of existing member, lb (N)	ϵ_{pi} = initial strain in prestressed steel reinforcement, in./in. (mm/mm)
V_s = nominal shear strength provided by steel stirrups, lb (N)	ϵ_{pnet} = net strain in flexural prestressing steel at limit state after prestress force is discounted (excluding strains due to effective prestress force after losses), in./in. (mm/mm)
w_f = width of FRP reinforcing plies, in. (mm)	$\epsilon_{pnet,s}$ = net strain in prestressing steel beyond decompression at service, in./in. (mm/mm)
y_b = distance from centroidal axis of gross section, neglecting reinforcement, to extreme bottom fiber, in./in. (mm/mm)	ϵ_{ps} = strain in prestressed reinforcement at nominal strength, in./in. (mm/mm)
y_t = vertical coordinate within compression region measured from neutral axis position. It corresponds to transition strain ϵ_r' , in. (mm)	$\epsilon_{ps,s}$ = strain in prestressing steel at service load, in./in. (mm/mm)
α = angle of application of primary FRP reinforcement direction relative to longitudinal axis of member	ϵ_s = strain in nonprestressed steel reinforcement, in./in. (mm/mm)
α_1 = multiplier on f_c' to determine intensity of an equivalent rectangular stress distribution for concrete	ϵ_{sy} = strain corresponding to yield strength of nonprestressed steel reinforcement, in./in. (mm/mm)
α_L = longitudinal coefficient of thermal expansion, in./in./°F (mm/mm/°C)	ϵ_t = net tensile strain in extreme tension steel at nominal strength, in./in. (mm/mm)
α_T = transverse coefficient of thermal expansion, in./in./°F (mm/mm/°C)	ϵ_t' = transition strain in stress-strain curve of FRP-confined concrete, in./in. (mm/mm)
β_1 = ratio of depth of equivalent rectangular stress block to depth of the neutral axis	ϕ = strength reduction factor
ϵ_b = strain in concrete substrate developed by a given bending moment (tension is positive), in./in. (mm/mm)	ϕ_D = design curvature for a confined concrete section
ϵ_{bi} = strain in concrete substrate at time of FRP installation (tension is positive), in./in. (mm/mm)	$\phi_{y,frp}$ = curvature of the FRP confined section at steel yielding
ϵ_c = strain in concrete, in./in. (mm/mm)	κ_a = efficiency factor for FRP reinforcement in determination of f_{cc}' (based on geometry of cross section)
ϵ_c' = compressive strain of unconfined concrete corresponding to f_c' , in./in. (mm/mm); may be taken as 0.002	κ_b = efficiency factor for FRP reinforcement in determination of ϵ_{ccu} (based on geometry of cross section)
ϵ_{ccu} = ultimate axial compressive strain of confined concrete corresponding to $0.85f_{cc}'$ in a lightly confined member (member confined to restore its concrete design compressive strength), or ultimate axial compressive strain of confined concrete corresponding to failure in a heavily confined member	κ_v = bond-dependent coefficient for shear
$\epsilon_{c,s}$ = strain in concrete at service, in./in. (mm/mm)	κ_e = efficiency factor equal to 0.55 for FRP strain to account for the difference between observed rupture strain in confinement and rupture strain determined from tensile tests
ϵ_{ct} = concrete tensile strain at level of tensile force resultant in post-tensioned flexural members, in./in. (mm/mm)	θ_p = plastic hinge rotation demand
ϵ_{cu} = ultimate axial strain of unconfined concrete corresponding to $0.85f_{co}'$ or maximum usable strain of unconfined concrete, in./in. (mm/mm), which can occur at $f_c = 0.85f_c'$ or $\epsilon_c = 0.003$, depending on the obtained stress-strain curve	ρ_f = FRP reinforcement ratio
ϵ_f = strain in the FRP reinforcement, in./in. (mm/mm)	ρ_g = ratio of area of longitudinal steel reinforcement to cross-sectional area of a compression member (A_s/bh)
ϵ_{fd} = debonding strain of externally bonded FRP reinforcement, in./in. (mm/mm)	ρ_l = longitudinal reinforcement ratio
ϵ_{fe} = effective strain in FRP reinforcement attained at failure, in./in. (mm/mm)	ρ_s = ratio of nonprestressed reinforcement
ϵ_{fu} = design rupture strain of FRP reinforcement, in./in. (mm/mm)	σ = standard deviation
$\bar{\epsilon}_{fu}$ = mean rupture strain of FRP reinforcement based on a population of 20 or more tensile tests per ASTM D3039/D3039M , in./in. (mm/mm)	τ_b = average bond strength for near-surface-mounted FRP bars, psi (MPa)
ϵ_{fu}^* = ultimate rupture strain of FRP reinforcement, in./in. (mm/mm)	ψ_e = factor used to modify development length based on reinforcement coating
	ψ_f = FRP strength reduction factor
	= 0.85 for flexure (calibrated based on design material properties)
	= 0.85 for shear (based on reliability analysis) for three-sided FRP U-wrap or two sided strengthening schemes
	= 0.95 for shear fully wrapped sections
	ψ_s = factor used to modify development length based on reinforcement size
	ψ_t = factor used to modify development length based on reinforcement location



2.2—Definitions

ACI provides a comprehensive list of definitions through an online resource, “ACI Concrete Terminology,” <https://www.concrete.org/store/productdetail.aspx?ItemID=CT13>. Definitions provided herein complement that source.

aramid fiber—fiber in which chains of aromatic polyamide molecules are oriented along the fiber axis to exploit the strength of the chemical bond.

aramid fiber-reinforced polymer—composite material comprising a polymer matrix reinforced with aramid fiber cloth, mat, or strands.

carbon fiber—fiber produced by heating organic precursor materials containing a substantial amount of carbon, such as rayon, polyacrylonitrile, or pitch in an inert environment.

carbon fiber-reinforced polymer—composite material comprising a polymer matrix reinforced with carbon fiber cloth, mat, or strands.

catalyst—substance that accelerates a chemical reaction and enables it to proceed under conditions more mild than otherwise required and that is not, itself, permanently changed by the reaction.

contact-critical application—strengthening or repair system that relies on load transfer from the substrate to the system material achieved through contact or bearing at the interface.

creep rupture—breakage of a material under sustained loading at stresses less than the tensile strength.

cross-linking—formation of covalent bonds linking one polymer molecule to another.

E-glass—family of glass fibers used in reinforced polymers with a calcium alumina borosilicate composition and a maximum alkali content of 2.0 percent.

fabric—two-dimensional network of woven, nonwoven, knitted, or stitched fibers; yarns; or tows.

fiber content—the amount of fiber present in a composite, expressed as a percentage volume fraction or mass fraction of the composite.

fiber fly—short filaments that break off dry fiber tows or yarns during handling and become airborne.

fire retardant—additive to the resin or a surface coating used to reduce the tendency of a resin to burn.

fiber volume fraction—ratio of the volume of fibers to the volume of the composite containing the fibers.

full cure—period at which components of a thermosetting resin have reacted sufficiently for the resin to produce specified properties.

glass fiber—filament drawn from an inorganic fusion typically comprising silica-based material that has cooled without crystallizing.

glass fiber-reinforced polymer—composite material comprising a polymer matrix reinforced with glass fiber cloth, mat, or strands.

glass-transition temperature—representative temperature of the temperature range over which an amorphous material (such as glass or a high polymer) changes from (or to) a brittle, vitreous state to (or from) a plastic state.

impregnate—to saturate fibers with resin or binder.

initiator—chemical used to start the curing process for unsaturated polyester and vinyl ester resins.

interlaminar shear—force tending to produce a relative displacement along the plane of the interface between two laminae.

intumescent coating—covering that swells, increasing volume and decreasing density, when exposed to fire imparting a degree of passive fire protection.

lamina—single layer of fiber reinforcement.

laminated—multiple plies or lamina molded together.

layup—process of placing reinforcing material and resin system in position for molding.

monomer—organic molecule of low molecular weight that creates a solid polymer by reacting with itself or other compounds of low molecular weight.

phenolic resin—thermosetting resin produced by the condensation reaction of an aromatic alcohol with an aldehyde (usually a phenol with formaldehyde).

pitch—viscid substance obtained as a residue of petroleum or coal tar for use as a precursor in the manufacture of some carbon fibers.

polyacrylonitrile—synthetic semi-crystalline organic polymer-based material that is spun into a fiber form for use as a precursor in the manufacture of some carbon fibers.

polyester—one of a large group of synthetic resins, mainly produced by reaction of dibasic acids with dihydroxy alcohols.

postcuring—application of elevated temperature to material containing thermosetting resin to increase the degree of polymer crosslinking and enhance the final material properties.

prepreg—sheet of fabric or mat preimpregnated with resin or binder that is partially cured and ready for final forming and curing.

pultrusion—continuous process for manufacturing fiber-reinforced polymer composites in which resin-impregnated fiber reinforcements (roving or mats) are pulled through a shaping and curing die to produce composites with uniform cross sections.

putty—thickened polymer-based resin used to prepare the concrete substrate.

resin content—amount of resin in a fiber-reinforced polymer composite laminate, expressed as either a percentage of total mass or total volume.

roving—parallel bundle of continuous yarns, tows, or fibers with little or no twist.

saturating resins (or saturants)—polymer-based resin used to impregnate the reinforcing fibers, fix them in place, and transfer load between fibers.

shelf life—length of time packaged materials can be stored under specified conditions and remain usable.

sizing—surface treatment applied to filaments to impart desired processing, durability, and bond attributes.

storage modulus—measure of the stored energy in a viscoelastic material undergoing cyclic deformation during dynamic mechanical analysis.

tow—untwisted bundle of continuous filaments.

vinylester resin—thermosetting reaction product of epoxy resin with a polymerizable unsaturated acid (usually meth-

acrylic acid) that is then diluted with a reactive monomer (usually styrene).

volatile organic compound—organic compound that vaporizes under normal atmospheric conditions.

wet layup—manufacturing process where dry fabric fiber reinforcement is impregnated on site with a saturating resin matrix and then cured in place.

wet-out—process of coating or impregnating roving, yarn, or fabric to fill the voids between the strands and filaments with resin; it is also the condition at which this state is achieved.

witness panel—small mockup manufactured under conditions representative of field application, to confirm that prescribed procedures and materials will yield specified mechanical and physical properties.

yarn—twisted bundle of continuous filaments.

CHAPTER 3—BACKGROUND INFORMATION

Externally bonded fiber-reinforced polymer (FRP) systems have been used to strengthen and retrofit existing concrete structures around the world since the mid-1980s. The number of projects using FRP systems worldwide has increased dramatically, from a few in the 1980s to many thousands today. Structural elements strengthened with externally bonded FRP systems include beams, slabs, columns, walls, joints/connections, chimneys and smokestacks, vaults, domes, tunnels, silos, pipes, and trusses. Externally bonded FRP systems have also been used to strengthen masonry, timber, steel, and cast-iron structures. Externally bonded FRP systems were developed as alternatives to traditional external reinforcing techniques such as steel plate bonding and steel or concrete column jacketing. The initial development of externally bonded FRP systems for the retrofit of concrete structures occurred in the 1980s in Europe and Japan.

3.1—Historical development

In Europe, FRP systems were developed as alternates to steel plate bonding. Bonding steel plates to the tension zones of concrete members with adhesive resins was shown to be a viable technique for increasing flexural strength (Fleming and King 1967). This technique has been used to strengthen many bridges and buildings around the world. Because steel plates can corrode, leading to a deterioration of the bond between the steel and concrete, and because they are difficult to install, requiring the use of heavy equipment, researchers looked to FRP materials as an alternative to steel. Experimental work using FRP materials for retrofitting concrete structures was reported as early as 1978 in Germany (Wolf and Miessler 1989). Research in Switzerland led to the first applications of externally bonded FRP systems to reinforced concrete bridges for flexural strengthening (Meier 1987; Rostasy 1987).

FRP systems were first applied to reinforced concrete columns for providing additional confinement in Japan in the 1980s (Fardis and Khalili 1981; Katsumata et al. 1987). A sudden increase in the use of FRPs in Japan was observed following the 1995 Hyogoken-Nanbu earthquake (Nanni 1995).

Researchers in the United States have had a continuous interest in fiber-based reinforcement for concrete structures since the 1930s. Development and research into the use of these materials for retrofitting concrete structures, however, started in the 1980s through the initiatives of the National Science Foundation (NSF) and the Federal Highway Administration (FHWA). The research activities led to the construction of many field projects that encompassed a wide variety of environmental conditions. Previous research and field applications for FRP rehabilitation and strengthening are described in ACI 440R and conference proceedings, including those of the Fiber Reinforced Polymers for Reinforced Concrete Structures (FRPRCS), Composites in Civil Engineering (CICE), and Conference on Durability of Composites for Construction (CDCC) series.

The development of codes and standards for externally bonded FRP systems is ongoing in Europe, Japan, Canada, and the United States. The first published codes and standards appeared in Japan (Japan Society of Civil Engineers 2001) and Europe (International Federation for Structural Concrete 2001). In the United States, ACI 440.8, ICC AC125, and NCHRP Report 655 (Zureick et al. 2010) provide criteria for evaluating FRP systems.

3.2—Commercially available externally bonded FRP systems

FRP systems come in a variety of forms, including wet layup systems and precured systems. FRP system forms can be categorized based on how they are delivered to the site and installed. The FRP system and its form should be selected based on the acceptable transfer of structural loads and the ease and simplicity of application. Common FRP system forms suitable for the strengthening of structural members are listed in 3.2.1 through 3.2.4.

3.2.1 Wet layup systems—Wet layup FRP systems consist of dry unidirectional or multidirectional fiber sheets or fabrics impregnated with a saturating resin on site. The saturating resin, along with the compatible primer and putty, bonds the FRP sheets to the concrete surface. Wet layup systems are saturated on site and cured in place and, in this sense, are analogous to cast-in-place concrete. Three common types of wet layup systems are listed as follows:

1. Dry unidirectional fiber sheets where the fibers run predominantly in one planar direction. ACI 440.8 provides specifications for unidirectional carbon fiber-reinforced polymer (CFRP) and glass fiber-reinforced polymer (GFRP) wet layup systems.
2. Dry multidirectional fiber sheets or fabrics where the fibers are oriented in at least two planar directions.
3. Dry fiber tows that are wound or otherwise mechanically applied to the concrete surface. The dry fiber tows are impregnated with resin on site during the winding operation.

3.2.2 Prepreg systems—Prepreg FRP systems consist of partially cured unidirectional or multidirectional fiber sheets or fabrics that are preimpregnated with a saturating resin in the manufacturer's facility. Prepreg systems are bonded to the concrete surface with or without an additional resin application, depending on specific system requirements.

Prepreg systems are saturated off site and, like wet layup systems, cured in place. Prepreg systems usually require additional heating for curing. Prepreg system manufacturers should be consulted for storage and shelf-life recommendations and curing procedures. Three common types of prepreg FRP systems are:

1. Preimpregnated unidirectional fiber sheets where the fibers run predominantly in one planar direction
2. Preimpregnated multidirectional fiber sheets or fabrics where the fibers are oriented in at least two planar directions
3. Preimpregnated fiber tows that are wound or otherwise mechanically applied to the concrete surface

3.2.3 Precured systems—Precured FRP systems consist of a wide variety of composite shapes manufactured off site. Typically, an adhesive, along with the primer and putty, is used to bond the precured shapes to the concrete surface. The system manufacturer should be consulted for recommended installation procedures. Precured systems are analogous to precast concrete. Three common types of precured systems are:

1. Precured unidirectional laminate sheets typically delivered to the site in the form of large flat stock or as thin ribbon strips coiled on a roll
2. Precured multidirectional grids, typically delivered to the site coiled on a roll
3. Precured shells, typically delivered to the site in the form of shell segments cut longitudinally so they can be opened and fitted around columns or other members; multiple shell layers are bonded to the concrete and to each other to provide confinement

3.2.4 Near-surface-mounted (NSM) systems—Surface-embedded NSM FRP systems consist of circular or rectangular bars or plates installed and bonded into grooves made on the concrete surface. A suitable adhesive is used to bond the FRP bar into the groove, and is cured in-place. The NSM system manufacturer should be consulted for recommended adhesives. Two common FRP bar types used for NSM applications are:

1. Round bars usually manufactured using pultrusion processes, typically delivered to the site in the form of single bars or in a roll, depending on bar diameter
2. Rectangular bars and plates usually manufactured using pultrusion processes, typically delivered to the site in a roll

CHAPTER 4—CONSTITUENT MATERIALS AND PROPERTIES

The physical and mechanical properties of fiber-reinforced polymer (FRP) materials presented in this chapter explain the behavior and properties affecting their use in concrete structures. The effects of factors such as loading history and duration, temperature, and moisture on the properties of FRP are discussed.

FRP strengthening systems come in a variety of forms (wet layup, prepreg, and precured). Factors such as fiber volume, type of fiber, type of resin, fiber orientation, dimensional effects, and quality control during manufacturing all play a role in establishing the characteristics of an FRP material. The material characteristics described in

this chapter are generic and do not apply to all commercially available products. Standard test methods are available to characterize certain FRP products (refer to [Appendix B](#)). [ACI 440.8](#) provides a specification for unidirectional carbon FRP (CFRP) and glass FRP (GFRP) materials made using the wet layup process. The licensed design professional should consult with the FRP system manufacturer to obtain the relevant characteristics for a specific product and the applicability of those characteristics.

4.1—Constituent materials

The constituent materials used in commercially available FRP repair systems, including all resins, primers, putties, saturants, adhesives, and fibers, have been developed for the strengthening of structural concrete members based on materials and structural testing.

4.1.1 Resins—A wide range of polymeric resins, including primers, putty fillers, saturants, and adhesives, are used with FRP systems. Commonly used resin types, including epoxy, vinyl esters, and polyesters, have been formulated for use in a wide range of environmental conditions. FRP system manufacturers use resins that have:

- a) Compatibility with and adhesion to the concrete substrate
- b) Compatibility with and adhesion to the FRP composite system
- c) Compatibility with and adhesion to the reinforcing fiber
- d) Resistance to environmental effects, including, but not limited to, moisture, salt water, temperature extremes, and chemicals normally associated with exposed concrete
- e) Filling ability
- f) Workability
- g) Pot life consistent with the application
- h) Development of appropriate mechanical properties for the FRP composite

4.1.1.1 Primer—Primer is used to penetrate the surface of the concrete, providing an improved adhesive bond for the saturating resin or adhesive.

4.1.1.2 Putty fillers—Putty is used to fill small surface voids in the substrate, such as bug holes, and to provide a smooth surface to which the FRP system can bond. Filled surface voids also prevent bubbles from forming during curing of the saturating resin.

4.1.1.3 Saturating resin—Saturating resin is used to impregnate the reinforcing fibers, fix them in place, and provide a shear load path to effectively transfer load between fibers. The saturating resin also serves as the adhesive for wet layup systems, providing a shear load path between the previously primed concrete substrate and the FRP system.

4.1.1.4 Adhesives—Adhesives are used to bond precured FRP laminate and near-surface mounted (NSM) systems to the concrete substrate. The adhesive provides a shear load path between the concrete substrate and the FRP reinforcing system. Adhesives are also used to bond together multiple layers of precured FRP laminates.

4.1.2 Fibers—Continuous glass, aramid, and carbon fibers are common reinforcements used in FRP systems. The fibers give the FRP system its strength and stiffness. Typical ranges

of the tensile properties of fibers are given in [Appendix A](#). A more detailed description of fiber types is given in [ACI 440R](#).

4.1.3 Protective coatings—The protective coating protects the bonded FRP reinforcement from potentially damaging environmental and mechanical effects. Coatings are typically applied to the exterior surface of the FRP system after some prescribed degree of adhesive or saturating resin cure. The protection systems are available in a variety of forms. These include:

- a) Polymer coatings that are generally epoxy or polyurethanes.
- b) Acrylic coatings that can be either straight acrylic systems or acrylic cement-based systems. The acrylic systems can also come in different textures.
- c) Cementitious systems that may require roughening of the FRP surface (such as broadcasting sand into wet resin) and can be installed in the same manner as they would be installed on a concrete surface.

d) Intumescent coatings that are polymer-based coatings used to provide a degree of passive fire protection and control flame spread and smoke generation per code requirements.

There are several reasons why protection systems are used to protect FRP systems that have been installed on concrete surfaces. These include:

a) *Ultraviolet light protection*—The epoxy used as part of the FRP strengthening system will be affected over time by exposure to ultraviolet light. There are many available methods used to protect the system from ultraviolet light. These include acrylic coatings, cementitious surfacing, aliphatic polyurethane coatings, and others. Certain types of vinyl ester resins have higher ultraviolet light durability than epoxy resins.

b) *Fire protection*—Fire protection systems are discussed in [1.2.1.2](#) and [9.2.1](#).

c) *Vandalism*—Protective systems that are to resist vandalism should be hard and durable. There are different levels of vandalism protection, ranging from polyurethane coatings that will resist cutting and scraping to cementitious overlays that provide greater protection.

d) *Impact, abrasion, and wear*—Protection systems for impact, abrasion, and wear are similar to those used for vandalism protection; however, abrasion and wear are different than vandalism in that they result from repeated exposure rather than a one-time event, and their protection systems are usually chosen for their hardness and durability.

e) *Aesthetics*—Protective topcoats may be used to conceal the FRP system. These may be acrylic latex coatings that are gray in color to match concrete, or they may be various other colors and textures to match the existing structure.

f) *Chemical resistance*—Exposure to harsh chemicals, such as strong acids, may damage the FRP system. In such environments, coatings with better chemical resistance, such as urethanes and novolac epoxies, may be used.

g) *Submersion in potable water*—In applications where the FRP system is to be submerged in potable water, the FRP system may leach compounds into the water supply. Protective coatings that do not leach harmful chemicals into the

water may be used as a barrier between the FRP system and the potable water supply.

4.2—Physical properties

4.2.1 Density—FRP materials have densities ranging from 75 to 130 lb/ft³ (1.2 to 2.1 g/cm³), which is four to six times lower than that of steel (Table 4.2.1).

Table 4.2.1—Typical densities of FRP materials, lb/ft³ (g/cm³)

Steel	Glass FRP (GFRP)	Carbon FRP (CFRP)	Aramid FRP (AFRP)
490 (7.9)	75 to 130 (1.2 to 2.1)	90 to 100 (1.5 to 1.6)	75 to 90 (1.2 to 1.5)

4.2.2 Coefficient of thermal expansion—The coefficients of thermal expansion of unidirectional FRP materials differ in the longitudinal and transverse directions, depending on the types of fiber, resin, and volume fraction of fiber. Table 4.2.2 lists the longitudinal and transverse coefficients of thermal expansion for typical unidirectional FRP materials. Note that a negative coefficient of thermal expansion indicates that the material contracts with increased temperature and expands with decreased temperature. For reference, the isotropic values of coefficient of thermal expansion for concrete and steel are also provided in Table 4.2.2. Refer to [9.3.1](#) for design considerations regarding thermal expansion.

4.2.3 Effects of high temperatures—Above the glass transition temperature T_g , the elastic modulus of a polymer is significantly reduced due to changes in its molecular structure. The value of T_g depends on the type of resin and is normally in the region of 140 to 180°F (60 to 82°C). In an FRP composite material, the fibers, which exhibit better thermal properties than the resin, can continue to support some load in the longitudinal direction until the temperature threshold of the fibers is reached. This can occur at temperatures exceeding 1800°F (1000°C) for carbon fibers, 530°F (275°C) for glass fibers, and 350°F (175°C) for aramid fibers. Due to a reduction in force transfer between fibers through bond to the resin, however, the tensile properties of the overall composite are reduced. Test results have indicated that temperatures of 480°F (250°C)—much higher than the resin T_g —will reduce the tensile strength of GFRP and CFRP materials exceeding 20 percent ([Kumahara et al. 1993](#)). Other properties affected by the shear transfer through the resin, such as bending strength, are reduced significantly at lower temperatures ([Wang and Evans 1995](#)).

For bond-critical applications of FRP systems, the properties of the polymer at the fiber-concrete interface are essential in maintaining the bond between FRP and concrete. At a temperature close to its T_g , the mechanical properties of the polymer are significantly reduced and the polymer begins to lose its ability to transfer stresses from the concrete to the fibers.

4.3—Mechanical properties

4.3.1 Tensile behavior—When loaded in direct tension, unidirectional fiber-reinforced polymer (FRP) materials do not exhibit any plastic behavior (yielding) before rupture.

Table 4.2.2—Typical coefficients of thermal expansion for FRP materials*

Direction	Coefficient of thermal expansion, $\times 10^{-6}/^{\circ}\text{F}$ ($\times 10^{-6}/^{\circ}\text{C}$)				
	Concrete	Steel	GFRP	CFRP	AFRP
Longitudinal, α_L	4.0 to 6.0 (7.0 to 11.0)	6.5 (11.7)	3.3 to 5.6 (6 to 10)	-0.6 to 0 (-1 to 0)	-3.3 to -1.1 (-6 to -2)
Transverse, α_T	4.0 to 6.0 (7.0 to 11.0)	6.5 (11.7)	10.4 to 12.6 (19 to 23)	12 to 27 (22 to 50)	33 to 44 (60 to 80)

*Typical values for fiber-volume fractions ranging from 0.5 to 0.7.

The tensile behavior of FRP materials consisting of a single type of fiber material is characterized by a linear elastic stress-strain relationship until failure, which is sudden and brittle.

The tensile strength and stiffness of an FRP material is dependent on several factors. Because the fibers in an FRP material are the main load-carrying constituents, the type of fiber, the orientation of fibers, the quantity of fibers, and method and conditions in which the composite is produced affect the tensile properties of the FRP material. Due to the primary role of the fibers and methods of application, the properties of an FRP repair system are sometimes reported based on the net-fiber area. In other instances, such as in precured laminates, the reported properties are based on the gross-laminate area.

The gross-laminate area of an FRP system is calculated using the total cross-sectional area of the cured FRP system, including all fibers and resin. The gross-laminate area is typically used for reporting precured laminate properties where the cured thickness is constant and the relative proportion of fiber and resin is controlled.

The net-fiber area of an FRP system is calculated using the known area of fiber, neglecting the total width and thickness of the cured system; thus, resin is excluded. The net-fiber area is typically used for reporting properties of wet layup systems that use manufactured fiber sheets and field-installed resins. The wet layup installation process leads to controlled fiber content and variable resin content. A method similar to net-fiber area reporting is to report the tensile force or stiffness per unit width of the FRP system as required by [ASTM D7565/D7565M](#).

System properties reported using the gross laminate area have higher relative thickness dimensions and lower relative strength and modulus values, whereas system properties reported using the net-fiber area have lower relative thickness dimensions and higher relative strength and modulus values. Regardless of the basis for the reported values, the load-carrying strength ($f_{fu}A_f$) and axial stiffness (A_fE_f) of the composite remain constant. Properties reported based on the net-fiber area are not the properties of the bare fibers. When tested as a part of a cured composite, the measured tensile strength and ultimate rupture strain of the net-fiber are typically lower than those measured based on a dry fiber test. The properties of an FRP system should be characterized as a composite, recognizing not just the material properties of the individual fibers, but also the efficiency of the fiber-resin system, the fabric architecture, and the method used to create the composite. The mechanical properties of all FRP systems, regardless of form, should be based on the testing of laminate samples with known fiber content.

The tensile properties of some commercially available FRP strengthening systems are given in Appendix A. The tensile properties of a particular FRP system, however, should be obtained from the FRP system manufacturer or using the appropriate test method described in [ASTM D3039/D3039M](#), [D7205/D7205M](#), or [D7565/D7565M](#). Manufacturers should report an ultimate tensile strength, which is defined as the mean tensile strength of a sample of test specimens minus three times the standard deviation ($f_{fu}^* = \bar{f}_{fu} - 3\sigma$) and, similarly, report an ultimate rupture strain ($\epsilon_{fu}^* = \bar{\epsilon}_{fu} - 3\sigma$). This approach provides a 99.87 percent probability that the actual ultimate tensile properties will exceed these statistically-based design values for a standard sample distribution ([Mutsuyoshi et al. 1990](#)). The elastic modulus should be calculated in accordance with [ASTM D3039/D3039M](#), [D7205/D7205M](#), or [D7565/D7565M](#). A minimum number of 20 replicate test specimens should be used to determine the ultimate tensile properties. The manufacturer should provide a description of the method used to obtain the reported tensile properties, including the number of tests, mean values, and standard deviations.

4.3.2 Compressive behavior—Externally bonded FRP systems should not be used as compression reinforcement due to insufficient testing to validate its use in this type of application. The mode of failure for FRP laminates subjected to longitudinal compression can include transverse tensile failure, fiber microbuckling, or shear failure. The mode of failure depends on the type of fiber, the fiber-volume fraction, and the type of resin. In general, compressive strengths are higher for materials with higher tensile strengths, except in the case of aramid FRP (AFRP), where the fibers exhibit nonlinear behavior in compression at a relatively low level of stress ([Wu 1990](#)). The compressive modulus of elasticity is usually smaller than the tensile modulus of elasticity of FRP materials ([Ehsani 1993](#)).

4.4—Time-dependent behavior

4.4.1 Creep rupture—FRP materials subjected to a sustained load can suddenly fail after a time period referred to as the endurance time. This type of failure is known as creep rupture. As the ratio of the sustained tensile stress to the short-term strength of the FRP laminate increases, endurance time decreases. The endurance time also decreases under adverse environmental conditions, such as high temperature, ultraviolet-radiation exposure, high alkalinity, wet and dry cycles, or freezing-and-thawing cycles.

In general, carbon fibers are the least susceptible to creep rupture, aramid fibers are moderately susceptible, and glass fibers are most susceptible. Creep rupture tests have been conducted on 0.25 in. (6 mm) diameter FRP bars reinforced

with glass, aramid, and carbon fibers. The FRP bars were tested at different load levels at room temperature. Results indicated that a linear relationship exists between creep rupture strength and the logarithm of time for all load levels. The ratios of stress to cause creep rupture after 500,000 hours (approximately 50 years) to the short-term ultimate strength of the GFRP, AFRP, and CFRP bars were extrapolated to be approximately 0.3, 0.5, and 0.9, respectively (Yamaguchi et al. 1997; Malvar 1998). Recommendations on sustained stress limits imposed to avoid creep rupture are given Chapter 9 through 15. As long as the sustained stress in the FRP is below the creep rupture stress limits, the strength of the FRP is available for nonsustained loads.

4.4.2 Fatigue—A substantial amount of data for fatigue behavior and life prediction of stand-alone FRP materials is available (National Research Council 1991). Most of these data were generated from materials typically used by the aerospace industry. Despite the differences in quality and consistency between aerospace and commercial-grade FRP materials, some general observations on the fatigue behavior of FRP materials can be made. Unless specifically stated otherwise, the following cases are based on a unidirectional material with approximately 60 percent fiber-volume fraction and subjected to tension-tension sinusoidal cyclic loading at:

- a) A frequency low enough to not cause self heating
- b) Ambient laboratory environments
- c) A stress ratio (ratio of minimum applied stress to maximum applied stress) of 0.1
- d) A direction parallel to the principal fiber alignment

Test conditions that raise the temperature and moisture content of FRP materials generally degrade the ambient environment fatigue behavior.

Of all types of FRP composites for infrastructure applications, CFRP is the least prone to fatigue failure. An endurance limit of 60 to 70 percent of the initial static ultimate strength of CFRP is typical. On a plot of stress versus the logarithm of the number of cycles at failure (S-N curve), the downward slope for CFRP is usually approximately 5 percent of the initial static ultimate strength per decade of logarithmic life (Curtis 1989). At 1 million cycles, the fatigue strength is generally between 60 and 70 percent of the initial static ultimate strength and is relatively unaffected by the moisture and temperature exposures of concrete structures unless the resin or fiber/resin interface is substantially degraded by the environment.

In ambient-environment laboratory tests (Mandell and Meier 1983), individual glass fibers demonstrated delayed rupture caused by stress corrosion, which had been induced by the growth of surface flaws in the presence of even minute quantities of moisture. When many glass fibers were embedded into a matrix to form an FRP composite, a cyclic tensile fatigue effect of approximately 10 percent loss in the initial static strength per decade of logarithmic lifetime was observed (Mandell 1982). This fatigue effect is thought to be due to fiber-fiber interactions and is not dependent on the stress corrosion mechanism described for individual fibers. Usually, no clear fatigue limit can be defined. Environmental factors can play an important role in the fatigue behavior of

glass fibers due to their susceptibility to moisture, alkaline, or acidic solutions.

Aramid fibers, for which substantial durability data are available, appear to behave reasonably well in fatigue. Neglecting in this context the rather poor durability of all aramid fibers in compression, the tension-tension fatigue behavior of an impregnated aramid fiber strand is excellent. Strength degradation per decade of logarithmic lifetime is approximately 5 to 6 percent (Roylance and Roylance 1981). While no distinct endurance limit is known for AFRP, 2-million-cycle endurance limits of commercial AFRP tendons for concrete applications have been reported in the range of 54 to 73 percent of the ultimate tensile strength (Odagiri et al. 1997). Because the slope of the applied stress versus logarithmic endurance time of AFRP is similar to the slope of the stress versus logarithmic cyclic lifetime data, the individual fibers appear to fail by a strain-limited creep rupture process. This lifetime-limiting mechanism in commercial AFRP bars is accelerated by exposure to moisture and elevated temperature (Roylance and Roylance 1981; Rostasy 1997).

4.5—Durability

Many FRP systems exhibit reduced mechanical properties after exposure to certain environmental factors, including high temperature, humidity, and chemical exposure. The exposure environment, duration of exposure, resin type and formulation, fiber type, and resin-curing method are some of the factors that influence the extent of the reduction in mechanical properties. These factors are discussed in more detail in 9.3. The tensile properties reported by the manufacturer are based on testing conducted in a laboratory environment, and do not reflect the effects of environmental exposure. These properties should be adjusted in accordance with the recommendations in 9.4 to account for the anticipated service environment to which the FRP system may be exposed during its service life.

4.6—FRP systems qualification

FRP systems should be qualified for use on a project based on independent laboratory test data of the FRP-constituent materials and the laminates made with them, structural test data for the type of application being considered, and durability data representative of the anticipated environment. Test data provided by the FRP system manufacturer demonstrating the proposed FRP system should meet all mechanical and physical design requirements, including tensile strength, durability, resistance to creep, bond to substrate, and T_g , should be considered. ACI 440.8 provides a specification for unidirectional carbon and glass FRP materials made using the wet layup process.

FRP composite systems that have not been fully tested should not be considered for use. Mechanical properties of FRP systems should be determined from tests on laminates manufactured in a process representative of their field installation. Mechanical properties should be tested in general conformance with the procedures listed in Appendix B. Modifications of standard testing procedures may be permitted to emulate field assemblies.

The specified material-qualification programs should require sufficient laboratory testing to measure the repeatability and reliability of critical properties. Testing of multiple batches of FRP materials is recommended. Independent structural testing can be used to evaluate a system's performance for the specific application.

CHAPTER 5—SHIPPING, STORAGE, AND HANDLING

5.1—Shipping

Fiber-reinforced polymer (FRP) system constituent materials should be packaged and shipped in a manner that conforms to all applicable federal and state packaging and shipping codes and regulations. Packaging, labeling, and shipping for thermosetting resin materials are controlled by [CFR 49](#).

5.2—Storage

5.2.1 Storage conditions—To preserve the properties and maintain safety in the storage of FRP system constituent materials, the materials should be stored in accordance with the manufacturer's recommendations. Certain constituent materials, such as reactive curing agents, hardeners, initiators, catalysts, and cleaning solvents, have safety-related requirements and should be stored in a manner as recommended by the manufacturer and OSHA. Catalysts and initiators (usually peroxides) should be stored separately.

5.2.2 Shelf life—The properties of the uncured resin components can change with time, temperature, or humidity. Such conditions can affect the reactivity of the mixed system and the uncured and cured properties. The manufacturer sets a recommended shelf life within which the properties of the resin-based materials should continue to meet or exceed stated performance criteria. Any component material that has exceeded its shelf life, has deteriorated, or has been contaminated should not be used. FRP materials deemed unusable should be disposed of in a manner specified by the manufacturer and acceptable to state and federal environmental control regulations.

5.3—Handling

5.3.1 Safety data sheet—Safety data sheets (SDSs) for all FRP-constituent materials and components should be obtained from the manufacturers, and should be accessible at the job site.

5.3.2 Information sources—Detailed information on the handling and potential hazards of FRP-constituent materials can be found in company literature and guides, OSHA guidelines, and other government informational documents.

5.3.3 General handling hazards—Thermosetting resins describe a generic family of products that includes unsaturated polyesters, vinyl esters, epoxy, and polyurethane resins. The materials used with them are generally described as hardeners, curing agents, peroxide initiators, isocyanates, fillers, and flexibilizers. There are precautions that should be observed when handling thermosetting resins and their component materials. Some general hazards that may be

encountered when handling thermosetting resins are listed as follows:

- a) Skin irritation, such as burns, rashes, and itching
- b) Skin sensitization, which is an allergic reaction similar to that caused by poison ivy, building insulation, or other allergens
- c) Breathing organic vapors from cleaning solvents, monomers, and diluents
- d) With a sufficient concentration in air, explosion or fire of flammable materials when exposed to heat, flames, pilot lights, sparks, static electricity, cigarettes, or other sources of ignition
- e) Exothermic reactions of mixtures of materials causing fires or personal injury
- f) Nuisance dust caused by grinding or handling of the cured FRP materials (manufacturer's literature should be consulted for specific hazards)

The complexity of thermosetting resins and associated materials makes it essential that labels and the SDS are read and understood by those working with these products. [CFR 16 Part 1500](#) regulates the labeling of hazardous substances and includes thermosetting-resin materials. [ANSI Z400.1/Z129.1-2010](#) provides further guidance regarding classification and precautions.

5.3.4 Personnel safe handling and clothing—Disposable suits and gloves are suitable for handling fiber and resin materials. Disposable rubber or plastic gloves are recommended and should be discarded after each use. Gloves should be resistant to resins and solvents. Safety glasses or goggles should be used when handling resin components and solvents. Respiratory protection, such as dust masks or respirators, should be used when fiber fly, dust, or organic vapors are present, or during mixing and placing of resins if required by the FRP system manufacturer.

5.3.5 Workplace safe handling—The workplace should be well ventilated. Surfaces should be covered as needed to protect against contamination and resin spills. Each FRP system constituent material has different handling and storage requirements to prevent damage. The material manufacturer should be consulted for guidance. Some resin systems are potentially dangerous during mixing of the components. The manufacturer's literature should be consulted for proper mixing procedures, and the SDS for specific handling hazards. Ambient cure resin formulations produce heat when curing, which in turn accelerates the reaction. Uncontrolled reactions, including fuming, fire, or violent boiling, may occur in containers holding a mixed mass of resin; therefore, containers should be monitored.

5.3.6 Cleanup and disposal—Cleanup can involve use of flammable solvents, and appropriate precautions should be observed. Cleanup solvents are available that do not present flammability concerns. All waste materials should be contained and disposed of as prescribed by the prevailing environmental authority.

CHAPTER 6—INSTALLATION

Procedures for installing fiber-reinforced polymer (FRP) systems have been developed by the system manufacturers and often differ between systems. In addition, installation

procedures can vary within a system, depending on the type and condition of the structure. This chapter presents general guidelines for the installation of FRP systems. Contractors trained in accordance with the installation procedures developed by the system manufacturer should install FRP systems. Deviations from the procedures developed by the FRP system manufacturer should not be allowed without consulting with the manufacturer.

6.1—Contractor competency

The FRP system installation contractor should demonstrate competency for surface preparation and application of the FRP system to be installed. Contractor competency can be demonstrated by providing evidence of training and documentation of related work previously completed by the contractor or by actual surface preparation and installation of the FRP system on portions of the structure. The FRP system manufacturer or its authorized agent should train the contractor's application personnel in the installation procedures of its system and ensure they are competent to install the system.

6.2—Temperature, humidity, and moisture considerations

Temperature, relative humidity, and surface moisture at the time of installation can affect the performance of the FRP system. Conditions to be observed before and during installation include surface temperature and moisture condition of the concrete, air temperature, relative humidity, and corresponding dew point.

Primers, saturating resins, and adhesives should generally not be applied to cold or frozen surfaces. When the surface temperature of the concrete surface falls below a minimum level as specified by the FRP system manufacturer, improper saturation of the fibers and improper curing of the resin constituent materials can occur, compromising the integrity of the FRP system. An auxiliary heat source can be used to raise the ambient and surface temperature during installation and maintain proper temperatures during curing. The heat source should be clean and not contaminate the surface or the uncured FRP system.

Resins and adhesives should generally not be applied to damp or wet surfaces unless they have been formulated for such applications. FRP systems should not be applied to concrete surfaces that are subject to moisture vapor transmission. The transmission of moisture vapor from a concrete surface through the uncured resin materials typically appears as surface bubbles and can compromise the bond between the FRP system and the substrate.


6.3—Equipment

Some FRP systems have unique, often system-specific, equipment designed specifically for their application. This equipment can include resin impregnators, sprayers, lifting/positioning devices, and winding machines. All equipment should be clean and in good operating condition. The contractor should have personnel trained in the operation of all equipment. Personal protective equipment, such as gloves, masks, eye guards, and coveralls, should be chosen and worn

for each employee's function. All supplies and equipment should be available in sufficient quantities to allow continuity in the installation project and quality assurance.

6.4—Substrate repair and surface preparation

The behavior of concrete members strengthened or retrofitted with FRP systems is highly dependent on a sound concrete substrate and proper preparation and profiling of the concrete surface. An improperly prepared surface can result in debonding or delamination of the FRP system before achieving the design load transfer. The general guidelines presented in this chapter should be applicable to all externally bonded FRP systems. Specific guidelines for a particular FRP system should be obtained from the FRP system manufacturer.

6.4.1 Substrate repair—All problems associated with the condition of the original concrete and the concrete substrate that can compromise the integrity of the FRP system should be addressed before surface preparation begins. **ACI 546R** and **ICRI 310.2R** detail methods for the repair and surface preparation of concrete. All concrete repairs should meet the requirements of the design drawings and project specifications. The FRP system manufacturer should be consulted on the compatibility of the FRP system with materials used for repairing the substrate. 

6.4.1.1 Corrosion-related deterioration—Externally bonded FRP systems should not be applied to concrete substrates suspected of containing actively corroding reinforcing steel. The expansive forces associated with the corrosion process are difficult to determine and could compromise the structural integrity of the externally applied FRP system. The cause(s) of the corrosion should be addressed, and the corrosion-related deterioration should be repaired before the application of any externally bonded FRP system.

6.4.1.2 Injection of cracks—Cracks that are 0.010 in. (0.3 mm) and wider can affect the performance of the externally bonded FRP systems. Consequently, cracks wider than 0.010 in. (0.3 mm) should be pressure-injected with epoxy before FRP installation in accordance with **ACI 224.1R**. Smaller cracks exposed to aggressive environments may require resin injection or sealing to prevent corrosion of existing steel reinforcement. Crack-width criteria for various exposure conditions are given in **ACI 224.1R**.

6.4.2 Surface preparation—Surface preparation requirements should be based on the intended application of the FRP system. Applications can be categorized as bond-critical or contact-critical. Bond-critical applications, such as flexural or shear strengthening of beams, slabs, columns, or walls, require an adhesive bond between the FRP system and the concrete. Contact-critical applications, such as confinement of columns, only require intimate contact between the FRP system and the concrete. Contact-critical applications do not require an adhesive bond between the FRP system and the concrete substrate, although one is typically provided to facilitate installation.

6.4.2.1 Bond-critical applications—Surface preparation for bond-critical applications should be in accordance with recommendations of **ACI 546R** and **ICRI 310.2R**. The

concrete or repaired surfaces to which the FRP system is to be applied should be freshly exposed and free of loose or unsound materials. Where fibers wrap around corners, the corners should be rounded to a minimum 0.5 in. (13 mm) radius to reduce stress concentrations in the FRP system and voids between the FRP system and the concrete. Roughened corners should be smoothed with putty. Obstructions, inside corners, concave surfaces, and embedded objects can affect the performance of the FRP system and should be addressed. Obstructions and embedded objects may need to be removed before installing the FRP system. Inside corners and concave surfaces may require special detailing to ensure that the bond of the FRP system to the substrate is maintained. Surface preparation can be accomplished using abrasive or water-blasting techniques. All laitance, dust, dirt, oil, curing compound, existing coatings, and any other matter that could interfere with the bond of the FRP system to the concrete should be removed. Bug holes and other small surface voids should be completely exposed during surface profiling. After the profiling operations are complete, the surface should be cleaned and protected before FRP installation so that no materials that can interfere with bond are redeposited on the surface.

The concrete surface should be prepared to a surface profile not less than CSP 3, as defined by [ICRI 310.2R](#) or to the tolerances recommended by the FRP system manufacturer. Localized out-of-plane variations, including form lines, should not exceed 1/32 in. (1 mm) or the tolerances recommended by the FRP system manufacturer. Localized out-of-plane variations can be removed by grinding, before abrasive or water blasting, or can be smoothed over using resin-based putty if the variations are very small. Bug holes and voids should be filled with resin-based putty.

All surfaces to receive the strengthening system should be as dry as recommended by the FRP system manufacturer. Water in the pores can inhibit resin penetration and reduce mechanical interlock. Moisture content should be evaluated in accordance with the requirements of [ACI 503.4](#).

6.4.2.2 Contact-critical applications—In applications involving confinement of structural concrete members, surface preparation should promote continuous intimate contact between the concrete surface and the FRP system. Surfaces to be wrapped should, at a minimum, be flat or convex to promote proper loading of the FRP system. Large voids in the surface should be patched with a repair material compatible with the existing concrete. Materials with low compressive strength and elastic modulus, such as plaster, can reduce the effectiveness of the FRP system and should be removed.

6.4.3 Near-surface mounted (NSM) systems—NSM systems are typically installed in grooves cut onto the concrete surface. The existing steel reinforcement should not be damaged while cutting the groove. The soundness of the concrete surface should be checked before installing the bar. The inside faces of the groove should be cleaned to ensure adequate bond with concrete. The resulting groove should be free of laitance or other compounds that may interfere with bond. The moisture content of the parent concrete should be controlled to suit the

bonding properties of the adhesive. The grooves should be completely filled with the adhesive. The adhesive should be specified by the NSM system manufacturer.

6.5—Mixing of resins

Mixing of resins should be done in accordance with the FRP system manufacturer's recommended procedure. All resin components should be at the proper temperature and mixed in the correct ratio until there is a uniform and complete mixing of components. Resin components are often contrasting colors, so full mixing is achieved when color streaks are eliminated. Resins should be mixed for the prescribed mixing time and visually inspected for uniformity of color. The material manufacturer should supply recommended batch sizes, mixture ratios, mixing methods, and mixing times.

Mixing equipment can include small electrically powered mixing blades or specialty units, or resins can be mixed by hand stirring, if needed. Resin mixing should be in quantities sufficiently small to ensure that all mixed resin can be used within the resin's pot life. Mixed resin that exceeds its pot life should not be used because the viscosity will continue to increase and will adversely affect the resin's ability to penetrate the surface or saturate the fiber sheet.

6.6—Application of FRP systems

Fumes can accompany the application of some FRP resins. FRP systems should be selected with consideration for their impact on the environment, including emission of volatile organic compounds and toxicology.

6.6.1 Primer and putty—Where required, primer should be applied to all areas on the concrete surface where the FRP system is to be placed. The primer should be placed uniformly on the prepared surface at the manufacturer's specified rate of coverage. The applied primer should be protected from dust, moisture, and other contaminants before applying the FRP system.

Putty should be used in an appropriate thickness and sequence with the primer as recommended by the FRP manufacturer. The system-compatible putty, which is typically a thickened resin-based paste, should be used only to fill voids and smooth surface discontinuities before the application of other materials. Rough edges or trowel lines of cured putty should be ground smooth before continuing the installation.

Before applying the saturating resin or adhesive, the primer and putty should be allowed to cure as specified by the FRP system manufacturer. If the putty and primer are fully cured, additional surface preparation may be required before the application of the saturating resin or adhesive. Surface preparation requirements should be obtained from the FRP system manufacturer.

6.6.2 Wet layup systems—Wet layup FRP systems are typically installed by hand using dry fiber sheets and a saturating resin, typically per the manufacturer's recommendations. The saturating resin should be applied uniformly to all prepared surfaces where the system is to be placed. The fibers can also be impregnated in a separate process using

a resin-impregnating machine before placement on the concrete surface.

The reinforcing fibers should be gently pressed into the uncured saturating resin in a manner recommended by the FRP system manufacturer. Entrapped air between layers should be released or rolled out before the resin sets. Sufficient saturating resin should be applied to achieve full saturation of the fibers.

Successive layers of saturating resin and fiber materials should be placed before the complete cure of the previous layer of resin. If previous layers are cured, interlayer surface preparation, such as light sanding or solvent application as recommended by the system manufacturer, may be required.

6.6.3 Machine-applied systems—Machine-applied systems can use resin-preimpregnated tows or dry-fiber tows. Prepreg tows are impregnated with saturating resin off site and delivered to the jobsite as spools of prepreg tow material. Dry fibers are impregnated at the jobsite during the winding process.

Wrapping machines are primarily used for the automated wrapping of concrete columns. The tows can be wound either horizontally or at a specified angle. The wrapping machine is placed around the column and automatically wraps the tow material around the perimeter of the column while moving up and down the column.

After wrapping, prepreg systems should be cured at an elevated temperature. Usually, a heat source is placed around the column for a predetermined temperature and time schedule in accordance with the manufacturer's recommendations. Temperatures are controlled to ensure consistent quality. The resulting FRP jackets do not have any seams or welds because the tows are continuous. In all the previous application steps, the FRP system manufacturer's recommendations should be followed.

6.6.4 Precured systems—Precured systems include shells, strips, and open grid forms that are typically installed with an adhesive. Adhesives should be uniformly applied to the prepared surfaces where precured systems are to be placed, except in certain instances of concrete confinement where adhesion of the FRP system to the concrete substrate may not be required.

Precured laminate surfaces to be bonded should be clean and prepared in accordance with the manufacturer's recommendation. The precured sheets or curved shells should be placed on or into the wet adhesive in a manner recommended by the FRP manufacturer. Entrapped air between layers should be released or rolled out before the adhesive sets. The adhesive should be applied at a rate recommended by the FRP manufacturer.

6.6.5 Near-surface mounted (NSM) systems—NSM systems consist of installing rectangular or circular FRP bars in grooves cut onto the concrete surface and bonded in place using an adhesive. Grooves should be dimensioned to ensure adequate adhesive around the bars. Typical groove dimensions for NSM FRP rods and plates are found in 14.3. NSM systems can be used on the topside of structural members and for overhead applications. Adhesive type and installation method should be specified by the NSM system manufacturer.

6.6.6 Protective coatings—Coatings should be compatible with the FRP strengthening system and applied in accordance with the manufacturer's recommendations. Typically, the use of solvents to clean the FRP surface before installing coatings is not recommended due to the deleterious effects that solvents can have on the polymer resins. The FRP system manufacturer should approve any use of solvent wipe preparation of FRP surfaces before the application of protective coatings. The coatings should be periodically inspected and maintenance should be provided to ensure the effectiveness of the coatings.

6.7—Alignment of FRP materials

The FRP ply orientation and ply stacking sequence should be specified. Small variations in angle, as little as 5 degrees, from the intended direction of fiber alignment can cause a substantial reduction in strength and modulus. Deviations in ply orientation should only be made if approved by the licensed design professional.

Sheet and fabric materials should be handled in a manner to maintain the fiber straightness and orientation. Fabric kinks, folds, or other forms of waviness should be reported to the licensed design professional.

6.8—Multiple plies and lap splices

Multiple plies can be used, provided that all plies are fully impregnated with the resin system, the resin shear strength is sufficient to transfer the shearing load between plies, and the bond strength between the concrete and FRP system is sufficient. For long spans, multiple lengths of fiber material or precured stock can be used to continuously transfer the load by providing adequate lap splices. Lap splices should be staggered unless noted otherwise by the licensed design professional. Lap splice details, including lap length, should be based on testing and installed in accordance with the manufacturer's recommendations. Due to the characteristics of some FRP systems, multiple plies and lap splices are not always possible. Specific guidelines on lap splices are given in Chapter 14.

6.9—Curing of resins

Curing of resins is a time-temperature-dependent phenomenon. Ambient-cure resins can take several days to reach full cure. Temperature extremes or fluctuations can retard or accelerate the resin curing time. The FRP system manufacturer may offer several prequalified grades of resin to accommodate these situations.

Elevated cure systems require the resin to be heated to a specific temperature for a specified time. Various combinations of time and temperature within a defined envelope should provide full cure of the system.

All resins should be cured according to the manufacturer's recommendation. Field modification of resin chemistry should not be permitted. Cure of installed plies should be monitored before placing subsequent plies. Installation of successive layers should be halted if there is a curing anomaly.

6.10—Temporary protection

Adverse temperatures; direct contact by rain, dust, or dirt; excessive sunlight; high humidity; or vandalism can damage an FRP system during installation and cause improper cure of the resins. Temporary protection, such as tents and plastic screens, may be required during installation and until the resins have cured. If temporary shoring is required, the FRP system should be fully cured before removing the shoring and allowing the structural member to carry the design loads. In the event of suspected damage to the FRP system during installation, the licensed design professional should be notified and the FRP system manufacturer consulted.

CHAPTER 7—INSPECTION, EVALUATION, AND ACCEPTANCE

Quality assurance and quality control (QA/QC) programs and criteria are to be maintained by the fiber-reinforced polymer (FRP) system manufacturers, the installation contractors, and others associated with the project. QA is typically an owner or a licensed professional activity whereas QC is a contractor or supplier activity. The QC program should be comprehensive and cover all aspects of the strengthening project, and should be detailed in the project specifications by a licensed professional. The degree of QC and the scope of testing, inspection, and record keeping depends on the size and complexity of the project.

Quality assurance is achieved through a set of inspections and applicable tests to document the acceptability of the installation. Project specifications should include a requirement to provide a QA plan for the installation and curing of all FRP materials. The plan should include personnel safety issues, application and inspection of the FRP system, location and placement of splices, curing provisions, means to ensure dry surfaces, QA samples, cleanup, and the suggested submittals listed in 15.3.

7.1—Inspection

FRP systems and all associated work should be inspected as required by the applicable codes. In the absence of such requirements, the inspection should be conducted by or under the supervision of a licensed design professional or a qualified inspector. Inspectors should be knowledgeable of FRP systems and be trained in the installation of FRP systems. The qualified inspector should require compliance with the design drawings and project specifications. During the installation of the FRP system, daily inspection should be conducted and should include:

- a) Date and time of installation
- b) Ambient temperature, relative humidity, and general weather observations
- c) Surface temperature of concrete
- d) Surface moisture
- e) Surface preparation methods and resulting profile using the ICRI surface profile chips
- f) Qualitative description of surface cleanliness
- g) Type of auxiliary heat source, if applicable
- h) Widths of cracks not injected with epoxy

- i) Fiber or precured laminate batch number(s) and approximate location in structure
- j) Batch numbers; mixture ratios; mixing time; and qualitative descriptions of the appearance of all mixed resins including primers, putties, saturants, adhesives, and coatings mixed for the day
- k) Observations of progress of cure of resins
- l) Conformance with installation procedures
- m) Pull-off test results: bond strength, failure mode, and location
- n) FRP properties from tests of field sample panels or witness panels, if required
- o) Location and size of any delaminations or air voids
- p) General progress of work

The inspector should provide the licensed design professional or owner with the inspection records and witness panels. Records and witness panels should be retained for a minimum of 10 years or a period specified by the licensed design professional. The installation contractor should retain sample cups of mixed resin and maintain a record of the placement of each batch.

7.2—Evaluation and acceptance

FRP systems should be evaluated and accepted or rejected based on conformance or nonconformance with the design drawings and specifications. FRP system material properties, installation within specified placement tolerances, presence of delaminations, cure of resins, and adhesion to substrate should be included in the evaluation. Placement tolerances, including fiber orientation, cured thickness, ply orientation, width and spacing, corner radii, and lap splice lengths, should be evaluated.

Witness panel and pull-off tests are used to evaluate the installed FRP system. In-place load testing can also be used to confirm the installed behavior of the FRP-strengthened member (Nanni and Gold 1998).

7.2.1 Materials—Before starting the project, the FRP system manufacturer should submit certification of specified material properties and identification of all materials to be used. Additional material testing can be conducted if deemed necessary based on the size and complexity of the project or other factors. Evaluation of delivered FRP materials can include tests for tensile strength, T_g , gel time, pot life, and adhesive shear strength. These tests are usually performed on material samples sent to a laboratory according to the QC test plan. Tests for pot life of resins and curing hardness are usually conducted on site. Materials that do not meet the minimum requirements as specified by the licensed design professional should be rejected.

Witness panels can be used to evaluate the tensile strength and modulus, lap splice strength, hardness, and T_g of the FRP system installed and cured on site using installation procedures similar to those used to install and cure the FRP system. During installation, flat panels of predetermined dimensions and thickness can be fabricated on site according to a predetermined sampling plan. After curing on site, the panels can then be sent to a laboratory for testing. Witness panels can be retained or submitted to an approved laboratory in a timely

manner for testing of strength and T_g . Strength and elastic modulus of FRP materials can be determined in accordance with the requirements of [ASTM D3039/D3039M](#), [D7205/D7205M](#), or [D7565/D7565M](#). The properties to be evaluated by testing should be specified. The licensed design professional may waive or alter the frequency of testing.

Some FRP systems, including precured and machine-wound systems, do not lend themselves to the fabrication of small, flat, witness panels. For these cases, the licensed design professional can modify the requirements to include test panels or samples provided by the manufacturer. During installation, sample cups of mixed resin should be prepared according to a predetermined sampling plan and retained for testing to determine the degree of cure (7.2.4).

7.2.2 Fiber orientation—Fiber or precured-laminate orientation should be evaluated by visual inspection. Fiber waviness—a localized appearance of fibers that deviate from the general straight-fiber line in the form of kinks or waves—should be evaluated for wet layup systems. Fiber or precured laminate misalignment of more than 5 degrees from that specified on the design drawings (approximately 1 in./ft [80 mm/m]) should be reported to the licensed design professional for evaluation and acceptance.

7.2.3 Delaminations—The cured FRP system should be evaluated for delaminations or air voids between multiple plies or between the FRP system and the concrete. Inspection methods should be capable of detecting delaminations of 2 in.² (1300 mm²) or greater. Methods such as acoustic sounding (hammer sounding), ultrasonics, and thermography can be used to detect delaminations.

The effect of delaminations or other anomalies on the structural integrity and durability of the FRP system should be evaluated. Delamination size, location, and quantity relative to the overall application area should be considered in the evaluation.

General acceptance guidelines for wet layup systems are:

- a) Small delaminations less than 2 in.² (1300 mm²) each are permissible as long as the delaminated area is less than 5 percent of the total laminate area and there are no more than 10 such delaminations per 10 ft² (1 m²).
- b) Large delaminations greater than 25 in.² (16,000 mm²) can affect the performance of the installed FRP and should be repaired by selectively cutting away the affected sheet and applying an overlapping sheet patch of equivalent plies.
- c) Delaminations less than 25 in.² (16,000 mm²) may be repaired by resin injection or ply replacement, depending on the size and number of delaminations and their locations.

For precured FRP systems, each delamination should be evaluated and repaired in accordance with the licensed design professional's direction. Upon completion of the repairs, the laminate should be reinspected to verify that the repair was properly accomplished.

7.2.4 Cure of resins—The relative cure of FRP systems can be evaluated by laboratory testing of witness panels or resin cup samples using [ASTM D3418](#). The relative cure of the resin can also be evaluated on the project site by physical observation of resin tackiness and hardness of work surfaces or hardness of retained resin samples. The FRP system

manufacturer should be consulted to determine the specific resin-cure verification requirements. For precured systems, adhesive hardness measurements should be made in accordance with the manufacturer's recommendation.

7.2.5 Adhesion strength—For bond-critical applications, tension adhesion testing of cored samples should be conducted in accordance with the requirements of [ASTM D7522/D7522](#). Such tests cannot be performed when using near-surface-mounted (NSM) systems. The sampling frequency should be specified. Tension adhesion strengths should exceed 200 psi (1.4 MPa) and should exhibit failure of the concrete substrate. Lower strengths or failure between the FRP system and the concrete or between plies should be reported to the licensed design professional for evaluation and acceptance. For NSM strengthening, sample cores may be extracted to visually verify the consolidation of the resin adhesive around the FRP bar. The location of this core should be chosen such that the continuity of the FRP reinforcement is maintained (that is, at the ends of the NSM bars).

7.2.6 Cured thickness—Small core samples, typically 0.5 in. (13 mm) in diameter, may be taken to visually ascertain the cured laminate thickness or number of plies. Cored samples required for adhesion testing also can be used to ascertain the laminate thickness or number of plies. The sampling frequency should be specified. Taking samples from high-stress areas or splice areas should be avoided. For aesthetic reasons, the cored hole can be filled and smoothed with a repair mortar or the FRP system putty. If required, a 4 to 8 in. (100 to 200 mm) overlapping FRP sheet patch of equivalent plies may be applied over the filled and smoothed core hole immediately after taking the core sample. The FRP sheet patch should be installed in accordance with the manufacturer's installation procedures.

CHAPTER 8—MAINTENANCE AND REPAIR

8.1—General

As with any strengthening or retrofit repair, the owner should periodically inspect and assess the performance of the fiber-reinforced polymer (FRP) system used for strengthening or retrofit repair of concrete members.

8.2—Inspection and assessment

8.2.1 General inspection—A visual inspection looks for changes in color, debonding, peeling, blistering, cracking, crazing, deflections, indications of reinforcing bar corrosion, and other anomalies. In addition, ultrasonic, acoustic sounding (hammer tap), or thermographic tests may indicate signs of progressive delamination.

8.2.2 Testing—Testing can include pull-off tension tests (7.2.5) or conventional structural loading tests ([ACI 437R](#)).

8.2.3 Assessment—Test data and observations are used to assess any damage and the structural integrity of the strengthening system. The assessment can include a recommendation for repairing any deficiencies and preventing recurrence of degradation.

8.3—Repair of strengthening system

The method of repair for the strengthening system depends on the causes of the damage, the type of material, the form of degradation, and the level of damage. Repairs to the fiber-reinforced polymer (FRP) system should not be undertaken without first identifying and addressing the causes of the damage.

Minor damage should be repaired, including localized FRP laminate cracking or abrasions that affect the structural integrity of the laminate. Minor damage can be repaired by bonding FRP patches over the damaged area. The FRP patches should possess the same characteristics, such as thickness or ply orientation, as the original laminate. The FRP patches should be installed in accordance with the material manufacturer's recommendation. Minor delaminations can be repaired by resin injection. Major damage, including peeling and debonding of large areas, may require removal of the affected area, reconditioning of the cover concrete, and replacement of the FRP laminate.

8.4—Repair of surface coating

In the event that the surface-protective coating should be replaced, the FRP laminate should be inspected for structural damage or deterioration. The surface coating may be replaced using a process approved by the system manufacturer.

CHAPTER 9—GENERAL DESIGN CONSIDERATIONS

General design recommendations are presented in this chapter. The recommendations presented are based on the traditional reinforced concrete design principles stated in the requirements of [ACI 318](#) and knowledge of the specific mechanical behavior of fiber-reinforced polymer (FRP) reinforcement.

FRP strengthening systems should be designed to resist tensile forces while maintaining strain compatibility between the FRP and the concrete substrate. FRP reinforcement should not be relied on to resist compressive forces. It is acceptable, however, for FRP tension reinforcement to experience compression due to moment reversals or changes in load pattern. The compressive strength of the FRP reinforcement, however, should be neglected.

9.1—Design philosophy

These design recommendations are based on limit-states-design principles. This approach sets acceptable levels of safety for the occurrence of both serviceability limit states (excessive deflections and cracking) and ultimate limit states (failure, stress rupture, and fatigue). In assessing the nominal strength of a member, the possible failure modes and subsequent strains and stresses in each material should be assessed. For evaluating the serviceability of a member, engineering principles, such as transformed section calculations using modular ratios, can be used.

FRP strengthening systems should be designed in accordance with [ACI 318](#) strength and serviceability requirements using the strength and load factors stated in [ACI 318](#). Additional reduction factors applied to the contribution of the FRP reinforcement are recommended by this guide to reflect

uncertainties inherent in FRP systems different from steel-reinforced and prestressed concrete. These reduction factors were determined based on statistical evaluation of variability in mechanical properties, predicted versus full-scale test results, and field applications. FRP-related reduction factors were calibrated to produce reliability indexes typically above 3.5. Reliability indexes between 3.0 and 3.5 can be encountered in cases where relatively low ratios of steel reinforcement combined with high ratios of FRP reinforcement are used. Such cases are less likely to be encountered in design because they violate the recommended strengthening limits of 9.2. Reliability indexes for FRP-strengthened members are determined based on the approach used for reinforced concrete buildings ([Nowak and Szerszen 2003](#); [Szerszen and Nowak 2003](#)). In general, lower reliability is expected in retrofitted and repaired structures than in new structures.

9.2—Strengthening limits

Careful consideration should be given to determine reasonable strengthening limits. These limits are imposed to guard against collapse of the structure should bond or other failure of the FRP system occur due to damage, vandalism, or other causes. The unstrengthened structural member, without FRP reinforcement, should have sufficient strength to resist a certain level of load. The existing strength of the structure should be sufficient to resist a level of load as described by Eq. (9.2)

$$(\phi R_n)_{existing} \geq (1.1S_{DL} + 0.75S_{LL})_{new} \quad (9.2)$$

A dead load factor of 1.1 is used because a relatively accurate assessment of the dead loads of the structure can be determined. A live load factor of 0.75 is used to exceed the statistical mean of the yearly maximum live load factor of 0.5, as given in [ASCE 7](#). The strengthening limit resulting from compliance with Eq. (9.2) will allow the strengthened member to maintain sufficient structural capacity until the damaged FRP is repaired.

In cases where the design live load acting on the member to be strengthened has a high likelihood of being present for a sustained period of time, a live load factor of 1.0 should be used instead of 0.75 in Eq. (9.2). Examples include library stack areas, heavy storage areas, warehouses, and other occupancies with a live load exceeding 150 lb/ft² (730 kg/m²). More specific limits for structures requiring a fire resistance rating are given in 9.2.1.

9.2.1 Structural fire resistance—The level of strengthening that can be achieved through the use of externally bonded FRP reinforcement can be limited by the code-required fire-resistance rating of a structure. The polymer resins typically used in wet layup and prepreg FRP systems and the polymer adhesives used in precured FRP systems suffer deterioration of mechanical and bond properties at temperatures close to or exceeding the T_g of the polymer, as described in [1.2.1.3](#).

Although the FRP system itself is significantly affected by exposure to elevated temperature, a combination of the FRP system with an existing concrete structure may still have an adequate fire resistance. When considering the fire resistance of an FRP-strengthened concrete element, it is important to

recognize that the strength of a reinforced concrete element is reduced during fire exposure due to heating of both the reinforcing steel and the concrete. Performance in fire of the existing concrete member can be enhanced by installing an insulation system, which will provide thermal protection to existing concrete and internal reinforcing steel, thus improving the overall fire rating, although the FRP system contribution may be reduced (Bisby et al. 2005a; Williams et al. 2006; Palmieri et al. 2011; Firmo et al. 2012).

By extending the methods in ACI 216.1 to FRP-strengthened reinforced concrete, limits on strengthening can be used to ensure a strengthened structure will not collapse in a fire event. A member's resistance to load effects, with reduced steel and concrete strengths and without the contribution of the FRP reinforcement, can be compared with the load demand on the member during the fire event to ensure the strengthened member can support these loads for the required fire duration (or fire rating time) without failure

$$R_{n0} \geq 1.0S_{DL} + 1.0S_{LL} \quad (9.2.1a)$$

Alternately, ACI 562 specifies the following

$$R_{n0} \geq 1.2S_{DL} + 0.5S_{LL} + 0.2S_{SL} + 1.0A_k \quad (9.2.1b)$$

where R_{n0} is the nominal resistance of the member at an elevated temperature, and S_{DL} , S_{LL} , and S_{SL} are the specified dead, live, and snow loads, respectively, calculated for the strengthened structure. For cases where the design live load has a high likelihood of being present for a sustained period of time, a live load factor of 1.0 should be used in place of 0.5 in Eq. (9.2.1b). Due to the lack of guidance for the calculation of A_k , the load or load effect resulting from the fire event, use of Eq. (9.2.1a) is recommended.

If the FRP system is meant to allow greater load-carrying capacity, such as an increase in live load, the load effects should be computed using these greater loads. If the FRP system is meant to address a loss in strength, such as deterioration, the resistance should reflect this loss.

The nominal resistance of the member at an elevated temperature R_{n0} may be determined using the procedure outlined in ACI 216.1 or through testing. The nominal resistance R_{n0} should be calculated based on the reduced material properties of the existing member. The resistance should be computed for the time required by the member's fire-resistance rating—for example, a 2-hour fire rating—and should not account for the contribution of the FRP system unless the continued effectiveness of the FRP can be proven through testing. More research is needed to accurately identify temperatures at which effectiveness is lost for different types of FRP. Until better information on the properties of FRP at high temperature is available, the critical temperature can be taken as the lowest T_g of the components of the system comprising the load path.

9.2.2 Overall structural strength—While FRP systems are effective in strengthening members for flexure and shear and providing additional confinement, other modes of failure, such as punching shear and bearing capacity of footings,

may be only marginally affected by FRP systems (Sharaf et al. 2006). All members of a structure should be capable of withstanding the anticipated increase in loads associated with the strengthened members.

Additionally, analysis should be performed on the member strengthened by the FRP system to check that, under overload conditions, the strengthened member will fail in a flexural mode rather than in a shear mode.

9.2.3 Seismic applications—Requirements for seismic strengthening using FRP are addressed in Chapter 13.

9.3—Selection of FRP systems

9.3.1 Environmental considerations—Environmental conditions uniquely affect resins and fibers of various FRP systems. The mechanical properties (for example, tensile strength, ultimate tensile strain, and elastic modulus) of some FRP systems degrade under exposure to certain environments such as alkalinity, salt water, chemicals, ultraviolet light, high temperatures, high humidity, and freezing-and-thawing cycles. The material properties used in design should account for this degradation in accordance with 9.4.

The licensed design professional should select an FRP system based on the known behavior of that system in the anticipated service conditions. Some important environmental considerations that relate to the nature of specific systems are given as follows. Specific information can be obtained from the FRP system manufacturer.

a) *Alkalinity/acidity*—The performance of an FRP system over time in an alkaline or acidic environment depends on the matrix material and the reinforcing fiber. Dry, unsaturated bare, or unprotected carbon fiber is resistant to both alkaline and acidic environments whereas bare glass fiber can degrade over time in these environments. A properly selected and applied resin matrix, however, should isolate and protect the fiber from the alkaline/acidic environment and resist deterioration. Sites with high alkalinity and high moisture or relative humidity favor the selection of carbon-fiber systems over glass-fiber systems.

b) *Thermal expansion*—FRP systems may have thermal expansion properties that are different from those of concrete. In addition, the thermal expansion properties of the fiber and polymer constituents of an FRP system can vary. Carbon fibers have a coefficient of thermal expansion near zero whereas glass fibers have a coefficient of thermal expansion similar to concrete. The polymers used in FRP strengthening systems typically have coefficients of thermal expansion roughly five times that of concrete. Calculation of thermally-induced strain differentials are complicated by variations in fiber orientation, fiber volume fraction, and thickness of adhesive layers. Experience indicates, however, that thermal expansion differences do not affect bond for small ranges of temperature change, such as $\pm 50^\circ\text{F}$ ($\pm 28^\circ\text{C}$) (Motavalli et al. 1997; Soudki and Green 1997; Green et al. 1998).

c) *Electrical conductivity*—Glass FRP (GFRP) and aramid FRP (AFRP) are effective electrical insulators, whereas carbon FRP (CFRP) is conductive. To avoid potential galvanic corrosion of steel elements, carbon-based FRP materials should not come in direct contact with steel.

9.3.2 Loading considerations—Loading conditions uniquely affect different fibers of FRP systems. The licensed design professional should select an FRP system based on the known behavior of that system in the anticipated service conditions. Some important loading considerations that relate to the nature of the specific systems are given in the following. Specific information should be obtained from material manufacturers.

a) *Impact tolerance*—AFRP and GFRP systems demonstrate better tolerance to impact than CFRP systems.

b) *Creep rupture and fatigue*—CFRP systems are highly resistive to creep rupture under sustained loading and fatigue failure under cyclic loading. GFRP systems are more sensitive to both loading conditions.

9.3.3 Durability considerations—Durability of FRP systems is the subject of considerable ongoing research (Dolan et al. 2008; Karbhari 2007). The licensed design professional should select an FRP system that has undergone durability testing consistent with the application environment. Durability testing may include hot-wet cycling, alkaline immersion, freezing-and-thawing cycling, ultraviolet exposure, dry heat, and salt water (Cromwell et al. 2011).

Any FRP system that completely encases or covers a concrete section should be investigated for the effects of a variety of environmental conditions including those of freezing and thawing, steel corrosion, alkali and silica aggregate reactions, water entrapment, vapor pressures, and moisture vapor transmission (Masoud and Soudki 2006; Soudki and Green 1997; Porter et al. 1997; Christensen et al. 1996; Toutanji 1999). Many FRP systems create a moisture-impermeable layer on the surface of the concrete. In areas where moisture vapor transmission is expected, adequate means should be provided to allow moisture to escape from the concrete structure.

9.3.4 Protective-coating selection considerations—A coating or insulation system can be applied to the installed FRP system to protect it from exposure to certain environmental conditions (Bisby et al. 2005a; Williams et al. 2006). The thickness and type of coating should be selected based on the requirements of the composite repair; resistance to environmental effects such as moisture, salt water, temperature extremes, fire, impact, and ultraviolet exposure; resistance to site-specific effects; and resistance to vandalism. Coatings are relied on to retard the degradation of the mechanical properties of the FRP systems. The coatings should be periodically inspected and maintained to ensure continued effectiveness.

External coatings or thickened coats of resin over fibers can protect them from damage due to impact or abrasion. In high-impact or traffic areas, additional levels of protection may be necessary. Portland cement plaster and polymer coatings are commonly used for protection where minor impact or abrasion is anticipated.

9.4—Design material properties

Unless otherwise stated, the material properties reported by manufacturers, such as the ultimate tensile strength, typically do not consider long-term exposure to environmental conditions and should be considered as initial properties.

Because long-term exposure to various types of environments can reduce the tensile properties and creep-rupture and fatigue endurance of FRP laminates, the material properties used in design equations should be reduced based on the environmental exposure condition.

Equations (9.4a) through (9.4c) give the tensile properties that should be used in all design equations. The design ultimate tensile strength should be determined using the environmental reduction factor given in Table 9.4 for the appropriate fiber type and exposure condition

$$f_{fu} = C_E f_{fu}^* \tag{9.4a}$$

Similarly, the design rupture strain should also be reduced for environmental exposure conditions

$$\epsilon_{fu} = C_E \epsilon_{fu}^* \tag{9.4b}$$

Because FRP materials are linear elastic until failure, the design modulus of elasticity for unidirectional FRP can be determined from Hooke’s law. The expression for the modulus of elasticity, given in Eq. (9.4c), recognizes that the modulus is typically unaffected by environmental conditions. The modulus given in this equation will be the same as the initial value reported by the manufacturer

$$E_f = f_{fu} / \epsilon_{fu} \tag{9.4c}$$

The constituent materials, fibers, and resins of an FRP system affect its durability and resistance to environmental exposure. The environmental reduction factors given in Table 9.4 are conservative estimates based on the relative durability of each fiber type.

As Table 9.4 illustrates, if the FRP system is located in a relatively benign environment, such as indoors, the reduction factor is closer to unity. If the FRP system is located in an aggressive environment where prolonged exposure to high humidity, freezing-and-thawing cycles, salt water, or alkalinity is expected, a lower reduction factor should be used. The reduction factor can be modified to reflect the use of a protective coating if the coating has been shown through testing to lessen the effects of environmental exposure and the coating is maintained for the life of the FRP system.

Table 9.4—Environmental reduction factor for various FRP systems and exposure conditions

Exposure conditions	Fiber type	Environmental reduction factor C_E
Interior exposure	Carbon	0.95
	Glass	0.75
	Aramid	0.85
Exterior exposure (bridges, piers, and unenclosed parking garages)	Carbon	0.85
	Glass	0.65
	Aramid	0.75
Aggressive environment (chemical plants and wastewater treatment plants)	Carbon	0.85
	Glass	0.50
	Aramid	0.70

CHAPTER 10—FLEXURAL STRENGTHENING

Bonding fiber-reinforced polymer (FRP) reinforcement to the tension face of a concrete flexural member with fibers oriented along the length of the member will provide an increase in flexural strength. Increases in overall flexural strength from 10 to 160 percent have been documented (Meier and Kaiser 1991; Ritchie et al. 1991; Sharif et al. 1994). When taking into account the strengthening limits of 9.2 and ductility and serviceability limits, however, strength increases of up to 40 percent are more reasonable.

This chapter does not apply to FRP systems used to enhance the flexural strength of members in the expected plastic hinge regions of ductile moment frames resisting seismic loads; these are addressed in Chapter 13.

10.1—Nominal strength

The strength design approach requires that the design flexural strength of a member exceed its required factored moment, as indicated by Eq. (10.1). The design flexural strength ϕM_n refers to the nominal strength of the member multiplied by a strength reduction factor, and the factored moment M_u refers to the moment calculated from factored loads (for example, $\alpha_{DL}M_{DL} + \alpha_{LL}M_{LL} + \dots$)

$$\phi M_n \geq M_u \quad (10.1)$$

This guide recommends that the factored moment M_u of a section be calculated by use of load factors as required by ACI 318. An additional strength reduction factor for FRP, ψ_f , should be applied to the flexural contribution of the FRP reinforcement alone, M_{nf} , as described in 10.2.10. The additional strength reduction factor, ψ_f , is used to improve the reliability of strength prediction and accounts for the different failure modes observed for FRP-strengthened members (delamination of FRP reinforcement).

The nominal flexural strength of FRP-strengthened concrete members with mild steel reinforcement and with bonded prestressing steel can be determined based on strain compatibility, internal force equilibrium, and the controlling mode of failure. For members with unbonded prestressed steel, strain compatibility does not apply and the stress in the unbonded tendons at failure depends on the overall deformation of the member and is assumed to be approximately the same at all sections.

10.1.1 Failure modes—The flexural strength of a section depends on the controlling failure mode. The following flexural failure modes should be investigated for an FRP-strengthened section (GangaRao and Vijay 1998):

- Crushing of the concrete in compression before yielding of the reinforcing steel
- Yielding of the steel in tension followed by rupture of the FRP laminate
- Yielding of the steel in tension followed by concrete crushing
- Shear/tension delamination of the concrete cover (cover delamination)
- Debonding of the FRP from the concrete substrate (FRP debonding)

Concrete crushing is assumed to occur if the compressive strain in the concrete reaches its maximum usable strain ($\epsilon_c = \epsilon_{cu} = 0.003$). Rupture of the externally bonded FRP is assumed to occur if the strain in the FRP reaches its design rupture strain ($\epsilon_f = \epsilon_{fu}$) before the concrete reaches its maximum usable strain.

Cover delamination or FRP debonding can occur if the force in the FRP cannot be sustained by the substrate (Fig. 10.1.1a). Such behavior is generally referred to as debonding, regardless of where the failure plane propagates within the FRP-adhesive-substrate region. Guidance to avoid the cover delamination failure mode is given in Chapter 13.

Away from the section where externally bonded FRP terminates, a failure controlled by FRP debonding may govern (Fig. 10.1.1a(b)). To prevent such an intermediate crack-induced debonding failure mode, the effective strain in FRP reinforcement should be limited to the strain at which debonding may occur, ϵ_{fd} , as defined in Eq. (10.1.1)

$$\begin{aligned} \epsilon_{fd} &= 0.083 \sqrt{\frac{f'_c}{nE_f t_f}} \leq 0.9\epsilon_{fu} \quad (\text{in.-lb}) \\ \epsilon_{fd} &= 0.41 \sqrt{\frac{f'_c}{nE_f t_f}} \leq 0.9\epsilon_{fu} \quad (\text{SI}) \end{aligned} \quad (10.1.1)$$

Equation (10.1.1) takes a modified form of the debonding strain equation proposed by Teng et al. (2003, 2004) that was based on committee evaluation of a significant database for flexural beam tests exhibiting FRP debonding failure. The proposed equation was calibrated using average measured values of FRP strains at debonding for flexural tests experiencing intermediate crack-induced debonding to determine the best-fit coefficient of 0.083 (0.41 in SI). Reliability of the FRP contribution to flexural strength is addressed by incorporating an additional strength reduction factor for FRP, ψ_f , in addition to the strength reduction factor ϕ per ACI 318 for structural concrete. Anchorage systems such as U-wraps, mechanical fasteners, fiber anchors, and U-anchors (examples are shown schematically in Fig. 10.1.1b) have been proven successful at delaying, and sometimes preventing, debonding failure of the longitudinal FRP (Kalfat et al. 2013; Grelle and Sneed 2013). Experimental studies have shown that these anchorage systems can increase the effective strain in the flexural FRP to values up to tensile rupture (Lee et al. 2010; Orton et al. 2008).

For near-surface-mounted (NSM) FRP applications, the value of ϵ_{fd} may vary from $0.6\epsilon_{fu}$ to $0.9\epsilon_{fu}$, depending on many factors such as member dimensions, steel and FRP reinforcement ratios, and surface roughness of the FRP bar. Based on analysis of a database of existing studies (Bianco et al. 2014), the committee recommends the use of $\epsilon_{fd} = 0.7\epsilon_{fu}$. To achieve the debonding design strain of NSM FRP bars, ϵ_{fd} , the bonded length should be greater than the development length given in Chapter 13.

10.2—Reinforced concrete members

This section presents guidance on the calculation of the flexural strengthening effect of adding longitudinal FRP

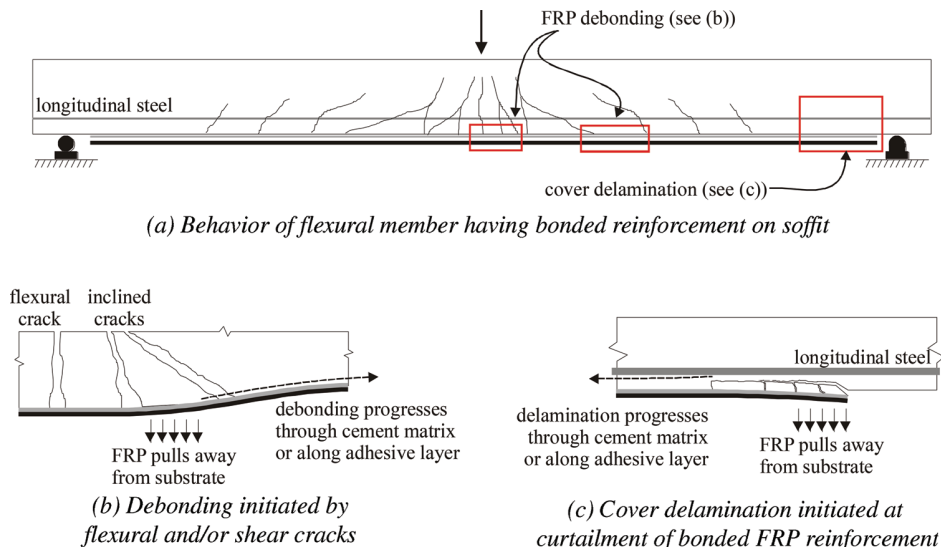


Fig. 10.1.1a—Debonding and delamination of externally bonded FRP systems.

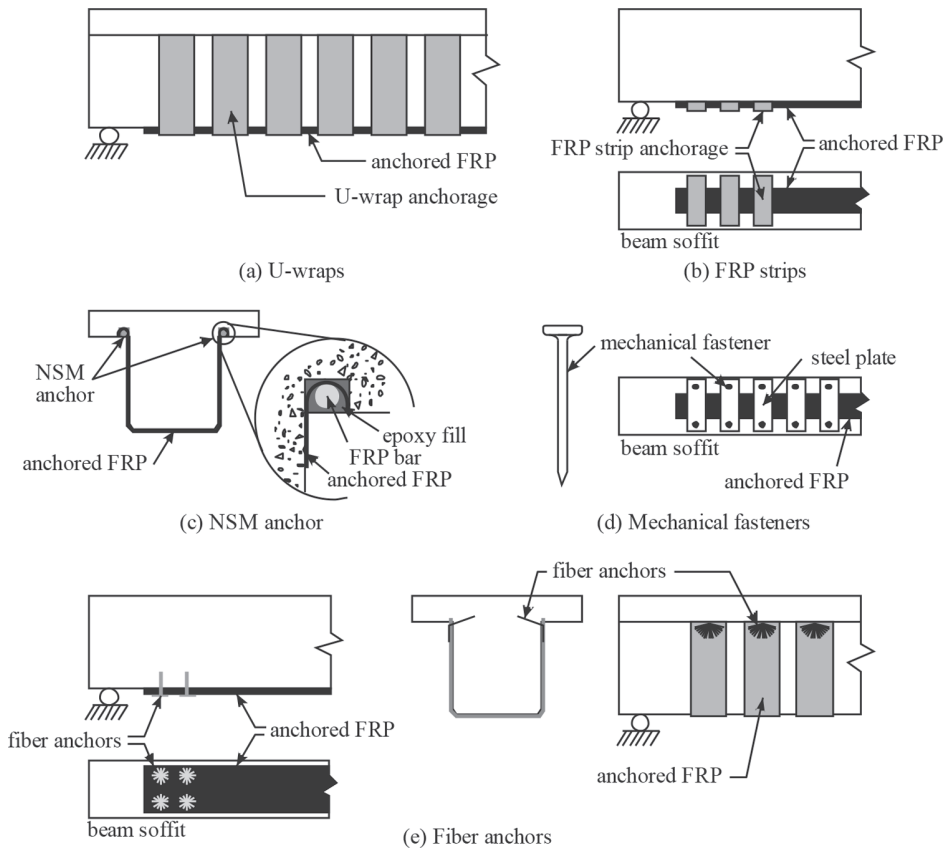


Fig. 10.1.1b—FRP anchorage systems.

reinforcement to the tension face of a reinforced concrete member. A specific illustration of the concepts in this section applied to strengthening of existing rectangular sections reinforced in the tension zone with nonprestressed steel is given. The general concepts outlined herein can, however, be extended to nonrectangular shapes (T-sections and I-sections) and to members with steel compression reinforcement.

10.2.1 Assumptions—The following assumptions are made in calculating the flexural resistance of a section strengthened with an externally applied FRP system:

- a) Design calculations are based on the dimensions, internal reinforcing steel arrangement, and material properties of the existing member being strengthened.
- b) The strains in the steel reinforcement and concrete are directly proportional to their distance from the neutral axis.

That is, a plane section before loading remains plane after loading.

c) There is no relative slip between external FRP reinforcement and the concrete.

d) The shear deformation within the adhesive layer is neglected because the adhesive layer is very thin with only slight variations in its thickness.

e) The maximum usable compressive strain in the concrete is 0.003.

f) The tensile strength of concrete is neglected.

g) The FRP reinforcement has a linear elastic stress-strain relationship to failure.

While some of these assumptions are necessary for the sake of computational ease, the assumptions do not accurately reflect the true fundamental behavior of FRP flexural reinforcement. For example, there will be shear deformation in the adhesive layer, causing relative slip between the FRP and the substrate. The inaccuracy of the assumptions will not, however, significantly affect the computed flexural strength of an FRP-strengthened member. An additional strength reduction factor (presented in 10.2.10) will conservatively compensate for any such discrepancies.

10.2.2 Shear strength—When FRP reinforcement is being used to increase the flexural strength of a member, the member should be capable of resisting the shear forces associated with the increased flexural strength. The potential for shear failure of the section should be considered by comparing the design shear strength of the section to the required shear strength. If additional shear strength is required, FRP laminates oriented transverse to the beam longitudinal axis can be used to resist shear forces, as described in Chapter 11.

10.2.3 Existing substrate strain—Unless all loads on a member, including self-weight and any prestressing forces, are removed before installation of FRP reinforcement, the substrate to which the FRP is applied will be strained. These strains should be considered initial strains and should be excluded from the strain in the FRP (Arduini and Nanni 1997; Nanni and Gold 1998). The initial strain on the bonded substrate, ϵ_{bi} , can be determined from an elastic analysis of the existing member, considering all loads that will be on the member during the installation of the FRP system. The elastic analysis of the existing member should be based on cracked section properties.

10.2.4 Flexural strengthening of concave soffits—The presence of curvature in the soffit of a concrete member may lead to the development of tensile stresses normal to the adhesive and surface to which the FRP is bonded. Such tensile stresses result when the FRP tends to straighten under load, and can promote the initiation of FRP debonding or interlaminar failures that reduce the effectiveness of the FRP flexural strengthening (Aiello et al. 2001; Eshwar et al. 2003). If the extent of the curved portion of the soffit exceeds a length of 40 in. (1.0 m) with a rise of 0.2 in. (5 mm), the surface should be made flat before strengthening. Alternately, anchorage systems such as U-wraps, mechanical fasteners, fiber anchors, or NSM anchors should be installed to mitigate delamination (Eshwar et al. 2005).

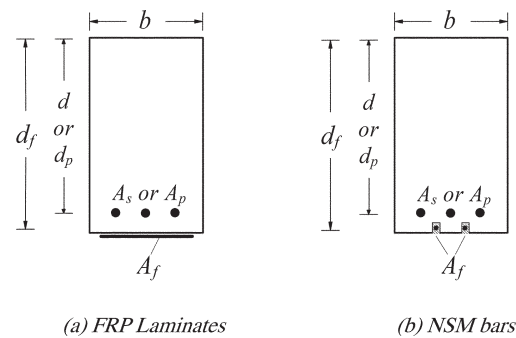


Fig. 10.2.5—Effective depth of FRP systems.

10.2.5 Strain in FRP reinforcement—It is important to determine the strain in the FRP reinforcement at the ultimate limit state. Because FRP materials are linear elastic until failure, the strain in the FRP will dictate the stress developed in the FRP. The maximum strain that can be achieved in the FRP reinforcement will be governed by either the strain developed in the FRP at the point at which concrete crushes, the point at which the FRP ruptures, or the point at which the FRP debonds from the substrate. The effective strain in the FRP reinforcement at the ultimate limit state can be found from Eq. (10.2.5)

$$\epsilon_{fe} = \epsilon_{cu} \left(\frac{d_f - c}{c} \right) - \epsilon_{bi} \leq \epsilon_{jd} \quad (10.2.5)$$

where ϵ_{bi} is the initial substrate strain as described in 10.2.3, and d_f is the effective depth of FRP reinforcement, as indicated in Fig. 10.2.5.

10.2.6 Stress in the FRP reinforcement—The effective stress in the FRP reinforcement is the maximum level of stress that can be developed in the FRP reinforcement before flexural failure of the section. This effective stress can be found from the strain in the FRP, assuming perfectly elastic behavior

$$f_{fe} = E_f \epsilon_{fe} \quad (10.2.6)$$

10.2.7 Strength reduction factor—The use of externally bonded FRP reinforcement for flexural strengthening will reduce the ductility of the original member. In some cases, the loss of ductility is negligible. Sections that experience a significant loss in ductility, however, should be addressed. To maintain a sufficient degree of ductility, the strain in the steel at the ultimate limit state should be checked. For reinforced concrete members with nonprestressed steel reinforcement, adequate ductility is achieved if the strain in the steel at the point of concrete crushing or failure of the FRP, including delamination or debonding, is at least 0.005, according to the definition of a tension-controlled section as given in ACI 318.

The approach taken by this guide follows the philosophy of ACI 318. A strength reduction factor given by Eq. (10.2.7) should be used, where ϵ_t is the net tensile strain in extreme tension steel at nominal strength, as defined in ACI 318.

$$\phi = \begin{cases} 0.90 & \text{for } \epsilon_t \geq 0.005 \\ 0.65 + \frac{0.25(\epsilon_t - \epsilon_{sy})}{0.005 - \epsilon_{sy}} & \text{for } \epsilon_{sy} < \epsilon_t < 0.005 \\ 0.65 & \text{for } \epsilon_t \leq \epsilon_{sy} \end{cases} \quad (10.2.7)$$

This equation sets the reduction factor at 0.90 for ductile sections and 0.65 for brittle sections where the steel does not yield, and provides a linear transition for the reduction factor between these two extremes. The use of Eq. (10.2.7) is limited to steel having a yield strength f_y less than 80 ksi (550 MPa) (ACI 318).

10.2.8 Serviceability—The serviceability of a member (deflections and crack widths) under service loads should satisfy applicable provisions of ACI 318. The effect of the FRP external reinforcement on the serviceability can be assessed using the transformed-section analysis.

To avoid inelastic deformations of reinforced concrete members with nonprestressed steel reinforcement strengthened with external FRP reinforcement, the existing internal steel reinforcement should be prevented from yielding under service load levels, especially for members subjected to cyclic loads (El-Tawil et al. 2001). The stress in the steel reinforcement under service load should be limited to 80 percent of the yield strength, as shown in Eq. (10.2.8a). In addition, the compressive stress in concrete under service load should be limited to 60 percent of the compressive strength, as shown in Eq. (10.2.8b)

$$f_{s,s} \leq 0.80f_y \quad (10.2.8a)$$

$$f_{c,s} \leq 0.60f'_c \quad (10.2.8b)$$

10.2.9 Creep rupture and fatigue stress limits—To avoid creep rupture of the FRP reinforcement under sustained stresses or failure due to cyclic stresses and fatigue of the FRP reinforcement, the stress in the FRP reinforcement under these stress conditions should be checked. Because this stress will be within the elastic response range of the member, the stresses can be computed by elastic analysis using cracked section properties as appropriate.

In 4.4, the creep rupture phenomenon and fatigue characteristics of FRP material were described and the resistance to its effects by various types of fibers was examined. As stated in 4.4.1, research has indicated that glass, aramid, and carbon fibers can sustain approximately 0.3, 0.5, and 0.9 times their ultimate strengths, respectively, before encountering a creep rupture problem (Yamaguchi et al. 1997; Malvar 1998). To avoid failure of an FRP-reinforced member due to creep rupture and fatigue of the FRP, stress limits for these conditions should be imposed on the FRP reinforcement. The stress in the FRP reinforcement can be computed using elastic analysis and an applied moment due to all sustained loads (dead loads and the sustained portion of the live load) plus the maximum moment induced in a fatigue loading cycle (Fig. 10.2.9). The sustained stress should be limited as expressed by Eq. (10.2.9) to maintain safety. Values for safe

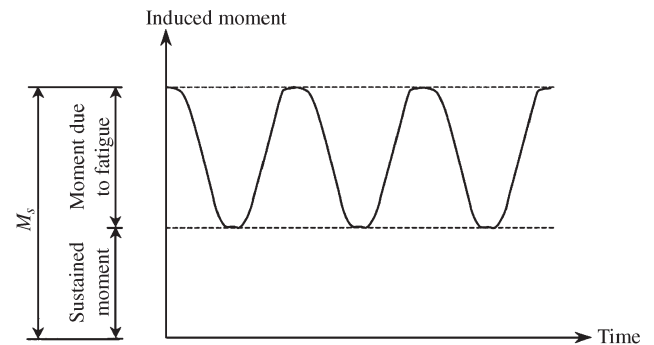


Fig. 10.2.9—Illustration of the level of applied moment to be used to check the stress limits in the FRP reinforcement.

sustained plus cyclic stress are given in Table 10.2.9. These values are based approximately on the stress limits previously stated in 4.4.1 with an imposed safety factor of 1/0.6

$$f_{f,s} \leq \text{sustained plus cyclic stress limit} \quad (10.2.9)$$

Table 10.2.9—Sustained plus cyclic service load stress limits in FRP reinforcement

Stress type	Fiber type		
	GFRP	AFRP	CFRP
Sustained plus cyclic stress limit	0.20 f_{fu}	0.30 f_{fu}	0.55 f_{fu}

10.2.10 Ultimate strength of singly reinforced rectangular section—To illustrate the concepts presented in this chapter, this section describes the application of these concepts to a nonprestressed singly-reinforced rectangular section. Figure 10.2.10 illustrates the internal strain and stress distribution for a rectangular section under flexure at the ultimate limit state.

The calculation procedure used to arrive at the ultimate strength should satisfy strain compatibility and force equilibrium, and should consider the governing mode of failure. Several calculation procedures can be derived to satisfy these conditions. The calculation procedure described herein illustrates an iterative method that involves selecting an assumed depth to the neutral axis, c , calculating the strain in each material using strain compatibility; calculating the associated stress in each material; and checking internal force equilibrium. If the internal force resultants do not equilibrate, the depth to the neutral axis should be revised and the procedure repeated.

For any assumed depth to the neutral axis, c , the strain in the FRP reinforcement can be computed from Eq. (10.2.5). This equation considers the governing mode of failure for the assumed neutral axis depth. If the left term of the inequality controls, concrete crushing controls flexural failure of the section. If the right term of the inequality controls, FRP failure (rupture or debonding) controls flexural failure of the section.

The effective stress in the FRP reinforcement can be found from the strain in the FRP, assuming perfectly elastic behavior using Eq. (10.2.6). Based on the strain in the FRP reinforcement, the strain in the nonprestressed steel rein-

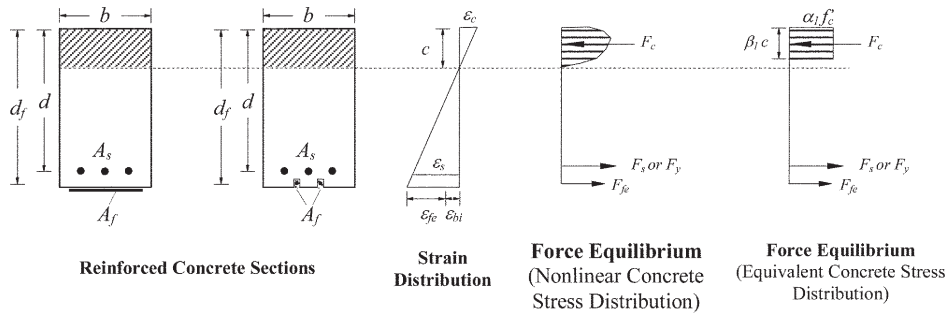


Fig. 10.2.10—Internal strain and stress distribution for a rectangular section under flexure at ultimate limit state.

forcement can be found from Eq. (10.2.10a) using strain compatibility

$$\epsilon_s = (\epsilon_{fe} + \epsilon_{bi}) \left(\frac{d-c}{d_f - c} \right) \quad (10.2.10a)$$

The stress in the steel is determined from the strain in the steel using its assumed elastic-perfectly plastic stress-strain curve

$$f_s = E_s \epsilon_s \leq f_y \quad (10.2.10b)$$

With the stress in the FRP and steel reinforcement determined for the assumed neutral axis depth, internal force equilibrium may be checked using Eq. (10.2.10c)

$$\alpha_1 f_c' \beta_1 b c = A_s f_s + A_f f_{fe} \quad (10.2.10c)$$

The terms α_1 and β_1 in Eq. (10.2.10c) are parameters defining a rectangular stress block in the concrete equivalent to the nonlinear distribution of stress. If concrete crushing is the controlling mode of failure (before or after steel yielding), α_1 and β_1 can be taken as the values associated with the Whitney stress block (ACI 318); that is, $\alpha_1 = 0.85$ and $\beta_1 = 0.85$ for f_c' between 2500 and 4000 psi (17 and 27 MPa), and β_1 is reduced linearly at a rate of 0.05 for each 1000 psi (7 MPa) of concrete strength exceeding 4000 psi (27 MPa). Note that β_1 shall not be taken less than 0.65. If FRP rupture, cover delamination, or FRP debonding occur, the Whitney stress block will give reasonably accurate results. A nonlinear stress distribution in the concrete or a more accurate stress block appropriate for the strain level reached in the concrete at the ultimate-limit state may be used.

The depth to the neutral axis, c , is found by simultaneously satisfying Eq. (10.2.5), (10.2.6), (10.2.10a), (10.2.10b), and (10.2.10c), thus establishing internal force equilibrium and strain compatibility. To solve for the depth of the neutral axis, c , an iterative solution procedure can be used. An initial value for c is first assumed and the strains and stresses are calculated using Eq. (10.2.5), (10.2.6), (10.2.10a), and (10.2.10b). A revised value for the depth of neutral axis, c , is then calculated from Eq. (10.2.10c). The calculated and assumed values for c are then compared. If they agree, then the proper value of c is reached. If the calculated and

assumed values do not agree, another value for c is selected, and the process is repeated until convergence is attained.

The nominal flexural strength of the section with FRP external reinforcement is computed from Eq. (10.2.10d). An additional reduction factor for FRP, ψ_f , is applied to the flexural-strength contribution of the FRP reinforcement. The recommended value of ψ_f is 0.85. This reduction factor for the strength contribution of FRP reinforcement is based on the reliability analysis discussed in 9.1, which was based on the experimentally calibrated statistical properties of the flexural strength (Okeil et al. 2007)

$$M_n = A_s f_s \left(d - \frac{\beta_1 c}{2} \right) + \psi_f A_f f_{fe} \left(d_f - \frac{\beta_1 c}{2} \right) \quad (10.2.10d)$$

10.2.10.1 Stress in steel under service loads—The stress in the steel reinforcement can be calculated based on a cracked-section analysis of the FRP-strengthened reinforced concrete section, as indicated by Eq. (10.2.10.1)

$$f_{s,s} = \frac{\left[M_s + \epsilon_{bi} A_f E_f \left(d_f - \frac{kd}{3} \right) \right] (d - kd) E_s}{\left[A_s E_s \left(d - \frac{kd}{3} \right) (d - kd) \right] + \left[A_f E_f \left(d_f - \frac{kd}{3} \right) (d_f - kd) \right]} \quad (10.2.10.1)$$

The distribution of strain and stress in the reinforced concrete section is shown in Fig. 10.2.10.1. Similar to conventional reinforced concrete, the depth to the neutral axis at service, kd , can be computed by taking the first moment of the areas of the transformed section. The transformed area of the FRP may be obtained by multiplying the area of FRP by the modular ratio of FRP to concrete. Although this method ignores the difference in the initial strain of the FRP, the initial strain does not greatly influence the depth to the neutral axis in the elastic response range of the member.

The stress in the steel under service loads computed from Eq. (10.2.10.1) should be compared against the limits described in 10.2.8. The value of M_s from Eq. (10.2.10.1) is equal to the moment due to all sustained loads (dead loads

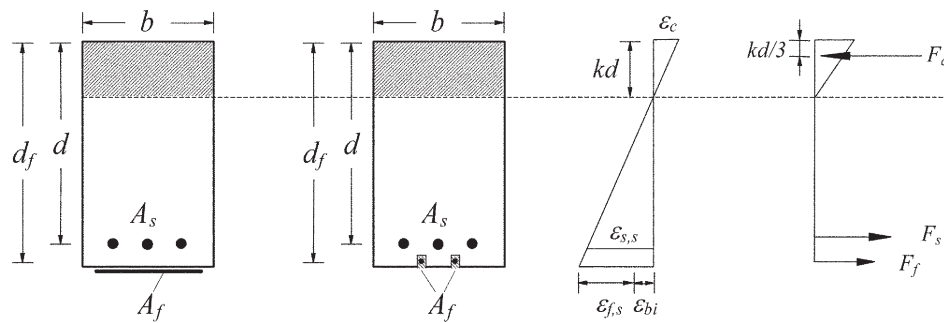


Fig. 10.2.10.1—Elastic strain and stress distribution.

and the sustained portion of the live load) plus the maximum moment induced in a fatigue loading cycle, as shown in Fig. 10.2.9.

10.2.10.2 Stress in FRP under service loads—The stress in the FRP reinforcement can be computed using Eq. (10.2.10.2) with $f_{s,s}$ from Eq. (10.2.10.1). Equation (10.2.10.2) gives the stress in the FRP reinforcement under an applied moment within the elastic response range of the member

$$f_{f,s} = f_{s,s} \left(\frac{E_f}{E_s} \right) \frac{d_f - kd}{d - kd} - \epsilon_{bi} E_f \quad (10.2.10.2)$$

The stress in the FRP under service loads computed from Eq. (10.2.10.2) should be compared against the limits described in 10.2.9.

10.3—Prestressed concrete members

This section presents guidance on the effect of adding longitudinal FRP reinforcement to the tension face of a rectangular prestressed concrete member. The general concepts outlined herein can be extended to nonrectangular shapes (T-sections and I-sections) and to members with tension, compression, or both, nonprestressed steel reinforcement.

10.3.1 Members with bonded prestressing steel

10.3.1.1 Assumptions—In addition to the basic assumptions for concrete and FRP behavior for a reinforced concrete section listed in 10.2.1, the following assumptions are made in calculating the flexural resistance of a prestressed section strengthened with an externally applied FRP system:

a) Strain compatibility can be used to determine strain in the externally bonded FRP, strain in the nonprestressed steel reinforcement, and the strain or strain change in the prestressing steel.

b) Additional flexural failure mode controlled by prestressing steel rupture should be investigated.

c) For cases where the prestressing steel is draped or harped, several sections along the span of the member should be evaluated to verify strength requirements.

d) The initial strain of the concrete substrate, ϵ_{bi} , should be calculated and excluded from the effective strain in the FRP. The initial strain can be determined from an elastic analysis of the existing member, considering all loads that will be applied to the member at the time of FRP installation. Analysis should

be based on the actual condition of the member (cracked or uncracked section) to determine the substrate initial strain.

10.3.1.2 Strain in FRP reinforcement—The maximum strain that can be achieved in the FRP reinforcement will be governed by strain limitations due to either concrete crushing, FRP rupture, FRP debonding, or prestressing steel rupture. The effective design strain for FRP reinforcement at the ultimate-limit state for failure controlled by concrete crushing can be calculated by the use of Eq. (10.2.5)

For failure controlled by prestressing steel rupture, Eq. (10.3.1.2a) can be used. For Grade 270 and 250 ksi (1860 and 1725 MPa) strand, the value of ϵ_{pu} to be used in Eq. (10.3.1.2a) is 0.035

$$\epsilon_{fe} = (\epsilon_{pu} - \epsilon_{pi}) \left(\frac{d_f - c}{d_p - c} \right) - \epsilon_{bi} \leq \epsilon_{fd} \quad (10.3.1.2a)$$

in which

$$\epsilon_{pi} = \frac{P_e}{A_p E_p} + \frac{P_e}{A_c E_c} \left(1 + \frac{e^2}{r^2} \right) \quad (10.3.1.2b)$$

10.3.1.3 Strength reduction factor—To maintain a sufficient degree of ductility, the strain in the prestressing steel at the nominal strength should be checked. Adequate ductility is achieved if the strain in the prestressing steel at the nominal strength is at least 0.013. Where this strain cannot be achieved, the strength reduction factor is decreased to account for a less ductile failure. The strength reduction factor for a member prestressed with standard 270 and 250 ksi (1860 and 1725 MPa) prestressing steel is given by Eq. (10.3.1.3), where ϵ_{ps} is the prestressing steel strain at the nominal strength

$$\phi = \begin{cases} 0.90 & \text{for } \epsilon_{ps} \geq 0.013 \\ 0.65 + \frac{0.25(\epsilon_{ps} - 0.010)}{0.013 - 0.010} & \text{for } 0.010 < \epsilon_{ps} < 0.013 \\ 0.65 & \text{for } \epsilon_{ps} \leq 0.010 \end{cases} \quad (10.3.1.3)$$

10.3.1.4 Serviceability—To avoid inelastic deformations of the strengthened member, the prestressing steel should

be prevented from yielding under service load levels. The stress in the steel under service load should be limited per Eq. (10.3.1.4a) and (10.3.1.4b). In addition, the compressive stress in the concrete under service load should be limited to 45 percent of the compressive strength

$$f_{ps,s} \leq 0.82f_{py} \quad (10.3.1.4a)$$

$$f_{ps,s} \leq 0.74f_{pu} \quad (10.3.1.4b)$$

When fatigue is a concern, the stress in the prestressing steel due to transient live loads should be limited to 18 ksi (125 MPa) when the radii of prestressing steel curvature exceeds 29 ft (9 m), or to 10 ksi (70 MPa) when the radii of prestressing-steel curvature does not exceed 12 ft (3.6 m). A linear interpolation should be used for radii between 12 and 29 ft (3.6 and 9 m) (AASHTO 2004). These limits have been verified experimentally for prestressed members with harped and straight strands strengthened with externally bonded FRP (Rosenboom and Rizkalla 2006).

10.3.1.5 Creep rupture and fatigue stress limits—To avoid creep rupture of the FRP reinforcement under sustained stresses or failure due to cyclic stresses and fatigue of the FRP reinforcement, the stress in the FRP reinforcement under these stress conditions should not exceed the limits provided in 10.2.9.

10.3.1.6 Nominal strength—The calculation procedure to compute nominal strength should satisfy strain compatibility and force equilibrium, and should consider the governing mode of failure. The calculation procedure described herein uses an iterative method similar to that discussed in 10.2.

For any assumed depth to the neutral axis, c , the effective strain and stress in the FRP reinforcement can be computed from Eq. (10.2.5) and (10.2.6), respectively. This equation considers the governing mode of failure for the assumed neutral axis depth. If the left term of the inequality in Eq. (10.2.5) controls, concrete crushing controls flexural failure of the section. If the right term of the inequality controls, FRP failure (rupture or debonding) controls flexural failure of the section.

The strain in the prestressed steel can be found from Eq. (10.3.1.6a) based on strain compatibility

$$\epsilon_{ps} = \epsilon_{pe} + \frac{P_e}{A_c E_c} \left(1 + \frac{e^2}{r^2} \right) + \epsilon_{pnet} \leq 0.035 \quad (10.3.1.6a)$$

in which ϵ_{pe} is the effective strain in the prestressing steel after losses, and ϵ_{pnet} is the net tensile strain in the prestressing steel beyond decompression, at the nominal strength. The value of ϵ_{pnet} will depend on the mode of failure, and can be calculated using Eq. (10.3.1.6b) and 10.3.1.6c)

$$\epsilon_{pnet} = 0.003 \left(\frac{d_p - c}{c} \right) \text{ for concrete crushing failure} \quad (10.3.1.6b)$$

$$\epsilon_{pnet} = (\epsilon_{fe} + \epsilon_{bi}) \left(\frac{d_p - c}{d_f - c} \right) \text{ for FRP rupture or debonding failure modes} \quad (10.3.1.6c)$$

The stress in the prestressing steel is calculated using the material properties of the steel. For a typical seven-wire low-relaxation prestressing strand, the stress-strain curve may be approximated by the following equations (Prestressed/Precast Concrete Institute 2004)

For Grade 250 ksi (1725 MPa) steel

$$f_{ps} = \begin{cases} 28,500\epsilon_{ps} & \text{for } \epsilon_{ps} \leq 0.0076 \\ 250 - \frac{0.04}{\epsilon_{ps} - 0.0064} & \text{for } \epsilon_{ps} > 0.0076 \end{cases} \text{ (in.-lb)} \quad (10.3.1.6d)$$

$$f_{ps} = \begin{cases} 196,500\epsilon_{ps} & \text{for } \epsilon_{ps} \leq 0.0076 \\ 1720 - \frac{0.276}{\epsilon_{ps} - 0.0064} & \text{for } \epsilon_{ps} > 0.0076 \end{cases} \text{ (SI)}$$

For Grade 270 ksi (1860 MPa) steel

$$f_{ps} = \begin{cases} 28,500\epsilon_{ps} & \text{for } \epsilon_{ps} \leq 0.0086 \\ 270 - \frac{0.04}{\epsilon_{ps} - 0.007} & \text{for } \epsilon_{ps} > 0.0086 \end{cases} \text{ (in.-lb)} \quad (10.3.1.6e)$$

$$f_{ps} = \begin{cases} 196,500\epsilon_{ps} & \text{for } \epsilon_{ps} \leq 0.0086 \\ 1860 - \frac{0.276}{\epsilon_{ps} - 0.007} & \text{for } \epsilon_{ps} > 0.0086 \end{cases} \text{ (SI)}$$

With the strain and stress in the FRP and prestressing steel determined for the assumed neutral axis depth, internal force equilibrium may be checked using Eq. (10.3.1.6f)

$$\alpha_1 f_c' \beta_1 b c = A_p f_p + A_f f_{fe} \quad (10.3.1.6f)$$

For the concrete crushing mode of failure, the equivalent compressive stress block factor α_1 can be taken as 0.85, and β_1 can be estimated as described in 10.2.10. If FRP rupture, cover delamination, or FRP debonding failure occurs, the use of equivalent rectangular concrete stress block factors is appropriate. Methods considering a nonlinear stress distribution in the concrete can also be used.

The depth to the neutral axis, c , is found by simultaneously satisfying Eq. (10.2.5), (10.2.6), and (10.3.1.6a) to (10.3.1.6f), thus establishing internal force equilibrium and strain compatibility. To solve for the depth of the neutral axis, c , an iterative solution procedure can be used. An initial

value for c is first assumed, and the strains and stresses are calculated using Eq. (10.2.5), (10.2.6), and (10.3.1.6a) to (10.3.1.6e). A revised value for the depth of neutral axis, c , is then calculated from Eq. (10.3.1.6f). The calculated and assumed values for c are then compared. If they agree, then the proper value of c is reached. If the calculated and assumed values do not agree, another value for c is selected, and the process is repeated until convergence is attained.

The nominal flexural strength of the section with FRP external reinforcement can be computed using Eq. (10.3.1.6g). The additional reduction factor $\psi_f = 0.85$ is applied to the flexural-strength contribution of the FRP reinforcement

$$M_n = A_p f_{ps} \left(d_p - \frac{\beta_1 c}{2} \right) + \psi_f A_f f_{fe} \left(d_f - \frac{\beta_1 c}{2} \right) \quad (10.3.1.6g)$$

10.3.1.7 Stress in prestressing steel under service loads—

The stress in the prestressing steel can be calculated based on the actual condition (cracked or uncracked section) of the strengthened reinforced concrete section. The strain in prestressing steel at service, $\epsilon_{ps,s}$, can be calculated as

$$\epsilon_{ps,s} = \epsilon_{pe} + \frac{P_e}{A_c E_c} \left(1 + \frac{e^2}{r^2} \right) + \epsilon_{pnet,s} \quad (10.3.1.7a)$$

in which ϵ_{pe} is the effective prestressing strain, and $\epsilon_{pnet,s}$ is the net tensile strain in the prestressing steel beyond decompression at service. The value of $\epsilon_{pnet,s}$ depends on the effective section properties at service, and can be calculated using Eq. (10.3.1.7b) and (10.3.1.7c)

$$\epsilon_{pnet,s} = \frac{M_s e}{E_c I_g} \text{ for uncracked section at service} \quad (10.3.1.7b)$$

$$\epsilon_{pnet,s} = \frac{M_{snet} e}{E_c I_{cr}} \text{ for cracked section at service} \quad (10.3.1.7c)$$

where M_{snet} is the net service moment beyond decompression. The stress in the prestressing steel under service loads can then be computed from Eq. (10.3.1.6d) and (10.3.1.6e), and compared against the limits described in 10.3.1.4.

10.3.1.8 Stress in FRP under service loads—Equation (10.3.1.8) gives the stress in the FRP reinforcement under an applied moment within the elastic response range of the member. The calculation procedure for the initial strain ϵ_{bi} at the time of FRP installation will depend on the state of the concrete section at the time of FRP installation and at service condition. Prestressed sections can be uncracked at installation/uncracked at service, uncracked at installation/cracked at service, or cracked at installation/cracked at service. The initial strain on the bonded substrate, ϵ_{bi} , can be determined from an elastic analysis of the existing member, considering all loads that will be on the member during the installation of the FRP system. The elastic analysis of the existing member should be

based on cracked or uncracked section properties, depending on existing conditions. In most cases, the initial strain before cracking is relatively small, and may conservatively be ignored

$$f_{f,s} = \left(\frac{E_f}{E_c} \right) \frac{M_s y_b}{I} - \epsilon_{bi} E_f \quad (10.3.1.8)$$

Depending on the actual condition at service (cracked or uncracked), the moment of inertia, I , can be taken as the moment of inertia of the uncracked section transformed to concrete, I_{tr} , or the moment of inertia of the cracked section transformed to concrete, I_{cr} . The variable y_b is the distance from the centroidal axis of the gross section, neglecting reinforcement, to the extreme bottom fiber. The computed stress in the FRP under service loads should not exceed the limits provided in 10.2.9.

10.4—Moment redistribution

Moment redistribution for continuous reinforced concrete beams strengthened using externally bonded FRP can be used to decrease factored moments calculated by elastic theory at sections of maximum negative or maximum positive moment for any assumed loading arrangement by not more than 1000 ϵ_r percent, to a maximum of 20 percent. Moment redistribution is only permitted when the strain in the tension steel reinforcement, ϵ_s , exceeds 0.0075 at the section at which moment is reduced. Moment redistribution is not permitted where approximate values of bending moments are used.

The reduced moment should be used for calculating redistributed moments at all other sections within the spans. Static equilibrium should be maintained after redistribution of moments for each loading arrangement. **El-Refaie et al. (2003)** demonstrated that continuous reinforced concrete beams strengthened with carbon FRP sheets can redistribute moment in the order of 6 to 31 percent. They also concluded that lower moment redistribution was achieved for beam sections retrofitted with higher amounts of carbon FRP reinforcement. **Silva and Ibell (2008)** demonstrated that sections that can develop a curvature ductility capacity greater than 2.0 can produce moment redistribution of at least 7.5 percent of the design moment.

CHAPTER 11—SHEAR STRENGTHENING

Fiber-reinforced polymer (FRP) systems have been shown to increase the shear strength of existing concrete beams and columns by wrapping or partially wrapping the members (**Malvar et al. 1995; Chajes et al. 1995; Norris et al. 1997; Kachlakev and McCurry 2000**). Orienting FRP fibers transverse to the axis of the member or perpendicular to potential shear cracks is effective in providing additional shear strength (**Sato et al. 1996**). An increase in shear strength may be required when flexural strengthening is implemented to ensure that flexural capacity remains critical. Flexural failures are relatively more ductile in nature compared with shear failures.

11.1—General considerations

This chapter presents guidance on the calculation of added shear strength resulting from the addition of FRP shear reinforcement to a reinforced concrete beam or column. The additional shear strength that can be provided by the FRP system is based on many factors, including geometry of the beam or column, wrapping scheme, and existing concrete strength, but should be limited in accordance with the recommendations of Chapter 9.

Shear strengthening using external FRP may be provided at locations of expected plastic hinges or stress reversal and for enhancing post-yield flexural behavior of members in moment frames resisting seismic loads, as described in Chapter 13.

11.2—Wrapping schemes

The three types of FRP wrapping schemes used to increase the shear strength of prismatic, rectangular beams, or columns are illustrated in Fig. 11.2. Completely wrapping the FRP system around the section on all four sides is the most efficient wrapping scheme and is most commonly used in column applications where access to all four sides of the column is available. In beam applications where an integral slab makes it impractical to completely wrap the member, the shear strength can be improved by wrapping the FRP system around three sides of the member (U-wrap) or bonding to two opposite sides of the member.

Although all three techniques have been shown to improve the shear strength of a rectangular member, completely wrapping the section is the most efficient, followed by the three-sided U-wrap. Bonding to two sides of a beam is the least efficient scheme.

For shear strengthening of circular members, only complete circumferential wrapping of the section in which the FRP is oriented perpendicular to the longitudinal axis of the member (that is, $\alpha = 90$ degrees) is recommended.

In all wrapping schemes, the FRP system can be installed continuously along the span of a member or placed as discrete strips. As discussed in 9.3.3, the potential effects of entrapping moisture in the substrate when using continuous reinforcement should be carefully considered. Specific means of allowing moisture vapor transmission out of the substrate should be employed where appropriate.

11.3—Nominal shear strength

The design shear strength of a concrete member strengthened with an FRP system should exceed the required shear strength (Eq. (11.3a)). The required shear strength of an FRP-strengthened concrete member should be computed with the load factors required by ACI 318. The design shear strength should be calculated by multiplying the nominal shear strength by the strength reduction factor ϕ , as specified by ACI 318

$$\phi V_n \geq V_u \tag{11.3a}$$

The nominal shear strength of an FRP-strengthened concrete member can be determined by adding the contribution of the FRP external shear reinforcement to the contribu-

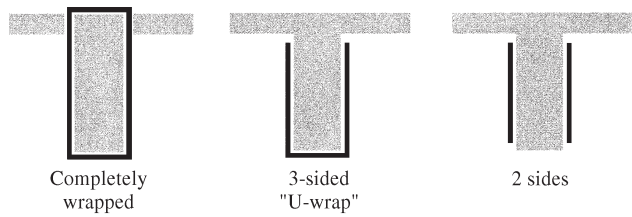


Fig. 11.2—Typical wrapping schemes for shear strengthening using FRP laminates.

tions from the reinforcing steel (stirrups, ties, or spirals) and the concrete (Eq. (11.3b)). An additional reduction factor ψ_f is applied to the contribution of the FRP system

$$\phi V_n = \phi(V_c + V_s + \psi_f V_f) \tag{11.3b}$$

where V_c and V_s are the concrete and internal reinforcing steel contributions to shear capacity calculated using the provisions of ACI 318, respectively. For prestressed members, V_c is the minimum of V_{ci} and V_{cw} defined by ACI 318.

Based on a reliability analysis using data from Boushelham and Chaallal (2006), Deniaud and Cheng (2001, 2003), Funakawa et al. (1997), Matthys and Triantafillou (2001), and Pellegrino and Modena (2002), the reduction factor ψ_f of 0.85 is recommended for the three-sided FRP U-wrap or two-opposite-sides strengthening schemes. Insufficient experimental data exist to perform a reliability analysis for fully-wrapped sections; however, there should be less variability with this strengthening scheme, as it is less bond-dependent and, therefore, the reduction factor ψ_f of 0.95 is recommended. The ψ_f factor was calibrated based on design material properties. These recommendations are given in Table 11.3.

Table 11.3—Recommended additional reduction factors for FRP shear reinforcement

$\psi_f = 0.95$	Completely wrapped members
$\psi_f = 0.85$	Three-side and two-opposite-sides schemes

11.4—FRP contribution to shear strength

Figure 11.4 illustrates the dimensional variables used in shear-strengthening calculations for FRP laminates. The contribution of the FRP system to shear strength of a member is based on the fiber orientation and an assumed crack pattern (Khalifa et al. 1998). The shear strength provided by the FRP reinforcement can be determined by calculating the force resulting from the tensile stress in the FRP across the assumed crack. The shear contribution of the FRP shear reinforcement is then given by Eq. (11.4a)

$$V_f = \frac{A_{fv} f_{fe} (\sin \alpha + \cos \alpha) d_{fv}}{s_f} \tag{11.4a}$$

For rectangular sections

$$A_{fv} = 2nt_f w_f \tag{11.4b}$$

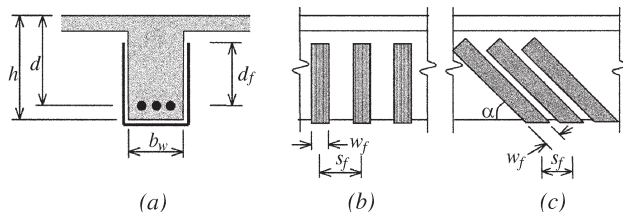


Fig. 11.4—Illustration of the dimensional variables used in shear-strengthening calculations for repair, retrofit, or strengthening using FRP laminates.

For circular sections, d_{fv} is taken as 0.8 times the diameter of the section and

$$A_{fv} = (\pi/2)nt_f w_f \quad (11.4c)$$

The tensile stress in the FRP shear reinforcement at nominal strength is directly proportional to the strain that can be developed in the FRP shear reinforcement at nominal strength

$$f_{fe} = E_f \epsilon_{fe} \quad (11.4d)$$

11.4.1 Effective strain in FRP laminates—The effective strain is the maximum strain that can be achieved in the FRP system at the nominal strength and is governed by the failure mode of the FRP system and of the strengthened reinforced concrete member. The licensed design professional should consider all possible failure modes and use an effective strain representative of the critical failure mode. The following subsections provide guidance on determining this effective strain for different configurations of FRP laminates used for shear strengthening of reinforced concrete members.

11.4.1.1 Completely wrapped members—For reinforced concrete column and beam members completely wrapped by FRP, loss of aggregate interlock of the concrete has been observed to occur at fiber strains less than the ultimate fiber strain. To preclude this mode of failure, the maximum strain used for design should be limited to 0.4 percent for members that are completely wrapped with FRP (Eq. (11.4.1.1))

$$\epsilon_{fe} = 0.004 \leq 0.75 \epsilon_{fu} \quad (11.4.1.1)$$

This strain limitation is based on testing (Priestley et al. 1996) and experience. Higher strains should not be used for FRP shear-strengthening applications.

11.4.1.2 Bonded U-wraps or bonded face plies—FRP systems that do not enclose the entire section (two- and three-sided wraps) have been observed to delaminate from the concrete before the loss of aggregate interlock of the section. For this reason, bond stresses have been analyzed to determine the efficiency of these systems and the effective strain that can be achieved (Triantafillou 1998). The effective strain is calculated using a bond-reduction coefficient κ_v , applicable to shear

$$\epsilon_{fe} = \kappa_v \epsilon_{fu} \leq 0.004 \quad (11.4.1.2a)$$

The bond-reduction coefficient is a function of the concrete strength, the type of wrapping scheme used, and the stiffness of the laminate. The bond-reduction coefficient can be computed from Eq. (11.4.1.2b) through (11.4.1.2e) (Khalifa et al. 1998)

$$\kappa_v = \frac{k_1 k_2 L_e}{468 \epsilon_{fu}} \leq 0.75 \quad (\text{in.-lb}) \quad (11.4.1.2b)$$

$$\kappa_v = \frac{k_1 k_2 L_e}{11,900 \epsilon_{fu}} \leq 0.75 \quad (\text{SI})$$

The active bond length L_e is the length over which the majority of the bond stress is maintained. This length is given by Eq. (11.4.1.2c)

$$L_e = \frac{2500}{(nt_f E_f)^{0.58}} \quad (\text{in.-lb}) \quad (11.4.1.2c)$$

$$L_e = \frac{23,300}{(nt_f E_f)^{0.58}} \quad (\text{SI})$$

The bond-reduction coefficient also relies on two modification factors, k_1 and k_2 , that account for the concrete strength and the type of wrapping scheme used, respectively. Expressions for these modification factors are given in Eq. (11.4.1.2d) and (11.4.1.2e)

$$k_1 = \left(\frac{f'_c}{4000} \right)^{2/3} \quad (\text{in.-lb}) \quad (11.4.1.2d)$$

$$k_1 = \left(\frac{f'_c}{27} \right)^{2/3} \quad (\text{SI})$$

$$k_2 = \begin{cases} \frac{d_{fv} - L_e}{d_{fv}} & \text{for U-wraps} \\ \frac{d_{fv} - 2L_e}{d_{fv}} & \text{for two sides bonded} \end{cases} \quad (11.4.1.2e)$$

The methodology for determining κ_v has been validated for members in regions of high shear and low moment, such as monotonically loaded simply supported beams. Although the methodology has not been confirmed for shear strengthening in areas subjected to combined high flexural and shear stresses or in regions where the web is primarily in compression (negative moment regions), it is suggested that κ_v is sufficiently conservative for such cases. The design procedures outlined herein have been developed by a combination of analytical and empirical results (Khalifa et al. 1998).

Anchorage details have been used to develop higher strains in bonded U-wraps used in shear strengthening applications. Anchorage systems include mechanical fasteners, FRP strips, fiber anchors, and near-surface mounted (NSM) anchors; examples are shown schematically in Fig. 10.1.1b. (Khalifa et al. 1999; Kalfat et al. 2013; Grelle and Sneed 2013). Properly anchored U-wraps can be designed to fail

by FRP rupture (Belarbi et al. 2011). In no case, however, should the effective strain in the anchored FRP U-wrap exceed the lesser of 0.004 or $0.75\varepsilon_{fu}$, and $\psi_f = 0.85$ remains appropriate for anchored U-wraps.

11.4.2 Spacing—Spaced FRP strips used for shear strengthening should be investigated to evaluate their contribution to the shear strength. Spacing should adhere to the limits prescribed by ACI 318 for internal steel shear reinforcement. The spacing of FRP strips is defined as the distance between the centerline of the strips.

11.4.3 Reinforcement limits—The total shear strength provided by reinforcement should be taken as the sum of the contribution of the FRP shear reinforcement and the steel shear reinforcement. The sum of the shear strengths provided by the shear reinforcement should be limited based on the criteria given for steel alone in ACI 318

$$\begin{aligned} V_s + V_f &\leq 8\sqrt{f'_c}b_w d && \text{(in.-lb)} \\ V_s + V_f &\leq 0.66\sqrt{f'_c}b_w d && \text{(SI)} \end{aligned} \quad (11.4.3)$$

For circular sections, $b_w d$ in Eq. (11.4.3) is taken as $0.8D^2$, where D is the member diameter.

CHAPTER 12—STRENGTHENING OF MEMBERS SUBJECTED TO AXIAL FORCE OR COMBINED AXIAL AND BENDING FORCES

Confinement of reinforced concrete columns by means of fiber-reinforced polymer (FRP) jackets can be used to enhance their strength and ductility. An increase in capacity is an immediate outcome typically expressed in terms of improved peak load resistance. Ductility enhancement, on the other hand, requires more complex calculations to determine the ability of a member to sustain rotation and drift without a substantial loss in strength. This chapter applies only to members confined with FRP systems.

12.1—Pure axial compression

FRP systems can be used to increase the axial compression strength of a concrete member by providing confinement with an FRP jacket (Nanni and Bradford 1995; Toutanji 1999). Confining a concrete member is accomplished by orienting the fibers transverse to the longitudinal axis of the member. In this orientation, the transverse or hoop fibers are similar to conventional spiral or tie reinforcing steel. Any contribution of longitudinally aligned fibers to the axial compression strength of a concrete member should be neglected.

FRP jackets provide passive confinement to the compression member, remaining unstressed until dilation and cracking of the wrapped compression member occur. For this reason, intimate contact between the FRP jacket and the concrete member is critical.

Depending on the level of confinement, the uniaxial stress-strain curve of a reinforced concrete column could be depicted by one of the curves in Fig. 12.1a, where f'_c and f'_{cc} represent the peak concrete strengths for unconfined and confined cases, respectively. These strengths are calculated as the peak load minus the contribution of the steel reinforce-

ment, all divided by the cross-sectional area of the concrete. The ultimate strain of the unconfined member corresponding to $0.85f'_c$ (Curve (a)) is ε_{cu} . The strain ε_{ccu} corresponds to: a) $0.85f'_{cc}$ in the case of the lightly confined member (Curve (b)); and b) the failure strain in both the heavily confined-softening case (the failure stress is larger than $0.85f'_{cc}$ (Curve (c)) or in the heavily confined-hardening case (Curve (d)).

The definition of ε_{ccu} at $0.85f'_{cc}$ or less is arbitrary, although consistent with modeling of conventional concrete (Hognestad 1951) and such that the descending branch of the stress-strain curve at that level of stress ($0.85f'_{cc}$ or higher) is not as sensitive to the test procedure in terms of rate of loading and stiffness of the equipment used.

The axial compressive strength of a nonslender, normal-weight concrete member confined with an FRP jacket may be calculated using the confined concrete strength (Eq. (12.1a) and (12.1b)). The axial force acting on an FRP-strengthened concrete member should be computed using the load factors required by ACI 318, and the values of the ϕ factors as established in ACI 318 for both types of transverse reinforcing steel (spirals or ties) apply.

For nonprestressed members with existing steel spiral reinforcement

$$\phi P_n = 0.85\phi[0.85f'_{cc}(A_g - A_{st}) + f_y A_{st}] \quad (12.1a)$$

For nonprestressed members with existing steel-tie reinforcement

$$\phi P_n = 0.8\phi[0.85f'_{cc}(A_g - A_{st}) + f_y A_{st}] \quad (12.1b)$$

Several models that simulate the stress-strain behavior of FRP-confined compression sections are available in the literature (Teng et al. 2002; De Lorenzis and Tepfers 2003; Lam and Teng 2003a). The stress-strain model by Lam and Teng (2003a,b) for FRP-confined concrete is illustrated in Fig. 12.1b and computed using the following expressions

$$f_c = \begin{cases} E_c \varepsilon_c - \frac{(E_c - E_2)^2}{4f'_c} & 0 \leq \varepsilon_c \leq \varepsilon'_t \\ f'_c + E_2 \varepsilon_c & \varepsilon'_t \leq \varepsilon_c \leq \varepsilon_{c,max} \end{cases} \quad (12.1c)$$

$$\varepsilon_{c,max} \leq \varepsilon_{ccu} \leq 0.01 \quad (12.1d)$$

$$E_2 = \frac{f'_{cc} - f'_c}{\varepsilon_{ccu}} \quad (12.1e)$$

$$\varepsilon'_t = \frac{2f'_c}{E_c - E_2} \quad (12.1f)$$

The maximum confined concrete compressive strength, f'_{cc} , and the maximum confinement pressure f'_l are calculated using Eq. (12.1g) and (12.1h), respectively (Lam and Teng 2003a,b) with the inclusion of an additional reduction factor $\psi_f = 0.95$

$$f'_c = f'_c + \psi_f 3.3 \kappa_a f'_t \quad (12.1g)$$

$$f'_t = \frac{2E_f n t_f \epsilon_{fe}}{D} \quad (12.1h)$$

In Eq. (12.1g), f'_c is the unconfined cylinder compressive strength of concrete, and the efficiency factor κ_a accounts for the geometry of the section, circular and noncircular, as defined in 12.1.1 and 12.1.2. In Eq. (12.1h), the effective strain in the FRP at failure, ϵ_{fe} , is given by

$$\epsilon_{fe} = \kappa_c \epsilon_{fu} \quad (12.1i)$$

The FRP strain efficiency factor κ_c accounts for the premature failure of the FRP system (Pessiki et al. 2001), related primarily to stress concentration regions caused by cracking of the concrete as it dilates. Based on experimental calibration using mainly carbon FRP (CFRP)-confined concrete specimens, an average value of 0.586 was computed for κ_c by Lam and Teng (2003a). Similarly, a database of 251 test results (Harries and Carey 2003) computed a value of $\kappa_c = 0.58$, whereas experimental tests on medium- and large-scale columns resulted in values of $\kappa_c = 0.57$ and 0.61, respectively (Carey and Harries 2005).

Based on tests by Lam and Teng (2003a,b), the ratio f'_t/f'_c should not be less than 0.08. This is the minimum level of confinement required to assure a nondescending second branch in the stress-strain performance, as shown by Curve (d) in Fig. 12.1a. This limitation was later confirmed for circular cross sections by Spoelstra and Monti (1999) using their analytical model. A strain efficiency factor κ_c of 0.55 and a minimum confinement ratio f'_t/f'_c of 0.08 should be used.

The maximum compressive strain in the FRP-confined concrete, ϵ_{ccu} , can be found using Eq. (12.1j) (Concrete Society 2004). The maximum concrete strain, $\epsilon_{c,max}$, used in Eq. (12.1c) should be limited to 0.01 to prevent excessive cracking and the resulting loss of concrete integrity.

$$\epsilon_{ccu} = \epsilon'_c \left(1.50 + 12 \kappa_b \frac{f'_t}{f'_c} \left(\frac{\epsilon_{fe}}{\epsilon'_c} \right)^{0.45} \right) \quad (12.1j)$$

In Eq. (12.1j), the efficiency factor κ_b accounts for the geometry of the section in the calculation of the ultimate axial strain, as defined in 12.1.1 and 12.1.2.

Strength enhancement for compression members with f'_c of 10,000 psi (70 MPa) or higher has not been experimentally verified. Enhancement of concrete having strength f'_c in excess of 10,000 psi (70 MPa) should be based on experimental testing.

12.1.1 Circular cross sections—FRP jackets are most effective at confining members with circular cross sections (Demers and Neale 1999; Pessiki et al. 2001; Harries and Carey 2003; Youssef 2003; Matthys et al. 2005; Rocca et al. 2006). The FRP system provides a circumferentially uniform confining pressure to the radial expansion of the compression member when the fibers are aligned transverse to the

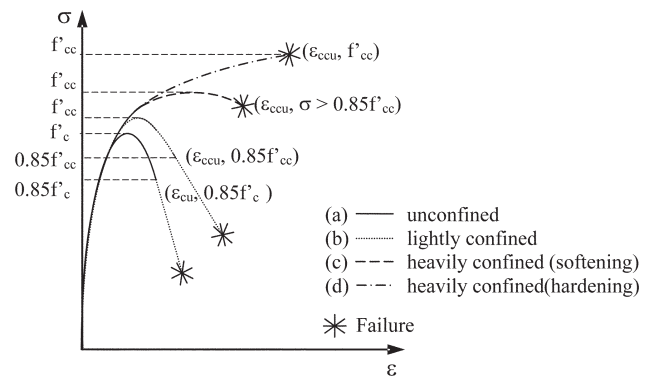


Fig. 12.1a—Schematic stress-strain behavior of unconfined and confined reinforced concrete columns (Rocca et al. 2006).

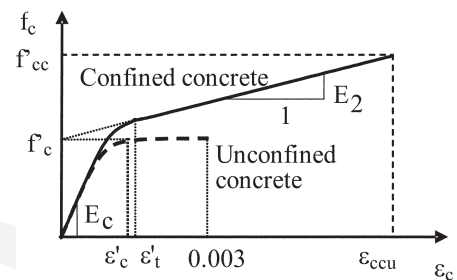


Fig. 12.1b—Stress-strain model for FRP-confined concrete (Lam and Teng 2003a).

longitudinal axis of the member. For circular cross sections, the shape factors κ_a and κ_b in Eq. (12.1g) and (12.1j), respectively, can be taken as 1.0.

12.1.2 Noncircular cross sections—Testing has shown that confining square and rectangular members with FRP jackets can provide marginal increases in the maximum axial compressive strength f'_{cc} of the member (Pessiki et al. 2001; Wang and Restrepo 2001; Harries and Carey 2003; Youssef 2003; Rocca et al. 2008). The provisions in this guide are not recommended for members featuring side aspect ratios h/b greater than 2.0, or face dimensions b or h exceeding 36 in. (900 mm), unless testing demonstrates their effectiveness.

For noncircular cross sections, f'_t in Eq. (12.1h) corresponds to the maximum confining pressure of an equivalent circular cross section with diameter D equal to the diagonal of the rectangular cross section

$$D = \sqrt{b^2 + h^2} \quad (12.1.2a)$$

The shape factors κ_a in Eq. (12.1g) and κ_b in Eq. (12.1j) depend on two parameters: the cross-sectional area of effectively confined concrete A_e , and the side-aspect ratio h/b , as shown in Eq. (12.1.2b) and (12.1.2c), respectively

$$\kappa_a = \frac{A_e}{A_c} \left(\frac{b}{h} \right)^2 \quad (12.1.2b)$$

$$\kappa_b = \frac{A_e}{A_c} \left(\frac{h}{b} \right)^{0.5} \quad (12.1.2c)$$

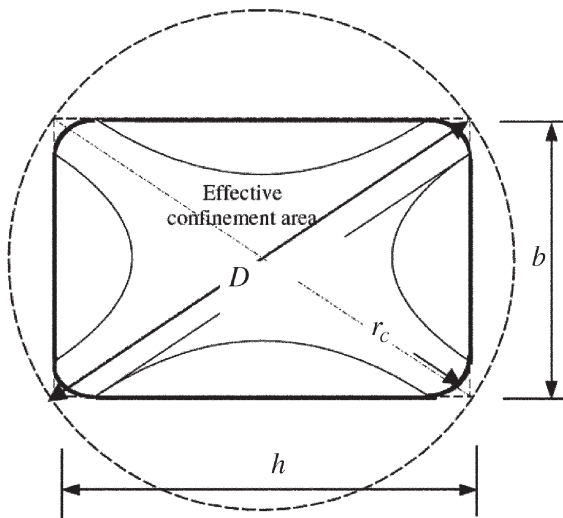


Fig. 12.1.2—Equivalent circular cross section (Lam and Teng 2003b).

The generally accepted theoretical approach for the definition of A_e consists of four parabolas within which the concrete is fully confined, outside of which negligible confinement occurs (Fig. 12.1.2). The shape of the parabolas and the resulting effective confinement area is a function of the dimensions of the column (b and h), the radius of the corners, r_c , and the longitudinal steel reinforcement ratio ρ_g , and can be expressed as

$$\frac{A_e}{A_c} = \frac{1 - \left[\left(\frac{b}{h} \right) (h - 2r_c)^2 + \left(\frac{h}{b} \right) (b - 2r_c)^2 \right] \rho_g}{3A_g - \rho_g} \quad (12.1.2d)$$

12.1.3 Serviceability considerations—As loads approach factored load levels, damage to the concrete in the form of significant cracking in the radial direction might occur. The FRP jacket contains the damage and maintains the structural integrity of the column. At service load levels, however, this type of damage should be avoided. In this way, the FRP jacket will only act during overloading conditions that are temporary in nature.

To ensure that radial cracking will not occur under service loads, the transverse strain in the concrete should remain below its cracking strain at service load levels. This corresponds to limiting the compressive stress in the concrete to $0.65f'_c$. In addition, the service stress in the longitudinal steel should remain below $0.60f_y$ to avoid plastic deformation under sustained or cyclic loads. By maintaining the specified stress in the concrete at service, the stress in the FRP jacket will be relatively low. The jacket is only stressed to significant levels when the concrete is transversely strained above the cracking strain and the transverse expansion becomes large. Service load stresses in the FRP jacket should never

exceed the creep rupture stress limit. In addition, axial deformations under service loads should be investigated to evaluate their effect on the performance of the structure.

12.2—Combined axial compression and bending

Wrapping with an FRP jacket can also provide strength enhancement for a member subjected to combined axial compression and flexure (Nosho 1996; Saadatmanesh et al. 1996; Chaallal and Shahawy 2000; Sheikh and Yau 2002; Iacobucci et al. 2003; Bousias et al. 2004; Elnabelsy and Saatcioglu 2004; Harajli and Rteil 2004; Sause et al. 2004; Memon and Sheikh 2005).

For predicting the effect of FRP confinement on strength enhancement, Eq. (12.1a) and (12.1b) are applicable when the eccentricity present in the member is less than or equal to $0.1h$. When the eccentricity is larger than $0.1h$, the methodology and equations presented in 12.1 can be used to determine the concrete material properties of the member cross section under compressive stress. Based on that, the axial load-moment (P - M) interaction diagram for the FRP-confined member can be constructed using well-established procedures (Bank 2006).

The following limitations apply for members subjected to combined axial compression and bending:

a) The effective strain in the FRP jacket should be limited to the value given in Eq. (12.2) to ensure the shear integrity of the confined concrete

$$\varepsilon_{fe} = 0.004 \leq \kappa_c \varepsilon_{fu} \quad (12.2)$$

b) The strength enhancement can only be considered when the applied ultimate axial force and bending moment, P_u and M_u , respectively, fall above the line connecting the origin and the balanced point in the P - M diagram for the unconfined member (Fig. 12.2). This limitation stems from the fact that strength enhancement is only significant for members in which compression failure is the controlling mode (Bank 2006).

P - M diagrams may be developed by satisfying strain compatibility and force equilibrium using the model for the stress-strain behavior for FRP-confined concrete presented in Eq. (12.1c) through (12.1f). For simplicity, the portion of the unconfined and confined P - M diagrams corresponding to compression-controlled failure can be reduced to two bilinear curves passing through three points (Fig 12.2). For values of eccentricity greater than $0.1h$ and up to the point corresponding to the balanced condition, the methodology provided in Appendix D may be used for the computation of a simplified interaction diagram. The values of the ϕ factors as established in ACI 318 for both types of transverse reinforcing steel (spirals or ties) apply.

12.3—Ductility enhancement

Increased ductility of a section results from the ability to develop greater compressive strains in the concrete before compressive failure (Seible et al. 1997). The FRP jacket can also serve to delay buckling of longitudinal steel reinforce-

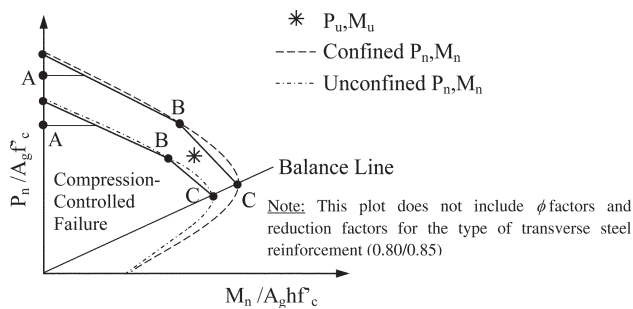


Fig. 12.2—Representative interaction diagram.

ment in compression and to clamp lap splices of longitudinal steel reinforcement.

For seismic applications, FRP jackets should be designed to provide a confining stress sufficient to develop concrete compression strains associated with the displacement demands as described in Chapter 13. Shear forces should also be evaluated in accordance with Chapter 11 to prevent brittle shear failure in accordance with ACI 318.

12.3.1 Circular cross sections—The maximum compressive strain for FRP-confined members with circular cross sections can be found from Eq. (12.1j) with f'_{cc} from Eq. (12.1g) and using $\kappa_b = 1.0$.

12.3.2 Noncircular cross sections—The maximum compressive strain for FRP-confined members with square or rectangular sections can be found from Eq. (12.1j), with f'_{cc} from Eq. (12.1g), and using κ_b as given in Eq. (12.1.2c). The confining effect of FRP jackets should be assumed to be negligible for rectangular sections with aspect ratio h/b exceeding 2.0, or face dimensions b or h exceeding 36 in. (900 mm), unless testing demonstrates their effectiveness.

12.4—Pure axial tension

FRP systems can be used to provide additional tensile strength to a concrete member. Due to the linear-elastic nature of FRP materials, the tensile contribution of the FRP system is directly related to its strain and is calculated using Hooke's Law.

The tension capacity provided by the FRP is limited by the design tensile strength of the FRP and the ability to transfer stresses into the substrate through bond (Nanni et al. 1997). The effective strain in the FRP can be determined based on the criteria given for shear strengthening in Eq. (11.4.1.1) through (11.4.1.2d). The value of k_2 in Eq. (11.4.1.2b) can be taken as 1.0. A minimum bonded length of ℓ_{df} , as calculated in 14.1.3, should be provided to develop this level of strain.

CHAPTER 13—SEISMIC STRENGTHENING

Many strengthening techniques have been developed and used for repair and rehabilitation of earthquake damaged and seismically deficient structures (Federal Emergency Management Agency 2006). Identification of an effective rehabilitation method is directly related to the outcome of a seismic evaluation of the structure and is based on consideration of many factors, including type of structure, rehabilitation objective, strengthening scheme effectiveness, constructability, and cost.

A classification of seismic rehabilitation methods for buildings in ASCE/SEI 41 and ACI 369R gives the following strategies: local modification of components, removal or lessening of existing irregularities and discontinuities, global structural stiffening, global structural strengthening, mass reduction, seismic isolation, and supplemental energy dissipation. Strengthening using FRP materials and systems allows for local modification of components and can be implemented in improving the overall seismic performance of the structure. The main advantages of FRP strengthening can be summarized as follows:

a) At the component level, FRP strengthening can be used to efficiently mitigate brittle mechanisms of failure. These may include shear failure of unconfined beam-column joints; shear failure of beams, columns, or both; and lap splice failure. FRP strengthening can also be used to increase the flexural capacity of reinforced concrete members, to resist the buckling of flexural steel bars, and to increase the inelastic rotational capacity of reinforced concrete members.

b) Implementing FRP strengthening schemes translates into an increase in the global displacement and energy dissipation capacities of the structure, thus improving the overall behavior of reinforced concrete structures subjected to seismic actions.

c) FRP shear strengthening and confinement has a small effect on the stiffness or mass of the structure. In such cases, a reevaluation of the seismic demand after strengthening is typically not required. When the structural stiffness needs to be increased, FRP strengthening of local components can be coupled with other traditional global upgrade techniques.

Many research programs have evaluated the adequacy of externally bonded FRP composites for seismic rehabilitation of concrete structures (Haroun et al. 2005; Pantelides et al. 2000; Ghobarah and Said 2002; Gergely et al. 2000; Antonopoulos and Triantafillou 2002; Hamed and Rabino-vitch 2005; Pampanin et al. 2007; Di Ludovico et al. 2008a). Other research programs have confirmed the potential of FRP techniques for upgrading the seismic performance of local elements such as reinforced concrete columns (Bousias et al. 2004) and connections (Antonopoulos and Triantafillou 2002; Prota et al. 2004). Research results for FRP applied at the local element or partial structural frame level were subsequently validated on full-scale structures (Pantelides et al. 2000; 2004; Balsamo et al. 2005; Engindeniz et al. 2008a,b). In addition, several structures that include FRP-strengthened members have experienced seismic events. Failure of these members has not been reported.

This chapter presents design guidelines for the seismic strengthening of reinforced concrete elements using externally bonded FRP composites. The design guidelines described herein are intended to be used in conjunction with the fundamental concepts, analysis procedures, design philosophy, seismic rehabilitation objectives, and acceptance criteria set forth in documents such as ASCE/SEI 41 and ACI 369R. Strengthening of RC building components or structures with FRP shall follow capacity protection principles. In capacity design (Hollings 1968; Park and Paulay 1976), a desirable mechanism of inelastic response

under seismic action is ensured by providing a strength hierarchy (strong column-weak beam; shear strength > flexural strength). Application of these design guidelines for the seismic rehabilitation of nonbuilding structures such as bridges, wharves, silos, and nuclear facilities warrant additional consideration.

These guidelines do not provide information required to complete a seismic evaluation of an existing structure, determine if retrofit is required, or identify the seismic deficiencies that need to be corrected to achieve the desired performance objective. These guidelines are also not meant to address post-seismic conditions or residual strength of the structure and the FRP retrofit system. After a seismic event, a structure that has been retrofitted with FRP composites could develop large displacements and excessive cracking, resulting in residual stresses or damage to the FRP system. In such cases, an investigation of the stability, ductility, and residual strength of the structure should be performed after the seismic event to assess the adequacy of the existing FRP retrofit system and to determine if additional remedial measures are needed.

13.1—Background

One of the most comprehensive documents developed to assess the need for seismic rehabilitation of reinforced concrete buildings is *ASCE/SEI 41*. FEMA P695 (*Federal Emergency Management Agency 2009*) provides further guidance in the selection of appropriate design criteria to achieve the seismic performance objectives. *ACI 369R* estimates the desired seismic performance of concrete components that are largely based on the format and content of *ASCE/SEI 41*.

FEMA (*Federal Emergency Management Agency 2006*) provides a complete list of references on technical design standards and analysis techniques that are available to design professionals. Other resources dealing with seismic upgrade of existing reinforced concrete structures can be obtained from *Japan Building Disaster Prevention Association (2005)*, *Eurocode 8 (2005)*, *International Federation for Structural Concrete (2003, 2006)*, *Italian National Research Council (2004)*, and *Sabnis et al. (1996)*.

Experience gained from examining the performance of reinforced concrete structures after a seismic event indicates that many structural deficiencies result from inadequate confinement of concrete, insufficient transverse and continuity reinforcement in connections and structural members, buckling of flexural reinforcement, lap splice failures, and anchorage failures (*Priestley et al. 1996; Haroun et al. 2003; Sezen et al. 2003; Pantelides et al. 1999, 2004*). These deficiencies have typically led to brittle failures, soft-story failure, and large residual displacements (*Moehle et al. 2002; Di Ludovico et al. 2008b; Prota et al. 2004; Pessiki et al. 1990*). Experimental work has also demonstrated that externally bonded FRP systems can be effective in addressing many of the aforementioned structural deficiencies (*Engin-deniz et al. 2005; Pantelides et al. 2008; Silva et al. 2007*).

13.2—FRP properties for seismic design

For seismic upgrades, the material environmental factors given in Table 9.4 should be used in the design of the FRP strengthening solution. The creep rupture limits in Table 10.2.9 need not be considered for seismic strengthening applications unless initial strains are imposed on the FRP as part of the retrofit scheme. Typically, when used for seismic retrofit, the FRP material will not be exposed to significant sustained service loads and creep rupture failure will not govern the design. Creep rupture limits should be considered, however, in cases where the application may impose initial or service strains that can produce sustained stresses on the FRP. Some examples include applications with expansive grouts, pre-tensioned FRP, or other methods that generate sustained stress in the FRP material. When this chapter is used in conjunction with *ASCE/SEI 41*, FRP material properties should be considered lower-bound material properties.

13.3—Confinement with FRP

Jacketing concrete structural members with FRP having the primary fibers oriented around the perimeter of the member provides confinement to plastic hinges, mitigates the splitting failure mode of poorly detailed lap splices, and prevents buckling of the main reinforcing bars.

13.3.1 General considerations—In seismic applications, jacketing concrete structural members with FRP is not recommended for rectangular sections with aspect ratios h/b greater than 1.5, or face dimensions b or h exceeding 36 in. (900 mm) (*Seible et al. 1997*), unless testing demonstrates the effectiveness of FRP for confinement of these members. For rectangular sections with an aspect ratio greater than 1.5, the section can be modified to be circular or oval to enhance the effectiveness of the FRP jacket (*Seible et al. 1997*). FRP anchors have been shown to increase the effectiveness of the FRP jacket in rectangular sections with aspect ratios greater than 1.5 (*Kim et al. 2011*).

13.3.2 Plastic hinge region confinement—FRP-jacketed reinforced concrete members achieve higher inelastic rotational capacity of the plastic hinge (*Seible et al. 1997*). FRP jacketing can be used to increase the concrete compressive strength when the concrete member complies with the condition in 12.3. For concrete members that do not satisfy this condition, only the ultimate concrete strains can be increased by FRP jacketing. Increase in flexural strength due to higher concrete compressive strength should be considered to verify that hinges can form prior to reaching the shear strength of members.

The design curvature ϕ_D for a confined reinforced concrete section at the plastic hinge can be calculated using Eq. (13.3.2a).

$$\phi_D = \frac{\theta_p}{L_p} + \phi_{y,frp} \leq \phi_{u,frp} \quad (13.3.2a)$$

where θ_p is the plastic rotation demand, which can be determined following the analytical procedures outlined in *ASCE/SEI 41*. In Eq. (13.3.2a), the curvatures of the FRP-confined section at steel yielding, $\phi_{y,frp}$, and at ultimate capacity, $\phi_{u,frp}$,

are determined by Eq. (13.3.2b) and (13.3.2c), and L_p is the plastic hinge length computed using Eq. (13.3.2d).

$$\phi_{y,frp} = \frac{\epsilon_y}{d - c_{y,frp}} \quad (13.3.2b)$$

where ϵ_y and $c_{y,frp}$ are the steel strain and depth of the neutral axis at steel yielding, respectively, and d is the distance from the extreme compression fibers to the extreme tension steel.

$$\phi_{u,frp} = \frac{\epsilon_{ccu}}{c_{u,frp}} \quad (13.3.2c)$$

where ϵ_{ccu} and $c_{u,frp}$ are the extreme compression fiber strain and depth of the neutral axis at ultimate, respectively.

For beams, the plastic hinge length L_p can be approximated as twice the beam height ($2h$). The plastic hinge length can also be determined using detailed analysis but should not be less than the beam height. In FRP-jacketed columns, the plastic hinge length L_p can be computed using Eq. (13.3.2d) (Priestley et al. 1996)

$$L_p = g + 0.0003f_y d_{bl} \quad (\text{in.-lb}) \quad (13.3.2d)$$

$$L_p = g + 0.044f_y d_{bl} \quad (\text{SI})$$

where d_{bl} and f_y are the diameter and yield stress of the flexural steel, respectively, and g is the clear gap between the FRP jacket and adjacent members, as shown in Fig. 13.3.2. The gap g should not be greater than 2 in. (50.8 mm).

In plastic hinge regions, the FRP confinement should be provided over a length not less than the larger of the plastic hinge length and ℓ_o , where ℓ_o is the length, measured along the member axis from the face of the joint, over which special transverse reinforcement must be provided as defined in Chapter 18 of ACI 318-14. It should be noted that plastic hinges may occur at locations other than the ends of the member. Complete wrapping around the perimeter of the member should be used for plastic hinge confinement. Continuous (full) coverage of the plastic hinge length with an FRP jacket is recommended. When a continuous jacket is not possible, discrete transverse FRP strips around the perimeter of the section can be used.

Once the design curvature ϕ_D has been established, the ultimate extreme compression fiber strain in the concrete at ultimate, ϵ_{ccu} , can be calculated using Eq. (13.3.2e)

$$\epsilon_{ccu} = \phi_D c_u \leq 0.01 \quad (13.3.2e)$$

where c_u is the neutral axis depth at the ultimate design limit state. For members subjected to combined axial and flexural forces, ϵ_{ccu} should be limited to 0.01.

Once ϵ_{ccu} is determined, the thickness of the FRP jacket can be determined in accordance with 12.1 and 12.2. To ensure the shear integrity of the confined concrete section,

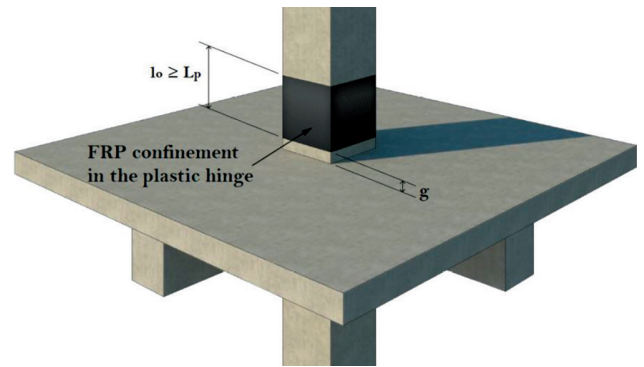


Fig. 13.3.2—Column plastic hinge confinement.

the effective design strain in the FRP jacket, ϵ_{fe} , should be limited to the value given by Eq. (12.2).

13.3.3 Lap splice clamping—The capacity of lap splices having inadequate lap length, especially those located in plastic hinge regions, can be improved by continuously confining the section over at least the length of the splice with externally bonded FRP (Seible et al. 1997; Haroun and Elsanadedy 2005). The required thickness of the FRP jacket can be calculated as follows

where D in inches and E_f in ksi,

circular sections: $nt_f = 145(D/E_f)$

rectangular sections: $nt_f = 218(D/E_f)$

(13.3.3a)

where D in mm and E_f is in MPa

circular sections: $nt_f = 1000(D/E_f)$

rectangular sections: $nt_f = 1500(D/E_f)$

where n is the number of FRP plies; t_f is the thickness per ply; D is the diameter of a circular member or the greater dimension of rectangular sections (per Eq. (12.1.2a)); and E_f is the tensile modulus of the FRP jacket.

While confining the section with FRP can mitigate the splitting mode of failure, the pullout failure mode may control the capacity of the confined lap splice. Therefore, regardless of FRP retrofit, the stress in the flexural reinforcing bar, f_s , should not exceed the limit given in Eq. (13.3.3b) (Harries et al. 2006).

$$f_s \leq \frac{33\ell_{prov}\sqrt{f'_c}}{d_{bl}\psi_t\psi_e\psi_s} \quad (\text{in.-lb}) \quad (13.3.3b)$$

$$f_s \leq \frac{2.75\ell_{prov}\sqrt{f'_c}}{d_{bl}\psi_t\psi_e\psi_s} \quad (\text{SI})$$

where ℓ_{prov} is the length of splice provided; d_{bl} is the diameter of the flexural reinforcement; and the ψ factors are those given in Section 25.4 of ACI 318-14.

13.3.4 Preventing buckling of flexural steel bars—Continuous or discrete FRP strips having the primary fibers oriented around the perimeter of the member can be used to prevent buckling of the flexural steel bars (Priestley et al.

1996). For circular sections, the volumetric reinforcement ratio provided by transverse FRP, ρ_f , is

$$\rho_f = \frac{4nt_f w_f}{D s_f} \quad (13.3.4a)$$

where n is the number of FRP plies; t_f is the thickness per ply; D is the diameter of the section; w_f is the FRP strip width; and s_f is the center-to-center spacing of the FRP strips. For continuous confinement, $w_f/s_f = 1$. In rectangular sections, the volumetric reinforcement ratio provided by the FRP, ρ_f , is (Priestley et al. 1996)

$$\rho_f = 2nt_f \left(\frac{b+h}{bh} \right) \frac{w_f}{s_f} \quad (13.3.4b)$$

where b and h are the dimensions of the rectangular section.

The amount of volumetric transverse reinforcement ratio should be at least

$$\rho_f \geq \frac{0.0052\rho_\ell D f_y}{d_{b\ell} f_{fe}} \quad (13.3.4c)$$

where ρ_ℓ is the flexural reinforcement ratio; D is the diameter of a circular section or the diagonal length of a rectangular section (Eq. (12.1.2a)); $d_{b\ell}$ and f_y are the diameter and the yield strength of the flexural reinforcement, respectively; ρ_f is the volumetric transverse reinforcement ratio computed by Eq. (13.3.4a) or (13.3.4b); and f_{fe} is the effective design stress in the FRP jacket computed by Eq. (13.3.4d)

$$f_{fe} = \varepsilon_{fe} E_f \quad (13.3.4d)$$

where ε_{fe} is the effective design strain in the FRP jacket given by Eq. (12.2) and E_f is the tensile modulus of the FRP jacket.

When discrete FRP strips rather than a continuous jacket are used, the clear spacing between FRP strips should not exceed the limits in Eq. (13.3.4e)

$$s_f \leq \left[3 - 6 \left(\frac{f_u}{f_y} - 1 \right) \right] d_{b\ell} \leq 6d_{b\ell} \quad (13.3.4e)$$

where f_u , f_y , and $d_{b\ell}$ are the ultimate and yield strengths and the smallest diameter of the internal flexural reinforcement, respectively. The clear spacing should not exceed 6 in. (150 mm). These requirements ensure that if the cover concrete spalls in the region between strips, the FRP can provide sufficient resistance against bar buckling. This approach neglects any contribution from the existing internal transverse reinforcement because the internal ties may not coincide within the open spaces between the FRP strips, and the interaction of the internal ties and external FRP strips has not been studied.

13.4—Flexural strengthening

The flexural capacity of reinforced concrete beams and columns in expected plastic hinge regions can be enhanced using FRP only in cases where strengthening will eliminate inelastic deformations in the strengthened region and transfer inelastic deformations to other locations in the member or the structure that are able to handle the ensuing ductility demands. The required flexural strength should be calculated in accordance with the design standard being used for rehabilitation, such as ASCE/SEI 41 and ACI 369R. When this chapter is used in conjunction with ASCE/SEI 41, the strengthened reinforced concrete members with FRP should be considered force-controlled unless a deformation-controlled classification can be justified based on experimental data.

The flexural capacity of reinforced concrete beams and columns can be enhanced using the design methodology presented in Chapter 10. The flexural strength ϕM_n should satisfy the requirement of Eq. (13.4)

$$\phi M_n \geq M_u \quad (13.4)$$

where M_u is the ultimate moment demand resulting from combined gravity and seismic demands. The flexural capacity of reinforced concrete members should be evaluated based on concrete and reinforcing steel strain limits set forth in the design standard. ASCE/SEI 41 provides a comprehensive list of concrete and reinforcing steel strain limits. In addition, the stress in the reinforcing steel should be limited to the stress that can be achieved based on the existing development lengths and lap-splice details. The strength reduction factor ϕ should be per the design standard being used for the rehabilitation. The additional strength reduction factor for FRP, ψ_f , shall be applied to the flexural contribution of the FRP reinforcement as described in 10.2.10.

13.4.2 Development and anchorage of flexural FRP reinforcement—This section provides conceptual methods for anchorage of flexural FRP reinforcement under seismic loads. Any anchorage method must be properly evaluated before it is selected for field implementation.

In seismic applications and within plastic hinge regions, the flexural FRP reinforcement should be confined using FRP strips that completely wrap around the perimeter of the section. Alternatively, the flexural FRP reinforcement could be confined over its entire length to provide higher resistance against debonding of the flexural FRP reinforcement. Because no anchorage design guidelines are currently available, the performance of any anchorage system should be substantiated through representative physical testing.

Such detailing provides higher resistance against debonding of the flexural FRP reinforcement. In applications involving floor systems, complete wrapping of the beam may require localized cutting of the slab to continue the FRP around the section.

Away from the plastic hinge region, transverse FRP U-wrap strips should be used to provide anchorage to the FRP flexural reinforcement. Other anchorage systems may also be used alone or in conjunction with FRP U-wrap strips.

Anchorage systems must be verified experimentally to demonstrate their effectiveness in preventing the debonding of the flexural FRP reinforcement. Several details for FRP anchorage at ends of retrofitted members are discussed in [Orton et al. \(2009\)](#).

The area of the transverse FRP wrap reinforcement, $A_{f,anchor}$, should be determined in accordance with Eq. (14.1.2). In addition, the length over which the FRP anchorage wraps are provided, $\ell_{d,E}$, should not be less than the value given by Eq. (13.4.2a).

$$\ell_{d,E} \geq \ell_o + \ell_{df} \quad (13.4.2a)$$

where ℓ_o is defined per Fig. 13.3.2, and ℓ_{df} is the required development length of the FRP system computed using Eq. (14.1.3).

For adequately anchored flexural FRP reinforcement, the effective design strain for FRP should be limited to

$$\varepsilon_{fd} \leq \min(0.90\varepsilon_{fu}, C_E\varepsilon_{fu}) \quad (13.4.2b)$$

Figure 13.4.2 depicts a conceptual detail for flexural strengthening of beams and columns at a joint and is intended to convey the critical elements of such a flexural strengthening. The design professional should detail the flexural FRP reinforcement to achieve continuity of the FRP across the joint. Appropriate development of the flexural FRP at both ends as well as adequate transverse reinforcement for confinement of the flexural FRP should be provided.

13.5—Shear strengthening

FRP shear strengthening can prevent brittle failures and promote the development of plastic hinges, resulting in an enhanced seismic behavior of concrete members. The design shear strength ϕV_n of a concrete member strengthened with FRP should satisfy Eq. (13.5)

$$\phi V_n \geq V_e \quad (13.5)$$

where ϕ should be per the design standard being used for the rehabilitation, and V_e is the design shear force. When this chapter is used in conjunction with [ASCE/SEI 41](#), the shear in the strengthened member should be considered force-controlled unless a deformation-controlled classification can be justified based on experimental data.

13.5.1 Design shear force V_e —The design shear force should be calculated in accordance with the design standard being used for the rehabilitation, such as [ASCE/SEI 41](#) and [ACI 369R](#). The shear capacity should be equal to or greater than the shear corresponding to the flexural capacity of the section. For example, when the rehabilitation is based on [ASCE/SEI 41](#), the design shear force is based on the seismic category and targeted seismic performance of the structure. When required by [ASCE/SEI 41](#) for the determination of the design shear force, the calculation of the probable flexural strength should be based on FRP stress taken as the lesser of $1.2f_{fd}$ and f_{fu} , ϕ should be taken as unity, and the FRP strength reduction factor ψ_f should be 1.0. Other limits for

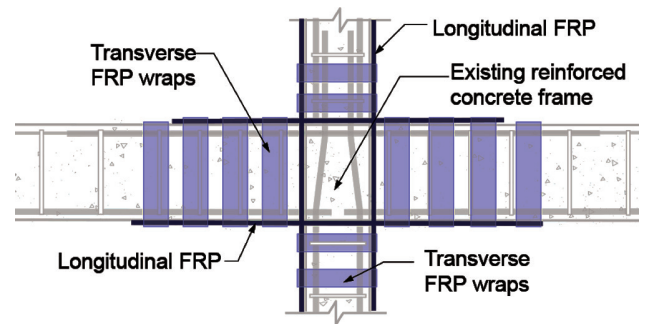


Fig. 13.4.2—Conceptual FRP strengthening detail (cross section elevation).

FRP strain and strength specified in this document should also be considered.

13.5.2 Nominal shear strength V_n —The shear strength of the existing member V_n^* should be determined following the procedures described in the design standard being used for rehabilitation, such as [ASCE/SEI 41](#) and [ACI 369R](#). The shear strength of an FRP-strengthened concrete member is calculated using Eq. (13.5.2).

$$V_n = V_n^* + \psi_f V_f \quad (13.5.2)$$

where ψ_f is the reduction factor applied to the contribution of the FRP system in accordance with [Chapter 11](#). The contributions of FRP to shear strength, V_f , should be determined in accordance with [Chapter 11](#). To account for effects of stress reversal, FRP shear strengthening should be provided with complete continuity around the perimeter of the section.

13.6—Beam-column joints

Experimental tests ([Bracci et al. 1992a](#); [Prota et al. 2004](#); [Pampanin et al. 2007](#)) and observations of post-seismic damage ([Moehle et al. 2002](#)) in structures designed to withstand only gravity loads show that unconfined beam-column joints frequently led to brittle failures and prevented structures from achieving higher global displacements before failure. Experimental evidence ([Pantelides et al. 2008](#); [Silva et al. 2007](#); [Pampanin et al. 2007](#); [Bracci et al. 1992b,c](#)) has shown that FRP systems can be effective for increasing the shear and energy dissipation capacity of unconfined joints. FRP layout and detailing will depend on the geometry of the existing joint and the number of members framing into it. FRP reinforcement in both directions is typically required at the joint to resist the cyclic loading effects of a seismic event ([Engindeniz et al. 2008a](#)). The FRP used to confine the joints should be anchored to be effective. [Pantelides et al. \(2008\)](#), [Silva et al. \(2007\)](#), and [Engindeniz et al. \(2008b\)](#) provide guidance on determining if FRP is a viable option for enhancing the performance of unconfined joints. Additionally, FRP reinforcement can be used to provide continuity across joints with discontinuous internal reinforcement ([Orton et al. 2009](#)).

13.7—Strengthening reinforced concrete shear walls

13.7.1 General considerations—This section presents design guidelines for the seismic strengthening of reinforced

concrete walls. Applying horizontal FRP strips along the height of the walls can increase the shear capacity of reinforced concrete shear walls. For short or squat walls, with height-to-length ratios less than 1.5, vertical FRP strips may also be required (ACI 318). Likewise, the in-plane flexural capacity of reinforced concrete shear walls can be increased by placing vertical FRP strips at the ends or boundaries of walls (Lombard et al. 2000; Hiotakis et al. 2004).

The shear strength of walls reinforced with FRP for flexure should be evaluated and compared to the shear strength corresponding to the nominal flexural strength of the retrofitted structure to promote a flexural failure rather than a brittle shear failure. Similarly, a shear retrofit should achieve greater shear capacity than the shear corresponding to the nominal flexural capacity of the wall. When this chapter is used in conjunction with ASCE/SEI 41, the flexure and shear in the strengthened portion of the wall should be considered force-controlled action unless a deformation-controlled classification is justified based on experimental data.

13.7.2 Flexural strengthening—FRP reinforcement for flexural strengthening of walls may be provided on one or both sides of the wall. Figure 13.7.2 shows a wall retrofitted with FRP reinforcement placed at the extreme ends of the wall. This figure also provides a description of the main variables required for design.

13.7.2.1 Concrete strain limits—The concrete compressive strains ϵ_c should be limited by Eq. (13.7.2.1a)

$$\epsilon_c = \epsilon_{fc} \left(\frac{1}{L_w/c - 1} \right) \leq \epsilon_{cu} \quad (13.7.2.1a)$$

where ϵ_{fd} corresponds to the strain at which debonding of the FRP may occur, per Eq. (10.1.1). In concrete shear walls, the concrete compressive strains at ultimate, ϵ_{cu} , should be limited to the following values (Wallace 1995)

$$\epsilon_{cu} \leq 0.010 \text{ for confined concrete at boundaries} \quad (13.7.2.1b)$$

$$\epsilon_{cu} \leq 0.003 \text{ for unconfined concrete at boundaries}$$

When confined boundary elements are required per Eq. (13.7.2.1b), means other than FRP may be required to meet the concrete strain requirements.

13.7.2.2 Anchorage of flexurally strengthened walls—Flexurally strengthened walls require anchorage to the foundations for load path continuity. Similarly, flexural FRP should be continuous through existing slabs to ensure continuity of the load path. Two conceptual methods for anchorage of a strengthened shear wall to the foundation are provided in Fig. 13.7.2.2. Any anchorage method, including the ones shown in Fig. 13.7.2.2, should be properly evaluated prior to field implementation. In shear walls, the vertical flexural FRP reinforcement does not need to be confined by transverse FRP strips or U-wraps that extend around the perimeter of the section.

13.7.3 Shear strengthening of reinforced concrete shear walls—Experimental investigations have demonstrated

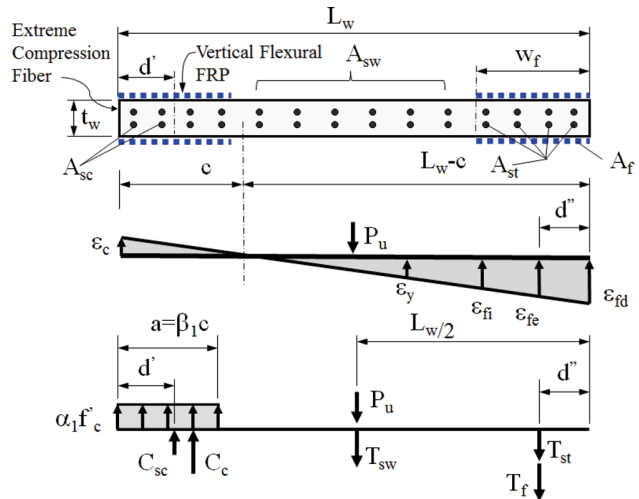


Fig. 13.7.2—FRP reinforcement for flexural strengthening.

the effectiveness of FRP for enhancing the shear performance of reinforced concrete walls subjected to seismic or cyclic loading (Haroun and Mosallam 2002; Khomwan and Foster 2005). The design shear strength ϕV_n of a reinforced concrete shear wall strengthened with FRP should satisfy Eq. (13.7.2.2a).

$$\phi V_n \geq V_u \quad (13.7.2.2a)$$

The strength reduction factor ϕ should be per the design standard being used for the rehabilitation.

For shear walls with externally bonded FRP, the nominal shear strength V_n can be computed using Eq. (13.7.2.2b)

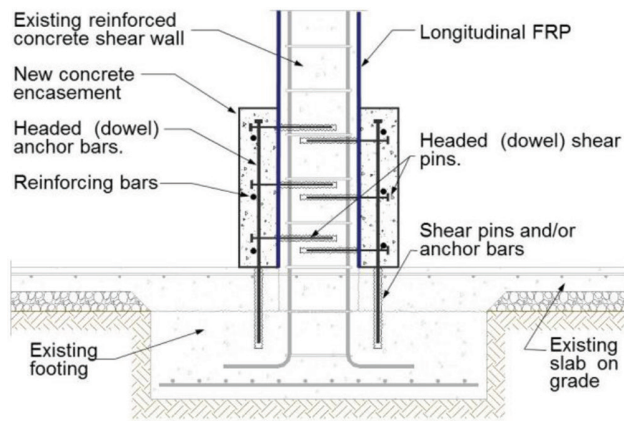
$$V_n = V_n^* + \psi_f V_f \quad (13.7.2.2b)$$

where V_n^* is the nominal shear strength of the existing shear wall; ψ_f is the reduction factor applied to the contribution of the FRP in accordance with Chapter 11; and V_f is the shear strength provided by the FRP. The shear strength enhancement for a wall section of length L_w in the direction of the applied shear force, with a laminate thickness t_f on two sides or one side of the wall, can be calculated using Eq. (13.7.2.2c) (Haroun et al. 2005)

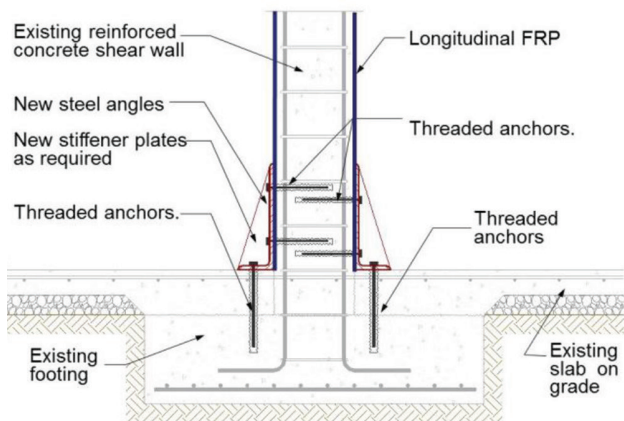
$$\text{for a two-sided retrofit: } V_f = 2t_f \epsilon_{fe} E_f d_{fv} \quad (13.7.2.2c)$$

$$\text{for a one-sided retrofit: } V_f = 0.75 t_f \epsilon_{fe} E_f d_{fv}$$

where d_{fv} is the effective depth of the shear wall, as defined by Chapter 18 of ACI 318-14, but not to exceed h_w , and ϵ_{fe} is according to 11.4.1 of this guide. FRP should be provided on two faces of the wall if the ratio of the existing transverse steel reinforcement to gross concrete area, ρ_t , is less than 0.0015. The intent of this provision is to ensure proper shear resistance of concrete in the event of severe cracking during a seismic event. The maximum nominal shear strength of a wall segment should not exceed the value given in Eq. (13.7.2.2d)



(a) Anchorage with concrete encasement



(b) Anchorage with steel angles

Fig. 13.7.2.2—Conceptual anchorage methods for strengthened shear wall.

$$V_n \leq 10\sqrt{f'_c}A_{cw} \quad (13.7.2.2d)$$

where A_{cw} is the area of the concrete section of an individual vertical wall.

13.7.3.1 Detailing of FRP shear reinforcement—Anchorage of shear FRP is considered good practice but it is not required to attain the shear strengths computed using the provisions of this chapter. Anchoring of the FRP shear reinforcement can be achieved by wrapping the FRP layers around the ends of the wall, by using mechanical anchorage devices such as steel anchors and steel plates (Paterson and Mitchell 2003), or by using FRP anchors (Binici and Ozcebe 2006).

The maximum clear spacing between the FRP shear strips should be limited to the minimum of one-fifth of the overall length of the wall, three times the thickness of the wall, or 18 in. (457 mm).

CHAPTER 14—FIBER-REINFORCED POLYMER REINFORCEMENT DETAILS

This chapter provides guidance for detailing externally bonded fiber-reinforced polymer (FRP) reinforcement. Detailing will typically depend on the geometry of the

structure, the soundness and quality of the substrate, and the levels of load that are to be sustained by the FRP sheets or laminates. Many bond-related failures can be avoided by following these general guidelines for detailing FRP sheets or laminates:

- Do not turn inside corners such as at the intersection of beams and joists or the underside of slabs
- Provide a minimum 1/2 in. (13 mm) radius when the sheet is wrapped around outside corners
- Provide adequate development length
- Provide sufficient overlap when splicing FRP plies

14.1—Bond and delamination

The actual distribution of bond stress in an FRP laminate is complicated by cracking of the substrate concrete. The general elastic distribution of interfacial shear stress and normal stress along an FRP laminate bonded to uncracked concrete is shown in Fig. 14.1.

The weak link in the concrete/FRP interface is the concrete. The soundness and tensile strength of the concrete substrate will limit the overall effectiveness of the bonded FRP system. Design requirements to mitigate FRP debonding failure modes are discussed in 10.1.1.

14.1.1 FRP debonding—In reinforced concrete members having relatively long shear spans or where the end peeling (refer to 14.1.2) has been effectively mitigated, debonding may initiate at flexural cracks, flexural/shear cracks, or both, near the region of maximum moment. Under loading, these cracks open and induce high local interfacial shear stress that initiates FRP debonding that propagates across the shear span in the direction of decreasing moment. Typically, this failure does not engage the aggregate in the concrete, progressing through the thin mortar-rich layer comprising the surface of the concrete substrate. This failure mode is exacerbated in regions having a high shear-moment ratio.

Anchorage systems, such as U-wraps, mechanical fasteners, fiber anchors, and near-surface-mounted (NSM) anchors, have been proven successful at delaying, and sometimes preventing, debonding failure of the longitudinal FRP (Kalfat et al. 2013; Grelle and Sneed 2013). Numerical and experimental studies have shown that these systems can increase the effective strain in the flexural FRP to values up to tensile rupture (Lee et al. 2010; Orton et al. 2008). A few studies have proposed analytical models to predict the behavior of specific anchor systems (Kim and Smith 2010); however, no published anchorage design guidelines are currently available. Therefore, the performance of any anchorage system should be substantiated through representative physical testing.

14.1.2 FRP end peeling—FRP end peeling (also referred to as concrete cover delamination) can result from the normal stresses developed at the ends of externally bonded FRP reinforcement. With this type of delamination, the existing internal reinforcing steel provides a weak horizontal plane along which the concrete cover pulls away from the rest of the beam, as shown in Fig. 14.1.2a.

The tensile concrete cover splitting failure mode is controlled, in part, by stress at the termination point of

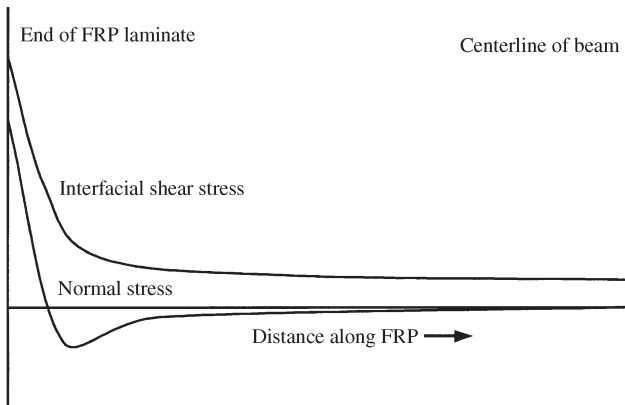


Fig. 14.1—Conceptual interfacial shear and normal stress distributions along the length of a bonded FRP laminate (Roberts and Haji-Kazemi 1989; Malek et al. 1998).

the FRP. In general, the FRP end peeling failure mode can be mitigated by using anchorage (U-wraps, mechanical fasteners, fiber anchors, or NSM anchors), by minimizing the stress at the FRP curtailment by locating the curtailment as close to the region of zero moment as possible, or by both. When the factored shear force at the termination point is greater than two-thirds of the concrete shear strength ($V_u > 0.67V_c$), the FRP laminates should be anchored with transverse reinforcement to prevent the concrete cover layer from splitting. The area of the transverse clamping FRP U-wrap reinforcement, $A_{fanchor}$, can be determined in accordance with Eq. (14.1.2) (Reed et al. 2005)

$$A_{fanchor} = \frac{(A_f f_{fe})_{longitudinal}}{(E_f \kappa_v \epsilon_{fu})_{anchor}} \quad (14.1.2)$$

in which κ_v is calculated using Eq. (11.4.1.2b). Instead of detailed analysis, the following general guidelines for the location of cutoff points for the FRP laminate can be used to avoid end peeling failure mode:

a) For simply supported beams, a single-ply FRP laminate should be terminated at least a distance equal to ℓ_{df} past the point along the span at which the resisted moment falls below the cracking moment M_{cr} . For multiple-ply laminates, the termination points of the plies should be tapered. The outermost ply should be terminated not less than ℓ_{df} past the point along the span at which the resisted moment falls below the cracking moment. Each successive ply should be terminated not less than an additional 6 in. (150 mm) beyond the previous ply (Fig. 14.1.2b).

b) For continuous beams, a single-ply FRP laminate should be terminated at least a distance $d/2$ or 6 in. (150 mm) beyond the inflection point (point of zero moment resulting from factored loads). For multiple-ply laminates, the termination points of the plies should be tapered. The outermost ply should be terminated no less than 6 in. (150 mm) beyond the inflection point. Each successive ply should be terminated not less than an additional 6 in. (150 mm) beyond the previous ply. For example, if a three-ply laminate is required, the ply directly in contact with the concrete substrate should

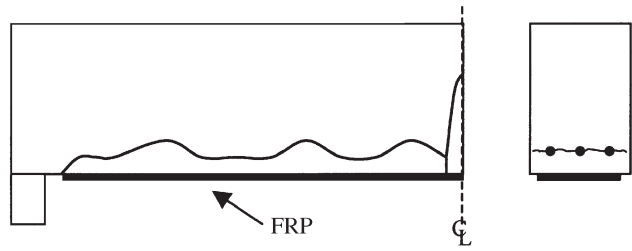


Fig. 14.1.2a—Delamination caused by tension failure of the concrete cover.

be terminated at least 18 in. (450 mm) past the inflection point (Fig. 14.1.2b). These guidelines apply for positive and negative moment regions.

14.1.3 Development length—The bond capacity of FRP is developed over a critical length ℓ_{df} . To develop the effective FRP stress at a section, the available anchorage length of FRP should exceed the value given by Eq. (14.1.3) (Teng et al. 2003).

$$\ell_{df} = 0.057 \sqrt{\frac{nE_f t_f}{\sqrt{f'_c}}} \quad (\text{in.-lb}) \quad (14.1.3)$$

$$\ell_{df} = \sqrt{\frac{nE_f t_f}{\sqrt{f'_c}}} \quad (\text{SI})$$

14.2—Detailing of laps and splices

Splices of FRP laminates should be provided only as permitted on drawings, specifications, or as authorized by the licensed design professional as recommended by the system manufacturer.

The fibers of FRP systems should be continuous and oriented in the direction of the largest tensile forces. Fiber continuity can be maintained with a lap splice. For FRP systems, a lap splice should be made by overlapping the fibers along their length. The required overlap, or lap-splice length, depends on the tensile strength and thickness of the FRP material system and on the bond strength between adjacent layers of FRP laminates. Sufficient overlap should be provided to promote the failure of the FRP laminate before debonding of the overlapped FRP laminates. The required overlap for an FRP system should be provided by the material manufacturer and substantiated through testing that is independent of the manufacturer.

Jacket-type FRP systems used for column members should provide appropriate development area at splices, joints, and termination points to ensure failure through the FRP jacket thickness rather than failure of the spliced sections.

For unidirectional FRP laminates, lap splices are required only in the direction of the fibers. Lap splices are not required in the direction transverse to the fibers. FRP laminates consisting of multiple unidirectional sheets oriented in more than one direction or multidirectional fabrics require lap splices in more than one direction to maintain the continuity of the fibers and the overall strength of the FRP laminates.

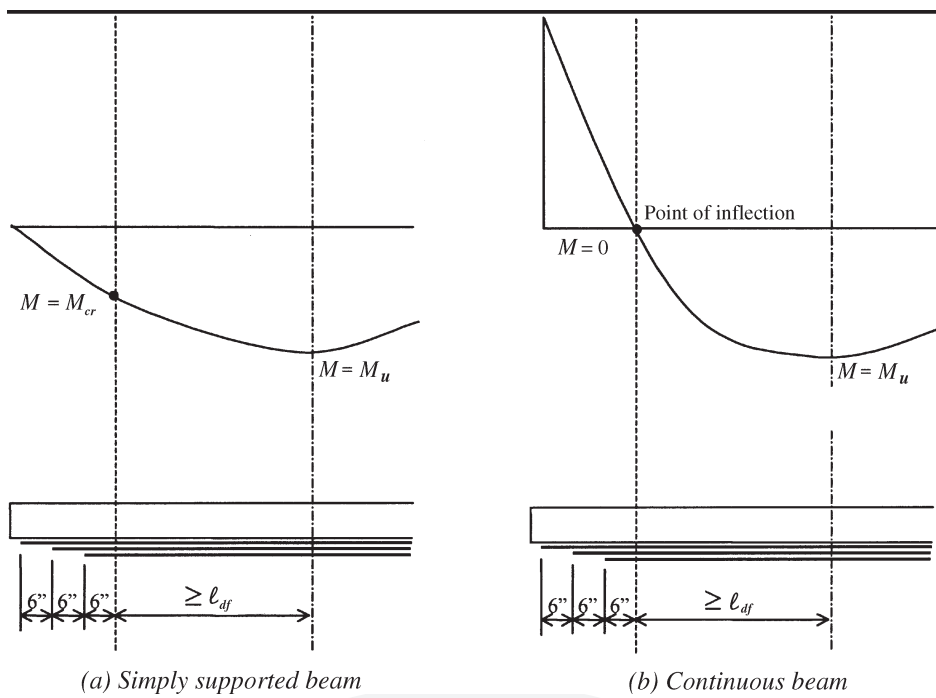


Fig. 14.1.2b—Graphical representation of the guidelines for allowable termination points of a three-ply FRP laminate.

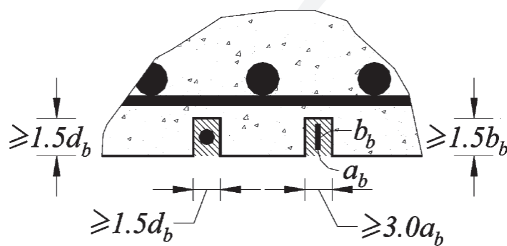


Fig. 14.3a—Minimum dimensions of grooves.

14.3—Bond of near-surface-mounted systems

For near-surface-mounted (NSM) systems, the minimum dimension of the grooves should be taken at least 1.5 times the diameter of the FRP bar (De Lorenzis and Nanni 2001; Hassan and Rizkalla 2003). When a rectangular bar with a large aspect ratio is used, however, the limit may lose significance due to constructibility. In such a case, a minimum groove size of $3.0a_b \times 1.5b_b$, as depicted in Fig. 14.3a, is suggested, where a_b is the smallest bar dimension. The minimum clear groove spacing for NSM FRP bars should be greater than twice the depth of the NSM groove to avoid overlapping of the tensile stresses around the NSM bars. Furthermore, a clear edge distance of four times the depth of the NSM groove should be provided to minimize edge effects that could accelerate debonding failure (Hassan and Rizkalla 2003).

Bond properties of NSM FRP bars depend on many factors such as cross-sectional shape and dimensions and surface properties of the FRP bar (Hassan and Rizkalla 2003; De Lorenzis et al. 2004). Figure 14.3b shows the equilibrium condition of an NSM FRP bar with an embedded length equal to its development length ℓ_{db} having a bond strength of τ_{max} . Using a triangular stress distribution, the average

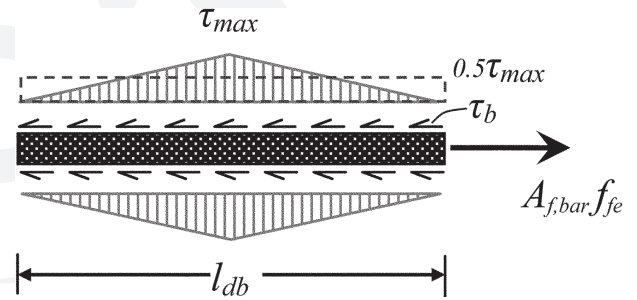


Fig. 14.3b—Transfer of force in NSM FRP bars.

bond strength can be expressed as $\tau_b = 0.5\tau_{max}$. Average bond strength τ_b for NSM FRP bars in the range of 500 to 3000 psi (3.5 to 20.7 MPa) has been reported (Hassan and Rizkalla 2003; De Lorenzis et al. 2004); therefore, $\tau_b = 1000$ psi (6.9 MPa) is recommended for calculating the bar development length. Using force equilibrium, the following equations for development length can be derived

$$\ell_{db} = \frac{d_b}{4\tau_b} f_{jd} \text{ for circular bars} \quad (14.3a)$$

$$\ell_{db} = \frac{a_b b_b}{2(a_b + b_b)(\tau_b)} f_{jd} \text{ for rectangular bars} \quad (14.3b)$$

CHAPTER 15—DRAWINGS, SPECIFICATIONS, AND SUBMITTALS

15.1—Engineering requirements

Although federal, state, and local codes for the design of externally bonded fiber-reinforced polymer (FRP) systems do not exist, other applicable code requirements may influence the selection, design, and installation of the FRP system. For example, code requirements related to fire or potable water may influence the selection of the coatings used with the FRP system. All design work should be performed under the guidance of a licensed design professional familiar with the properties and applications of FRP strengthening systems.

15.2—Drawings and specifications

The licensed design professional should document calculations summarizing the assumptions and parameters used to design the FRP strengthening system and should prepare design drawings and project specifications. The drawings and specifications should show, at a minimum, the following information specific to externally applied FRP systems:

- a) FRP system to be used
- b) Location of the FRP system relative to the existing structure
- c) Dimensions and orientation of each ply, laminate, or near-surface-mounted (NSM) bar
- d) Number of plies and bars and the sequence of installation
- e) Location of splices and lap length
- f) General notes listing design loads and allowable strains in the FRP laminates
- g) Material properties of the FRP laminates and concrete substrate
- h) Concrete surface preparation requirements, including corner preparation, groove dimensions for NSM bars, and maximum irregularity limitations
- i) Installation procedures, including surface temperature and moisture limitations, and application time limits between successive plies
- j) Curing procedures for FRP systems
- k) Protective coatings and sealants, if required
- l) Shipping, storage, handling, and shelf-life guidelines
- m) Quality control and inspection procedures, including acceptance criteria
- n) In-place load testing of installed FRP system, if necessary

15.3—Submittals

Specifications should require the FRP system manufacturer, installation contractor, and inspection agency (if required) to submit product information and evidence of their qualifications and experience to the licensed design professional for review.

15.3.1 FRP system manufacturer—Submittals required of the FRP system manufacturer should include:

- a) Indication of compliance with existing specifications (such as ACI 440.8) as applicable
- b) Product data sheets indicating the physical, mechanical, and chemical characteristics of the FRP system and all its constituent materials
- c) Tensile properties of the FRP system, including the method of reporting properties (net fiber or gross laminate), test methods used, and the statistical basis used for determining the properties (4.3)
- d) Installation instructions, maintenance instructions, and general recommendations regarding each material to be used; installation procedures should include surface preparation requirements
- e) Manufacturer's Safety Data Sheets (SDSs) for all materials to be used
- f) Quality control procedure for tracking FRP materials and material certifications
- g) Durability test data for the FRP system in the types of environments expected
- h) Structural test reports pertinent to the proposed application
- i) Reference projects

15.3.2 FRP system installation contractor—Submittals required of the FRP system installation contractor should include:

- a) Documentation from the FRP system manufacturer of having been trained to install the proposed FRP system
- b) Project references, including installations similar to the proposed installation (for example, for an overhead application, the contractor should submit a list of previous installations involving the installation of the proposed FRP system in an overhead application)
- c) Evidence of competency in surface preparation techniques
- d) Quality control testing procedures including voids and delaminations, FRP bond to concrete, and FRP tensile properties
- e) Daily log or inspection forms used by the contractor

15.3.3 FRP system inspection agency—If an independent inspection agency is used, submittals required of that agency should include:

- a) A list of inspectors to be used on the project and their qualifications
- b) Sample inspection forms
- c) A list of previous projects inspected by the inspector

CHAPTER 16—DESIGN EXAMPLES

16.1—Calculation of FRP system tensile properties

This example calculation shown in Table 16.1b illustrates the derivation of material properties based on net-fiber area versus the properties based on gross-laminate area. As described in 4.3.1, both methods of determining material properties are valid. It is important, however, that any design calculations consistently use material properties based on only one of the two methods (for example, if the gross-laminate thickness is used in any calculation, the strength based on gross-laminate area should be used in the calculations as well). Reported design properties should be based on a population of 20 or more coupons tested in accordance with ASTM D3039/D3039M. Reported properties should be statistically adjusted by subtracting three standard deviations from the mean tensile stress and strain, as discussed in 4.3.1.

A test panel is fabricated from two plies of a carbon fiber/resin unidirectional fiber-reinforced polymer (FRP) system

Table 16.1a—FRP system tension test results

Coupon ID	Specimen width		Measured coupon thickness		Measured rupture load	
	in.	mm.	in.	mm.	kips	kN
T-1	2	50.8	0.055	1.40	17.8	79.2
T-2	2	50.8	0.062	1.58	16.4	72.9
T-3	2	50.8	0.069	1.75	16.7	74.3
T-4	2	50.8	0.053	1.35	16.7	74.3
T-5	2	50.8	0.061	1.55	17.4	77.4
Average	2	50.8	0.060	1.52	17.0	75.6

using the wet layup technique. Based on the known fiber content of this FRP system, the net-fiber area is 0.0065 in.²/in. (0.165 mm²/mm) width per ply. After the system has cured, five 2 in. (50.8 mm) wide test coupons are cut from the panel. The test coupons are tested in tension to failure in accordance with ASTM D3039/D3039M. Tabulated in Table 16.1a are the results of the tension tests.

Table 16.1b—FRP system net fiber and gross laminate property calculations

Net-fiber area property calculations		Gross-laminate area property calculations	
Calculate A_f using the known, net-fiber area ply thickness: $A_f = nt_p w_f$	$A_f = (2)(0.0065 \text{ in.}^2/\text{in.})(2 \text{ in.}) = 0.026 \text{ in.}^2$ $A_f = (2)(0.165 \text{ mm}^2/\text{mm})(50.8 \text{ mm}) = 16.8 \text{ mm}^2$	Calculate A_f using the average, measured laminate thickness: $A_f = t_p w_f$	$A_f = (0.060 \text{ in.})(2 \text{ in.}) = 0.120 \text{ in.}^2$ $A_f = (1.52 \text{ mm})(50.8 \text{ mm}) = 77.4 \text{ mm}^2$
Calculate the average FRP system tensile strength based on net-fiber area: $\bar{f}_{fu} = \frac{\text{average rupture load}}{A_f}$	$\bar{f}_{fu} = \frac{17 \text{ kip}}{0.026 \text{ in.}^2} = 650 \text{ ksi}$ $\bar{f}_{fu} = \frac{75.62 \text{ kN}}{16.8 \text{ mm}^2} = 4.5 \text{ kN/mm}^2$	Calculate the average FRP system tensile strength based on gross-laminate area: $\bar{f}_{fu} = \frac{\text{average rupture load}}{A_f}$	$\bar{f}_{fu} = \frac{17 \text{ kip}}{0.120 \text{ in.}^2} = 140 \text{ ksi}$ $\bar{f}_{fu} = \frac{75.62 \text{ kN}}{77.4 \text{ mm}^2} = 0.997 \text{ kN/mm}^2$
Calculate the average FRP system tensile strength per unit width based on net-fiber area: $\bar{p}_{fu} = \frac{\bar{f}_{fu} A_f}{w_f}$	$\bar{p}_{fu} = \frac{(650 \text{ ksi})(0.026 \text{ in.}^2)}{2 \text{ in.}} = 8.4 \text{ kip/in.}$ $\bar{p}_{fu} = \frac{(4.5 \text{ kN/mm}^2)(16.8 \text{ mm}^2)}{50.8 \text{ mm}} = 1.49 \text{ kN/mm}$	Calculate the average FRP system tensile strength per unit width based on laminate area: $\bar{p}_{fu} = \frac{\bar{f}_{fu} A_f}{w_f}$	$\bar{p}_{fu} = \frac{(140 \text{ ksi})(0.120 \text{ in.}^2)}{2 \text{ in.}} = 8.4 \text{ kip/in.}$ $\bar{p}_{fu} = \frac{(0.98 \text{ kN/mm}^2)(77.4 \text{ mm}^2)}{50.8 \text{ mm}} = 1.49 \text{ kN/mm}$

16.2—Comparison of FRP systems' tensile properties

Two FRP systems are being considered for strengthening concrete members. The mechanical properties of two FRP systems are available from respective manufacturers. System A consists of dry, carbon-fiber unidirectional sheets and is installed with an adhesive resin using the wet layup technique. System B consists of precured carbon fiber/resin laminates that are bonded to the concrete surface with an

adhesive resin. Excerpts from the data sheets provided by the FRP system manufacturers are given in Table 16.2a. After reviewing the material data sheets sent by the FRP system manufacturers, the licensed design professional compares the tensile strengths of the two systems.

Because the data sheets for both systems are reporting statistically based properties, it is possible to directly compare the tensile strength and modulus of both systems, as shown in Table 16.2b.

Table 16.2a—Material properties and description of two types of FRP systems

System A (excerpts from data sheet)	System B (excerpts from data sheet)
System type: dry, unidirectional sheet Fiber type: high-strength carbon Polymer resin: epoxy System A is installed using a wet layup procedure where the dry carbon-fiber sheets are impregnated and adhered with an epoxy resin on-site.	System type: precured, unidirectional laminate Fiber type: high-strength carbon Polymer resin: epoxy System B's precured laminates are bonded to the concrete substrate using System B's epoxy paste adhesive.
Mechanical properties**†	Mechanical properties*†
$t_f = 0.013$ in. (0.33 mm)	$t_f = 0.050$ in. (1.27 mm)
$f_{fu}^* = 550$ ksi (3792 N/mm ²)	$f_{fu}^* = 380$ ksi (2620 N/mm ²)
$\epsilon_{fu}^* = 1.6\%$	$\epsilon_{fu}^* = 1.5\%$
$E_f = 33,000$ ksi (227,527 N/mm ²)	$E_f = 22,000$ ksi (151,724 N/mm ²)

*Reported properties are based on a population of 20 or more coupons tested in accordance with ASTM D3039/D3039M.

†Reported properties have been statistically adjusted by subtracting three standard deviations from the mean tensile stress and strain.

**Thickness is based on the net-fiber area for one ply of the FRP system. Resin is excluded. Actual installed thickness of cured FRP is 0.04 to 0.07 in. (1.0 to 1.8 mm) per ply.

Table 16.2b—Procedure comparing two types of FRP systems

Procedure	Calculation in in.-lb units	Calculation in SI units
Step 1A—Calculate the tensile strength per unit width of System A $p_{fu}^* = f_{fu}^* t_f$	$p_{fu}^* = (550 \text{ ksi})(0.013 \text{ in.}) = 7.15 \text{ kip/in.}$	$p_{fu}^* = (3.79 \text{ kN/mm}^2)(0.33 \text{ mm}) = 1.25 \text{ kN/mm}$
Step 1B—Calculate the tensile strength per unit width of System B $p_{fu}^* = f_{fu}^* t_f$	$p_{fu}^* = (380 \text{ ksi})(0.050 \text{ in.}) = 19 \text{ kip/in.}$	$p_{fu}^* = (2.62 \text{ kN/mm}^2)(1.27 \text{ mm}) = 3.33 \text{ kN/mm}$
Step 2A—Calculate the tensile modulus per unit width of System A $k_f = E_f t_f$	$k_f = (33,000 \text{ ksi})(0.013 \text{ in.}) = 429 \text{ kip/in.}$	$k_f = (227.5 \text{ kN/mm}^2)(0.33 \text{ mm}) = 75.1 \text{ kN/mm}$
Step 2B—Calculate the tensile modulus per unit width of System B $k_f = E_f t_f$	$k_f = (22,000 \text{ ksi})(0.050 \text{ in.}) = 1100 \text{ kip/in.}$	$k_f = (151.7 \text{ kN/mm}^2)(1.27 \text{ mm}) = 192.7 \text{ kN/mm}$
Step 3—Compare the two systems Compare the tensile strengths: p_{fu}^* (System A) p_{fu}^* (System B)	$\frac{p_{fu}^* (\text{System B})}{p_{fu}^* (\text{System A})} = \frac{19 \text{ kip/in.}}{7.15 \text{ kip/in.}} = 2.66$ \therefore three plies of System A are required for each ply of System B for an equivalent tensile strength	$\frac{p_{fu}^* (\text{System B})}{p_{fu}^* (\text{System A})} = \frac{3.33 \text{ kN/mm}}{1.25 \text{ kN/mm}} = 2.66$ \therefore three plies of System A are required for each ply of System B for an equivalent tensile strength
Compare the stiffnesses: k_f (System A) k_f (System B)	$\frac{k_f (\text{System B})}{k_f (\text{System A})} = \frac{1100 \text{ kip/in.}}{429 \text{ kip/in.}} = 2.56$ \therefore three plies of System A are required for each ply of System B for an equivalent stiffness	$\frac{k_f (\text{System A})}{k_f (\text{System B})} = \frac{192.7 \text{ kN/mm}}{75.1 \text{ kN/mm}} = 2.56$ \therefore three plies of System A are required for each ply of System B for an equivalent stiffness

Because all the design procedures outlined in this document limit the strain in the FRP material, the full nominal strength of the material is not used and should not be the basis of comparison between two material systems. When considering various FRP material systems for a particular application, the FRP systems should be compared based on equivalent stiffness only. In addition, each FRP system under consideration should have the ability to develop the strain associated with the effective strain required by the application without rupturing, $\varepsilon_{fu} > \varepsilon_{fe}$.

In many instances, it may be possible to vary the width of the FRP strip as opposed to the number of plies (use larger widths for systems with lower thicknesses and vice versa). In such instances, equivalent stiffness calculations typically will not yield equivalent contributions to the strength of a member. In general, thinner (lower nt_f) and wider (higher w_f) FRP systems will provide a higher level of strength to a member due to lower bond stresses. The exact equivalency, however, can only be found by performing complete calculations (according to procedures described in [Chapters 10, 11, and 12](#) of this guide) for each system.



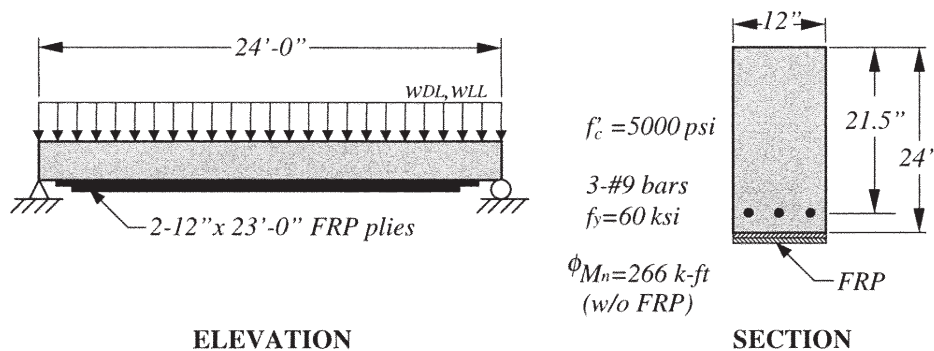
16.3—Flexural strengthening of an interior reinforced concrete beam with FRP laminates

A simply supported concrete beam reinforced with three No. 9 bars (Fig. 16.3) is located in an unoccupied warehouse and is subjected to a 50 percent increase in its live-load-carrying requirements. An analysis of the existing beam indicates that the beam still has sufficient shear strength to resist the new required shear strength and meets the deflection and crack-control serviceability requirements. Its flexural strength, however, is inadequate to carry the increased live load.

Summarized in Table 16.3a are the existing and new loadings and associated midspan moments for the beam. The

existing reinforced concrete beam should be strengthened with the FRP system described in Table 16.3b, specifically, two 12 in. (305 mm) wide x 23.0 ft (7 m) long plies bonded to the soffit of the beam using the wet layup technique.

By inspection, the degree of strengthening is reasonable in that it does meet the strengthening limit criteria specified in Eq. (9.2). That is, the existing moment strength without FRP, $(\phi M_n)_{w/o} = 266$ kip-ft (361 kN-m), is greater than the unstrengthened moment limit, $(1.1M_{DL} + 0.75M_{LL})_{new} = 177$ kip-ft (240 kN-m). The design calculations used to verify this configuration follow in Table 16.3c.



Length of the beam ℓ	24 ft	7.32 m
Width of the beam w	12 in.	305 mm
d	21.5 in.	546 mm
h	24 in.	609.6 mm
f'_c	5000 psi	34.5 N/mm ²
f_y	60 ksi	414 N/mm ²
ϕM_n without FRP	266 k-ft	361 kN-m
Bars	No. 9	$\phi = 28.6$ mm

Fig. 16.3—Schematic of the idealized simply supported beam with FRP external reinforcement.

Table 16.3a—Loadings and corresponding moments

Loading/moment	Existing loads		Anticipated loads	
Dead loads w_{DL}	1.00 kip/ft	14.6 N/mm	1.00 kip/ft	14.6 N/mm
Live load w_{LL}	1.20 kip/ft	17.5 N/mm	1.80 kip/ft	26.3 N/mm
Unfactored loads ($w_{DL} + w_{LL}$)	2.20 kip/ft	32.1 N/mm	2.80 kip/ft	40.9 N/mm
Unstrengthened load limit ($1.1w_{DL} + 0.75w_{LL}$)	NA	NA	2.50 kip/ft	35.8 N/mm
Factored loads ($1.2w_{DL} + 1.6w_{LL}$)	3.12 kip/ft	45.5 N/mm	4.08 kip/ft	59.6 N/mm
Dead-load moment M_{DL}	72 kip-ft	98 kN-m	72 kip-ft	98 kN-m
Live-load moment M_{LL}	86 kip-ft	117 kN-m	130 kip-ft	176 kN-m
Service-load moment M_s	158 kip-ft	214 kN-m	202 kip-ft	274 kN-m
Unstrengthened moment limit ($1.1M_{DL} + 0.75M_{LL}$)	NA	NA	177 kip-ft	240 kN-m
Factored moment M_u	224 kip-ft	304 kN-m	294.4 kip-ft	399 kN-m

Table 16.3b—Manufacturer’s reported FRP system properties

Thickness per ply t_f	0.040 in.	1.02 mm
Ultimate tensile strength f_{fu}^*	90 ksi	621 N/mm ²
Rupture strain ϵ_{fu}^*	0.015 in./in.	0.015 mm/mm
Modulus of elasticity of FRP laminates E_f	5360 ksi	37,000 N/mm ²

Table 16.3c—Procedure for flexural strengthening of an interior reinforced concrete beam with fiber-reinforced polymer laminates

Procedure	Calculation in in.-lb units	Calculation in SI metric units
Step 1—Calculate the FRP system design material properties The beam is located in an interior space and a carbon FRP (CFRP) material will be used. Therefore, per Table 9.4, an environmental reduction factor of 0.95 is suggested. $f_{fu} = C_E f_{fu}^*$ $\epsilon_{fu} = C_E \epsilon_{fu}^*$	$f_{fu} = (0.95)(90 \text{ ksi}) = 85 \text{ ksi}$ $\epsilon_{fu} = (0.95)(0.015 \text{ in./in.}) = 0.0142 \text{ in./in.}$	$f_{fu} = (0.95)(621 \text{ N/mm}^2) = 590 \text{ N/mm}^2$ $\epsilon_{fu} = (0.95)(0.015 \text{ mm/mm}) = 0.0142 \text{ mm/mm}$
Step 2—Preliminary calculations Properties of the concrete: β_1 from ACI 318-14, Section 22.2.2.4.3 $E_c = 57,000 \sqrt{f'_c}$ Properties of the existing reinforcing steel: Properties of the externally bonded FRP reinforcement: $A_f = n t_f w_f$	$\beta_1 = 1.05 - 0.05(f'_c/1000) = 0.80$ $E_c = 57,000 \sqrt{5000 \text{ psi}} = 4,030,000 \text{ psi}$ $A_s = 3(1.00 \text{ in.}^2) = 3.00 \text{ in.}^2$ $A_f = (2 \text{ plies})(0.040 \text{ in./ply})(12 \text{ in.}) = 0.96 \text{ in.}^2$	$\beta_1 = 1.05 - 0.05(f'_c/1000) = 0.80$ $E_c = 4700 \sqrt{34.5 \text{ N/mm}^2} = 27,600 \text{ N/mm}^2$ $A_s = 3(645 \text{ mm}^2) = 1935 \text{ mm}^2$ $A_f = (2 \text{ plies})(1.02 \text{ mm/ply})(305 \text{ mm}) = 619 \text{ mm}^2$
Step 3—Determine the existing state of strain on the soffit The existing state of strain is calculated assuming the beam is cracked and the only loads acting on the beam at the time of the FRP installation are dead loads. A cracked section analysis of the existing beam gives $k = 0.334$ and $I_{cr} = 5937 \text{ in.}^4 = 2471 \times 10^6 \text{ mm}^4$ $\epsilon_{bi} = \frac{M_{DL}(d_f - kd)}{I_{cr} E_c}$	$\epsilon_{bi} = \frac{(864 \text{ kip-in.})[24 \text{ in.} - (0.334)(21.5 \text{ in.})]}{(5937 \text{ in.}^4)(4030 \text{ ksi})}$ $= 0.00061$	$\epsilon_{bi} = \frac{(97.6 \text{ kN-mm})[609.6 \text{ mm} - (0.334)(546.1 \text{ mm})]}{(2471 \times 10^6 \text{ mm}^4)(27.6 \text{ kN/mm}^2)}$ $= 0.00061$
Step 4—Determine the design strain of the FRP system The design strain of FRP accounting for debonding failure mode ϵ_{fd} is calculated using Eq. (10.1.1) Because the design strain is smaller than the rupture strain, debonding controls the design of the FRP system.	$\epsilon_{fd} = 0.083 \sqrt{\frac{5000 \text{ psi}}{2(5,360,000 \text{ psi})(0.04 \text{ in.})}}$ $= 0.009 \leq 0.9(0.0142) = 0.0128$	$\epsilon_{fd} = 0.41 \sqrt{\frac{34.5 \text{ N/mm}^2}{2(37,000 \text{ N/mm}^2)(1.02 \text{ mm})}}$ $= 0.009 \leq 0.9(0.0142) = 0.0128$

Table 16.3c (cont.)—Procedure for flexural strengthening of an interior reinforced concrete beam with fiber-reinforced polymer laminates

Procedure	Calculation in in.-lb units	Calculation in SI metric units
<p>Step 5—Estimate c, the depth to the neutral axis</p> <p>A reasonable initial estimate of c is $0.20d$. The value of the c is adjusted after checking equilibrium.</p> $c = 0.20d$	$c = (0.20)(21.5 \text{ in.}) = 4.30 \text{ in.}$	$c = (0.20)(546.1 \text{ mm}) = 109 \text{ mm}$
<p>Step 6—Determine the effective level of strain in the FRP reinforcement</p> <p>The effective strain level in the FRP may be found from Eq. (10.2.5).</p> $\epsilon_{fe} = 0.003 \left(\frac{d_f - c}{c} \right) = \epsilon_{bi} \leq \epsilon_{fd}$ <p>Note that for the neutral axis depth selected, FRP debonding would be in the failure mode because the second expression in this equation controls. If the first expression governed, then concrete crushing would be in the failure mode. Because FRP controls the failure of the section, the concrete strain at failure ϵ_c may be less than 0.003 and can be calculated using similar triangles:</p> $\epsilon_c = (\epsilon_{fe} + \epsilon_{bi}) \left(\frac{c}{d_f - c} \right)$	$\epsilon_{fe} = 0.003 \left(\frac{24 \text{ in.} - 4.3 \text{ in.}}{4.3 \text{ in.}} \right) - 0.00061 \leq 0.009$ $\epsilon_{fe} = 0.0131 > 0.009$ $\epsilon_{fe} = \epsilon_{fd} = 0.009$ $\epsilon_c = (0.09 + 0.00061) \left(\frac{4.3 \text{ in.}}{24 \text{ in.} - 4.3 \text{ in.}} \right) = 0.0021$	$\epsilon_{fe} = 0.003 \left(\frac{609.6 \text{ mm} - 109.2 \text{ mm}}{109.2 \text{ mm}} \right) - 0.00061 \leq 0.009$ $\epsilon_{fe} = 0.0131 > 0.009$ $\epsilon_{fe} = \epsilon_{fd} = 0.009$ $\epsilon_c = (0.009 + 0.00061) \left(\frac{109.2 \text{ mm}}{609.6 \text{ mm} - 109.2 \text{ mm}} \right) = 0.0021$
<p>Step 7—Calculate the strain in the existing reinforcing steel</p> <p>The strain in the reinforcing steel can be calculated using similar triangles according to Eq. (10.2.6).</p> $\epsilon_s = (\epsilon_{fe} + \epsilon_{bi}) \left(\frac{c}{d_f - c} \right)$	$\epsilon_s = (0.09 + 0.00061) \left(\frac{21.5 \text{ in.} - 4.3 \text{ in.}}{24 \text{ in.} - 4.3 \text{ in.}} \right) = 0.0084$	$\epsilon_s = (0.09 + 0.00061) \left(\frac{546.1 \text{ mm} - 109.2 \text{ mm}}{609.6 \text{ mm} - 109.2 \text{ mm}} \right) = 0.0084$
<p>Step 8—Calculate the stress level in the reinforcing steel and FRP</p> <p>The stresses are calculated using Eq. (10.2.10b) and Hooke's Law.</p> $f_s = E_s \epsilon_s \leq f_y$ $f_{fe} = E_f \epsilon_{fe}$	$f_s = (29,000 \text{ ksi})(0.0084) \leq 60 \text{ ksi}$ $f_s = 244 \text{ ksi} \leq 60 \text{ ksi}$ <p>Hence, $f_s = 60 \text{ ksi}$</p> $f_{fe} = (5360 \text{ ksi})(0.009) = 48.2 \text{ ksi}$	$f_s = (200 \text{ kN/mm}^2)(0.0084) \leq 0.414 \text{ kN/mm}^2$ $f_s = 1.68 \text{ kN/mm}^2 \leq 0.414 \text{ kN/mm}^2$ <p>Hence, $f_s = 0.414 \text{ kN/mm}^2$</p> $f_{fe} = (37 \text{ kN/mm}^2)(0.009) = 0.33 \text{ kN/mm}^2$

Table 16.3c (cont.)—Procedure for flexural strengthening of an interior reinforced concrete beam with fiber-reinforced polymer laminates

Procedure	Calculation in in.-lb units	Calculation in SI metric units
<p>Step 9—Calculate the internal force resultants and check equilibrium</p> <p>Concrete stress block factors may be calculated using ACI 318. Approximate stress block factors may also be calculated based on the parabolic stress-strain relationship for concrete as follows:</p> $\beta_1 = \frac{4\epsilon'_c - \epsilon_c}{6\epsilon'_c - 2\epsilon_c}$ $\alpha_1 = \frac{3\epsilon'_c \epsilon_c - \epsilon_c^2}{3\beta_1 \epsilon_c^2}$ <p>where ϵ'_c is strain corresponding to f'_c calculated as</p> $\epsilon'_c = \frac{1.7f'_c}{E_c}$ <p>Force equilibrium is verified by checking the initial estimate of c with Eq. (10.3.1.6g).</p> $c = \frac{A_s f_s + A_f f_{fe}}{\alpha_1 f_c \beta_1 b}$	$\beta_1 = \frac{4(0.0021) - 0.0021}{6(0.0021) - 2(0.0021)} = 0.749$ $\alpha_1 = \frac{3(0.0021)(0.0021) - (0.0021)^2}{3(0.749)(0.0021)^2} = 0.886$ $\epsilon'_c = \frac{1.7(5000)}{4.03 \times 10^6} = 0.0021$ $c = \frac{(3.00 \text{ in.}^2)(60 \text{ ksi}) + (0.96 \text{ in.}^2)(48.2 \text{ ksi})}{(0.886)(5 \text{ ksi})(0.749)(12 \text{ in.})}$ <p>$c = 5.68 \text{ in.} \neq 4.30 \text{ in. n.g.}$ \therefore revise estimate of c and repeat Steps 6 through 9 until equilibrium is achieved.</p>	$\beta_1 = \frac{4(0.0021) - 0.0021}{6(0.0021) - 2(0.0021)} = 0.749$ $\alpha_1 = \frac{3(0.0021)(0.0021) - (0.0021)^2}{3(0.749)(0.0021)^2} = 0.886$ $\epsilon'_c = \frac{1.7(34.5)}{27,600} = 0.0021$ $c = \frac{(1935.48 \text{ mm}^2)(414 \text{ N/mm}^2) + (619 \text{ mm}^2)(330 \text{ N/mm}^2)}{(0.886)(34.5 \text{ N/mm}^2)(0.749)(304.8 \text{ mm})}$ <p>$c = 149 \text{ mm} \neq 109 \text{ mm n.g.}$ \therefore revise estimate of c and repeat Steps 6 through 9 until equilibrium is achieved.</p>
<p>Step 10—Adjust c until force equilibrium is satisfied</p> <p>Steps 6 through 9 were repeated several times with different values of c until equilibrium was achieved. The results of the final iteration are</p> <p>$c = 5.17 \text{ in.}; \epsilon_s = 0.0083; f_s = f_y = 60 \text{ ksi}; \beta_1 = 0.786; \alpha_1 = 0.928; \text{ and } f_{fd} = 48.2 \text{ ksi}$</p>	$c = \frac{(3.00 \text{ in.}^2)(60 \text{ ksi}) + (0.96 \text{ in.}^2)(48.2 \text{ ksi})}{(0.925)(5 \text{ ksi})(0.786)(12 \text{ in.})}$ <p>$c = 5.17 \text{ in.}$ \therefore the value of c selected for the final iteration is correct.</p>	$c = \frac{(1935.5 \text{ mm}^2)(414 \text{ N/mm}^2) + (619 \text{ mm}^2)(330 \text{ N/mm}^2)}{(0.928)(34.5 \text{ N/mm}^2)(0.786)(304.8 \text{ mm})}$ <p>$c = 131 \text{ mm}$ \therefore the value of c selected for the final iteration is correct.</p>
<p>Step 11—Calculate flexural strength components</p> <p>The design flexural strength is calculated using Eq. (10.2.10d). An additional reduction factor, $\psi_f = 0.85$, is applied to the contribution of the FRP system.</p> <p>Steel contribution to bending:</p> $M_{ns} = A_s f_s \left(d - \frac{\beta_1 c}{2} \right)$ <p>FRP contribution to bending:</p> $M_{nf} = A_f f_{fe} \left(d_f - \frac{\beta_1 c}{2} \right)$	$M_{ns} = (3.00 \text{ in.}^2)(60 \text{ ksi}) \left(21.5 \text{ in.} - \frac{0.786(5.17 \text{ in.})}{2} \right)$ <p>$M_{ns} = 3504 \text{ kip-in.} = 292 \text{ kip-ft}$</p> $M_{nf} = (0.96 \text{ in.}^2)(48.2 \text{ ksi}) \left(24 \text{ in.} - \frac{0.786(5.17 \text{ in.})}{2} \right)$ <p>$M_{nf} = 1020 \text{ kip-in.} = 85 \text{ kip-ft}$</p>	$M_{ns} = (1935.5 \text{ mm}^2)(414 \text{ N/mm}^2) \left(546.1 \text{ mm} - \frac{0.786(131 \text{ mm})}{2} \right)$ <p>$M_{ns} = 3.963 \times 10^8 \text{ N-mm} = 396.3 \text{ kN-m}$</p> $M_{nf} = (619 \text{ mm}^2)(330 \text{ N/mm}^2) \left(609.6 \text{ mm} - \frac{0.786(131 \text{ mm})}{2} \right)$ <p>$M_{nf} = 1.140 \times 10^8 \text{ N-mm} = 114 \text{ kN-m}$</p>

Table 16.3c (cont.)—Procedure for flexural strengthening of an interior reinforced concrete beam with fiber-reinforced polymer laminates

Procedure	Calculation in in.-lb units	Calculation in SI metric units
<p>Step 12—Calculate design flexural strength of the section</p> <p>The design flexural strength is calculated using Eq. (10.1) and (10.2.10d). Because $\epsilon_s = 0.0083 > 0.005$, a strength reduction factor of $\phi = 0.90$ is appropriate per Eq. (10.2.7).</p> $\phi M_n = \phi [M_{ns} + \psi_f M_{nf}]$	$\phi M_n = 0.9[292 \text{ kip-ft} + 0.85(85 \text{ kip-ft})]$ $\phi M_n = 327 \text{ kip-ft} \geq M_u = 294 \text{ kip-ft}$ <p>\therefore the strengthened section is capable of sustaining the new required moment strength.</p>	$\phi M_n = 0.9[396.3 \text{ kN-m} + 0.85(114 \text{ kN-m})]$ $\phi M_n = 443 \text{ kN-m} \geq M_u = 399 \text{ kN-m}$ <p>\therefore the strengthened section is capable of sustaining the new required moment strength.</p>
<p>Step 13—Check service stresses in the reinforcing steel and the FRP.</p> <p>Calculate the elastic depth to the cracked neutral axis. This can be simplified for a rectangular beam without compression reinforcement as follows:</p> $k = \frac{\sqrt{\left(\rho_s \frac{E_s}{E_c} + \rho_f \frac{E_f}{E_c}\right)^2 + 2\left(\rho_s \frac{E_s}{E_c} + \rho_f \frac{E_f}{E_c} \left(\frac{d_f}{d}\right)\right) - \left(\rho_s \frac{E_s}{E_c} + \rho_f \frac{E_f}{E_c}\right)}{2}$ <p>Calculate the stress level in the reinforcing steel using Eq. (10.2.10.1) and verify that it is less than the recommended limit per Eq. (10.2.8a).</p> $f_{s,s} = \frac{\left[M_s + \epsilon_w A_s E_f \left(d_f - \frac{kd}{3}\right)\right] (d - kd) E_s}{A_s E_s \left(d - \frac{kd}{3}\right) (d - kd) + A_f E_f \left(d_f - \frac{kd}{3}\right) (d_f - kd)}$ $f_{s,s} \leq 0.80 f_y$	$k = 0.343$ $kd = (0.343)(21.5 \text{ in.}) = 7.37 \text{ in.}$ $f_{s,s} = 40.4 \text{ ksi} \leq (0.80)(60 \text{ ksi}) = 48 \text{ ksi}$ <p>\therefore the stress level in the reinforcing steel is within the recommended limit.</p>	$k = 0.343$ $kd = (0.343)(546.1 \text{ mm}) = 187 \text{ mm}$ $f_{s,s} = 279 \text{ N/mm}^2 \leq (0.80)(410 \text{ N/mm}^2) = 330 \text{ N/mm}^2$ <p>\therefore the stress level in the reinforcing steel is within the recommended limit.</p>

Table 16.3c (cont.)—Procedure for flexural strengthening of an interior reinforced concrete beam with fiber-reinforced polymer laminates

Procedure	Calculation in in.-lb units	Calculation in SI metric units
Step 14—Check creep rupture limit at service of the FRP Calculate the stress level in the FRP using Eq. (10.2.10.2) and verify that it is less than creep-rupture stress limit given in Table 10.2.9. Assume that the full service load is sustained.		
$f_{f,s} = f_{s,s} \left(\frac{E_f}{E_s} \right) \left(\frac{d_f - kd}{d - kd} \right) - \epsilon_{st} E_f$	$f_{f,s} = 40.4 \text{ ksi} \left(\frac{5360 \text{ ksi}}{29,000 \text{ ksi}} \right) \left(\frac{24 \text{ in.} - 7.37 \text{ in.}}{21.5 \text{ in.} - 7.37 \text{ in.}} \right) - (0.00061)(5360 \text{ ksi})$	$f_{f,s} = 0.278 \text{ kN/mm}^2 \left(\frac{37 \text{ kN/mm}^2}{200 \text{ kN/mm}^2} \right) \left(\frac{609.6 \text{ mm} - 187 \text{ mm}}{546 \text{ mm} - 187 \text{ mm}} \right) - (0.00061)(38 \text{ N/mm}^2)$
For a carbon FRP system, the sustained plus cyclic stress limit is obtained from Table 10.2.9:	$f_{f,s} = 5.60 \text{ ksi} \leq (0.55)(85 \text{ ksi}) = 47 \text{ ksi}$	$f_{f,s} = 38 \text{ N/mm}^2 \leq (0.55)(590 \text{ N/mm}^2) = 324 \text{ N/mm}^2$
Sustained plus cyclic stress limit = $0.55f_{fu}$	\therefore the stress level in the FRP is within the recommended sustained plus cyclic stress limit.	\therefore the stress level in the FRP is within the recommended sustained plus cyclic stress limit.

$$k = \sqrt{\left[0.0116 \left(\frac{29,000}{4030} \right) + 0.00372 \left(\frac{5360}{4030} \right) \right]^2 + 2 \left[0.0116 \left(\frac{29,000}{4030} \right) + 0.00372 \left(\frac{5360}{4030} \right) \left(\frac{24 \text{ in.}}{21.5 \text{ in.}} \right) \right]} - \left[0.0116 \left(\frac{29,000}{4030} \right) + 0.00372 \left(\frac{5360}{4030} \right) \right]$$

$$f_{s,s} = \frac{\left[2424 \text{ kip-in.} + \left[(0.00061)(0.96 \text{ in.}^3) \times (5360 \text{ ksi}) \left(24 \text{ in.} - \frac{7.37 \text{ in.}}{3} \right) \right] \times \left[(21.5 \text{ in.} - 7.37 \text{ in.})(29,000 \text{ ksi}) \right] \right]}{\left[(3.00 \text{ in.}^3)(29,000 \text{ ksi}) \times \left(21.5 \text{ in.} - \frac{7.37 \text{ in.}}{3} \right) (21.5 \text{ in.} - 7.37 \text{ in.}) \right] + \left[(0.96 \text{ in.}^3)(5360 \text{ ksi}) \left(24 \text{ in.} - \frac{7.37 \text{ in.}}{3} \right) (24 \text{ in.} - 7.37 \text{ in.}) \right]}$$

$$k = \sqrt{\left[0.0116 \left(\frac{200}{27.6} \right) + 0.00372 \left(\frac{37}{27.6} \right) \right]^2 + 2 \left[0.0116 \left(\frac{200}{27.6} \right) + 0.00372 \left(\frac{37}{27.6} \right) \left(\frac{609.6 \text{ mm}}{546 \text{ mm}} \right) \right]} - \left[0.0116 \left(\frac{200}{27.6} \right) + 0.00372 \left(\frac{37}{27.6} \right) \right]$$

$$f_{s,s} = \frac{\left[273,912 \text{ kN-mm} + \left[(0.00061)(619 \text{ mm}^3)(37 \text{ kN/mm}^2) \times \left(609.6 \text{ mm} - \frac{187 \text{ mm}}{3} \right) \right] \times \left[(546 \text{ mm} - 187 \text{ mm})(200 \text{ kN/mm}^2) \right] \right]}{\left[(1935 \text{ mm}^3)(200 \text{ kN/mm}^2) \times \left(546 \text{ mm} - \frac{187 \text{ mm}}{3} \right) (546 \text{ mm} - 187 \text{ mm}) \right] + \left[(619 \text{ mm}^3)(37 \text{ kN/mm}^2) \left(607 \text{ mm} - \frac{187 \text{ mm}}{3} \right) (607 \text{ mm} - 187 \text{ mm}) \right]}$$

In detailing the FRP reinforcement, the FRP should be terminated a minimum of ℓ_{df} , calculated per Eq. (14.1.3), past the point on the moment diagram that represents cracking. The factored shear force at the termination should also be checked against the shear force that causes FRP end peeling,

estimated as two-thirds of the concrete shear strength. If the shear force is greater than two-thirds of the concrete shear strength, the FRP strips should be extended further toward the supports. U-wraps may also be used to reinforce against cover delamination.

16.4—Flexural strengthening of an interior reinforced concrete beam with near-surface-mounted FRP bars

An existing reinforced concrete beam (Fig. 16.4) is to be strengthened using the loads given in Table 16.3a and the near-surface-mounted (NSM) FRP system described in Table 16.4a. Specifically, three No. 3 carbon FRP (CFRP) bars are to be used at a distance 23.7 in. (602.1 mm) from the extreme top fiber of the beam.

By inspection, the degree of strengthening is reasonable in that it does meet the strengthening limit criteria put forth in Eq. (10.1). That is, the existing flexural strength without FRP, $(\phi M_n)_{w/o} = 266$ kip-ft (361 kN-m), is greater than the unstrengthened moment limit, $(1.1M_{DL} + 0.75M_{LL})_{new} = 177$ kip-ft (240 kN-m). The design calculations used to verify this configuration follow in Table 16.4b.

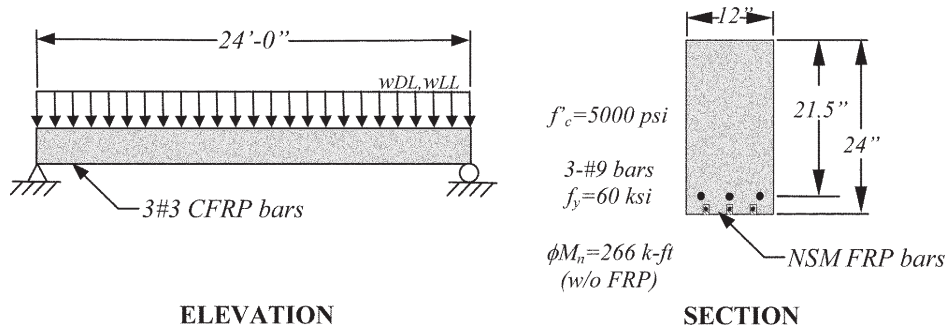


Fig. 16.4—Schematic of the idealized simply supported beam with FRP external reinforcement.

Table 16.4a—Manufacturer's reported NSM FRP system properties

Area per No. 3 bar	0.10 in. ²	64.5 mm ²
Ultimate tensile strength f_{fu}^*	250 ksi	1725 N/mm ²
Rupture strain ϵ_{fu}^*	0.013 in./in.	0.013 mm/mm
Modulus of elasticity of FRP laminates E_f	19,230 ksi	132,700 N/mm ²
Length of the beam ℓ	29 ft	8.84 m
Bay width l_2	30 ft	9.14 m
Width of beam w	24 in.	610 mm
d_p	22.5 in.	571 mm
h	25 in.	635 mm
Effective flange width b_f	87 in.	2210 mm
Flange thickness h_f	4 in.	102 mm
f'_c	4000 psi	27.6 N/mm ²
Strands diameter	1/2 in.	12.7 mm
f_{pe}	165 ksi	1138 N/mm ²
f_{py}	230 ksi	1586 N/mm ²
f_{pu}	270 ksi	1860 N/mm ²
E_p	28,500 ksi	1.96×10^5 N/mm ²
ϕM_n without FRP	336 kip-ft	455 kN-m

Table 16.4b—Procedure for flexural strengthening of an interior reinforced concrete beam with NSM FRP bars

Procedure	Calculation in in.-lb units	Calculation in SI metric units
<p>Step 1—Calculate the FRP system design material properties</p> <p>The beam is located in an interior space and a CFRP material will be used. Therefore, per Table 9.4, an environmental reduction factor of 0.95 is suggested.</p> $f_{fu} = C_E f_{fu}^*$ $\epsilon_{fu} = C_E \epsilon_{fu}^*$	$f_{fu} = (0.95)(250 \text{ ksi}) = 237.5 \text{ ksi}$ $\epsilon_{fu} = (0.95)(0.013 \text{ in./in.}) = 0.0123 \text{ in./in.}$	$f_{fu} = (0.95)(1725 \text{ N/mm}^2) = 1639 \text{ N/mm}^2$ $\epsilon_{fu} = (0.95)(0.013 \text{ mm/mm}) = 0.0123 \text{ mm/mm}$
<p>Step 2—Preliminary calculations</p> <p>Properties of the concrete:</p> <p>β_1 from ACI 318-14, Section 22.2.2.4.3</p> $E_c = 57,000\sqrt{f'_c}$	$\beta_1 = 1.05 - 0.05 \frac{f'_c}{1000} = 0.85$ $E_c = 57,000\sqrt{5000 \text{ psi}} = 4,030,00 \text{ psi}$ $A_s = 3(1.00 \text{ in.}^2) = 3.00 \text{ in.}^2$ $A_f = (3 \text{ bars})(0.01 \text{ in.}^2/\text{bar}) = 0.3 \text{ in.}^2$	$\beta_1 = 1.05 - 0.05 \frac{f'_c}{6.9} = 0.85$ $E_c = 4700\sqrt{34.5 \text{ N/mm}^2} = 27,600 \text{ N/mm}^2$ $A_s = 3(645.2 \text{ mm}^2) = 1935 \text{ mm}^2$ $A_f = (3 \text{ bars})(64.5 \text{ mm}^2/\text{bar}) = 194 \text{ mm}^2$
<p>Step 3—Determine the existing state of strain on the soffit</p> <p>The existing state of strain is calculated assuming the beam is cracked and the only loads acting on the beam at the time of the FRP installation are dead loads. A cracked section analysis of the existing beam gives $k = 0.334$ and $I_{cr} = 5937 \text{ in.}^4 = 2471 \times 10^6 \text{ mm}^4$</p> $\epsilon_{bi} = \frac{M_{DL}(d_f - kd)}{I_{cr}E_c}$	$\epsilon_{bi} = \frac{(864 \text{ kip-in.})[23.7 \text{ in.} - (0.334)(21.5 \text{ in.})]}{(5937 \text{ in.}^4)(4030 \text{ ksi})} = 0.00061$	$\epsilon_{bi} = \frac{(97.6 \text{ kN-mm})[602 \text{ mm} - (0.334)(546 \text{ mm})]}{(2471 \times 10^6 \text{ mm}^4)(27.6 \text{ kN/mm}^2)} = 0.00061$
<p>Step 4—Determine the bond-dependent coefficient of the FRP system</p> <p>Based on the manufacturer's recommendation, the dimensionless bond-dependent coefficient for flexure κ_m is 0.7.</p>	$\kappa_m = 0.7$	$\kappa_m = 0.7$
<p>Step 5—Estimate c, the depth to the neutral axis</p> <p>A reasonable initial estimate of c is $0.20d$. The value of the c is adjusted after checking equilibrium.</p> $c = 0.20d$	$c = (0.20)(21.5 \text{ in.}) = 4.30 \text{ in.}$	$c = (0.20)(546 \text{ mm}) = 109 \text{ mm}$

Table 16.4b (cont.)—Procedure for flexural strengthening of an interior reinforced concrete beam with NSM FRP bars

Procedure	Calculation in in.-lb units	Calculation in SI metric units
<p>Step 6—Determine the effective level of strain in the FRP reinforcement</p> <p>The effective strain level in the FRP may be found from Eq. (10.2.5).</p> $\epsilon_{fe} = \left(\frac{d_f - c}{c} \right) \epsilon_{bi} \leq \kappa_m \epsilon_{fd}$ <p>Note that for the neutral axis depth selected, FRP debonding would be the failure mode because the second expression in this equation controls. If the first expression governed, then concrete crushing would be the failure mode. Because FRP controls the failure of the section, the concrete strain at failure, ϵ_c, may be less than 0.003 and can be calculated using similar triangles:</p> $\epsilon_c = (\epsilon_{fd} + \epsilon_{bi}) \left(\frac{c}{d_f - c} \right)$	$\epsilon_{fe} = 0.003 \left(\frac{23.7 \text{ in.} - 4.3 \text{ in.}}{4.3 \text{ in.}} \right) - 0.00061 = 0.0129$ $\kappa_m \epsilon_{fd} = 0.7(0.0123) = 0.00865$ <p>Hence, $\epsilon_{fe} = 0.00865$ (Mode of failure is FRP debonding)</p> $\epsilon_c = (0.00865 + 0.00061) \left(\frac{4.3}{23.7 - 4.3} \right) = 0.0020$	$\epsilon_{fe} = 0.003 \left(\frac{602 \text{ mm} - 109 \text{ mm}}{109 \text{ mm}} \right) - 0.00061 = 0.0129$ $\kappa_m \epsilon_{fd} = 0.7(0.0123) = 0.00865$ <p>Hence, $\epsilon_{fe} = 0.00865$ (Mode of failure is FRP debonding)</p> $\epsilon_c = (0.00865 + 0.00061) \left(\frac{109}{602 - 109} \right) = 0.0020$
<p>Step 7—Calculate the strain in the existing reinforcing steel</p> <p>The strain in the reinforcing steel can be calculated using similar triangles according to Eq. (10.2.10a).</p> $\epsilon_s = (\epsilon_{fe} + \epsilon_{bi}) \left(\frac{d - c}{d_f - c} \right)$	$\epsilon_s = (0.00865 + 0.00061) \left(\frac{21.5 - 4.3}{23.7 - 4.3} \right) = 0.0082$	$\epsilon_s = (0.00865 + 0.00061) \left(\frac{546 - 109}{602 - 109} \right) = 0.0082$
<p>Step 8—Calculate the stress level in the reinforcing steel and FRP.</p> <p>The stresses are calculated using Eq. (10.2.10b) and Hooke's Law.</p> $f_s = E_s \epsilon_s \leq f_y$ $f_{fe} = E_f \epsilon_{fe}$	$f_s = (29,000 \text{ ksi})(0.0082) \leq 60 \text{ ksi}$ $f_s = 238 \text{ ksi} > 60 \text{ ksi}$ <p>therefore, $f_s = 60 \text{ ksi}$</p> $f_{fe} = (19,230 \text{ ksi})(0.00865) = 166 \text{ ksi}$	$f_s = (200 \text{ kN/mm}^2)(0.0082) \leq 0.414 \text{ kN/mm}^2$ $f_s = 1.64 \text{ kN/mm}^2 \leq 0.414 \text{ kN/mm}^2$ <p>therefore, $f_s = 0.414 \text{ kN/mm}^2$</p> $f_{fe} = (132,700 \text{ N/mm}^2)(0.00865) = 1147 \text{ N/mm}^2$

Table 16.4b (cont.)—Procedure for flexural strengthening of an interior reinforced concrete beam with NSM FRP bars

Procedure	Calculation in in.-lb units	Calculation in SI metric units
<p>Step 9—Calculate the internal force resultants and check equilibrium</p> <p>Concrete stress block factors may be calculated using ACI 318. Approximate stress block factors may also be calculated based on the parabolic stress-strain relationship for concrete as follows:</p> $\beta_1 = \frac{4\epsilon'_c - \epsilon_c}{6\epsilon'_c - 2\epsilon_c}$ $\alpha_1 = \frac{3\epsilon'_c \epsilon_c - \epsilon_c^2}{3\beta_1 \epsilon_c'^2}$ <p>where ϵ'_c is strain corresponding to f'_c calculated as</p> $\epsilon'_c = \frac{1.7f'_c}{E_c}$ <p>Force equilibrium is verified by checking the initial estimate of c with Eq. (10.3.1.6g).</p> $c = \frac{A_s f_s + A_f f_{fe}}{\alpha_1 f'_c \beta_1 b}$	$\beta_1 = \frac{4(0.0021) - 0.002}{6(0.0021) - 2(0.002)} = 0.743$ $\alpha_1 = \frac{3(0.0021)(0.002) - (0.002)^2}{3(0.743)(0.0021)^2} = 0.870$ $\epsilon'_c = \frac{1.7(5000)}{4030 \times 10^6} = 0.0021$ $c = \frac{(3.00 \text{ in.}^2)(60 \text{ ksi}) + (0.3 \text{ in.}^2)(166 \text{ ksi})}{(0.87)(5 \text{ ksi})(0.743)(12 \text{ in.})}$ <p>$c = 5.92 \text{ in.} \neq 4.30 \text{ in. n.g.}$</p> <p>$\therefore$ revise estimate of c and repeat Steps 6 through 9 until equilibrium is achieved.</p>	$\beta_1 = \frac{4(0.0021) - 0.002}{6(0.0021) - 2(0.002)} = 0.743$ $\alpha_1 = \frac{3(0.0021)(0.002) - (0.002)^2}{3(0.743)(0.0021)^2} = 0.870$ $\epsilon'_c = \frac{1.7(34.5)}{27,606} = 0.0021$ $c = \frac{(1935 \text{ mm}^2)(414 \text{ N/mm}^2) + (194 \text{ mm}^2)(1147 \text{ N/mm}^2)}{(0.87)(34.5 \text{ N/mm}^2)(0.743)(305 \text{ mm})}$ <p>$c = 150 \text{ mm} \neq 109 \text{ in. n.g.}$</p> <p>$\therefore$ revise estimate of c and repeat Steps 6 through 9 until equilibrium is achieved.</p>
<p>Step 10—Adjust c until force equilibrium is satisfied</p> <p>Steps 6 through 9 were repeated several times with different values of c until equilibrium was achieved. The results of the final iteration are</p> <p>$c = 5.26 \text{ in.}; \epsilon_s = 0.0082; f_s = f_y = 60 \text{ ksi}; \epsilon_{fe} = 0.00865; \epsilon_c = 0.0027; \beta_1 = 0.786; \alpha_1 = 0.928; \text{ and } f_{fe} = 166 \text{ ksi}$</p>	$c = \frac{(3.00 \text{ in.}^2)(60 \text{ ksi}) + (0.3 \text{ in.}^2)(166 \text{ ksi})}{(0.928)(5 \text{ ksi})(0.786)(12 \text{ in.})}$ <p>$c = 5.25 \text{ in.} \approx 5.26 \text{ in.}$</p> <p>$\therefore$ the value of c selected for the final iteration is correct.</p>	$c = \frac{(1935 \text{ mm}^2)(414 \text{ N/mm}^2) + (193 \text{ mm}^2)(1147 \text{ N/mm}^2)}{(0.928)(34.5 \text{ N/mm}^2)(0.786)(305 \text{ mm})}$ <p>$c = 133 \text{ mm} \approx 134 \text{ mm}$</p> <p>$\therefore$ the value of c selected for the final iteration is correct.</p>

Table 16.4b (cont.)—Procedure for flexural strengthening of an interior reinforced concrete beam with NSM FRP bars

Procedure	Calculation in in.-lb units	Calculation in SI metric units
<p>Step 11—Calculate flexural strength components.</p> <p>The design flexural strength is calculated using Eq. (10.2.10d). An additional reduction factor, $\psi_f = 0.85$, is applied to the contribution of the FRP system. Steel contribution to bending:</p> $M_{ns} = A_s f_s \left(d - \frac{\beta_1 c}{2} \right)$ <p>FRP contribution to bending:</p> $M_{nf} = A_s f_{fc} \left(d_f - \frac{\beta_1 c}{2} \right)$	$M_{ns} = (3.0 \text{ in.}^2)(60 \text{ ksi}) \left(21.5 \text{ in.} - \frac{0.786(5.25 \text{ in.})}{2} \right)$ $M_{ns} = 3498 \text{ kip-in.} = 291 \text{ kip-ft}$ $M_{nf} = (0.3 \text{ in.}^2)(166 \text{ ksi}) \left(23.7 \text{ in.} - \frac{0.786(5.25 \text{ in.})}{2} \right)$ $M_{nf} = 1077 \text{ kip-in.} = 90 \text{ kip-ft}$	$M_{ns} = (1935 \text{ mm}^2)(414 \text{ N/mm}^2) \left(546 \text{ mm} - \frac{0.786(133 \text{ mm})}{2} \right)$ $M_{ns} = 394 \text{ kN-m}$ $M_{nf} = (194 \text{ mm}^2)(1147 \text{ N/mm}^2) \left(602.1 \text{ mm} - \frac{0.786(133 \text{ mm})}{2} \right)$ $M_{nf} = 122 \text{ kN-m}$
<p>Step 12—Calculate design flexural strength of the section</p> <p>The design flexural strength is calculated using Eq. (10-1) and (10.2.10d). Because $\epsilon_s = 0.0082 > 0.005$, a strength reduction factor of $\phi = 0.90$ is appropriate per Eq. (10.2.7).</p> $\phi M_n = \phi [M_{ns} + \psi_f M_{nf}]$	$\phi M_n = 0.9 [291 \text{ kip-ft} + 0.85(90 \text{ kip-ft})]$ $\phi M_n = 331 \text{ kip-ft} \geq M_u = 294 \text{ kip-ft}$ <p>\therefore the strengthened section is capable of sustaining the new required flexural strength.</p>	$\phi M_n = 0.9 [394 \text{ kN-m} + 0.85(122 \text{ kN-m})]$ $\phi M_n = 448 \text{ kN-m} \geq M_u = 398 \text{ kN-m}$ <p>\therefore the strengthened section is capable of sustaining the new required flexural strength.</p>
<p>Step 13—Check service stresses in the reinforcing steel and the FRP</p> <p>Calculate the elastic depth to the cracked neutral axis. This can be simplified for a rectangular beam without compression reinforcement as follows:</p> $k = \frac{\left(\rho_s \frac{E_s}{E_c} + \rho_f \frac{E_f}{E_c} \right)^2}{+2 \left(\rho_s \frac{E_s}{E_c} + \rho_f \frac{E_f}{E_c} \left(\frac{d_f}{d} \right) \right) - \left(\rho_s \frac{E_s}{E_c} + \rho_f \frac{E_f}{E_c} \right)}$ <p>Calculate the stress level in the reinforcing steel using Eq. (10.2.10.1) and verify that it is less than the recommended limit per Eq. (10.2.8a).</p> $f_{s,s} = \frac{\left[M_s + \epsilon_u A_s E_s \left(d_f - \frac{kd}{3} \right) \right] (d - kd) E_s}{A_s E_s \left(d - \frac{kd}{3} \right) (d - kd) + A_s E_s \left(d_f - \frac{kd}{3} \right) (d_f - kd)}$ $f_{s,s} \leq 0.80 f_y$	$k = 0.345$ $kd = (0.345)(21.5 \text{ in.}) = 7.4 \text{ in.}$ $f_{s,s} = 40.3 \text{ ksi} \leq (0.80)(60 \text{ ksi}) = 48 \text{ ksi}$ <p>\therefore the stress level in the reinforcing steel is within the recommended limit.</p>	$k = 0.345$ $kd = (0.345)(546 \text{ mm}) = 188 \text{ mm}$ $f_{s,s} = 278 \text{ N/mm}^2 \leq (0.80)(410 \text{ N/mm}^2) = 330 \text{ N/mm}^2$ <p>\therefore the stress level in the reinforcing steel is within the recommended limit.</p>

Table 16.4b (cont.)—Procedure for flexural strengthening of an interior reinforced concrete beam with NSM FRP bars

Procedure	Calculation in in.-lb units	Calculation in SI metric units
Step 14—Check creep rupture limit at service of the FRP Calculate the stress level in the FRP using Eq. (10.2.10.2) and verify that it is less than creep-rupture stress limit given in Table 10.2.9. Assume that the full service load is sustained. $f_{f,s} = f_{s,s} \left(\frac{E_f}{E_s} \right) \left(\frac{d_f - kd}{d - kd} \right) - \epsilon_{bi} E_f$ For a carbon FRP system, the sustained plus cyclic stress limit is obtained from Table 10.2.9: Sustained plus cyclic stress limit = $0.55f_{fu}$	$f_{f,s} = 40.3 \text{ ksi} \left(\frac{19,230 \text{ ksi}}{29,000 \text{ ksi}} \right) \left(\frac{23.7 \text{ in.} - 7.4 \text{ in.}}{21.5 \text{ in.} - 7.4 \text{ in.}} \right) - (0.00061)(19,230 \text{ ksi})$ $f_{f,s} = 19 \text{ ksi} \leq (0.55)(85 \text{ ksi}) = 50 \text{ ksi}$ ∴ the stress level in the FRP is within the recommended sustained plus cyclic stress limit.	$f_{f,s} = 0.278 \text{ kN/mm}^2 \left(\frac{133 \text{ kN/mm}^2}{200 \text{ kN/mm}^2} \right) \left(\frac{602 \text{ mm} - 188 \text{ mm}}{546 \text{ mm} - 188 \text{ mm}} \right) - (0.00061)(133 \text{ N/mm}^2)$ $f_{f,s} = 134 \text{ N/mm}^2 \leq (0.55)(590 \text{ N/mm}^2) = 324.5 \text{ N/mm}^2$ ∴ the stress level in the FRP is within the recommended sustained plus cyclic stress limit.

$$* k = \sqrt{\left[0.0116 \left(\frac{29,000}{4030} \right) + 0.0012 \left(\frac{19,230}{4030} \right) \right]^2 + 2 \left[0.0116 \left(\frac{29,000}{4030} \right) + 0.0012 \left(\frac{19,230}{4030} \right) \left(\frac{23.7 \text{ in.}}{21.5 \text{ in.}} \right) \right]} - \left[0.0116 \left(\frac{29,000}{4030} \right) + 0.0012 \left(\frac{19,230}{4030} \right) \right]$$

$$† f_{s,s} = \frac{\left(\left[2424 \text{ kip-in.} + \left[(0.00061)(0.3 \text{ in.}^2) \times (19,230 \text{ ksi}) \left(23.7 \text{ in.} - \frac{7.4 \text{ in.}}{3} \right) \right] \right) \times (21.5 \text{ in.} - 7.4 \text{ in.})(29,000 \text{ ksi}) \right)}{\left(\left[(3.00 \text{ in.}^2)(29,000 \text{ ksi}) \left(21.5 \text{ in.} - \frac{7.4 \text{ in.}}{3} \right) \times (21.5 \text{ in.} - 7.4 \text{ in.}) \right] + \left[(0.3 \text{ in.}^2)(19,230 \text{ ksi}) \left(23.7 \text{ in.} - \frac{7.4 \text{ in.}}{3} \right) \times (23.7 \text{ in.} - 7.4 \text{ in.}) \right] \right)}$$

$$‡ k = \sqrt{\left[0.0116 \left(\frac{200}{27.6} \right) + 0.0012 \left(\frac{133}{27.6} \right) \right]^2 + 2 \left[0.0116 \left(\frac{200}{27.6} \right) + 0.0012 \left(\frac{133}{27.6} \right) \left(\frac{602 \text{ mm}}{546 \text{ mm}} \right) \right]} - \left[0.0116 \left(\frac{200}{27.6} \right) + 0.0012 \left(\frac{133}{27.6} \right) \right]$$

$$§ f_{s,s} = \frac{\left(\left[273,912 \text{ kN-mm} + \left[(0.00061)(194 \text{ mm}^2) \times (132.7 \text{ kN/mm}^2) \times \left(602 \text{ mm} - \frac{188 \text{ mm}}{3} \right) \right] \right) \times \left[(546 \text{ mm} - 188 \text{ mm})(200 \text{ kN/mm}^2) \right] \right)}{\left(\left[(1935 \text{ mm}^2)(200 \text{ kN/mm}^2) \times \left(546 \text{ mm} - \frac{188 \text{ mm}}{3} \right) \right] (546 \text{ mm} - 188 \text{ mm}) \right) + \left[(194 \text{ mm}^2)(132.7 \text{ kN/mm}^2) \times \left(602 \text{ mm} - \frac{188 \text{ mm}}{3} \right) \right] (602 \text{ mm} - 188 \text{ mm}) \right)}$$

In detailing the FRP reinforcement, FRP bars should be terminated at a distance equal to the bar development length past the point on the moment diagram that represents cracking.

16.5—Flexural strengthening of an interior prestressed concrete beam with FRP laminates

A number of continuous prestressed concrete beams with five 1/2 in. (12.7 mm) diameter bonded strands (Fig. 16.5) are located in a parking garage that is being converted to an office space. All prestressing strands are Grade 270 ksi (1860 N/mm²) low-relaxation seven-wire strands. The beams require an increase in their live-load-carrying capacity from 50 to 75 lb/ft² (244 to 366 kg/m²). The beams are also required to support an additional dead load of 10 lb/ft² (49 kg/m²). Analysis indicates that each existing beam has adequate flexural capacity to carry the new loads in the negative moment region at the supports but is deficient in flexure at midspan and in shear at the supports. The beam meets the deflection and crack control serviceability require-

ments. The cast-in-place beams support a 4 in. (100 mm) slab. For bending at midspan, beams should be treated as T-sections. Summarized in Table 16.5a are the existing and new loads and associated midspan moments for the beam. FRP system properties are shown in Table 16.3b.

By inspection, the degree of strengthening is reasonable in that it does meet the strengthening limit criteria put forth in Eq. (10.1). That is, the existing flexural strength without FRP, $(\phi M_n)_{w/o} = 336$ kip-ft (455 kN-m), is greater than the unstrengthened moment limit, $(1.1M_{DL} + 0.75M_{LL})_{new} = 273$ kip-ft (370 kN-m). The design calculations used to verify this configuration follow. The beam is to be strengthened using the FRP system described in Table 16.3b. A one-ply, 24 in. (610 mm) wide strip of FRP is considered for this evaluation.

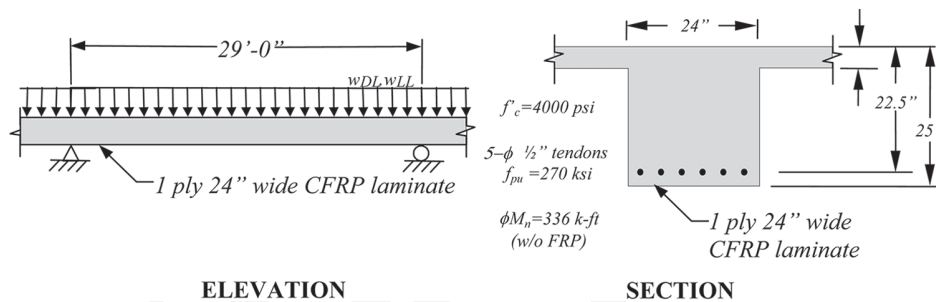


Fig. 16.5—Schematic of the idealized continuous prestressed beam with FRP external reinforcement.

Table 16.5a—Loadings and corresponding moments

Loading/moment	Existing loads		Anticipated loads	
Dead loads w_{DL}	2.77 kip/ft	40.4 N/mm	3.09 kip/ft	45.1 N/mm
Live load w_{LL}	1.60 kip/ft	23.3 N/mm	2.4 kip/ft	35 N/mm
Unfactored loads ($w_{DL} + w_{LL}$)	4.37 kip/ft	63.8 N/mm	5.49 kip/ft	80.2 N/mm
Unstrengthened load limit ($1.1w_{DL} + 0.75w_{LL}$)	NA	NA	5.2 kip/ft	75.9 N/mm
Factored loads ($1.2w_{DL} + 1.6w_{LL}$)	5.88 kip/ft	85.9 N/mm	7.55 kip/ft	110.2 N/mm
Dead-load moment M_{DL}	147 kip-ft	199 kN-m	162 kip-ft	220.2 kN-m
Live-load moment M_{LL}	85 kip-ft	115 kN-m	126 kip-ft	171.1 kN-m
Service-load moment M_s	232 kip-ft	314 kN-m	288 kip-ft	391.3 kN-m
Unstrengthened moment limit ($1.1M_{DL} + 0.75M_{LL}$) _{new}	NA	NA	273 kip-ft	371 kN-m
Factored moment M_u	312 kip-ft	423 kN-m	397 kip-ft	538 kN-m

Table 16.5b—Procedure for flexural strengthening of an interior prestressed concrete beam with FRP laminates

Procedure	Calculation in in.-lb units	Calculation in SI metric units
<p>Step 1—Calculate the FRP-system design material properties</p> <p>The beam is located in an interior space and a CFRP material will be used. Therefore, per Table 9.4, an environmental reduction factor of 0.95 is suggested.</p> $f_{fu} = C_E f_{fu}^*$ $\epsilon_{fu} = C_E \epsilon_{fu}^*$	$f_{fu} = (0.95)(90 \text{ ksi}) = 85 \text{ ksi}$ $\epsilon_{fu} = (0.95)(0.015 \text{ in./in.}) = 0.0142 \text{ in./in.}$	$f_{fu} = (0.95)(621 \text{ N/mm}^2) = 590 \text{ N/mm}^2$ $\epsilon_{fu} = (0.95)(0.015 \text{ mm/mm}) = 0.0142 \text{ mm/mm}$
<p>Step 2—Preliminary calculations</p> <p>Properties of the concrete:</p> <p>β_1 from ACI 318-14, Section 22.2.2.4.3</p> $E_c = 57,000\sqrt{f'_c}$ <p>Properties of the existing prestressing steel:</p> <p>Area of FRP reinforcement:</p> $A_f = n_f w_f$ <p>Cross-sectional area:</p> $A_{cg} = b_f h_f + b_w (h - h_f)$ <p>Distance from the top fiber to the section centroid:</p> $y_t = \frac{b_f \frac{h_f^2}{2} + b_w (h - h_f) \left(h_f + \frac{(h - h_f)}{2} \right)}{A_{cg}}$ <p>Gross moment of inertia:</p> $I_g = \frac{b_f h_f^3}{12} + b_f h_f \left(y_t - \frac{h_f}{2} \right)^2 + \frac{b_w (h - h_f)^3}{12} + b_w (h - h_f) \left(y_t - \frac{h - h_f}{2} \right)^2$ <p>Radius of gyration:</p> $r = \sqrt{\frac{I_g}{A_{cg}}}$ <p>Effective prestressing strain:</p> $\epsilon_{pe} = \frac{f_{pe}}{E_p}$ <p>Effective prestressing force:</p> $P_e = A_{ps} f_{pe}$ <p>Eccentricity of prestressing force:</p> $e = d_p - y_t$	$\beta_1 = 1.05 - 0.05 \frac{f'_c}{1000} = 0.85$ $E_c = 57,000\sqrt{4000 \text{ psi}} = 3,605,00 \text{ psi}$ $A_{ps} = 5(0.153 \text{ in.}^2) = 0.765 \text{ in.}^2$ $A_f = (1 \text{ ply})(0.040 \text{ in./ply})(24 \text{ in.}) = 0.96 \text{ in.}^2$ $A_{cg} = (87 \text{ in.})(4 \text{ in.}) + (24 \text{ in.})(25 \text{ in.} - 4 \text{ in.}) = 852 \text{ in.}^2$ $y_t = \frac{87 \text{ in.} \times \frac{4 \text{ in.}^2}{2} + 24 \text{ in.} \times 21 \times 14.5}{852} = 9.39 \text{ in.}$ $I_g = \frac{87 \text{ in.} \times 4 \text{ in.}^3}{12} + 87 \text{ in.} \times 4 \text{ in.} (9.39 \text{ in.} - 2)^2 + \frac{24 \text{ in.} \times 21^3}{12} + 24 \text{ in.} \times 21 (9.39 - 10.5)^2 = 38,610 \text{ in.}^4$ $r = \sqrt{\frac{38,610}{852}} = 6.73 \text{ in.}$ $\epsilon_{pe} = \frac{165}{28,500} = 0.00578$ $P_e = 0.765 \times 165 = 126.2 \text{ kip}$ $e = 22.5 - 9.39 = 13.1 \text{ in.}$	$\beta_1 = 1.05 - 0.05 \frac{f'_c}{6.9} = 0.85$ $E_c = 4700\sqrt{27.6 \text{ N/mm}^2} = 24,700 \text{ N/mm}^2$ $A_{ps} = 5(99 \text{ mm}^2) = 495 \text{ mm}^2$ $A_f = (1 \text{ ply})(1.0 \text{ mm/ply})(610 \text{ mm}) = 610 \text{ mm}^2$ $A_{cg} = (2210 \text{ mm})(102 \text{ mm}) + (610 \text{ mm})(612 \text{ mm} - 102 \text{ mm}) = 5.5 \times 10^5 \text{ mm}^2$ $y_t = \frac{2210 \text{ mm} \times \frac{102 \text{ mm}^2}{2} + 610 \text{ mm} \times 533 \times 368}{5.5 \times 10^5} = 238 \text{ mm}$ $I_g = \frac{2210 \text{ mm} \times 102 \text{ mm}^3}{12} + 2210 \text{ mm} \times 102 \text{ mm} (238 - 51)^2 + \frac{610 \text{ mm} \times 533^3}{12} + 610 \text{ mm} \times 533 (238 - 266.7)^2 = 1.61 \times 10^{10} \text{ mm}^4$ $r = \sqrt{\frac{1.61 \times 10^{10}}{5.5 \times 10^5}} = 171 \text{ mm}$ $\epsilon_{pe} = \frac{1138}{1.96 \times 10^5} = 0.00579$ $P_e = 495 \times 1138 = 563,310 \text{ N}$ $e = 571 - 238 = 333 \text{ mm}$

Table 16.5b (cont.)—Procedure for flexural strengthening of an interior prestressed concrete beam with fiber-reinforced polymer laminates

Procedure	Calculation in in.-lb units	Calculation in SI metric units
<p>Step 3—Determine the existing state of strain on the soffit</p> <p>The existing state of strain is calculated assuming the beam is uncracked and the only loads acting on the beam at the time of the FRP installation are dead loads. Distance from extreme bottom fiber to the section centroid:</p> $y_b = h - y_t$ <p>Initial strain in the beam soffit:</p> $\epsilon_{bi} = \frac{-P_e}{E_c A_{cg}} \left(1 + \frac{e y_b}{r^2} \right) + \frac{M_{DL} y_b}{E_c I_g}$	$y_b = 25 - 9.39 = 15.61 \text{ in.}$ $\epsilon_{bi} = \frac{-126.2}{3605 \times 852} \left(1 + \frac{13.1 \times 15.6}{6.73^2} \right) + \frac{147 \times 12 \times 15.6}{3605 \times 38,610}$ $\epsilon_{bi} = -2.88 \times 10^{-5}$	$y_b = 635 - 238 = 397 \text{ mm}$ $\epsilon_{bi} = \frac{-563,310}{24,700 \times 5.5 \times 10^5} \left(1 + \frac{333 \times 397}{171^2} \right) + \frac{199 \times 10^6 \times 397}{24,700 \times 1.61 \times 10^{10}}$ $\epsilon_{bi} = -2.88 \times 10^{-5}$
<p>Step 4—Determine the design strain of the FRP system</p> <p>The design strain of FRP accounting for debonding failure mode ϵ_{fd} is calculated using Eq. (10.2.1.1)</p> <p>Because the design strain is smaller than the rupture strain, debonding controls the design of the FRP system.</p>	$\epsilon_{fd} = 0.083 \sqrt{\frac{4000 \text{ psi}}{1(5,360,000 \text{ psi})(0.04 \text{ in.})}}$ $= 0.0113 \leq 0.9(0.0142) = 0.0128$	$\epsilon_{fd} = 0.042 \sqrt{\frac{27.6 \text{ N/mm}^2}{1(37,000 \text{ N/mm}^2)(1.016 \text{ mm})}}$ $= 0.0113 \leq 0.9(0.0142) = 0.0128$
<p>Step 5—Estimate c, the depth to the neutral axis</p> <p>A reasonable initial estimate of c is $0.1h$. The value of the c is adjusted after checking equilibrium.</p> $c = 0.1h$	$c = (0.1)(25 \text{ in.}) = 2.50 \text{ in.}$	$c = (0.1)(635 \text{ mm}) = 63.5 \text{ mm}$
<p>Step 6—Determine the effective level of strain in the FRP reinforcement</p> <p>The effective strain level in the FRP may be found from Eq. (10.3.1.6c).</p> $\epsilon_{fe} = 0.003 \left(\frac{d_f - c}{c} \right) - \epsilon_{bi} \leq \epsilon_{fd}$ <p>Note that for the neutral axis depth selected, FRP debonding would be the failure mode because the second expression in this equation controls. If the first (limiting) expression governed, then FRP rupture would be the failure mode.</p>	$\epsilon_{fe} = 0.003 \left(\frac{25 - 2.5}{2.5} \right) - 0.00003 = 0.027$ $> \epsilon_{fd} = 0.0113$ <p>Failure is governed by FRP debonding</p> $\epsilon_{fe} = \epsilon_{fd} = 0.0113$	$\epsilon_{fe} = 0.003 \left(\frac{635 - 63.5}{63.5} \right) - 0.00003 = 0.027$ $> \epsilon_{fd} = 0.0113$ <p>Failure is governed by FRP debonding</p> $\epsilon_{fe} = \epsilon_{fd} = 0.0113$

Table 16.5b (cont.)—Procedure for flexural strengthening of an interior prestressed concrete beam with fiber-reinforced polymer laminates

Procedure	Calculation in in.-lb units	Calculation in SI metric units
<p>Step 7—Calculate the strain in the existing prestressing steel</p> <p>The strain in the prestressing steel can be calculated using Eq. (10.3.1.6c) and (10.3.1.6a).</p> $\epsilon_{pnet} = (\epsilon_{fe} + \epsilon_{bi}) \left(\frac{d_p - c}{d_f - c} \right)$ $\epsilon_{ps} = \epsilon_{pe} + \frac{P_e}{A_{cs} E_c} \left(1 + \frac{e^2}{r^2} \right) + \epsilon_{pnet} \leq 0.035$	$\epsilon_{pnet} = (0.0113 + 0.00003) \left(\frac{22.5 - 2.5}{25 - 2.5} \right)$ $\epsilon_{pnet} = 0.01$ $\epsilon_{ps} = 0.00589 + \frac{126.2}{852 \times 3605} \left(1 + \frac{13.1^2}{6.73^2} \right) + 0.01$ $\epsilon_{ps} = 0.016 \leq 0.035$	$\epsilon_{pnet} = (0.0113 + 0.00003) \left(\frac{571 - 63.5}{635 - 63.5} \right)$ $\epsilon_{pnet} = 0.01$ $\epsilon_{ps} = 0.00589 + \frac{563,310}{5.5 \times 10^5 \times 24,700} \left(1 + \frac{333^2}{171^2} \right) + 0.01$ $\epsilon_{ps} = 0.016 \leq 0.035$
<p>Step 8—Calculate the stress level in the prestressing steel and FRP</p> <p>The stresses are calculated using Eq. (10.3.1.6e) and Hooke's Law.</p> $f_{ps} = \begin{cases} 28,500\epsilon_{ps} & \text{for } \epsilon_{ps} \leq 0.0086 \\ 270 - \frac{0.04}{\epsilon_{ps} - 0.007} & \text{for } \epsilon_{ps} > 0.0086 \end{cases}$ $f_{fe} = E_f \epsilon_{fe}$	$f_{ps} = 270 - \frac{0.04}{0.016 - 0.007} = 265.6 \text{ ksi}$ $f_{fe} = (5360 \text{ ksi})(0.0113) = 60.6 \text{ ksi}$	$f_{ps} = 1860 - \frac{0.276}{0.016 - 0.007} = 1831 \text{ N/mm}^2$ $f_{fe} = (37,000 \text{ N/mm}^2)(0.0113) = 418 \text{ N/mm}^2$
<p>Step 9—Calculate the equivalent concrete compressive stress block parameters α_1 and β_1.</p> <p>The strain in concrete at failure can be calculated from strain compatibility as follows:</p> $\epsilon_c = (\epsilon_{fe} + \epsilon_{bi}) \left(\frac{c}{d_f - c} \right)$ <p>The strain ϵ'_c corresponding to f'_c is calculated as</p> $\epsilon'_c = \frac{1.7f'_c}{E_c}$ <p>Concrete stress block factors can be estimated using ACI 318. Approximate stress block factors may be calculated from the parabolic stress-strain relationship for concrete and is expressed as follows:</p> $\beta_1 = \frac{4\epsilon'_c - \epsilon_c}{6\epsilon'_c - 2\epsilon_c}$ $\alpha_1 = \frac{\epsilon'_c \epsilon_c - \epsilon_c}{\beta \epsilon'}$	$\epsilon_c = (0.0113 + 0.00003) \left(\frac{2.5}{25 - 2.5} \right) = 0.0013$ $\epsilon'_c = \frac{1.7(4000)}{3605 \times 10^6} = 0.0019$ $\beta_1 = \frac{4(0.0019) - 0.0013}{6(0.0019) - 2(0.0013)} = 0.716$ $\alpha_1 = \frac{3(0.0019)(0.0013) - (0.0013)^2}{3(0.716)(0.0019)^2} = 0.738$	$\epsilon_c = (0.0113 + 0.00003) \left(\frac{63.5}{635 - 63.5} \right) = 0.0013$ $\epsilon'_c = \frac{1.7(27.6)}{24,700} = 0.0019$ $\beta_1 = \frac{4(0.0019) - 0.0013}{6(0.0019) - 2(0.0013)} = 0.716$ $\alpha_1 = \frac{3(0.0019)(0.0013) - (0.0013)^2}{3(0.716)(0.0019)^2} = 0.738$

Table 16.5b (cont.)—Procedure for flexural strengthening of an interior prestressed concrete beam with fiber-reinforced polymer laminates

Procedure	Calculation in in.-lb units	Calculation in SI metric units
<p>Step 10—Calculate the internal force resultants and check equilibrium</p> <p>Force equilibrium is verified by checking the initial estimate of c with Eq. (10.2.10c).</p>	$c = 1.42 \text{ in.} \neq 2.50 \text{ in.} \quad \text{n.g.}$ <p>\therefore revise estimate of c and repeat Steps 6 through 10 until equilibrium is achieved.</p>	$c = 36 \text{ mm} \neq 63.5 \text{ in.} \quad \text{n.g.}$ <p>\therefore revise estimate of c and repeat Steps 6 through 10 until equilibrium is achieved.</p>
<p>Step 11—Adjust c until force equilibrium is satisfied</p> <p>Steps 6 through 10 were repeated several times with different values of c until equilibrium was achieved. The results of the final iteration are</p> <p>$c = 1.86 \text{ in.}$; $\epsilon_{ps} = 0.016$; $f_{ps} = f_y = 265.6 \text{ ksi}$; $\epsilon_{fe} = 0.0113$; $f_{fe} = 60.6 \text{ ksi}$; $\epsilon_c = 0.00091$; $\alpha_1 = 0.577$; and $\beta_1 = 0.698$.</p>	$c = 1.86 \text{ in.} = 1.86 \text{ in.}$ <p>\therefore the value of c selected for the final iteration is correct.</p>	$c = 47 \text{ mm} = 47 \text{ mm}$ <p>\therefore the value of c selected for the final iteration is correct.</p>
<p>Step 12—Calculate flexural strength components</p> <p>The design flexural strength is calculated using Eq. (10.3.1.6g). An additional reduction factor, $\psi_f = 0.85$, is applied to the contribution of the FRP system.</p> <p>Prestressing steel contribution to bending:</p> <p>FRP contribution to bending:</p>	$M_{np} = 4440 \text{ kip-in.} = 370 \text{ kip-ft}$ $M_{nf} = 1417 \text{ kip-in.} = 118 \text{ kip-ft}$	$M_{np} = 501.6 \times 10^6 \text{ N-mm} = 501.6 \text{ kN-m}$ $M_{nf} = 160.1 \times 10^6 \text{ N-mm} = 160.1 \text{ kN-m}$
<p>Step 13—Calculate design flexural strength of the section</p> <p>The design flexural strength is calculated using Eq. (10.1) and (10.3.1.6g). Because $\epsilon_{ps} = 0.016 > 0.015$, a strength reduction factor of $\phi = 0.90$ should be used per Eq. (10.2.7). An additional reduction factor $\psi_f = 0.85$ is used to calculate the FRP contribution to nominal capacity.</p> $\phi M_n = \phi [M_{np} + \psi_f M_{nf}]$	$\phi M_n = 0.9 [370 \text{ kip-ft} + 0.85 (118 \text{ kip-ft})]$ $\phi M_n = 423 \text{ kip-ft} \geq M_u = 397 \text{ kip-ft}$ <p>\therefore the strengthened section is capable of sustaining the new required flexural strength.</p>	$\phi M_n = 0.9 [506.1 \text{ kN-m} + 0.85 (160.1 \text{ kN-m})]$ $\phi M_n = 573 \text{ kN-m} \geq M_u = 538 \text{ kN-m}$ <p>\therefore the strengthened section is capable of sustaining the new required flexural strength.</p>
<p>Step 14—Check service condition of the section</p> <p>Calculate the cracking moment and compare the service moment:</p>	$f_r = 7.5\sqrt{4000} = 474 \text{ psi} = 0.474 \text{ ksi}$ $M_{cr} = 3695 \text{ kip-in.} = 308 \text{ kip-ft}$ $> M_s = 288 \text{ kip-ft}$ <p>\therefore the strengthened section is uncracked at service.</p>	$f_r = 0.6\sqrt{27.6} = 3.15 \text{ N/mm}^2$ $M_{cr} = 411,654,013 \text{ N-mm} = 412 \text{ kN-m}$ $> M_s = 391.3 \text{ kN-m}$ <p>\therefore the strengthened section is uncracked at service.</p>

Table 16.5b (cont.)—Procedure for flexural strengthening of an interior prestressed concrete beam with fiber-reinforced polymer laminates

Procedure	Calculation in in.-lb units	Calculation in SI metric units
<p>Step 15—Check stress in prestressing steel at service condition</p> <p>Calculate the cracking moment and compare to service moment:</p> $\epsilon_{ps,s} = \epsilon_{pe} + \frac{P_e}{A_c E_c} \left(1 + \frac{e^2}{r^2} \right) + \frac{M_s e}{E_c I_g}$ <p>Calculate the steel stress using Eq. (10.3.1.6d):</p> $f_{ps,s} = \begin{cases} 28,500\epsilon_{ps,s} & \text{for } \epsilon_{ps,s} \leq 0.0086 \\ 270 - \frac{0.04}{\epsilon_{ps,s} - 0.07} & \text{for } \epsilon_{ps,s} > 0.0086 \end{cases}$ <p>Check the service stress limits of Eq. (10.3.1.4a) and (10.3.1.4b):</p> $f_{ps,s} \leq 0.82f_{py}$ $f_{ps,s} \leq 0.74f_{pu}$	$\epsilon_{ps,s} = 0.0063 \leq 0.0086$ $f_{ps,s} = 28,500(0.0063) = 180 \text{ ksi}$ $f_{ps,s} = 180 \text{ ksi} < 0.82(230) = 189 \text{ ksi} \quad \text{OK}$ $f_{ps,s} = 180 \text{ ksi} < 0.74(270) = 200 \text{ ksi} \quad \text{OK}$	$\epsilon_{ps,s} = 0.0063 \leq 0.0086$ $f_{ps,s} = 1.96 \times 10^5(0.0063) = 1238 \text{ N/mm}^2$ $f_{ps,s} = 1238 \text{ N/mm}^2 < 0.82(1586) = 1300 \text{ N/mm}^2 \quad \text{OK}$ $f_{ps,s} = 1238 \text{ N/mm}^2 < 0.74(1860) = 1376 \text{ N/mm}^2 \quad \text{OK}$
<p>Step 16—Check stress in concrete at service condition</p> <p>Calculate the cracking moment and compare to service moment:</p> $\epsilon_{c,s} = \frac{-P_e}{A_c E_c} \left(1 + \frac{e^2}{r^2} \right) - \frac{M_s y_t}{E_c I_g}$ $f_{c,s} = E_c \epsilon_{c,s}$ $f_{c,s} \leq 0.45f'_c$	$\epsilon_{c,s} = \frac{-26.2}{852 \times 3605} \left(1 + \frac{13.1^2}{7.75^2} \right) - \frac{289 \times 12 \times 9.39}{3605 \times 51,150}$ $\epsilon_{c,s} = 0.00016$ $f_{c,s} = 3,605,000 \text{ psi} (0.00016) = 577 \text{ psi}$ $0.45f'_c = 0.45(4000) = 1800 \text{ psi}$ $f_{c,s} = 577 \text{ psi} < 0.45f'_c = 1800 \text{ psi} \quad \text{OK}$	$\epsilon_{c,s} = \frac{-563,310}{5.5 \times 10^5 \times 24,700} \left(1 + \frac{333^2}{197^2} \right) - \frac{391.3 \times 10^6 \times 238}{24,700 \times 2.13 \times 10^{10}}$ $\epsilon_{c,s} = 0.00016$ $f_{c,s} = 24,700 \text{ N/mm}^2 (0.00016) = 3.95 \text{ N/mm}^2$ $0.45f'_c = 0.45(27.6) = 12.42 \text{ N/mm}^2$ $f_{c,s} = 3.95 \text{ N/mm}^2 < 0.45f'_c = 12.42 \text{ N/mm}^2 \quad \text{OK}$
<p>Step 17—Check service stresses in the FRP reinforcement</p> <p>The stress in the FRP at service condition can be calculated using Eq. (10.3.1.8):</p> $f_{f,s} = \left(\frac{E_f}{E_c} \right) \frac{M_s y_b}{I} - \epsilon_{bi} E_f$ <p>Because the section is uncracked at service, the gross moment of inertia of the section must be used.</p> <p>The calculated stress in FRP should be checked against the limits in Table 10.2.9. For carbon FRP:</p> $f_{f,s} \leq 0.55f_{fu}$	$f_{f,s} = \left(\frac{5360 \text{ ksi}}{3605 \text{ ksi}} \right) \frac{289 \text{ kip-ft} \times 12 \text{ in./ft} \times 15.61 \text{ in.}}{51,150 \text{ in.}^4} - 0.00003 \times 5360 \text{ ksi}$ $f_{f,s} = 1.41 \text{ ksi}$ $0.55f_{fu} = 0.55(85) = 47 \text{ ksi}$ $f_{f,s} = 1.41 \text{ ksi} < 0.55f_{fu} = 47 \text{ ksi} \quad \text{OK}$	$f_{f,s} = \left(\frac{37,700 \text{ N/mm}^2}{24,700 \text{ N/mm}^2} \right) \frac{391.3 \times 10^6 \text{ N/mm} \times 397 \text{ mm}}{2.13 \times 10^{10} \text{ mm}^4} - 0.00003 \times 37,700 \text{ N/mm}^2$ $f_{f,s} = 9.7 \text{ N/mm}^2$ $0.55f_{fu} = 0.55(586) = 322 \text{ N/mm}^2$ $f_{f,s} = 9.7 \text{ N/mm}^2 < 0.55f_{fu} = 322 \text{ N/mm}^2 \quad \text{OK}$

In detailing the FRP reinforcement, the FRP should be terminated a minimum of ℓ_{df} , calculated per Eq. (14.1.3), past the point on the moment diagram that represents cracking. The factored shear force at the termination should also be checked against the shear force that causes FRP end peeling,

estimated as two-thirds of the concrete shear strength. If the shear force is greater than two-thirds of the concrete shear strength, FRP strips should be extended further toward the supports. U-wraps may also be used to reinforce against cover delamination.

16.6—Shear strengthening of an interior T-beam

A reinforced concrete T-beam ($f'_c = 3000$ psi [20.7 N/mm²]) located inside of an office building is subjected to an increase in its live-load-carrying requirements. An analysis of the existing beam indicates that the beam is still satisfactory for flexural strength; however, its shear strength is inadequate to carry the increased live load. Based on the analysis, the nominal shear strength provided by the concrete is $V_c = 44.2$ kip (196.6 kN), and the nominal shear strength provided by steel reinforcement is $V_s = 19.6$ kip (87.2 kN). Thus, the design shear strength of the existing beam is $\phi V_{n,existing} = 0.75(44.2 \text{ kip} + 19.6 \text{ kip}) = 47.85$ kip (213 kN). The factored required shear strength, including the increased live load, at a distance d away from the support is $V_u = 57$ kip (253.5 kN). Figure 16.6a shows the shear diagram with the locations where shear strengthening is required along the length of the beam.

Supplemental FRP shear reinforcement is designed as shown in Fig. 16.6b and summarized in Table 16.6a. Each FRP strip consists of one ply ($n = 1$) of a flexible carbon sheet installed by wet layup. The FRP system manufacturer’s reported material properties are shown in Table 16.6b.

The design calculations used to arrive at this configuration follow in Table 16.6c.

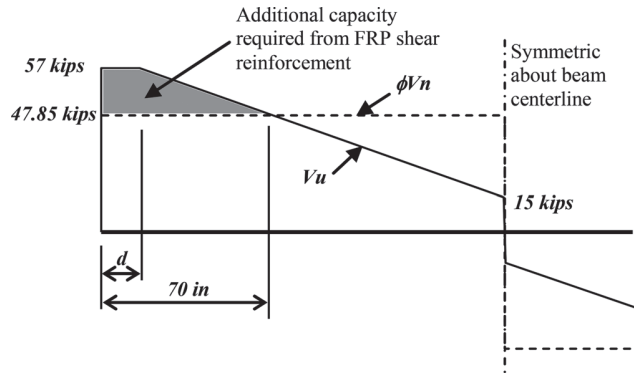


Fig. 16.6a—Shear diagram showing demand versus existing strength. The FRP reinforcement should correct the deficiency shown shaded.

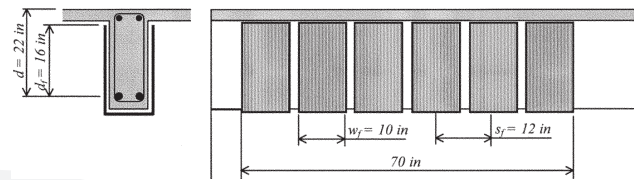


Fig. 16.6b—Configuration of the supplemental FRP shear reinforcement.

Table 16.6a—Configuration of the supplemental FRP shear reinforcement

d	22 in.	559 mm
d_{fv}	16 in.	406 mm
Width of each sheet w_f	10 in.	254 mm
Span between each sheet s_f	12 in.	305 mm
FRP strip length	70 in.	1778 mm

Table 16.6b—Manufacturer’s reported FRP system properties

Thickness per ply t_f	0.0065 in.	0.165 mm
Ultimate tensile strength f_{fu}^*	550,000 psi	3790 N/mm ²
Rupture strain ϵ_{fu}^*	0.017 in./in.	0.017 mm/mm
Modulus of elasticity E_f	33,000,000 psi	227,530 N/mm ²

Table 16.6c—Procedure for shear strengthening of an interior T-beam

Procedure	Calculation in in.-lb units	Calculation in SI metric units
<p>Step 1—Compute the design material properties</p> <p>The beam is located in an enclosed and conditioned space and a CFRP material will be used. Therefore, per Table 9.4, an environmental-reduction factor of 0.95 is suggested.</p> $f_{fu} = C_E f_u^*$ $\epsilon_{fu} = C_E \epsilon_{fu}^*$	$f_{fu} = (0.95)(550 \text{ ksi}) = 522.5 \text{ ksi}$ $\epsilon_{fu} = (0.95)(0.017) = 0.016$	$f_{fu} = (0.95)(3.79 \text{ kN/mm}^2) = 3.60 \text{ kN/mm}^2$ $\epsilon_{fu} = (0.95)(0.017) = 0.016$
<p>Step 2—Calculate the effective strain level in the FRP shear reinforcement</p> <p>The effective strain in FRP U-wraps should be determined using the bond-reduction coefficient κ_v. This coefficient can be computed using Eq. (11.4.1.2b) through (11.4.2.1e).</p> $L_e = \frac{2500}{(n_f E_f)^{0.58}}$ $k_1 = \left(\frac{f'_c}{4000} \right)^{2/3}$ $k_2 = \left(\frac{d_{fv} - L_e}{d_{fv}} \right)$ $\kappa_v = \frac{k_1 k_2 L_e}{468 \epsilon_{fu}} \leq 0.75$ <p>The effective strain can then be computed using Eq. (11.4.1.2a) as follows:</p> $\epsilon_{fe} = \kappa_v \epsilon_{fu} \leq 0.004$	$L_e = \frac{2500}{[(1)(0.0065 \text{ in.})(33 \times 10^6 \text{ psi})]^{0.58}} = 2.0 \text{ in.}$ $k_1 = \left(\frac{3000 \text{ psi}}{4000} \right)^{2/3} = 0.825$ $k_2 = \left(\frac{16 \text{ in.} - 2.0 \text{ in.}}{16 \text{ in.}} \right) = 0.875$ $\kappa_v = \frac{(0.82)(0.875)(2 \text{ in.})}{468(0.016)} = 0.193 \leq 0.75$ $\epsilon_{fe} = 0.193(0.016) = 0.0031 \leq 0.004$	$L_e = \frac{416}{[(1)(0.1651 \text{ mm})(227.5 \times 10^3 \text{ kN/mm}^2)]^{0.58}} = 50.8 \text{ mm}$ $k_1 = \left(\frac{20.7 \text{ kN/mm}^2}{254} \right)^{2/3} = 0.825$ $k_2 = \left(\frac{406 \text{ mm} - 50.8 \text{ mm}}{406 \text{ mm}} \right) = 0.875$ $\kappa_v = \frac{(0.82)(0.875)(50.8 \text{ mm})}{11,910(0.016)} = 0.193 \leq 0.75$ $\epsilon_{fe} = 0.193(0.016) = 0.0031 \leq 0.004$
<p>Step 3—Calculate the contribution of the FRP reinforcement to the shear strength</p> <p>The area of FRP shear reinforcement can be computed as:</p> $A_{fv} = 2n_f w_f$ <p>The effective stress in the FRP can be computed from Hooke's law.</p> $f_{fe} = \epsilon_{fe} E_f$ <p>The shear contribution of the FRP can be then calculated from Eq. (11.4a):</p> $V_f = \frac{A_{fv} f_{fe} (\sin \alpha + \cos \alpha) d_{fv}}{s_f}$	$A_{fv} = 2(1)(0.0065 \text{ in.})(10 \text{ in.}) = 0.13 \text{ in.}^2$ $f_{fe} = (0.0031)(33,000 \text{ ksi}) = 102 \text{ ksi}$ $V_f = \frac{(0.13 \text{ in.}^2)(102 \text{ ksi})(1)(16 \text{ in.})}{(12 \text{ in.})}$ $V_f = 17.7 \text{ kip}$	$A_{fv} = 2(1)(0.1651 \text{ mm})(254 \text{ mm}) = 83.87 \text{ mm}^2$ $f_{fe} = (0.0031)(227.6 \text{ kN/mm}^2) = 0.703 \text{ kN/mm}^2$ $V_f = \frac{(83.87 \text{ mm}^2)(0.703 \text{ kN/mm}^2)(1)(406 \text{ mm})}{(304.8 \text{ mm})}$ $V_f = 78.5 \text{ kN}$

Table 16.6c (cont.)—Procedure for shear strengthening of an interior T-beam

Procedure	Calculation in in.-lb units	Calculation in SI metric units
<p>Step 4—Calculate the shear strength of the section</p> <p>The design shear strength can be computed from Eq. (11.3b) with $\psi_f = 0.85$ for U-wraps.</p> $\phi V_n = \phi(V_c + V_s + \psi_f V_f)$	$\phi V_n = 0.75[44.2 + 19.6 + (0.85)(17.7)]$ $\phi V_n = 59 \text{ kip} > V_u = 57 \text{ kip}$ <p>\therefore the strengthened section is capable of sustaining the required shear strength.</p>	$\phi V_n = 0.75[196.6 + 87.2 + (0.85)(78.5)]$ $\phi V_n = 263 \text{ kN} > V_u = 253.3 \text{ kN}$ <p>\therefore the strengthened section is capable of sustaining the required shear strength.</p>



16.7—Shear strengthening of an exterior column

A 24 x 24 in. (610 x 610 mm) square column requires an additional 60 kip (267 kN) of shear strength ($\Delta V_u = 60$ kip [267 kN]). The column is located in an unenclosed parking garage and experiences a wide variation in temperature and climate. A method of strengthening the column using FRP is sought.

An E-glass-based FRP complete wrap is selected to retrofit the column. The properties of the FRP system, as reported by the manufacturer, are shown in Table 16.7. The design calculations to arrive at the number of complete wraps required follow.

Table 16.7a—Manufacturer’s reported FRP system properties*

Thickness per ply t_f	0.051 in.	1.3 mm
Guaranteed ultimate tensile strength f_{fu}^*	80,000 psi	552 N/mm ²
Guaranteed rupture strain ϵ_{fu}^*	0.020 in./in.	0.020 mm/mm
Modulus of elasticity E_f	4,000,000 psi	27,600 N/mm ²
*The reported properties are laminate properties.		



Table 16.7b—Procedure for shear strengthening of an exterior column

Procedure	Calculation in in.-lb units	Calculation in SI metric units
<p>Step 1—Compute the design material properties</p> <p>The column is located in an exterior environment and a glass FRP (GFRP) material will be used. Therefore, per Table 9.4, an environmental reduction factor of 0.65 is suggested.</p> $f_{fu} = C_E f_{fu}^*$ $\varepsilon_{fu} = C_E \varepsilon_{fu}^*$	$f_{fu} = (0.65)(80 \text{ ksi}) = 52 \text{ ksi}$ $\varepsilon_{fu} = (0.65)(0.020) = 0.013$	$f_{fu} = (0.65)(552 \text{ N/mm}^2) = 358.5 \text{ N/mm}^2$ $\varepsilon_{fu} = (0.65)(0.020) = 0.013$
<p>Step 2—Calculate the effective strain level in the FRP shear reinforcement</p> <p>The effective strain in a complete FRP wrap can be determined from Eq. (11.4.1.1):</p> $\varepsilon_{fe} = 0.004 \leq 0.75\varepsilon_{fu}$	$\varepsilon_{fe} = 0.004 \leq 0.75(0.013) = 0.010$ <p>∴ use an effective strain of $\varepsilon_{fe} = 0.004$.</p>	$\varepsilon_{fe} = 0.004 \leq 0.75(0.013) = 0.010$ <p>∴ use an effective strain of $\varepsilon_{fe} = 0.004$.</p>
<p>Step 3—Determine the area of FRP reinforcement required</p> <p>The required shear contribution of the FRP reinforcement can be computed based on the increase in strength needed, the strength reduction factor for shear, and a partial-reduction factor $\psi_f = 0.95$ for completely wrapped sections in shear.</p> $V_{f,reqd} = \frac{\Delta V_u}{\phi(\psi_f)}$ <p>The required area of FRP can be determined by reorganizing Eq. (11.4a). The required area is left in terms of the spacing.</p> $A_{fv,reqd} = \frac{V_{f,reqd} s_f}{\varepsilon_{fe} E_f (\sin \alpha + \cos \alpha) d_f}$	$V_{f,reqd} = \frac{60 \text{ kip}}{0.85(0.95)} = 74.3 \text{ kip}$ $A_{fv,reqd} = \frac{(74.3 \text{ kip})s_f}{(0.004)(4000 \text{ ksi})(1)(24 \text{ in.})} = 0.194s_f$	$V_{f,reqd} = \frac{266.9 \text{ kN}}{0.85(0.95)} = 330.5 \text{ kN}$ $A_{fv,reqd} = \frac{(330.5 \text{ kN})s_f}{(0.004)(27.6 \text{ kN/mm}^2)(1)(610 \text{ mm})} = 4.91s_f$
<p>Step 4—Determine the number of plies, and strip width and spacing.</p> <p>The number of plies can be determined in terms of the strip width and spacing as follows:</p> $n = \frac{A_{fv,reqd}}{2t_f w_f}$	$n = \frac{0.194s_f}{2(0.051 \text{ in.})w_f} = 1.90 \frac{s_f}{w_f}$ <p>∴ use two plies ($n = 2$) continuously along the height of the column ($s_f = w_f$).</p>	$n = \frac{4.91s_f}{2(1.3 \text{ mm})w_f} = 1.90 \frac{s_f}{w_f}$ <p>∴ use two plies ($n = 2$) continuously along the height of the column ($s_f = w_f$).</p>

16.8—Strengthening of a noncircular concrete column for axial load increase

A 24 x 24 in. (610 x 610 mm) square column requires an additional 20 percent of axial load-carrying capacity. Concrete and steel reinforcement material properties as well as details of the cross section of the column are shown in Table 16.8a. The column is located in an interior envi-

ronment, and a CFRP material will be used. A method of strengthening the column is sought.

A carbon-based FRP complete wrap is selected to retrofit the columns. The properties of the FRP system, as reported by the manufacturer, are shown in Table 16.8b. The design calculations to arrive at the number of required complete wraps follow.

Table 16.8a—Column cross section details and material properties

	f'_c	6.5 ksi	45 MPa
	f_y	60 ksi	400 MPa
	r_c	1 in.	25 mm
	Bars	12 No. 10	12 ϕ 32
	A_g	576 in. ²	3716 cm ²
	A_{st}	15.24 in. ²	98 cm ²
	$\rho_g, \%$	2.65	2.65
	ϕP_n without FRP	2087 kip	9281 kN
	$\phi P_{n(req)}$	2504 kip	11,138 kN
	Note: The column features steel ties for transverse reinforcement.		

Table 16.8b—Manufacturer’s reported FRP system properties

Thickness per ply t_f	0.013 in.	0.33 mm
Ultimate tensile strength f_{fu}^*	550 ksi	3792 MPa
Rupture strain ϵ_{fu}^*	0.0167 in./in.	0.0167 mm/mm
Modulus of elasticity E_f	33,000 ksi	227,527 MPa

Table 16.8c—Procedure for strengthening of a noncircular concrete column for axial load increase

Procedure	Calculation in in.-lb units	Calculation in SI metric units
<p>Step 1—Compute the design FRP material properties</p> <p>The column is located in an interior environment and a CFRP material will be used. Therefore, per Table 9.4, an environmental reduction factor of 0.95 is suggested.</p> $f_{fu} = C_E f_{fu}^*$ $\varepsilon_{fu} = C_E \varepsilon_{fu}^*$	$f_{fu} = (0.95)(550 \text{ ksi}) = 522.5 \text{ ksi}$ $\varepsilon_{fu} = (0.95)(0.0167) = 0.0159 \text{ in./in.}$	$f_{fu} = (0.95)(3792 \text{ MPa}) = 3603 \text{ MPa}$ $\varepsilon_{fu} = (0.95)(0.0167) = 0.0159 \text{ mm/mm}$
<p>Step 2—Determine the required maximum compressive strength of confined concrete f'_{cc}</p> <p>f'_{cc} can be obtained by reordering Eq. (12.1b):</p> $f'_{cc} = \frac{1}{0.85(A_g - A_{st})} \left(\frac{\phi P_{n,req}}{0.80\phi} - f_y A_{st} \right)$	$f'_{cc} = \frac{1}{0.85 \times (576 \text{ in.}^2 - 15.24 \text{ in.}^2)} \times \left(\frac{2504 \text{ kip}}{0.80 \times 0.65} - 60 \text{ ksi} \times 15.24 \text{ in.}^2 \right)$ $f'_{cc} = 8.18 \text{ ksi}$	$f'_{cc} = \frac{1}{0.85 \times (371,612 \text{ mm}^2 - 9832 \text{ mm}^2)} \times \left(\frac{11,138 \text{ kN}}{0.80 \times 0.65} - 414 \text{ MPa} \times 9832 \text{ mm}^2 \right)$ $f'_{cc} = 56.4 \text{ MPa}$
<p>Step 3—Determine the maximum confining pressure due to the FRP jacket f_t</p> <p>f_t can be obtained by reordering Eq. (12.1g):</p> $f_t = \frac{f'_{cc} - f'_c}{3.3\kappa_a}$ <p>where</p> $\kappa_a = \frac{A_e}{A_c} \left(\frac{b}{h} \right)^2$ $\frac{A_e}{A_c} = \frac{1 - \left[\left(\frac{b}{h} \right) (h - 2r_c)^2 + \left(\frac{h}{b} \right) (b - 2r_c)^2 \right]}{3A_g} - \rho_g$	$f_t = \frac{8.18 \text{ ksi} - 6.5 \text{ ksi}}{0.95 \times 3.3 \times 0.425} = 1.26 \text{ ksi}$ $\kappa_a = 0.425(1)^2 = 0.425$ $\frac{A_e}{A_c} = \frac{1 - [2 \times (1)(24 \text{ in.} - 2 \times 1 \text{ in.})^2]}{3 \times 576 \text{ in.}^2} - 0.0265$ $\frac{A_e}{A_c} = 0.425$	$f_t = \frac{56.4 \text{ MPa} - 44.8 \text{ MPa}}{0.95 \times 3.3 \times 0.425} = 8.7 \text{ MPa}$ $\kappa_a = 0.425(1)^2 = 0.425$ $\frac{A_e}{A_c} = \frac{1 - [2 \times (1)(610 \text{ mm} - 2 \times 25 \text{ mm})^2]}{3 \times 371,612 \text{ mm}^2} - 0.0265$ $\frac{A_e}{A_c} = 0.425$
<p>Step 4—Determine the number of plies n.</p> <p>n can be obtained by reordering Eq. (12.1h):</p> $n = \frac{f_t \sqrt{b^2 + h^2}}{2E_f t_f \varepsilon_{fe}}$ $\varepsilon_{fe} = \kappa_c \varepsilon_{fu}$ <p>Checking the minimum confinement ratio:</p> $\frac{f_t}{f'_c} \geq 0.08$	$n = \frac{1.26 \text{ ksi} \sqrt{(24 \text{ in.})^2 + (24 \text{ in.})^2}}{2(33,000 \text{ ksi})(0.013 \text{ in.})(8.8 \times 10^{-3} \text{ in./in.})}$ $n = 5.7 \approx 6 \text{ plies}$ $\varepsilon_{fe} = 0.55 \times 0.0159 \text{ in./in.} = 8.8 \times 10^{-3} \text{ in./in.}$ $\frac{f_t}{f'_c} = \frac{1.26 \text{ ksi}}{6.5 \text{ ksi}} = 0.19 > 0.08 \quad \text{OK}$	$n = \frac{8.7 \text{ MPa} \sqrt{(610 \text{ mm})^2 + (610 \text{ mm})^2}}{2(227,527 \text{ MPa})(0.33 \text{ mm})(8.8 \times 10^{-3} \text{ mm/mm})}$ $n = 5.7 \approx 6 \text{ plies}$ $\varepsilon_{fe} = 0.55 \times 0.0159 \text{ mm/mm} = 8.8 \times 10^{-3} \text{ mm/mm}$ $\frac{f_t}{f'_c} = \frac{8.7 \text{ MPa}}{44.8 \text{ MPa}} = 0.19 > 0.08 \quad \text{OK}$

Table 16.8c (cont.)—Procedure for strengthening of a noncircular concrete column for axial load increase

Procedure	Calculation in in.-lb units	Calculation in SI metric units
<p>Step 5—Verify that the ultimate axial strain of the confined concrete $\epsilon_{ccu} \leq 0.01$</p> <p>ϵ_{ccu} can be obtained using Eq. (12.1j):</p> $\epsilon_{ccu} = \epsilon'_c \left(1.5 + 12\kappa_b \frac{f'_c}{f'_c} \left(\frac{\epsilon_{f'e}}{\epsilon'_c} \right)^{0.45} \right)$ <p>where</p> $\kappa_b = \frac{A_g}{A_c} \left(\frac{h}{b} \right)^{0.5}$ <p>If the case that ϵ_{ccu} was to be greater than 0.01, then f'_{cc} should be recalculated from the stress-strain model using Eq. (12.1c).</p>	<p>$\epsilon_{cc} = (0.002 \text{ in./in.})$</p> $\times \left(1.5 + 12 \times 0.425 \times \frac{1.2 \text{ ksi}}{6.5 \text{ ksi}} \left(\frac{8.8 \times 10^{-3} \text{ in./in.}}{0.002 \text{ in./in.}} \right)^{0.45} \right)$ <p>$\epsilon_{cc} = 0.0067 \text{ in./in.} < 0.01 \quad \text{OK}$</p> <p>$\kappa_b = 0.425(1)^{0.5} = 0.425$</p>	<p>$\epsilon_{cc} = (0.002 \text{ mm/mm})$</p> $\times \left(1.5 + 12 \times 0.425 \times \frac{8.3 \text{ MPa}}{44.8 \text{ MPa}} \left(\frac{8.8 \times 10^{-3} \text{ mm/mm}}{0.002 \text{ mm/mm}} \right)^{0.45} \right)$ <p>$\epsilon_{cc} = 0.0067 \text{ mm/mm} < 0.01 \quad \text{OK}$</p> <p>$\kappa_b = 0.425(1)^{0.5} = 0.425$</p>



16.9—Strengthening of a noncircular concrete column for increase in axial and bending forces

The column described in 16.8 is subjected to an ultimate axial compressive load $P_u = 1900$ kip (8451 kN) and an ultimate bending moment $M_u = 380$ kip-ft (515 kN-m) ($e =$

$0.1h$). It is sought to increase load demands by 30 percent at constant eccentricity ($P_u = 2470$ kip, $M_u = 494$ kip-ft).

The calculations to determine moment-axial interaction for the FRP confined column follow in Table 16.9

Table 16.9—Procedure for strengthening of a noncircular concrete column for increase in axial and bending forces

Procedure	Calculation in in.-lb units	Calculation in SI metric units
<p>Step 1—Determine the simplified curve for the unstrengthened column ($n = 0$ plies)</p> <p>Points A, B, and C can be obtained by well-known procedures, and also by using Eq. (D-1) to (D-5) considering $\psi_f = 1$, $f_{cc}' = f_c'$, $E_2 = 0$, and $\epsilon_{ccu} = \epsilon_{cu} = 0.003$.</p>	<p>$\phi P_{n(A)} = 2087$ kip; $\phi M_{n(A)} = 0$ kip-ft $\phi P_{n(B)} = 1858$ kip; $\phi M_{n(B)} = 644$ kip-ft $\phi P_{n(C)} = 928$ kip; $\phi M_{n(C)} = 884$ kip-ft</p>	<p>$\phi P_{n(A)} = 9283$ kN; $\phi M_{n(A)} = 0$ kN-m $\phi P_{n(B)} = 8265$ kN; $\phi M_{n(B)} = 873$ kN-m $\phi P_{n(C)} = 4128$ kN; $\phi M_{n(C)} = 1199$ kN-m</p>



Table 16.9 (cont.)—Procedure for strengthening of a noncircular concrete column for increase in axial and bending forces

Procedure	Calculation in in.-lb units	Calculation in SI metric units
<p>Step 2—Determine the simplified curve for a strengthened column</p> <p>A wrapping system composed of six plies will be the starting point to construct the bilinear Curve A-B-C and then be compared with the position of the required P_u and M_u.</p> <p>Points A, B, and C of the curve can be computed using Eq. (12-1), (D-1), and (D-2):</p> $\phi P_{n(A)} = \phi 0.8(0.85f'_{cc}(A_g - A_{sr}) + f_y A_{sr})$ $\phi P_{n(B,C)} = \phi(A(y_i)^3 + B(y_i)^2 + C(y_i) + D) + \frac{\sum A_{sif_{si}}}{\sum A_{sif_{si}}}$ $\phi M_{n(B,C)} = \phi(E(y_i)^4 + F(y_i)^3 + G(y_i)^2 + H(y_i) + I) + \sum A_{sif_{si}} d_i$ <p>The coefficients $A, B, C, D, E, F, G, H,$ and I of the previous expressions are given by Eq. (D-3):</p> $A = \frac{-b(E_c - E_2)^2 \left(\frac{\epsilon_{ccu}}{c}\right)^2}{12f'_c}$ $B = \frac{b(E_c - E_2) \left(\frac{\epsilon_{ccu}}{c}\right)}{2}$ $C = bf'_c$ $D = bf'_c + \frac{bcE_2}{2} (\epsilon_{ccu})$ $E = \frac{-b(E_c - E_2)^2 \left(\frac{\epsilon_{ccu}}{c}\right)^2}{16f'_c}$ $F = b\left(c - \frac{h}{2}\right) \frac{(E_c - E_2)^2 \left(\frac{\epsilon_{ccu}}{c}\right)^2}{12f'_c} + \frac{b(E_c - E_2) \left(\frac{\epsilon_{ccu}}{c}\right)}{3}$ $G = -\left(\frac{b}{2} f'_c + b\left(c - \frac{h}{2}\right) \frac{(E_c - E_2) \left(\frac{\epsilon_{ccu}}{c}\right)}{2}\right)$ $H = bf'_c \left(c - \frac{h}{2}\right)$ $I = \frac{bc^2}{2} f'_c - bcf'_c \left(c - \frac{h}{2}\right) + \frac{bc^2 E_2}{3} (\epsilon_{ccu}) - \frac{bcE_2}{2} \left(c - \frac{h}{2}\right) (\epsilon_{ccu})$	<p>Point A: Nominal axial capacity:</p> $\phi P_{n(A)} = 0.65 \times 0.8(0.85 \times 8.26 \text{ ksi} \times (576 \text{ in.}^2 - 15.24 \text{ in.}^2) + 60 \text{ ksi} \times 15.24 \text{ in.}^2)$ $\phi P_{n(A)} = 2523 \text{ kip}$ <p>where</p> $f'_{cc} = 6.5 \text{ ksi} + 3.3(0.425)(1.26 \text{ ksi})$ $f'_{cc} = 8.26 \text{ ksi}$ $f_t = \frac{0.95 \times 2 \times 33,000 \text{ ksi} \times 6 \times 0.013 \text{ in.} \times \left(0.55 \times 0.0159 \frac{\text{in.}}{\text{in.}}\right)}{\sqrt{(24 \text{ in.})^2 + (24 \text{ in.})^2}}$ $f_t = 1.26 \text{ ksi}$ <p>Point B: Nominal axial capacity:</p> $\phi P_{n(B)} = 0.65[-0.22 \text{ kip/in.}^3(15.33 \text{ in.})^3 + 10.17 \text{ ksi}(15.33 \text{ in.})^2 - 56 \text{ kip/in.}(15.33 \text{ in.}) + 3645.2 \text{ kip}] + 5.08 \text{ in.}^2(60 \text{ ksi}) + 2.54 \text{ in.}^2(60 \text{ ksi}) + 2.54 \text{ in.}^2(37.21 \text{ ksi})]$ $\phi P_{n(B)} = 2210 \text{ kip}$ <p>where</p> $A = \frac{-24 \text{ in.}(4595 \text{ ksi} - 190.7 \text{ ksi})^2 \left(\frac{0.0042 \text{ in./in.}}{22 \text{ in.}}\right)^2}{12 \times 6.5 \text{ ksi}}$ $A = -0.22 \text{ kip/in.}^3$ $B = \frac{24 \text{ in.}(4595 \text{ ksi} - 190.7 \text{ ksi}) \left(\frac{0.0042 \text{ in./in.}}{22 \text{ in.}}\right)}{2}$ $B = 10.17 \text{ ksi}$ $C = -24 \text{ in.} \times 6.5 \text{ ksi} = -156 \text{ kip/in.}$ $D = 24 \text{ in.} \times 22 \text{ in.} \times 6.5 \text{ ksi} + \frac{24 \text{ in.} \times 22 \text{ in.} \times 190.7 \text{ ksi}}{2} \times (0.0042 \text{ in./in.}) = 3645.2 \text{ kip}$	<p>Point A: Nominal axial capacity:</p> $\phi P_{n(A)} = 0.65 \times 0.8(0.85 \times 56.96 \text{ MPa} \times (371,612 \text{ mm}^2 - 9832 \text{ mm}^2) + 414 \text{ MPa} \times 9232 \text{ mm}^2)$ $\phi P_{n(A)} = 11,223 \text{ kN}$ <p>where</p> $f'_{cc} = 44.8 \text{ MPa} + 3.3(0.425)(8.7 \text{ MPa})$ $f'_{cc} = 56.96 \text{ MPa}$ $f_t = \frac{0.95 \times 2 \times 227,500 \text{ MPa} \times 6 \times 0.33 \text{ mm} \times \left(0.55 \times 0.0159 \frac{\text{mm}}{\text{mm}}\right)}{\sqrt{(610 \text{ mm})^2 + (610 \text{ mm})^2}}$ $f_t = 8.67 \text{ MPa}$ <p>Point B: Nominal axial capacity:</p> $\phi P_{n(B)} = 0.65[-6.003 \times 10^{-5} \text{ kN/mm}^3(389 \text{ mm})^3 + 70.14 \times 10^{-3} \text{ kN/mm}^2(389 \text{ mm})^2 - 27.32 \text{ kN/mm}(389 \text{ mm}) + 16,215 \text{ kN}] + 3277 \text{ mm}^2(414 \text{ MPa}) + 1639 \text{ mm}^2(414 \text{ MPa}) + 1639 \text{ mm}^2(257 \text{ ksi})]$ $\phi P_{n(B)} = 9892 \text{ kN}$ <p>where</p> $A = \frac{-610 \text{ mm}(31,685 \text{ MPa} - 1315 \text{ MPa})^2 \left(\frac{0.0042 \text{ mm/mm}}{559 \text{ mm}}\right)^2}{12 \times 44.8 \text{ MPa}}$ $A = -6.003 \times 10^{-5} \text{ kN/mm}^3$ $B = \frac{600 \text{ mm}(31,685 \text{ MPa} - 1315 \text{ MPa}) \left(\frac{0.0042 \text{ mm/mm}}{559 \text{ mm}}\right)}{2}$ $B = 70.14 \times 10^{-3} \text{ kN/mm}^2$ $C = -610 \text{ mm} \times 44.84 \text{ MPa} = -27.32 \text{ kN/mm}$ $D = 610 \text{ mm} \times 559 \text{ mm} \times 44.8 \text{ MPa} + \frac{610 \text{ mm} \times 559 \text{ mm} \times 1315 \text{ MPa}}{2} \times (0.0042 \text{ mm/mm}) = 16,215 \text{ kN}$

Table 16.9 (cont.)—Procedure for strengthening of a noncircular concrete column for increase in axial and bending forces

Procedure	Calculation in in.-lb units	Calculation in SI metric units
<p>Key parameters of the stress-strain model:</p> $y_t = c \frac{\epsilon'_t}{\epsilon_{ccu}}$ $c = \begin{cases} d & \text{for Point B} \\ d \frac{\epsilon_{ccu}}{\epsilon_{sy} + \epsilon_{ccu}} & \text{for Point C} \end{cases}$ $\epsilon'_t = \frac{2f'_c}{E_c - E_2}$ $E_2 = \frac{f'_{cc} - f'_c}{\epsilon_{ccu}}$ $f'_{cc} = f'_c + 3.3\kappa_a f'_t$ $\epsilon_{ccu} = \epsilon'_c \left(1.5 + 12\kappa_b \frac{f'_t}{f'_c} \left(\frac{\epsilon_{fe}}{\epsilon'_c} \right)^{0.45} \right)$ $\epsilon_{fe} = \min(0.004, \kappa_c \epsilon_{fu})$ $\kappa_a = \frac{A_e}{A_c} \left(\frac{b}{h} \right)^2$ $\kappa_b = \frac{A_e}{A_c} \left(\frac{h}{b} \right)^{0.5}$ $\frac{\Psi_f E_f n t_f \epsilon_{fe}}{\sqrt{b^2 h^2}}$	<p>For the calculation of the coefficients, it is necessary to compute key parameters from the stress-strain model:</p> $y_t = 22 \text{ in.} \times \frac{0.003 \text{ in./in.}}{0.0042 \text{ in./in.}} = 15.33 \text{ in.}$ $c = 22 \text{ in.}$ $\epsilon'_t = \frac{2 \times 6.5 \text{ ksi}}{4595 \text{ ksi} - 190.7 \text{ ksi}} = 0.003 \text{ in./in.}$ $E_2 = \frac{7.31 \text{ ksi} - 6.5 \text{ ksi}}{0.0042 \text{ in./in.}} = 190.7 \text{ ksi}$ $f'_{cc} = 6.5 \text{ ksi} + 3.3(0.425)(0.58 \text{ ksi}) = 7.31 \text{ ksi}$ $\epsilon_{ccu} = 0.002 \text{ in./in.}$ $\times \left(1.5 + 12 \times 0.425 \left(\frac{0.58 \text{ ksi}}{6.5 \text{ ksi}} \right) \left(\frac{0.004 \text{ in./in.}}{0.002 \text{ in./in.}} \right)^{0.45} \right)$ $\epsilon_{ccu} = 0.0042 \text{ in./in.}$ $\kappa_a = \kappa_b = 0.425$ $f_t = \frac{0.95 \times 2 \times 33,000 \text{ ksi} \times 6 \times 0.013 \text{ in.} \times (0.004 \text{ in./in.})}{\sqrt{(24 \text{ in.})^2 + (24 \text{ in.})^2}}$ <p>Checking the minimum confinement ratio: $f_t/f'_c = 0.58 \text{ ksi}/6.5 \text{ ksi} = 0.09 \geq 0.08$ OK</p> <p>The strains in each layer of steel are determined by similar triangles in the strain distribution. The corresponding stresses are then given by: $f_{s1} = \epsilon_{s1} E_s = 0.0038 \text{ in./in.} \times 29,000 \text{ ksi} \rightarrow 60 \text{ ksi}$ $f_{s2} = \epsilon_{s2} E_s = 0.0026 \text{ in./in.} \times 29,000 \text{ ksi} \rightarrow 60 \text{ ksi}$ $f_{s3} = \epsilon_{s3} E_s = 0.0013 \text{ in./in.} \times 29,000 \text{ ksi} = 37.2 \text{ ksi}$ $f_{s4} = \epsilon_{s4} E_s = 0 \text{ in./in.} \times 29,000 \text{ ksi} = 0 \text{ ksi}$</p> <p>Nominal bending moment: $\phi M_{n(B)} = 0.65[-0.166 \text{ kip/in.}^3(15.33 \text{ in.})^4 + 8.99 \text{ ksi}(15.33 \text{ in.})^3 - 179.73 \text{ kip/in.}(15.33 \text{ in.})^2 + 1560 \text{ kip}(15.33 \text{ in.}) + 4427 \text{ kip-in.}] + 5.08 \text{ in.}^2(60 \text{ ksi})(10 \text{ in.}) + 2.54 \text{ in.}^2(60 \text{ ksi})(3.3 \text{ in.}) - 2.54 \text{ in.}^2(37.21 \text{ ksi})(3.3 \text{ in.})$ $\phi M_{n(B)} = 682 \text{ kip-ft}$</p> <p>where</p> $E = \frac{-24 \text{ in.}(4595 \text{ ksi} - 190.7 \text{ ksi})^2 \left(\frac{0.0042 \text{ in./in.}}{22 \text{ in.}} \right)^2}{16 \times 6.5 \text{ ksi}} = -0.166 \text{ kip/in.}^3$	<p>For the calculation of the coefficients, it is necessary to compute key parameters from the stress-strain model:</p> $y_t = 559 \text{ mm} \times \frac{0.003 \text{ mm/mm}}{0.0042 \text{ mm/mm}} = 389 \text{ mm}$ $c = 559 \text{ mm}$ $\epsilon'_t = \frac{2 \times 44.8 \text{ MPa}}{31,685 \text{ MPa} - 1315 \text{ MPa}} = 0.003 \text{ mm/mm}$ $E_2 = \frac{50.4 \text{ MPa} - 44.8 \text{ MPa}}{0.0042 \text{ mm/mm}} = 1315 \text{ MPa}$ $f'_{cc} = 44.8 \text{ MPa} + 3.3(0.425)(3.97 \text{ MPa}) = 50.4 \text{ MPa}$ $\epsilon_{ccu} = 0.002 \text{ mm/mm}$ $\times \left(1.5 + 12 \times 0.425 \left(\frac{3.97 \text{ MPa}}{44.8 \text{ MPa}} \right) \left(\frac{0.004 \text{ mm/mm}}{0.002 \text{ mm/mm}} \right)^{0.45} \right)$ $\epsilon_{ccu} = 0.0042 \text{ mm/mm}$ $\kappa_a = \kappa_b = 0.425$ $f_t = \frac{0.95 \times 2 \times 227,527 \text{ MPa} \times 6 \times 0.33 \text{ mm} \times (0.004 \text{ mm/mm})}{\sqrt{(610 \text{ mm})^2 + (610 \text{ mm})^2}}$ <p>Checking the minimum confinement ratio: $f_t/f'_c = 3.97 \text{ MPa}/44.8 \text{ MPa} = 0.09 \geq 0.08$ OK</p> <p>The strains in each layer of steel are determined by similar triangles in the strain distribution. The corresponding stresses are then given by: $f_{s1} = \epsilon_{s1} E_s = 0.0038 \text{ mm/mm} \times 200,000 \text{ MPa} \rightarrow 414 \text{ MPa}$ $f_{s2} = \epsilon_{s2} E_s = 0.0026 \text{ mm/mm} \times 200,000 \text{ MPa} \rightarrow 414 \text{ MPa}$ $f_{s3} = \epsilon_{s3} E_s = 0.0013 \text{ mm/mm} \times 200,000 \text{ MPa} = 257 \text{ MPa}$ $f_{s4} = \epsilon_{s4} E_s = 0 \text{ mm/mm} \times 200,000 \text{ MPa} = 0 \text{ MPa}$</p> <p>Nominal bending moment: $\phi M_{n(B)} = 0.65[-4.502 \times 10^{-5} \text{ kN/mm}^3(389 \text{ mm})^4 + 62.01 \times 10^{-3} \text{ kN/mm}^3(389 \text{ mm})^3 - 31.48 \text{ kN/mm}(389 \text{ mm})^2 + 6939 \text{ kN}(389 \text{ mm}) + 500,162 \text{ kN-mm}] + 3277 \text{ mm}^2(414 \text{ MPa})(254 \text{ mm}) + 1639 \text{ mm}^2(414 \text{ MPa})(85 \text{ mm}) - 1639 \text{ mm}^2(257 \text{ MPa})(85 \text{ mm})$ $\phi M_{n(B)} = 924 \text{ kN-m}$</p> <p>where</p> $E = \frac{-610 \text{ mm}(31,685 \text{ MPa} - 1315 \text{ MPa})^2}{16 \times 44.8 \text{ MPa}} \times \left(\frac{0.0042 \text{ mm/mm}}{559 \text{ mm}} \right)^2 = -0.452 \times 10^{-5} \text{ kN/mm}^3$
<p>Notes: The designer should bear in mind that, for the case of pure compression, the effective strain in the FRP, ϵ_{fe}, is limited by $\kappa_c \epsilon_{fu}$ and, in the case of combined axial and bending, by $\epsilon_{fe} = \min(0.004, \kappa_c \epsilon_{fu})$.</p>		



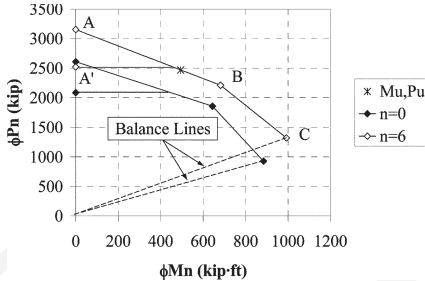
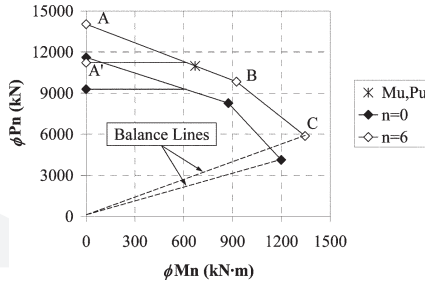
Table 16.9 (cont.)—Procedure for strengthening of a noncircular concrete column for increase in axial and bending forces

Procedure	Calculation in in.-lb units	Calculation in SI metric units
	$F = 24 \text{ in.}(22 \text{ in.} - 12 \text{ in.})$ $\times \frac{(4595 \text{ ksi} - 190.7 \text{ ksi})^2}{12 \times 6.5 \text{ ksi}} \times \left(\frac{0.0042 \text{ in./in.}}{22 \text{ in.}}\right)^2$ $+ \frac{24 \text{ in.}(4595 \text{ ksi} - 190.7 \text{ ksi})}{3} \times \left(\frac{0.0042 \text{ in./in.}}{22 \text{ in.}}\right)$ $= 0.899 \text{ ksi}$ $G = 6.5 \text{ ksi} \times 12 \text{ in.} + 24 \text{ in.}(22 \text{ in.} - 12 \text{ in.})$ $\times \left(\frac{4595 \text{ ksi} - 190.7 \text{ ksi}}{2}\right) \left(\frac{0.0042 \text{ in./in.}}{22 \text{ in.}}\right)$ $= -179.73 \text{ kip/in.}$ $H = 6.5 \text{ ksi} \times 24 \text{ in.}(22 \text{ in.} - 12 \text{ in.}) = 1560 \text{ kip}$ $I = 6.5 \text{ ksi} \times 24 \text{ in.} \times ([22 \text{ in.}]^2/2) - 6.5 \text{ ksi}(22 \text{ in.} - 12 \text{ in.}) \times 22 \text{ in.} \times 24 \text{ in.} + 190.7 \text{ ksi} \times 24 \text{ in.} \times ([22 \text{ in.}]^2/3)(0.0042 \text{ in./in.}) - 190.7 \text{ ksi} \times 24 \text{ in.} \times (22 \text{ in.}/3)(22 \text{ in.} - 12 \text{ in.})(0.0042 \text{ in./in.}) = 4427 \text{ kip-in.}$ <p>The distances from each layer of steel reinforcement to the geometric centroid of the cross section are:</p> $d_1 = 10 \text{ in.}$ $d_2 = d_3 = 3.3 \text{ in.}$ <p>Point C: Nominal axial capacity:</p> $\phi P_{ni} = 0.65[-0.49 \text{ kip/in.}^3(10.3 \text{ in.})^3 + 15.14 \text{ ksi}(10.3 \text{ in.})^2 - 156 \text{ kip-in.}(10.3 \text{ in.}) + 2448.71 \text{ kip}] + 5.08 \text{ in.}^2(60 \text{ ksi}) + 2.54 \text{ in.}^2(50.79 \text{ ksi}) + 2.54 \text{ in.}^2(-4.61 \text{ ksi}) + 5.08 \text{ in.}^2(-60 \text{ ksi})$ $\phi P_{ni} = 1320 \text{ kip}$ <p>where</p> $A = \frac{-24 \text{ in.}(4595 \text{ ksi} - 190.7 \text{ ksi})^2}{12 \times 6.5 \text{ ksi}} \left(\frac{0.0042 \text{ in./in.}}{14.78 \text{ in.}}\right)^2$ $= -0.49 \text{ kip/in.}^3$ $B = \frac{-24 \text{ in.}(4595 \text{ ksi} - 190.7 \text{ ksi})}{2} \left(\frac{0.0042 \text{ in./in.}}{14.78 \text{ in.}}\right)$ $= 15.14 \text{ ksi}$ $C = -24 \text{ in.} \times 6.5 \text{ ksi} = -156 \text{ kip/in.}$ $D = 24 \text{ in.} \times 14.78 \text{ in.} \times 6.5 \text{ ksi}$ $+ \frac{24 \text{ in.} \times 14.78 \text{ in.} \times 190.7 \text{ ksi}}{2}$ $\times (0.0042 \text{ in./in.}) = 2448.71 \text{ kip}$	$F = 610 \text{ mm}(559 \text{ mm} - 305 \text{ mm})$ $\times \frac{(31,685 \text{ MPa} - 1315 \text{ MPa})^2}{12 \times 44.8 \text{ MPa}} \times \left(\frac{0.0042 \text{ mm/mm}}{559 \text{ mm}}\right)^2$ $+ \frac{610 \text{ mm}(31,685 \text{ MPa} - 1315 \text{ MPa})}{3}$ $\times \left(\frac{0.0042 \text{ mm/mm}}{559 \text{ mm}}\right) = 62.01 \times 10^{-3} \text{ kN/mm}^2$ $G = 44.8 \text{ MPa} \times 305 \text{ mm} + 610 \text{ mm}(559 \text{ mm} - 305 \text{ mm})$ $\times \left(\frac{31,685 \text{ MPa} - 1315 \text{ MPa}}{2}\right) \left(\frac{0.0042 \text{ mm/mm}}{559 \text{ mm}}\right)$ $= -31.48 \text{ kN/mm}$ $H = 44.8 \text{ MPa} \times 610 \text{ mm}(559 \text{ mm} - 305 \text{ mm}) = 6939 \text{ kN}$ $I = 44.8 \text{ MPa} \times 610 \text{ mm} \times ([559 \text{ mm}]^2/2) - 44.8 \text{ MPa}(559 \text{ mm} - 305 \text{ mm}) \times (559 \text{ mm})(610 \text{ mm}) + 1315 \text{ MPa} \times 610 \text{ mm} \times ([559 \text{ mm}]^2/3)(0.0042 \text{ mm/mm}) - 1315 \text{ MPa} \times 610 \text{ mm} \times (559 \text{ mm}/3)(559 \text{ mm} - 305 \text{ mm})(0.0042 \text{ mm/mm}) = 500,162 \text{ kN-mm}$ <p>The distances from each layer of steel reinforcement to the geometric centroid of the cross section are:</p> $d_1 = 254 \text{ mm}$ $d_2 = d_3 = 85 \text{ mm}$ <p>Point C: Nominal axial capacity:</p> $\phi P_{n(C)} = 0.65[-1.33 \times 10^{-4} \text{ kN/mm}^3(262 \text{ mm})^3 + 104.41 \times 10^{-3} \text{ kN/mm}^2 \times (262 \text{ mm})^2 - 27.32 \text{ kN/mm}(262 \text{ mm}) + 10,892 \text{ kN}] + 3277 \text{ mm}^2(414 \text{ MPa}) + 1315 \text{ mm}^2(350 \text{ MPa}) + 1315 \text{ mm}^2(-31.8 \text{ MPa}) + 3277 \text{ mm}^2(-414 \text{ MPa})$ $\phi P_{n(C)} = 5870 \text{ kN}$ <p>where</p> $A = \frac{-610 \text{ mm}(31,681 \text{ MPa} - 1315 \text{ MPa})^2}{12 \times 44.8 \text{ MPa}}$ $\times \left(\frac{0.0042 \text{ mm/mm}}{375 \text{ mm}}\right)^2 = 1.33 \times 10^{-4} \text{ kN/mm}^3$ $B = \frac{-610 \text{ mm}(31,681 \text{ MPa} - 1315 \text{ MPa})}{2}$ $\times \left(\frac{0.0042 \text{ mm/mm}}{375 \text{ mm}}\right) = -104.41 \times 10^{-3} \text{ kN/mm}^2$ $C = -610 \text{ mm} \times 44.8 \text{ MPa} = -27.32 \text{ kN/mm}$ $D = 610 \text{ mm} \times 375 \text{ mm} \times 44.8 \text{ MPa}$ $+ \frac{610 \text{ mm} \times 375 \text{ mm} \times 1315 \text{ MPa}}{2}$ $\times (0.0042 \text{ mm/mm}) = 10,892 \text{ kN}$

Table 16.9 (cont.)—Procedure for strengthening of a noncircular concrete column for increase in axial and bending forces

Procedure	Calculation in in.-lb units	Calculation in SI metric units
	<p>For the calculation of the coefficients, it is necessary to compute key parameters from the stress-strain model:</p> $c = 22 \text{ in.} \times \left(\frac{0.0042 \text{ in./in.}}{0.0021 \text{ in./in.} + 0.0042 \text{ in./in.}} \right)$ $= 14.67 \text{ in.}$ $y_t = 14.64 \text{ in.} \frac{0.003 \text{ in./in.}}{0.0042 \text{ in./in.}} = 10.5 \text{ in.}$ <p>The strains in each layer of steel are determined by similar triangles in the strain distribution. The corresponding stresses are then given by:</p> $f_{s1} = \epsilon_{s1} E_s = 0.0037 \text{ in./in.} \times 29,000 \text{ ksi} \rightarrow 60 \text{ ksi}$ $f_{s2} = \epsilon_{s2} E_s = 0.0018 \text{ in./in.} \times 29,000 \text{ ksi} = 50.78 \text{ ksi}$ $f_{s3} = \epsilon_{s3} E_s = -1.59 \times 10^{-4} \text{ in./in.} \times 29,000 \text{ ksi} = -4.61 \text{ ksi}$ $f_{s4} = \epsilon_{s4} E_s = -0.0021 \text{ in./in.} \times 29,000 \text{ ksi} = -60 \text{ ksi}$ <p>Nominal bending moment:</p> $\phi M_{n(C)} = 0.65[-0.37 \text{ kip/in.}^3 (10.3 \text{ in.})^4 + 11.46 \text{ ksi} (10.3 \text{ in.})^3 - 120.08 \text{ kip/in.} (10.3 \text{ in.})^2 + 433.5 \text{ kip} (10.3 \text{ in.}) + 11,643 \text{ kip-in.}] + 5.08 \text{ in.}^2 (60 \text{ ksi}) (10 \text{ in.}) + 2.54 \text{ in.}^2 (50.79 \text{ ksi}) (3.33 \text{ in.}) - 2.54 \text{ in.}^2 (-4.61 \text{ ksi}) (3.33 \text{ in.}) - 5.08 \text{ in.}^2 (-60 \text{ ksi}) (10 \text{ in.})$ <p style="text-align: center;">$\phi M_{n(C)} = 992 \text{ kip-ft}$</p> <p>where</p> $E = \frac{-24 \text{ in.} (4595 \text{ ksi} - 190.7 \text{ ksi})^2 \left(\frac{0.0042 \text{ in./in.}}{14.78 \text{ in.}} \right)^2}{16 \times 6.5 \text{ ksi}}$ $= -0.37 \text{ kip/in.}^3$ $F = 24 \text{ in.} (14.78 \text{ in.} - 12 \text{ in.}) \times \frac{(4595 \text{ ksi} - 190.7 \text{ ksi})^2 \left(\frac{0.0042 \text{ in./in.}}{14.78 \text{ in.}} \right)^2}{12 \times 6.5 \text{ ksi}} + \frac{24 \text{ in.} (4595 \text{ ksi} - 190.7 \text{ ksi})}{3} \times \left(\frac{0.0042 \text{ in./in.}}{14.78 \text{ in.}} \right) = 11.46 \text{ ksi}$ $G = -6.5 \text{ ksi} \times 12 \text{ in.} + 24 \text{ in.} (14.78 \text{ in.} - 12 \text{ in.}) \times \left(\frac{4595 \text{ ksi} - 190.7 \text{ ksi}}{2} \right) \left(\frac{0.0042 \text{ in./in.}}{14.78 \text{ in.}} \right) = -120.08 \text{ kip/in.}$ $H = 6.5 \text{ ksi} \times 24 \text{ in.} (14.78 \text{ in.} - 12 \text{ in.}) = 433.5 \text{ kip}$ $I = 6.5 \text{ ksi} \times 24 \text{ in.} \times ((14.78 \text{ in.})^2/2) - 6.5 \text{ ksi} (14.78 \text{ in.} - 12 \text{ in.}) (14.78 \text{ in.}) (24 \text{ in.}) + 190.7 \text{ ksi} \times 24 \text{ in.} \times ((14.78 \text{ in.})^2/3) (0.0042 \text{ in./in.}) - 190.7 \text{ ksi} \times 24 \text{ in.} \times (14.78 \text{ in.}/3) (14.78 \text{ in.} - 12 \text{ in.}) (0.0042 \text{ in./in.}) = 11,643 \text{ kip-in.}$	<p>For the calculation of the coefficients, it is necessary to compute key parameters from the stress-strain model:</p> $c = 560 \text{ mm} \times \left(\frac{0.0042 \text{ mm/mm}}{0.0021 \text{ mm/mm} + 0.0042 \text{ mm/mm}} \right)$ $= 373 \text{ mm}$ $y_t = 373 \text{ mm} \frac{0.003 \text{ in./in.}}{0.0042 \text{ in./in.}} = 266 \text{ mm}$ <p>The strains in each layer of steel are determined by similar triangles in the strain distribution. The corresponding stresses are then given by:</p> $f_{s1} = \epsilon_{s1} E_s = 0.0037 \text{ mm/mm} \times 200,000 \text{ MPa} \rightarrow 414 \text{ MPa}$ $f_{s2} = \epsilon_{s2} E_s = 0.0018 \text{ mm/mm} \times 200,000 \text{ MPa} = 350 \text{ MPa}$ $f_{s3} = \epsilon_{s3} E_s = -1.59 \times 10^{-4} \text{ mm/mm} \times 200,000 \text{ MPa} = -31.8 \text{ MPa}$ $f_{s4} = \epsilon_{s4} E_s = -0.0021 \text{ mm/mm} \times 200,000 \text{ MPa} = -414 \text{ MPa}$ <p>Nominal bending moment:</p> $\phi M_{n(C)} = 0.65[-9.98 \times 10^{-5} \text{ kN/mm}^3 (262 \text{ mm})^4 + 79 \times 10^{-3} \text{ kN/mm}^2 (262 \text{ mm})^3 - 21.03 \text{ kN/mm} (262 \text{ mm})^2 + 1928 \text{ kN} (262 \text{ mm}) + 1,315,453 \text{ kN-mm}] + 3277 \text{ mm}^2 (414 \text{ MPa}) (254 \text{ mm}) + 1639 \text{ mm}^2 (-31.8 \text{ MPa}) (85 \text{ mm}) - 3277 \text{ mm}^2 (-414 \text{ MPa}) (254 \text{ mm})$ <p style="text-align: center;">$\phi M_{n(C)} = 1345 \text{ kN-m}$</p> <p>where</p> $E = \frac{-610 \text{ mm} (31,681 \text{ MPa} - 1315 \text{ MPa})^2 \left(\frac{0.0042 \text{ mm/mm}}{375 \text{ mm}} \right)^2}{16 \times 44.8 \text{ MPa}}$ $= -9.98 \times 10^{-5} \text{ kN/mm}^3$ $F = 610 \text{ mm} (375 \text{ mm} - 305 \text{ mm}) \times \frac{(31,681 \text{ MPa} - 1315 \text{ MPa})^2 \left(\frac{0.0042 \text{ mm/mm}}{375 \text{ mm}} \right)^2}{12 \times 44.8 \text{ MPa}} + \frac{610 \text{ mm} (31,681 \text{ MPa} - 1315 \text{ MPa})}{3} \times \left(\frac{0.0042 \text{ mm/mm}}{375 \text{ mm}} \right) = 79 \times 10^{-3} \text{ kN/mm}^2$ $G = -44.8 \text{ MPa} \times 305 \text{ mm} + 610 \text{ mm} (375 \text{ mm} - 305 \text{ mm}) \times \left(\frac{31,681 \text{ MPa} - 1315 \text{ MPa}}{2} \right) \left(\frac{0.0042 \text{ mm/mm}}{375 \text{ mm}} \right) = -21.03 \text{ kN/mm}$ $H = 44.8 \text{ MPa} \times 610 \text{ mm} (375 \text{ mm} - 305 \text{ mm}) = 1928 \text{ kN}$ $I = 44.8 \text{ MPa} \times 610 \text{ mm} \times ((375 \text{ mm})^2/2) - 44.8 \text{ MPa} (375 \text{ mm} - 305 \text{ mm}) \times (375 \text{ mm}) (610 \text{ mm}) + 1315 \text{ MPa} \times 610 \text{ mm} \times ((375 \text{ mm})^2/3) (0.0042 \text{ mm/mm}) - 1315 \text{ MPa} \times 610 \text{ mm} \times (375 \text{ mm}/2) (375 \text{ mm} - 305 \text{ mm}) (0.0042 \text{ mm/mm}) = 1,315,453 \text{ kN-mm}$

Table 16.9 (cont.)—Procedure for strengthening of a noncircular concrete column for increase in axial and bending forces

Procedure	Calculation in in.-lb units	Calculation in SI metric units																																																
<p>Step 3—Comparison of simplified partial interaction diagram with required P_u and M_u</p>	<p>The following table summarizes the axial and bending nominal capacities (unstrengthened and strengthened) for Points A, B, and C. These points are plotted in the following figure</p> <table border="1" data-bbox="555 501 1000 728"> <thead> <tr> <th rowspan="2">Point</th> <th colspan="2">$n = 0$ plies (unstrengthened member)</th> <th colspan="2">$n = 6$ plies</th> </tr> <tr> <th>ϕP_n, kip</th> <th>ϕM_n, kip-ft</th> <th>ϕP_n, kip</th> <th>ϕM_n, kip-ft</th> </tr> </thead> <tbody> <tr> <td>A</td> <td>2087</td> <td>0</td> <td>2523</td> <td>0</td> </tr> <tr> <td>B</td> <td>1858</td> <td>644</td> <td>2210</td> <td>682</td> </tr> <tr> <td>C</td> <td>928</td> <td>884</td> <td>1320</td> <td>992</td> </tr> </tbody> </table> 	Point	$n = 0$ plies (unstrengthened member)		$n = 6$ plies		ϕP_n , kip	ϕM_n , kip-ft	ϕP_n , kip	ϕM_n , kip-ft	A	2087	0	2523	0	B	1858	644	2210	682	C	928	884	1320	992	<p>The following table summarizes the axial and bending nominal capacities (unstrengthened and strengthened) for Points A, B, and C. These points are plotted in the following figure.</p> <table border="1" data-bbox="1023 501 1468 728"> <thead> <tr> <th rowspan="2">Point</th> <th colspan="2">$n = 0$ plies (unstrengthened member)</th> <th colspan="2">$n = 6$ plies</th> </tr> <tr> <th>ϕP_n, kN</th> <th>ϕM_n, kN-m</th> <th>ϕP_n, kN</th> <th>ϕM_n, kN-m</th> </tr> </thead> <tbody> <tr> <td>A</td> <td>9283</td> <td>0</td> <td>11,223</td> <td>0</td> </tr> <tr> <td>B</td> <td>8264</td> <td>873</td> <td>9829</td> <td>924</td> </tr> <tr> <td>C</td> <td>4128</td> <td>1199</td> <td>5870</td> <td>1345</td> </tr> </tbody> </table> 	Point	$n = 0$ plies (unstrengthened member)		$n = 6$ plies		ϕP_n , kN	ϕM_n , kN-m	ϕP_n , kN	ϕM_n , kN-m	A	9283	0	11,223	0	B	8264	873	9829	924	C	4128	1199	5870	1345
Point	$n = 0$ plies (unstrengthened member)		$n = 6$ plies																																															
	ϕP_n , kip	ϕM_n , kip-ft	ϕP_n , kip	ϕM_n , kip-ft																																														
A	2087	0	2523	0																																														
B	1858	644	2210	682																																														
C	928	884	1320	992																																														
Point	$n = 0$ plies (unstrengthened member)		$n = 6$ plies																																															
	ϕP_n , kN	ϕM_n , kN-m	ϕP_n , kN	ϕM_n , kN-m																																														
A	9283	0	11,223	0																																														
B	8264	873	9829	924																																														
C	4128	1199	5870	1345																																														



16.10—Plastic hinge confinement for seismic strengthening

This example illustrates the design of an FRP retrofit to enhance the plastic rotation capacity of a nonductile reinforced concrete column. In this example, the column cannot efficiently resist seismic loads for two reasons: (1) the tie spacing does not conform to current seismic design codes; and (2) the ties do not project into the core and under seismic loads may open once the cover concrete begins to spall. The aforementioned deficiencies indicate that the column may have inadequate shear strength, inadequate confinement of the plastic hinge region, and inadequate clamping of lap splices. In addition, the designer should ensure adequate resistance against buckling of the main longitudinal reinforcement. In this example, the deficiency under consideration is inadequate plastic rotation capacity, which can be enhanced by confinement of the plastic hinge region with FRP. A seismic analysis has already determined that the column is capable of resisting the required seismic moments. Thus, there is no need to increase the flexural capacity of the section. This example is limited in scope to the FRP design requirements, and does not cover the seismic analysis. ASCE/SEI 41 is used as the base standard for this example.

The column, which is to be part of a lateral load-resisting system, is illustrated in Fig. 16.10a. Expected material proper-

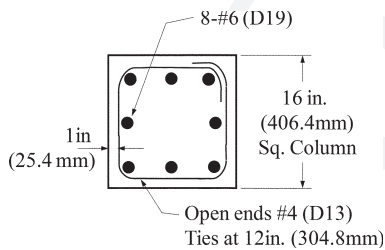


Fig. 16.10a—As-built column details.

ties and other relevant information are listed in Table 16.10a. From a seismic analysis, the column should be capable of developing a plastic rotation $\theta_p = 0.025$ rad. The axial load on the column, including gravity plus seismic loads, is $P_u = 75$ kip (334 kN). This plastic rotation demand exceeds the limiting value of 0.015 stipulated in ASCE/SEI 41 numerical acceptance criteria for reinforced concrete columns that do not conform to current seismic design codes. The concrete and reinforcing steel strain limitations of ASCE/SEI 41 as listed in Table 16.10b should not be exceeded.

The column is strengthened with CFRP laminates having the composite properties listed in Table 16.10c and bonded around the column using the wet layup technique. Glass FRP (GFRP), however, can similarly be used if desired. The design process was initiated by considering a wrapping system composed of three plies. After two iterations, the final wrapping system was found to require five plies. Only the calculations used to verify the final configuration are provided. These calculations are shown in Table 16.10d.

Figure 16.10b shows the moment curvature analysis of the as-built and retrofit rectangular sections. The moment curvature analysis results show the as-built ultimate curvature capacity is significantly lower than the required curvature demand.

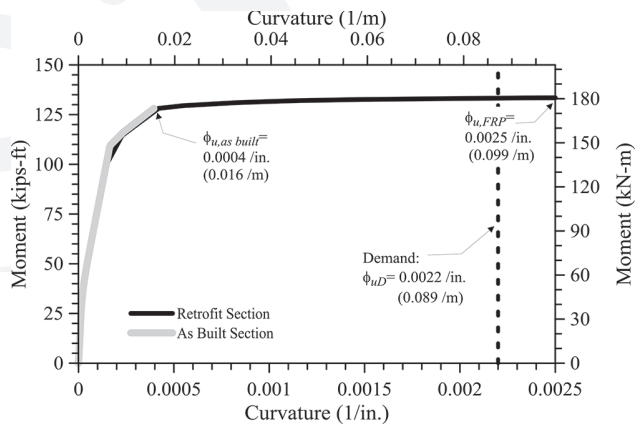


Fig. 16.10b—Moment-curvature analysis.

Table 16.10a—Column material properties

Concrete strength f_c'	4000 psi	27.6 MPa
Concrete elastic modulus $E_c = 57,000\sqrt{f_c'}$ (psi) $E_c = 4700\sqrt{f_c'}$ (MPa)	3605 ksi	25 GPa
Longitudinal reinforcing steel: yield strength f_y	44,000 psi	303 MPa
Modulus of elasticity of steel E_s	29,000 ksi	200 GPa
Longitudinal reinforcing steel: yield strain ϵ_y	0.0015	0.0015
Column height between plastic hinges L	10 ft	3.05 m
Distance to extreme tension steel d	14.625 in.	371 mm

Table 16.10b—Maximum usable strain levels (ASCE/SEI 41)

	Strain limits	
	Unconfined sections	Confined sections per 13.3.1
Compressive (concrete)	0.003	ϵ_{ccu}
Tensile (steel)	0.005	0.05
Compressive (steel)	Limited by the concrete	0.02

Table 16.10c—Manufacturer’s reported composite properties

Thickness per ply t_f	0.023 in.	0.584 mm
Ultimate tensile strength f_{fu}^*	155 ksi	1072 MPa
Rupture strain ϵ_{fu}^*	0.015	0.015
Modulus of elasticity, E_f	9326 ksi	64.3 GPa



Table 16.10d—Procedure for designing plastic hinge confinement for seismic strengthening

Procedure	Calculation in in.-lb units	Calculation in SI units
Step 1—FRP-system design material properties $\epsilon_{fu} = C_E \epsilon_{fu}^*$ $C_E = 0.95$ The column is located in an interior space. Therefore, per Table 9.4, an environmental-reduction factor of 0.95 is used. $\epsilon_{fe} = 0.004 \leq \kappa_c \epsilon_{fu}$	$\epsilon_{fu} \leq 0.95 \times 0.015 = 0.014$ $\kappa_c = 0.55$ $\epsilon_{fe} = 0.004 \leq 0.55 \times 0.014 = 0.0078 \therefore \epsilon_{fe} = 0.04$	$\therefore \epsilon_{fe} = 0.04$
Step 2—Plastic hinge length In FRP jacketed columns, the plastic hinge length is: $L_p = g + 0.0003 f_y d_{bt}$ (psi and in.) $L_p = g + 0.044 f_y d_{bt}$ (MPa and mm)	$L_p = 2 + 0.0003 \times 44,000 \times 0.75 = 12$ in.	$L_p = 50.8 + 0.044 \times 303.4 \times 19 = 305$ in.
Step 3—Preliminary calculations $b = h = 16$ in. (406 mm) From 12.1.2: $D = \sqrt{h^2 + b^2}$ $\kappa_a = \frac{A_e}{A_c} \left(\frac{b}{h}\right)^2$ $\kappa_b = \frac{A_e}{A_c} \sqrt{\frac{h}{b}}$ where A_e/A_c is calculated as: $\frac{A_e}{A_c} = \frac{1 - \left[\frac{\left(\frac{b}{h}\right)(h - 2r_c)^2 + \left(\frac{h}{b}\right)(b - 2r_c)^2}{3A_g} \right]}{1 - \rho_g}$	$D = \sqrt{16^2 + 16^2} = 22.63$ in. $A_e/A_c = 0.62$ $\kappa_a = 0.62 \left(\frac{A_e}{A_c}\right)^2 = 0.62$ $\kappa_b = 0.62 \sqrt{\frac{16}{16}} = 0.62$ $\epsilon_c' = 0.002$	$D = \sqrt{406.4^2 + 406.4^2} = 575$ mm $A_e/A_c = 0.62$ $\kappa_a = 0.62$ $\kappa_b = 0.62$ $\epsilon_c' = 0.002$
Step 4—Confining concrete model variables Using the trial design of five plies, compute the confined concrete model parameters listed in the following: $f_t = \frac{2E_f t_f n_f \epsilon_{fe}}{D}$ $f_{cc}' = f_c' + \psi_f 3.3 \kappa_d f_t$ $\epsilon_{ccu} = \epsilon_c' \left(1.50 + 12 \kappa_b \frac{f_t}{f_c'} \left(\frac{\epsilon_{fe}}{\epsilon_c'} \right)^{0.45} \right)$	$f_t = \frac{2 \times 9,326,000 \times 0.023 \times 5 \times 0.004}{22.63} = 380$ psi $\psi_f = 095$ for fully wrapped sections $f_{cc}' = 4000 + 0.95 \times 3.3 \times 0.62 \times 380 = 4740$ psi $\epsilon_{ccu} = 0.002 \left(1.50 + 12 \times 0.62 \times \frac{380}{4000} \left(\frac{0.004}{0.002} \right)^{0.45} \right)$ $= 0.0049 \leq 0.01$	$f_t = \frac{2 \times 64,300 \times 0.584 \times 5 \times 0.004}{575} = 2.61$ MPa $\psi_f = 095$ $f_{cc}' = 27.6 + 0.95 \times 3.3 \times 0.62 \times 2.61 = 32.66$ MPa $\epsilon_{ccu} = 0.002 \left(1.50 + 12 \times 0.62 \times \frac{2.61}{27.60} \left(\frac{0.004}{0.002} \right)^{0.45} \right)$ $= 0.0049 \leq 0.01$
	$h/b = 1.00$	
	Note: For rectangular members, plastic hinge confinement by jacketing is not recommended for members featuring side aspect ratios, h/b , greater than 1.5, or face dimensions, b or h , exceeding 36 in. (900 mm), unless testing demonstrates their effectiveness (13.3.1).	
	ϵ_{ccu} is limited to 0.01 to prevent excessive cracking and the resulting loss of concrete integrity	
Note: The expressions presented previously are used in conjunction with a moment-curvature ($M-\phi$) analysis program to obtain the yield and ultimate curvature. These curvatures are presented in Steps 5 and 6.		

Table 16.10d (cont.)—Procedure for designing plastic hinge confinement for seismic strengthening

Procedure	Calculation in in.-lb units	Calculation in SI units
Step 5—Output from $M-\phi$ analysis program obtain the neutral axis at yielding of longitudinal reinforcement, $c_{y,frp}$	Neutral axis: $c_{y,frp} = 5.34$ in.	Neutral axis: $c_{y,frp} = 136$ mm
	Note: Yield strain of longitudinal reinforcement: $\epsilon_y = 0.0049$	
Step 6—Output from $M-\phi$ analysis program obtain the neutral axis at ultimate, $c_{u,frp}$	Neutral axis: $c_{u,frp} = 1.95$ in.	Neutral axis: $c_{u,frp} = 50$ mm
	Note: The ultimate concrete compressive strain is computed per Step 4: $\epsilon_{ccu} = 0.0049$	
1. Concrete compression strain: $\epsilon_{ccu} = 0.0049$		
2. Steel tension strain: $\epsilon_s = \epsilon_{ccu} \left(\frac{d}{c_u} - 1 \right)$	$\epsilon_s = 0.0049 \left(\frac{14.625}{5.34} - 1 \right) = 0.032 < 0.05$	$\epsilon_s = 0.0049 \left(\frac{371}{136} - 1 \right) = 0.032 < 0.05$
Step 7—Compute the yield curvature $\phi_{y,frp} = \frac{\epsilon_y}{d - c_{y,frp}}$	From a $M-\phi$ analysis the yield curvature is: $\phi_{y,frp} = \frac{0.0015}{14.625 - 5.34} = 0.000163/\text{in.}$	From a $M-\phi$ analysis the yield curvature is: $\phi_{y,frp} = \frac{0.0015}{371 - 136} = 0.0064/\text{m}$
Step 8—Compute the ultimate curvature capacity: $\phi_{u,frp} = \frac{\epsilon_{ccu}}{c_{u,FRP}}$	From a $M-\phi$ analysis the ultimate curvature is: $\phi_{u,frp} = \frac{0.0049}{1.95} = 0.0025/\text{in.}$	From a $M-\phi$ analysis the ultimate curvature is: $\phi_{u,frp} = \frac{0.0049}{50} = 0.099/\text{m}$
Step 9—Compute the ultimate curvature demand $\phi_D = \frac{\theta_D}{L_p} + \phi_{y,frp}$	$\phi_D = \frac{0.025}{12} + 0.000163 = 0.0022/\text{in.}$	$\phi_D = \frac{0.025}{3.05} + 0.0064 = 0.084/\text{m}$
Step 10—Verify design: $\phi_D < \phi_{u,frp}$	$\phi_D = 0.0022/\text{in.} < 0.0025/\text{in.}$ OK	$\phi_D = 0.084/\text{m} < 0.099/\text{m}$ OK
Step 11—Length of confined region, l_o Transverse reinforcement as specified per Section 18.7 of ACI 318-14 shall be provided over a length l_o	$l_o \geq \begin{cases} 16 \text{ in.} \\ \frac{120/2}{6} = 10 \text{ in.} \\ 18 \text{ in.} \end{cases}$	$l_o \geq \begin{cases} 406.4 \text{ mm} \\ \frac{3050/2}{6} = 254 \text{ mm} \\ 457 \text{ mm} \end{cases}$
	$l_o > L_p = 18 \text{ in. (457 mm)}$	
Design summary: Completely wrap the section with five transverse plies. Confining jacket should extend at least 18 in. (457 mm) beyond the joint interface.		

16.11—Lap-splice clamping for seismic strengthening

This example illustrates the design of an FRP retrofit to improve the seismic performance of a reinforced concrete column that is constructed with a lap splice in a region of plastic rotations. Material properties, details, and other relevant information are provided in Table 16.11a and Fig. 16.11. The column is strengthened with CFRP laminates having the composite properties listed in Table 16.11b and bonded around the column using the wet layup technique. Glass FRP, however, can similarly be used if desired.

The final wrapping system was found to require five plies. Only the calculations used to verify the final configuration are provided. These calculations are shown in Table 16.11c.

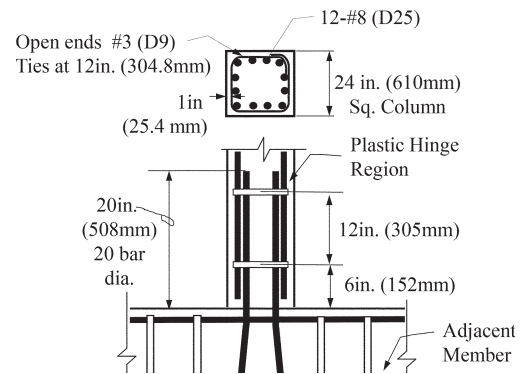


Fig. 16.11—Detail of lap splice in a plastic hinge region.

Table 16.11a—Column material properties

Concrete strength f'_c	4000 psi	27.6 MPa
Concrete elastic modulus		
$E_c = 57,000\sqrt{f'_c}$ (psi)	3605 ksi	25 GPa
$E_c = 4700\sqrt{f'_c}$ (MPa)		
Longitudinal reinforcing steel: yield strength f_y	44,000 psi	303.4 MPa
Modulus of elasticity of steel E_s	29,000 ksi	200 GPa
Longitudinal reinforcing steel: yield strain ϵ_y	0.0015	0.0015
Column height between plastic hinges, L	10 ft	3.05 m
Distance to extreme tension steel, d	14.625 in.	371 mm

Table 16.11b—Manufacturer's reported composite properties

Thickness per ply t_f	0.08 in.	2 mm
Ultimate tensile strength	143 ksi	986 MPa
Rupture strain	0.010	0.010
Modulus of elasticity E_f	13,900 ksi	95.8 GPa

Table 16.11c—Procedure for designing lap-splice clamping for seismic strengthening

Procedure	Calculation in in.-lb units	Calculation in SI units
<p>Step 1—Compute the tensile stress that existing splice can develop: (ACI 318-14 Section 25.4)</p> $f_s = \frac{40 \ell_d \lambda \sqrt{f'_c} \left(\frac{c_b K_{tr}}{d_b} \right)}{3 d_b \Psi_t \Psi_e \Psi_s} \text{ (in. and psi)}$ $f_s = \frac{3.33 \ell_d \lambda \sqrt{f'_c} \left(\frac{c_b K_{tr}}{d_b} \right)}{3 d_b \Psi_t \Psi_e \Psi_s} \text{ (mm and MPa)}$ $K_{tr} = \frac{40 A_{tr}}{sn}$ $\Psi_t = \Psi_e = \Psi_s = 1.00$ $\lambda = 1.00 \text{ (normalweight concrete)}$	<p>$s = 12 \text{ in.}$ $n = 1$ Longitudinal bars in the potential plane of splitting</p> $K_{tr} = \frac{40 \times 1 \times 0.11}{12 \times 1} = 0.37 \text{ in.}$ $\frac{c_b + K_{tr}}{d_b} = \frac{(1.00 + 0.375 + 0.5) + 0.37}{1.00} = 2.24 \leq 2.50$ <p>Per Eq. (25.4.2.3a) of ACI 318-14 the value $\frac{c_b + K_{tr}}{d_b}$ cannot be greater than 2.5.</p> $f_s = \frac{40 \times 20.0 \times 1.0 \sqrt{4000} \times 2.24}{3 \times 1.0 \times 1.0 \times 1.0 \times 1.0} = 37,779 \text{ psi} \leq 44,000 \text{ psi}$	<p>$s = 305 \text{ mm}$ $n = 1$</p> $K_{tr} = \frac{40 \times 1 \times 71}{305 \times 1} = 9.3 \text{ mm}$ $\frac{c_b + K_{tr}}{d_b} = \frac{(25.4 + 9.53 + 12.7) + 9.3}{25.4} = 2.24 \leq 2.50$ $f_s = \frac{3.33 \times 508 \times 1.0 \sqrt{27.6} \times 2.24}{3 \times 25.4 \times 1.0 \times 1.0 \times 1.0} = 260 \text{ MPa} \leq 303 \text{ MPa}$
<p>Note: Computed stress f_s does not reach f_y, longitudinal bar yield strength, and as such lap splice must be clamped.</p>		
<p>Step 2—Stress corresponding to pullout capacity of splice</p> $f_s \leq \frac{33 \ell_d \lambda \sqrt{f'_c}}{d_{bt} \Psi_t \Psi_e \Psi_s} \text{ (in. and psi)}$ $f_s \leq \frac{2.75 \ell_d \lambda \sqrt{f'_c}}{d_{bt} \Psi_t \Psi_e \Psi_s} \text{ (mm and MPa)}$	<p>$\ell_{prov} = 20 d_{bt} = 20 \times 1.0 = 20 \text{ in.}$</p> <p>Pullout capacity of splice:</p> $f_s = \frac{33 \times 20.0 \times \sqrt{4000}}{1.0 \times 1.0 \times 1.0 \times 1.0} = 41,742 \text{ psi}$	<p>$\ell_{prov} = 20 d_{bt} = 20 \times 25.4 = 508 \text{ mm}$</p> <p>Pullout capacity of splice:</p> $f_s = \frac{2.75 \times 508 \times \sqrt{27.6}}{25.4 \times 1.0 \times 1.0 \times 1.0} = 289 \text{ MPa}$
<p>Step 3—Compute the required jacket thickness, t_j</p> $nt_j = 1500 \times \frac{D}{E_f} \text{ (ksi and in.)}$ $nt_j = 1500 \times \frac{D}{E_f} \text{ (MPa and mm)}$	<p>$D = 24 \text{ in.}$ (maximum dimension in a rectangular member)</p> <p>$E_f = 13,900 \text{ ksi}$</p> $t_j = 218 \times \frac{24}{13,900} = 0.38 \text{ in.}$	<p>$D = 610 \text{ mm}$</p> <p>$E_f = 95,800 \text{ MPa}$</p> $t_j = 1500 \times \frac{610}{95,800} = 9.6 \text{ mm}$
<p>Step 4—Compute the required number of plies, n</p> $n = t_j / t_f$	<p>$t_f = 0.08 \text{ in.}$</p> <p>$n = 0.38 / 0.08 = \text{five plies}$</p>	<p>$t_f = 2 \text{ mm}$</p> <p>$n = 9.60 / 2 = \text{five plies}$</p>
<p>Design summary: Completely wrap the section with five transverse plies. Confining jacket should extend at least full height of lap splice; that is, 20 in. (508 mm) Using five plies of the FRP-specified results in a splice capacity of 41,742 psi (289 MPa), which is controlled by the maximum pull-out capacity calculated in Step 2.</p>		

16.12—Seismic shear strengthening

This example illustrates the main steps in calculating the amount of FRP required for the shear strengthening of a reinforced concrete member. The member used in this example is illustrated in Fig. 16.12. Column material properties are shown in Table 16.12a, the configuration of the FRP shear reinforcement is described in Table 16.12b, and the CFRP laminate material properties are listed in Table 16.12c. ASCE/SEI 41 is used as the standard for this example. Glass FRP (GFRP) can similarly be used if desired. Calculations for determining the FRP required as shown in Table 16.12d.

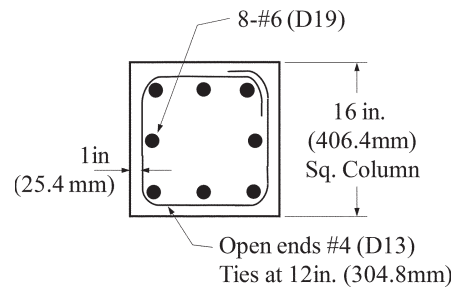


Fig. 16.12—As-built column details.

Table 16.12a—Column material properties

Concrete strength f'_c	4000 psi	27.6 MPa
Concrete elastic modulus		
$E_c = 57,000\sqrt{f'_c}$ (psi)	3605 ksi	25 GPa
$E_c = 4700\sqrt{f'_c}$ (MPa)		
Longitudinal reinforcing steel: yield strength f_y	44,000 psi	303.4 MPa
Modulus of elasticity of steel E_s	29,000 ksi	200 GPa
Longitudinal reinforcing steel: yield strain ϵ_y	0.0015	0.0015
Column height between plastic hinges, L	10 ft	3.05 m
Distance to extreme tension steel, d	14.625 in.	371 mm
Ultimate axial load P_u	75 kip	333.62 kN

Table 16.12b—Configuration of supplemental FRP shear reinforcement

Minimum section dimension	16 in.	406 mm
d_f (governed by minimum section dimension)	16 in.	406 mm
Width w_f	8 in.	203 mm
Spacing s_f (full coverage)	8 in.	203 mm

Table 16.12c—Manufacturer's reported composite properties

Thickness per ply t_f	0.023 in.	0.584 mm
Ultimate tensile strength f_{fu}^*	155 ksi	1072 MPa
Rupture strain ϵ_{fu}^*	0.015	0.015
Modulus of elasticity E_f	9326 ksi	64.3 GPa

Table 16.12d—Procedure for seismic shear strengthening

Design steps	Calculation in in.-lb units	Calculation in SI units
<p>Step 1—Compute the probable moment capacity of the member, M_{pr}</p> <p>Per 13.5.1; in calculating the probable moment $\phi = 1$ and $\psi_f = 1$ are used.</p>	<p>From a $M-\phi$ analysis, the probable moment capacity is: $M_{pr} = 322$ kip-ft</p>	<p>From a $M-\phi$ analysis, the probable moment capacity is: $M_{pr} = 437$ kN-m</p>
	<p>Notes: (1) In seismic applications, the shear design process initiates with the calculation of the probable moment capacity of the section. (2) Moment M_{pr} is computed at both top and bottom ends of the member.</p>	
<p>Step 2—Obtain the yield and ultimate curvature from a $M-\phi$ analysis</p>	<p>Yield curvature: $\phi_{y,frp} = 0.000163/\text{in.}$</p> <p>Ultimate curvature: $\phi_{u,frp} = 0.0019/\text{in.}$</p>	<p>Yield curvature: $\phi_{y,frp} = 0.0064/\text{m}$</p> <p>Ultimate curvature: $\phi_{u,frp} = 0.074/\text{m}$</p>
<p>Step 3—Compute the displacement ductility and reduction factor, k</p> <p>In FRP jacketed columns, the plastic hinge length is (Eq. (1)): $L_p = g + 0.0003f_y d_b$ f_y is in ksi and d_b is in inches</p> <p>$L_p = g + 0.044f_y d_b$ f_y is in MPa and d_b is in mm</p> <p>In this example:</p> <p>$L_{eff} = \frac{L}{2} = 60$ in. (1524 mm)</p> <p>Yield deflection $\Delta_{y,frp}$:</p> $\Delta_{y,frp} = \frac{\phi_{y,frp} L_{eff}^2}{3}$ <p>Plastic deflection $\Delta_{p,frp}$:</p> $\Delta_{p,frp} = (\phi_u - \phi_y) L_p \left(L_{eff} - \frac{L_p}{2} \right)$ <p>Displacement ductility μ_Δ:</p> $\mu_\Delta = 1 + \frac{\Delta_p}{\Delta_y}$ <p>Shear reduction factor per ASCE/SEI 41</p> $\begin{cases} \mu_\Delta \leq 2; & k = 1.0 \\ 2 \leq \mu_\Delta \leq 6; & k = 0.7 + \frac{0.30 \times (6 - \mu_\Delta)}{4} \\ \mu_\Delta > 6; & k = 0.7 \end{cases}$	<p>Plastic hinge length: $L_p = 2 + 0.0003 \times 44,000 \times 0.75 = 12$ in.</p> <p>Note: Use a maximum gap between the FRP and the column base of 2 in.</p> <p>Yield deflection: $\Delta_{y,frp} = \frac{0.000163 \times 60^2}{3} = 0.20$ in.</p> <p>Plastic deflection: $\Delta_{p,frp} = (0.0019 - 0.000163) \times 12 \left(60 - \frac{12}{2} \right) = 1.13$ in.</p> <p>Displacement ductility: $\mu_\Delta = 1 + \frac{1.13}{0.20} = 6.7$</p> <p>Reduction factor: $k = 0.70$</p>	<p>Plastic hinge length: $L_p = 50.8 + 0.044 \times 303.4 \times 19 = 305$ mm</p> <p>Note: Use a maximum gap between the FRP and the column base of 50.8 mm.</p> <p>Yield deflection: $\Delta_y = \frac{0.0065 \times 1524^2}{3 \times 1000} = 5.1$ mm</p> <p>Plastic deflection: $\Delta_{p,frp} = \frac{(0.074 - 0.0064)}{1000} \times 305 \left(1524 - \frac{305}{2} \right) = 28.6$ mm</p> <p>Displacement ductility: $\mu_\Delta = 1 + \frac{28.6}{5.1} = 6.7$</p> <p>Reduction factor: $k = 0.70$</p>
<p>Step 4—Compute the shear design force, V_u</p> <p>Per ACI 318-14 Section 18.7.6:</p> $V_u = \frac{M_{pr,top} + M_{pr,bot}}{L} \pm \frac{w_u L}{2}$	<p>In this example, with the exception of the earthquake forces, there are no applied uniform loads on the member, as such:</p> <p>$W_u = 0.00$</p> <p>From Step 1, the probable moment capacity is:</p> <p>$M_{pr,top} = M_{pr,bot} = 322$ kip-ft (437 kN-m)</p> <p>Design shear force: $V_u = \frac{322 + 322}{120/12} \pm 0 = 64.4$ kip</p>	<p>Design shear force: $V_u = \frac{437 + 437}{3.05} \pm 0 = 286$ kN</p>

Table 16.12d (cont.)—Procedure for seismic shear strengthening

Design steps	Calculation in in.-lb units	Calculation in SI units
<p>Step 5—Calculate the concrete, V_c, and steel contribution, V_s</p> <p>Concrete contribution, V_c:</p> <p>Per ACI 318-14 Section 18.7.6.2.1, and because:</p> $\frac{M_{pr,r} + M_{pr,l}}{\ell_n} \geq \left(\frac{w_u \ell_n}{2}\right) \frac{1}{2} \Rightarrow V_c = 0$ <p>Steel contribution V_s</p> $V_s = A_{sh} f_y \frac{d}{s}$	<p>Concrete contribution to shear capacity:</p> $V_c = 0$ <p>Steel contribution to shear capacity:</p> $V_s = 2 \times 0.20 \times 44 \times \frac{14.625}{12} = 21.4 \text{ kip}$ <p>Combined concrete and steel contribution:</p> $k(V_c + V_s) = 0.70(0 + 21.4) = 14.98 \text{ kip}$	<p>Concrete contribution to shear capacity:</p> $V_c = 0$ <p>Steel contribution to shear capacity:</p> $V_s = 2 \times 129 \times 303.4 \times \frac{371.475}{305} = 95.2 \text{ kN}$ <p>Combined concrete and steel contribution:</p> $k(V_c + V_s) = 0.70(0 + 95.2) = 66.6 \text{ kN}$
<p>Step 6—Calculate the required FRP force, V_f</p> $V_{f,R} = \frac{\left[\frac{V_u}{\phi} - k(V_c + V_s) \right]}{\psi_f}$ <p>Per ASCE/SEI 41, $\phi = 1.00$</p> <p>For completely wrapped members, Table 11.3 recommends $\psi_f = 0.95$.</p>	<p>Required FRP force:</p> $V_{f,R} = \frac{\left[\frac{64.4}{1.00} - 14.98 \right]}{0.95} = 45.26 \text{ kip}$	<p>Required FRP force:</p> $V_{f,R} = \frac{\left[\frac{286}{1.00} - 66.6 \right]}{0.95} = 201.3 \text{ kN}$
<p>Step 7—Calculate the effective stress, f_{fe}.</p> <p>For fully wrapped members, the effective strain is computed using Eq. (11.4.1.1):</p> $\epsilon_{fe} = 0.75 C_E \epsilon_{fti}^* \leq 0.004$ $C_E = 0.95$ <p>The column is located in an interior space. Therefore, per Table 9.4, an environmental-reduction factor of 0.95 is used.</p> <p>The effective FRP stress can be computed from Hooke's law:</p> $f_{fe} = \epsilon_{fe} E_f$	<p>Effective strain:</p> $\epsilon_{fe} = 0.75 \times 0.95 \times 0.015 = 0.11 \leq 0.004$ <p>Effective stress:</p> $f_{fe} = 0.004 \times 9326 = 37.3 \text{ ksi}$	<p>Effective strain:</p> $\epsilon_{fe} = 0.75 \times 0.95 \times 0.015 = 0.11 \leq 0.004$ <p>Effective stress:</p> $f_{fe} = 0.004 \times 64,300 = 257 \text{ MPa}$
<p>Step 8—Calculate the number of plies, n_f</p> <p>Area of a single ply for a fully wrapped member (Eq. (11.4a)):</p> $A_{fv} = 2t_f w_f$ <p>The shear contribution of the FRP can be then calculated from Eq. (11-3).</p> $V_f = A_{fv} f_{fe} \frac{(\sin \alpha + \cos \alpha) d_{fv}}{s_f}$	<p>Area per ply:</p> $A_{fv} = 2 \times 0.023 \times 8 = 0.37 \text{ in.}^2$ <p>Force per ply:</p> $V_f = 0.37 \times 37.3 \frac{(1)16}{8} = 27.6 \text{ kip}$ <p>Number of plies:</p> $n_f = \frac{V_{f,R}}{V_f} = \frac{45.26}{27.6} = 2 \text{ (minimum)}$	<p>Area per ply:</p> $A_{fv} = 2 \times 0.584 \times 203 = 237 \text{ mm}^2$ <p>Force per ply:</p> $V_f = 237 \times 257 \frac{(1)406}{203} = 122 \text{ kN}$ <p>Number of plies:</p> $n_f = \frac{V_{f,R}}{V_f} = \frac{201.3}{122} = 2 \text{ (minimum)}$
<p>Design summary: Completely wrap the section with two transverse plies</p>		

16.13—Flexural and shear seismic strengthening of shear walls

This example illustrates the use of an FRP retrofit to increase the shear and flexural strength of an existing cantilevered concrete wall. The shear strengthening is achieved by installing horizontally oriented FRP on one face of the wall. The flexural strengthening is achieved by installing multiple layers of vertically oriented FRP on both faces of the wall near the wall ends. Details for anchorage of the FRP to the foundation are not addressed. Carbon FRP (CFRP) is used in this example. Glass FRP (GFRP) can similarly be used if desired.

The example incorporates the following two major phases:

1. Determine the shear and flexural capacity of the existing wall
2. Design the FRP to achieve the required strength

Details of the wall and relevant information are provided in Fig. 16.13a and Table 16.13a. The wall is assumed to be an ordinary shear wall. The wall is strengthened with FRP having the composite properties listed in Table 16.13b. A factored axial load, P_u , of 12 kip (53 kN) is assumed in addition to the lateral force. ASCE/SEI 41 is assumed to be the standard used as the basis for the rehabilitation.

This example illustrates a manual calculation approach for the design of FRP strengthening of a shear wall. A moment curvature analysis of the existing and repaired wall, shown in Fig. 16.13b, is used to assess the accuracy of the manual approach. The reasonably good agreement of the flexural results from the design example with those from a moment-curvature analysis validates the illustrative example. The design calculations are shown in Table 16.13c.

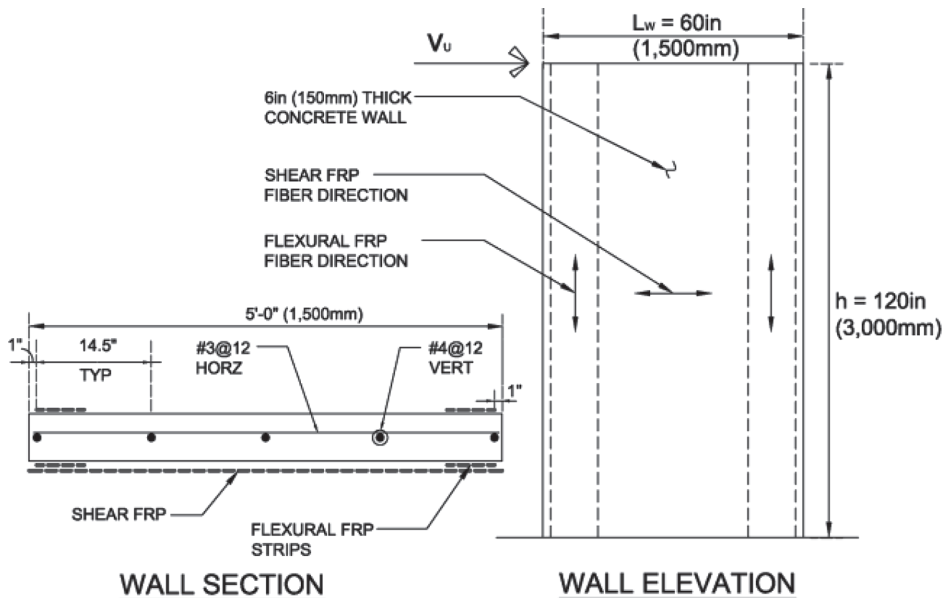


Fig. 16.13a—Concrete wall details.

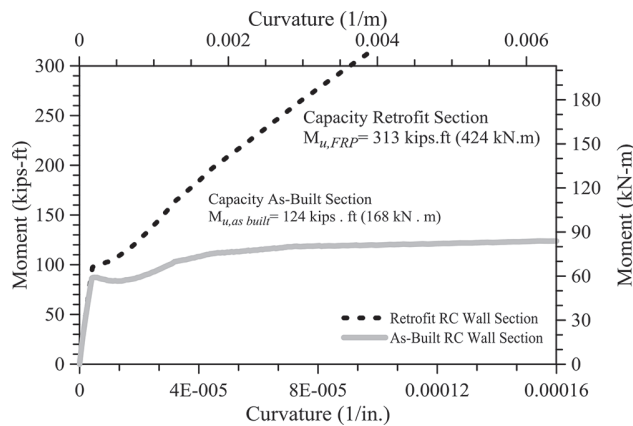


Fig. 16.13b—Moment-curvature analysis for shear wall example.

Table 16.13a—As-built shear wall properties and demands

Concrete strength	2500 psi	17.23 MPa
Longitudinal reinforcing steel yield strength	40.0 ksi	275.8 MPa
Modulus of elasticity of steel	29,000 ksi	200 GPa
Longitudinal reinforcing yield strain	0.0014 in./in.	0.0014 mm/mm
Shear wall height h	10 ft	3000 mm
Shear wall length	60.0 in.	1500 mm
Shear wall thickness	6 in.	150 mm
Existing wall reinforcement Horizontal: No. 3 at 12 in. (305 mm) on center => $\rho_t = 0.0015$ Vertical: No. 4 at 12 in. (305 mm) on center => $\rho_l = \rho_b = 0.0027$	—	—
Axial factored load P_u	12 kip	53.4 kN
Ultimate shear demand V_u	52 kip	232 kN
Ultimate moment demand at wall base M_u	260 kip-ft	348 kN-m
A_{sw} = area of wall web steel => area of four No. 4 bars (neglecting one bar within the compression zone)	0.8 in. ²	500 mm ²

Table 16.13b—Manufacturer's reported composite properties

Thickness per ply t_f	0.023 in.	0.575 mm
Ultimate tensile strength f_{fu}^*	140 ksi	965.3 MPa
Rupture strain ϵ_{fu}^*	0.012 in./in.	0.012 mm/mm
Modulus of elasticity E_f	9600 ksi	66.2 GPa

Table 16.13c—Procedure for flexural and shear seismic strengthening of shear walls

Procedure	Calculation in in.-lb units	Calculation in SI units
<p>Step 1—Compute existing wall capacity</p> <p>Shear capacity: Shear capacity per ACI 318:</p> $V_c = 2\lambda\sqrt{f'_c}t_w d_{fv}$ $V_c = \frac{0.167b_w d\sqrt{f'_c}}{1000}$ $V_{sw} = \frac{A_v f_y d_{fv}}{s}$ $V_n = V_c + V_{sw}$ <p>Using $\phi = 1.0$ for shear (per ASCE/SEI 41):</p> <p>Flexural capacity: A quick method to assess the flexural capacity is shown in the following. Assume that all web steel in the wall yields. This includes all the longitudinal reinforcement except for the one bar that is adjacent to the compression face, that is, four No. 4 bars can be considered to yield.</p> $a = \frac{A_{sw}f_y + P_u}{0.85f'_c t_w}$ $M_n = (A_{sw}f_y + P_u)(d - a/2)$ <p>where $d = L_w/2$</p> <p>Using $\phi = 1.0$:</p> <p>It can be observed that the wall does not have adequate capacity.</p>	$V_c = \frac{2(6 \times 0.8 \times 60)\sqrt{2500}}{1000}$ $V_c = 28.8 \text{ kip}$ $V_{sw} = 0.11 \times 40,000 \times \frac{0.8 \times 60}{12}$ $V_{sw} = 17.6 \text{ kip}$ $V_n = 28.8 \text{ kip} + 17.6 \text{ kip}$ $V_n = 46.4 \text{ kip}$ $\phi V_n = 46.4 \text{ kip} < V_u = 52 \text{ kip}$ $a = \frac{0.8 \text{ in.}^2 \times 40 \text{ ksi} + 12 \text{ kip}}{0.85 \times 2.5 \text{ ksi} \times 6 \text{ in.}} = 3.45 \text{ in.}$ $d = L_w/2 = 30 \text{ in.}$ $M_n = 104 \text{ kip-ft}$ $\phi M_n = 104 \text{ kip-ft} < M_u = 260 \text{ kip-ft}$	$V_c = \frac{(0.167 \times 0.8 \times 1500)\sqrt{17.23}}{1000}$ $V_c = 124.8 \text{ kN}$ $V_{sw} = \frac{71 \times 275.8 \times 0.8 \times \frac{1500}{305}}{1000}$ $V_{sw} = 77.0 \text{ kN}$ $V_n = 124.8 \text{ kN} + 77.0 \text{ kN}$ $V_n = 201.8 \text{ kN}$ $\phi V_n = 201.8 \text{ kN} < V_u = 232 \text{ kN}$ $a = \frac{\left(\frac{500 \text{ mm}^2 \times 275.8 \text{ MPa}}{1000}\right) + 53.4 \text{ kN}}{\left(\frac{0.85 \times 17.23 \text{ MPa} \times 150 \text{ mm}}{1000}\right)} = 87.1 \text{ mm}$ $d = 750 \text{ mm}$ $M_n = 135.1 \text{ kN-m}$ $\phi M_n = 135.1 \text{ kN-m} < M_u = 348 \text{ kN-m}$
<p>Step 2—FRP design material properties</p> <p>Use environmental reduction factors from Table 9.4.</p> <p>Per 9.4:</p> $f_{fu} = C_E f_{fu}^*$ $\epsilon_{fu} = C_E \epsilon_{fu}^*$	<p>For interior exposure for carbon FRP: $C_E = 0.95$</p> $f_{fu} = 133 \text{ ksi}$ $\epsilon_{fu} = 0.0114 \text{ in./in.}$	$f_{fu} = 917 \text{ MPa}$ $\epsilon_{fu} = 0.0114 \text{ mm/mm}$
<p>Step 3—Flexural strengthening</p> <p>Step 3a—Compute the debonding strain limit, ϵ_{fd}</p> <p>This is the limit for the effective strain in the FRP.</p> <p>Per Eq. (10.2.1.1):</p> $\epsilon_{fd} = 0.083 \sqrt{\frac{f'_c}{nE_f t_f}} \leq 0.9\epsilon_{fu} \quad (\text{in.-lb})$ $\epsilon_{fd} = 0.41 \sqrt{\frac{f'_c}{nE_f t_f}} \leq 0.9\epsilon_{fu} \quad (\text{SI})$	<p>For one layer of FRP, $\epsilon_{fd} = 0.0088$ For two layers of FRP, $\epsilon_{fd} = 0.0062$ For three layers of FRP, $\epsilon_{fd} = 0.0051$</p>	<p>For one layer of FRP, $\epsilon_{fd} = 0.0088$ For two layers of FRP, $\epsilon_{fd} = 0.0062$ For three layers of FRP, $\epsilon_{fd} = 0.0051$</p>

Table 16.13c (cont.)—Procedure for flexural and shear seismic strengthening of shear walls

Procedure	Calculation in in.-lb units	Calculation in SI units
Flexural design involves iteration to achieve equilibrium across the section. Usually, the first step is to assume the depth of the neutral axis c .	Use the available information to assist with an assumption for the depth of the neutral axis c .	
Assume that the flexural strengthening will require three layers of 8 in. (200 mm) wide strips on each side of the wall at each end. Assume that the effective strain is at the centroid of the FRP area. Knowing the maximum effective strain in the FRP, compute the force in the FRP	$w_f = 8$ in. $n_f = 3$ $t_f = 0.023$ in. $A_f = \text{two sides} \times 3(0.023)(8)$ $A_f = 1.104$ in. ²	$w_f = 200$ mm $n_f = 3$ $t_f = 0.575$ mm $A_f = 690$ mm ²
$T_f = C_E A_f \epsilon_{fd} E_f$	$T_f = 0.85(1.104)(0.0051)(9600 \text{ ksi}) = 45.94$ kip	$T_f = \frac{0.85(690)(0.0051)(66,200 \text{ MPa})}{1000} = 198.0$ kN
Depth of corresponding compression block:		
$a = \frac{A_{sw} f_y + P_u + T_f}{0.85 f'_c t_w}$	$a = 7.05$ in.	$a = 177.2$ mm
Compute an estimate of the depth of the neutral axis, c :	$c = a/0.85 = 8.3$ in.	$c = a/0.85 = 208.5$ mm
Check actual strain at centroid of FRP area and corresponding force in the FRP:	$\epsilon_{feCG} = \epsilon_{fd} \left(1 + \frac{W_f/2}{c+1-L_w} \right) = 0.00469$	$\epsilon_{feCG} = \epsilon_{fd} \left(1 + \frac{W_f/2}{c+25.4-L_w} \right) = 0.00469$
It is observed that the force in the FRP does not agree with that based on the initial assumption. However, the above steps provide a reasonable starting point for an assumption for c .	Corresponding force in FRP, $T_f = C_E A_f \epsilon_{feCG} E_f = 42.32$ kip	Corresponding force in FRP, $T_f = C_E A_f \epsilon_{feCG} E_f = 182.1$ kN
Compute concrete strain at extreme compression surface per Eq. (13.7.2.1a):	Assume $c = 8.0$ in.	Assume $c = 200$ mm
$\epsilon_c = \epsilon_{fd} \left(\frac{1}{(L_w/c)-1} \right) \leq \epsilon_{cu}$	$\epsilon_c = 0.0008$ $\epsilon_c < \epsilon_{cu} = 0.003$ OK	$\epsilon_c = 0.0008$ $\epsilon_c < \epsilon_{cu} = 0.003$ OK
Compute strain in the bar in the compression zone:	$\epsilon_{sc} = 0.007$ where $d' = 1$ in. $\epsilon_{sc} < \epsilon_y = 0.0014$	$\epsilon_{sc} = 0.007$ where $d' = 25$ mm $\epsilon_{sc} < \epsilon_y = 0.0014$
Compute strain in the bars in the tension zone:	$\epsilon_{st1} = \left(\frac{\epsilon_c}{c} \right) (14.5 + 1 - 8.0)$ $\epsilon_{st1} = 0.0075 < \epsilon_y$	$\epsilon_{st1} = \left(\frac{\epsilon_c}{c} \right) (362.5 + 25 - 200)$ $\epsilon_{st1} = 0.0075 < \epsilon_y$
Compute strain at centroid of FRP area:	Similarly, $\epsilon_{st2} = 0.0022 > \epsilon_y$ $\epsilon_{st3} = 0.0037 > \epsilon_y$ $\epsilon_{st4} = 0.0051 > \epsilon_y$ $\epsilon_{feCG} = 0.0047$	Similarly, $\epsilon_{st2} = 0.0022 > \epsilon_y$ $\epsilon_{st3} = 0.0037 > \epsilon_y$ $\epsilon_{st4} = 0.0051 > \epsilon_y$ $\epsilon_{feCG} = 0.0047$
Recompute total tensile force components at the above determined strain levels:		
Recalculate depth of compression block and depth to neutral axis:	$T_f = 42.34$ kip	$T_f = 182.5$ kN
Iterate as required to reach convergence:	$T_{sw} = 0.2 \times 0.00075 \times 29,000 + 3 \times 0.2 \times 40 = 28.35$ kip	$T_{sw} = 125 \times 0.00075 \times 200,000 + 3 \times 125 \times 275.8 = 122.175$ kN = 122.2 kN

Table 16.13c (cont.)—Procedure for flexural and shear seismic strengthening of shear walls

Procedure	Calculation in in.-lb units	Calculation in SI units
Step 3b—Calculate the strains and force components in concrete, FRP and reinforcing steel	$a = 6.48 \text{ in.}$ $c = 7.63 \text{ in.}$	$a = 163 \text{ mm}$ $c = 191.8 \text{ mm}$
Force in the bar in the compression zone:	Final value of the depth of the neutral axis is achieved after iteration. $c = 7.648 \text{ in.}$ $a = 6.5 \text{ in.}$	$c = 191 \text{ mm}$ $a = 162.4 \text{ mm}$
Strains and forces in bars in tensile zone:	$\epsilon_c = 0.00076 < \epsilon_{cu}$ $\epsilon_{sc} = 0.00066 < \epsilon_y$ $C_{sc} = 0.2 \times 0.00066 \times 29,000 = 3.83 \text{ kip}$	$\epsilon_c = 0.00076 < \epsilon_{cu}$ $\epsilon_{sc} = 0.00066 < \epsilon_y$ $C_{sc} = 125 \times 0.00066 \times 200 = 16.5 \text{ kN}$
Strain and force in FRP:	$\epsilon_{st1} = 0.0078 < \epsilon_y$ $\epsilon_{st2} = 0.0022 > \epsilon_y$ $\epsilon_{st3} = 0.0037 > \epsilon_y$ $\epsilon_{st4} = 0.0051 > \epsilon_y$	$\epsilon_{st1} = 0.0078 < \epsilon_y$ $\epsilon_{st2} = 0.0022 > \epsilon_y$ $\epsilon_{st3} = 0.0037 > \epsilon_y$ $\epsilon_{st4} = 0.0051 > \epsilon_y$
From equilibrium, compressive force in concrete:	$T_{s1} = 4.52 \text{ kip}$ $T_{s2} = T_{s3} = T_{s4} = 8.0 \text{ kip}$ $\sum T_s = 28.52 \text{ kip}$	$T_{s1} = 19.5 \text{ kN}$ $T_{s2} = T_{s3} = T_{s4} = 34.48 \text{ kN}$ $\sum T_s = 122.94 \text{ kN}$
Step 3c—Calculate the moment capacity of the section	$\epsilon_{fcG} = 0.0047$ $T_f = 42.37 \text{ kip}$	$\epsilon_{fcG} = 0.0047$ $T_f = 182.5 \text{ kN}$
Compute lever arm for different force components:	$C_c = (\sum T_s + T_f + P_u + C_{sc}) = 79.06 \text{ kip}$ Bar in compression: $d_1 = c - 1 \text{ in.} = 7.648 - 1 = 6.65 \text{ in.}$ Concrete compression: $\left(c - \frac{a}{2}\right) = 7.648 - \frac{6.5}{2} = 4.4 \text{ in.}$ First bar in tension: $(1 \text{ in.} + 14.5 \text{ in.} - c) = 7.85 \text{ in.}$ Second bar in tension: 22.35 in. Third bar in tension: 36.85 in. Fourth bar in tension: 51.35 in. FRP: $L_w - c - W_f/2 - 1 \text{ in.} = 47.35 \text{ in.}$ P_u : $L_w/2 - c = 22.35 \text{ in.}$	$C_c = (\sum T_s + T_f + P_u + C_{sc}) = 342.4 \text{ kN}$ Bar in compression: $d_1 = c - 25 = 166 \text{ mm}$ Concrete compression: $\left(c - \frac{a}{2}\right) = 109.8 \text{ mm}$ First bar in tension: $(25 \text{ mm} + 362.5 \text{ mm} - c) = 196.5 \text{ mm}$ Second bar in tension: 559 mm Third bar in tension: 921.5 mm Fourth bar in tension: 1284 mm FRP: $L_w - c - W_f/2 - 25 \text{ mm} = 1184 \text{ mm}$ P_u : $L_w/2 - c = 559 \text{ mm}$
Nominal moment capacity, M_n :	$M_n = 79.06 \times 4.4 + 3.83 \times 6.65 + 4.52 \times 7.85 + 8 \times 22.35 + 8 \times 36.85 + 8 \times 51.35 + 0.85 \times 42.37 \times 47.35 + 12 \times 22.35 = 272.2 \text{ kip-ft}$	$M_n = 353 \text{ kN}\cdot\text{m}$
Per Section 10.2.10, include reduction factor for FRP contribution, $\psi = 0.85$.	$\phi M_n = 272.2 \text{ kip-ft} > M_u = 260 \text{ kip-ft}$ $\phi M_n > M_u \therefore \text{OK}$	$\phi M_n = 353 \text{ kN}\cdot\text{m} > M_u = 348 \text{ kN}\cdot\text{m}$ $\phi M_n > M_u \therefore \text{OK}$

Table 16.13c (cont.)—Procedure for flexural and shear seismic strengthening of shear walls

Procedure	Calculation in in.-lb units	Calculation in SI units
<p>Step 4—Shear strengthening</p> <p>Per 13.7.3, Eq. (13.7.2.2b):</p> <p>V_f is the shear contribution of FRP and is computed in accordance with Chapter 11.</p> <p>Step 4a—Calculate V_f</p> <p>Because the FRP is only on one side of the wall, per Eq. (13.7.2.2c):</p> <p>Since the FRP will be face-bonded to the wall, the effective FRP strain will be: $\epsilon_{fe} = \kappa_v \epsilon_{fu} \leq 0.004$</p> <p>Use Eq. (11.4.1.2b7), (11.4.1.2c), (11.4.1.2d), and (11.4.2.1e) to compute κ_v.</p> <p>Corresponding tensile stress in the FRP: Per ACI 318-14, Section 11.5.4.2, d_{fv} is taken as $0.8L_w$.</p> <p>Compute shear capacity of FRP strengthened wall using $\phi = 1.0$:</p> <p>Step 4b — Compute the shear corresponding to the nominal flexural strength. See Section 13.7.1.</p> <p>Note: The FRP for shear strengthening could be optimized by using horizontal strips rather than full coverage. For anchorage of shear FRP see Section 13.6.3.1.</p>	<p>From Step 1, $V_n^* = 46.4$ kip</p> <p>For one layer of the FRP: $L_e = 1.99$ in. $k_1 = 0.731$ $k_2 = 0.91$ $\kappa_v = 0.2$</p> <p>$\epsilon_{fe} = 0.2 \times 0.014 = 0.0028$ $f_{fe} = 0.0028 \times 9600 = 26.9$ ksi</p> <p>It is assumed that FRP is installed over the full height of the wall and not in discrete strips. $d_{fv} = 0.8L_w = 48$ in. $V_f = 0.75 \times 0.023 \times 0.0028 \times 9600 \times 48 = 22.25$ kip</p> <p>Reduction factor for FRP shear contribution, $\psi_f = 0.85$. $\psi_f V_f = 18.9$ kip</p> <p>Shear capacity of the retrofitted wall: $\phi V_n = 1.0(46.4 + 18.9)$ kip $\phi V_n = 65.3$ kip $> V_u = 52$ kip $\phi V_n > V_u \therefore$ OK $M_n = 272.2$ kip-ft</p> <p>Shear corresponding to the nominal flexural strength: $V_{Mnom} = 272.2$ kip-ft/10 ft = 27.2 kip The shear strength of the wall is: $V_n = 65.3$ kip $V_n \geq V_{Mnom} \therefore$ OK</p>	<p>From Step 1, $V_n^* = 1.0(201.8 + 81.5$ kN)</p> <p>$\epsilon_{fe} = 0.2 \times 0.014 = 0.0028$ $f_{fe} = 0.0028 \times 66.2 = 0.185$ GPa</p> <p>$d_{fv} = 0.8L_w = 1200$ mm $V_f = 0.75 \times 0.575 \times 0.0028 \times 66.2 \times 1200 = 95.9$ kN</p> <p>$\psi_f V_f = 81.5$ kN</p> <p>$\phi V_n = 1.0(203.1 + 81.5)$ kN $\phi V_n = 283.3$ kN $> V_u = 232$ kN $\phi V_n > V_u \therefore$ OK $M_n = 353$ kN·m</p> <p>$V_{Mnom} = 353$ kN·m/3 m = 117.1 kN The shear strength of the wall is: $V_n = 284.6$ kN $V_n \geq V_{Mnom} \therefore$ OK</p>

CHAPTER 17—REFERENCES

Committee documents are listed first by document number and year of publication followed by authored documents listed alphabetically.

American Concrete Institute (ACI)

ACI 216.1-14—Code Requirements for Determining Fire Resistance of Concrete and Masonry Construction Assemblies

ACI 224.1R-07—Causes, Evaluation, and Repair of Cracks in Concrete Structures

ACI 318-14—Building Code Requirements for Structural Concrete and Commentary

ACI 364.1R-07—Guide for Evaluation of Concrete Structures before Rehabilitation

ACI 369R-11—Guide for Seismic Rehabilitation of Existing Concrete Frame Buildings and Commentary

ACI 437R-03—Strength Evaluation of Existing Concrete Buildings

ACI 440R-07—Report on Fiber-Reinforced Polymer (FRP) Reinforcement for Concrete Structures

ACI 440.3R-12—Guide Test Methods for Fiber-Reinforced Polymers (FRPs) for Reinforcing or Strengthening Concrete Structures

ACI 440.7R-10—Guide for the Design and Construction of Externally Bonded Fiber-Reinforced Polymer Systems for Strengthening Unreinforced Masonry Structures

ACI 440.8-13—Specification for Carbon and Glass Fiber-Reinforced Polymer (FRP) Materials Made by Wet Layup for External Strengthening of Concrete and Masonry Structures

ACI 503.4-92—Standard Specification for Repairing Concrete with Epoxy Mortars (Reapproved by 2003)

ACI 546R-14—Guide to Concrete Repair

ACI 562-13—Code Requirements for Evaluation, Repair, and Rehabilitation of Concrete Buildings and Commentary

American National Standards Institute (ANSI)

ANSI Z400.1/Z129.1-2010—Hazardous Workplace Chemicals - Hazard Evaluation and Safety Data Sheet and Precautionary Labeling Preparation

American Society of Civil Engineers (ASCE)

ASCE 7-10—Minimum Design Loads for Buildings and Other Structures

ASCE/SEI 41-13—Seismic Rehabilitation and Retrofit of Existing Buildings

ASTM International

ASTM C1583/C1583M-13—Standard Test Method for Tensile Strength of Concrete Surfaces and the Bond Strength or Tensile Strength of Concrete Repair and Overlay Materials by Direct Tension (Pull-off Method)

ASTM D648-16—Test Method for Deflection Temperature of Plastics Under Flexural Load in the Edgewise Position

ASTM D696-16—Standard Test Method for Coefficient of Linear Thermal Expansion of Plastics Between -30°C and 30°C with a Vitreous Silica Dilatometer

ASTM D790-15—Standard Test Methods for Flexural Properties of Unreinforced and Reinforced Plastics and Electrical Insulating Materials

ASTM D2240-15—Standard Test Method for Rubber Property—Durometer Hardness

ASTM D2538-02(2010)—Standard Practice for Fusion of Poly(Vinyl Chloride) (PVC) Compounds Using a Torque Rheometer

ASTM D2584-11—Standard Test Method for Ignition Loss of Cured Reinforced Resins

ASTM D2990-09—Standard Test Methods for Tensile, Compressive, and Flexural Creep and Creep-Rupture of Plastics

ASTM D3039/D3039M-14—Standard Test Method for Tensile Properties of Polymer Matrix Composite Materials

ASTM D3171-15—Standard Test Methods for Constituent Content of Composite Materials

ASTM D3418-15—Standard Test Method for Transition Temperatures and Enthalpies of Fusion and Crystallization of Polymers by Differential Scanning Calorimetry

ASTM D3479/D3479M-12—Standard Test Method for Tension-Tension Fatigue of Polymer Matrix Composite Materials

ASTM D4476/D4476M-14—Standard Test Method for Flexural Properties of Fiber Reinforced Pultruded Plastic Rods

ASTM D7205/D7205M-06(2011)—Standard Test Method for Tensile Properties of Fiber Reinforced Polymer Matrix Composite Bars

ASTM D7337/D7337M-12—Standard Test Method for Tensile Creep Rupture of Fiber Reinforced Polymer Matrix Composite Bars

ASTM D7522/D7522M-15—Standard Test Method for Pull-Off Strength for FRP Bonded to Concrete Substrate

ASTM D7565/D7565M-10(2017)—Standard Test Method for Determining Tensile Properties of Fiber Reinforced Polymer Matrix Composites Used for Strengthening of Civil Structures

ASTM D7616/D7616M-11—Standard Test Method for Determining Apparent Overlap Splice Shear Strength Properties of Wet Lay-Up Fiber-Reinforced Polymer Matrix Composites Used for Strengthening Civil Structures

ASTM D7617/D7617M-11—Standard Test Method for Transverse Shear Strength of Fiber-Reinforced Polymer Matrix Composite Bars

ASTM E84-16—Standard Test Method for Surface Burning Characteristics of Building Materials

ASTM E328-13—Standard Test Methods for Stress Relaxation Tests for Materials and Structures

ASTM E831-14—Standard Test Method for Linear Thermal Expansion of Solid Materials by Thermomechanical Analysis

ASTM E1356-08(2014)—Standard Test Method for Assignment of the Glass Transition Temperatures by Differential Scanning Calorimetry

ASTM E1640-13—Standard Test Method for Assignment of the Glass Transition Temperature by Dynamic Mechanical Analysis

ASTM E2092-13—Test Method for Distortion Temperature in Three-Point Bending by Thermomechanical Analysis

Code of Federal Regulations (CFR)

CFR 16 Part 1500-2015—Hazardous Substances and Articles; Administration and Enforcement Regulations
CFR 49-2015—Transportation

International Code Council (ICC)

ICC AC125(2013)—Acceptance Criteria for Concrete and Reinforced and Unreinforced Masonry Strengthening Using Externally Bonded Fiber-Reinforced Polymer (FRP) Composite Systems

International Concrete Repair Institute (ICRI)

ICRI 210.3R-2009—Guide for Using In-Situ Tensile Pull-Off Tests to Evaluate Bond of Concrete Surface Materials

ICRI 310.2R-2013—Selecting and Specifying Concrete Surface Preparation for Sealers, Coatings, Polymer Overlays, and Concrete Repair

Authored documents

AASHTO, 2004, “LRFD Bridge Design Specifications,” third edition, American Association of State Highway and Transportation Officials Washington, DC.

Aiello, M. A.; Galati, N.; and Tegola, L. A., 2001, “Bond Analysis of Curved Structural Concrete Elements Strengthened using FRP Materials,” *Fifth International Symposium on Non-Metallic (FRP) Reinforcement for Concrete Structures (FRPRCS-5)*, Cambridge-Thomas Telford, London, pp. 680-688.

Antonopoulos, C. P., and Triantafillou, T. C., 2002, “Analysis of FRP-Strengthened RC Beam-Column Joints,” *Journal of Composites for Construction*, V. 6, No. 1, pp. 41-51. doi: [10.1061/\(ASCE\)1090-0268\(2002\)6:1\(41\)](https://doi.org/10.1061/(ASCE)1090-0268(2002)6:1(41))

Apicella, F., and Imbrogno, M., 1999, “Fire Performance of CFRP-Composites Used for Repairing and Strengthening Concrete,” *Proceedings of the 5th ASCE Materials Engineering Congress*, Cincinnati, OH, pp. 260-266.

Arduini, M., and Nanni, A., 1997, “Behavior of Pre-Cracked RC Beams Strengthened with Carbon FRP Sheets,” *Journal of Composites for Construction*, V. 1, No. 2, pp. 63-70. doi: [10.1061/\(ASCE\)1090-0268\(1997\)1:2\(63\)](https://doi.org/10.1061/(ASCE)1090-0268(1997)1:2(63))

Balsamo, A.; Manfredi, G.; Mola, E.; Negro, P.; and Prota, A., 2005, “Seismic Rehabilitation of a Full-Scale RC Structure using GFRP Laminates,” *7th International Symposium on Fiber-Reinforced (FRP) Polymer Reinforcement for Concrete Structures*, SP-230, C. K. Shield, J. P. Busel, S. L. Walkup, and D. D. Gremel, eds., American Concrete Institute, Farmington Hills, MI, pp. 1325-1344.

Bank, L. C., 2006, *Composites for Construction: Structural Design with FRP Materials*, John Wiley & Sons, Hoboken, NJ, 560 pp.

Belarbi, A.; Bae, S.; Ayou, A.; Kuchma, D.; Mirmiran, A.; and Okeil, A., 2011, “Design of FRP Systems for Strengthening Concrete Girders in Shear,” NCHRP Report 678, National Cooperative Highway Research Program, 130 pp.

Bianco, V.; Monti, G.; and Barros, J. A. O., 2014, “Design Formula to Evaluate the NSM FRP Strips Shear Strength Contribution to a RC Beam,” *Composites. Part B, Engineering*, V. 56, pp. 960-971. doi: [10.1016/j.compositesb.2013.09.001](https://doi.org/10.1016/j.compositesb.2013.09.001)

Binici, B., and Ozcebe, G., 2006, “Seismic Evaluation of Infilled Reinforced Concrete Frames Strengthened with FRPS,” *Proceedings of the 8th U.S. National Conference on Earthquake Engineering*, Earthquake Engineering Research Center, San Francisco, CA, 10 pp.

Bisby, L. A.; Green, M. F.; and Kodur, V. K. R., 2005a, “Fire Endurance of Fiber-Reinforced Polymer-Confined Concrete Columns,” *ACI Structural Journal*, V. 102, No. 6, Nov.-Dec., pp. 883-891.

Bisby, L. A.; Green, M. F.; and Kodur, V. K. R., 2005b, “Response to Fire of Concrete Structures that Incorporate FRP,” *Progress in Structural Engineering and Materials*, V. 7, No. 3, pp. 136-149. doi: [10.1002/pse.198](https://doi.org/10.1002/pse.198)

Bousias, S.; Triantafillou, T.; Fardis, M.; Spathis, L.; and O’Regan, B., 2004, “Fiber-Reinforced Polymer Retrofitting of Rectangular Reinforced Concrete Columns with or without Corrosion,” *ACI Structural Journal*, V. 101, No. 4, July-Aug., pp. 512-520.

Bousselham, A., and Chaallal, O., 2006, “Behavior of Reinforced Concrete T-Beams Strengthened in Shear with Carbon Fiber-Reinforced Polymer—An Experimental Study,” *ACI Structural Journal*, V. 103, No. 3, May-June, pp. 339-347.

Bracci, J. M.; Mander, J. B.; and Reinhorn, A. M., 1992a, “Seismic Resistance of Reinforced Concrete Frame Structures Designed only for Gravity Loads: Part I - Design and Properties of a One-Third Scale Model Structure,” *Technical Report NCEER-92-0027*, National Center for Earthquake Engineering Research, State University of New York, SUNY, Buffalo, New York, 186 pp.

Bracci, J. M.; Mander, J. B.; and Reinhorn, A. M., 1992b, “Seismic Resistance of Reinforced Concrete Frame Structures Designed only for Gravity Loads: Part II - Experimental Performance and Analytical Study of Retrofitted Structural Model,” *Technical Report NCEER-92-0031*, National Center for Earthquake Engineering Research, State University of New York, SUNY, Buffalo, New York, 166 pp.

Bracci, J. M.; Mander, J. B.; and Reinhorn, A. M., 1992c, “Seismic Resistance of Reinforced Concrete Frame Structures Designed only for Gravity Loads: Part III - Experimental Performance and Analytical Study of Structural Model,” *Technical Report NCEER-92-0029*, National Center for Earthquake Engineering Research, State University of New York, SUNY, Buffalo, New York, 168 pp.

Carey, S. A., and Harries, K. A., 2005, “Axial Behavior and Modeling of Small-, Medium-, and Large-Scale Circular Sections Confined with CFRP Jackets,” *ACI Structural Journal*, V. 102, No. 4, July-Aug., pp. 596-604.

Chaallal, O., and Shahawy, M., 2000, “Performance of Fiber-Reinforced Polymer-Wrapped Reinforced Concrete Column under Combined Axial-Flexural Loading,” *ACI Structural Journal*, V. 97, No. 4, July-Aug., pp. 659-668.

- Chajes, M.; Januska, T.; Mertz, D.; Thomson, T.; and Finch, W., 1995, "Shear Strengthening of Reinforced Concrete Beams Using Externally Applied Composite Fabrics," *ACI Structural Journal*, V. 92, No. 3, May-June, pp. 295-303.
- Christensen, J. B.; Gilstrap, J. M.; and Dolan, C. W., 1996, "Composite Materials Reinforcement of Existing Masonry Structures," *Journal of Architectural Engineering*, V. 2, No. 2, pp. 63-70. doi: [10.1061/\(ASCE\)1076-0431\(1996\)2:2\(63\)](https://doi.org/10.1061/(ASCE)1076-0431(1996)2:2(63))
- Concrete Society, 2004, "Design Guidance for Strengthening Concrete Structures Using Fibre Composite Materials," *Technical Report No. 55 (TR55)*, second edition, Surrey, UK, 128 pp.
- Cromwell, J. R.; Harries, K. A.; and Shahrooz, B. M., 2011, "Environmental Durability of Externally Bonded FRP Materials Intended for Repair of Concrete Structures," *Journal of Construction and Building Materials*, V. 25, No. 5, pp. 2528-2539. doi: [10.1016/j.conbuildmat.2010.11.096](https://doi.org/10.1016/j.conbuildmat.2010.11.096)
- Curtis, P. T., 1989, "Fatigue Behavior of Fibrous Composite Materials," *Journal of Strain Analysis*, V. 24, No. 4, pp. 235-244. doi: [10.1243/03093247V244235](https://doi.org/10.1243/03093247V244235)
- Das, S., 2011, "Life Cycle Assessment of Carbon Fiber-Reinforced Polymer Composites," *The International Journal of Life Cycle Assessment*, V. 16, No. 3, pp. 268-282. doi: [10.1007/s11367-011-0264-z](https://doi.org/10.1007/s11367-011-0264-z)
- De Lorenzis, L., and Nanni, A., 2001, "Characterization of FRP Rods as Near Surface Mounted Reinforcement," *Journal of Composites for Construction*, V. 5, No. 2, pp. 114-121. doi: [10.1061/\(ASCE\)1090-0268\(2001\)5:2\(114\)](https://doi.org/10.1061/(ASCE)1090-0268(2001)5:2(114))
- De Lorenzis, L., and Tepfers, R., 2003, "Comparative Study of Models on Confinement of Concrete Cylinders with Fiber-Reinforced Polymer Composites," *Journal of Composites for Construction*, V. 7, No. 3, pp. 219-237. doi: [10.1061/\(ASCE\)1090-0268\(2003\)7:3\(219\)](https://doi.org/10.1061/(ASCE)1090-0268(2003)7:3(219))
- De Lorenzis, L.; Lundgren, K.; and Rizzo, A., 2004, "Anchorage Length of Near-Surface-Mounted FRP Bars for Concrete Strengthening—Experimental Investigation and Numerical Modeling," *ACI Structural Journal*, V. 101, No. 2, Mar.-Apr., pp. 269-278.
- Demers, M., and Neale, K., 1999, "Confinement of Reinforced Concrete Columns with Fibre Reinforced Composites Sheets—An Experimental Study," *Canadian Journal of Civil Engineering*, V. 26, No. 2, pp. 226-241. doi: [10.1139/198-067](https://doi.org/10.1139/198-067)
- Deniaud, C., and Cheng, J. J. R., 2001, "Shear Behavior of Reinforced Concrete T-Beams with Externally Bonded Fiber-Reinforced Polymer Sheets," *ACI Structural Journal*, V. 98, No. 3, May-June, pp. 386-394.
- Deniaud, C., and Cheng, J. J. R., 2003, "Reinforced Concrete T-Beams Strengthened in Shear with Fiber Reinforced Polymer Sheets," *Journal of Composites for Construction*, V. 7, No. 4, pp. 302-310. doi: [10.1061/\(ASCE\)1090-0268\(2003\)7:4\(302\)](https://doi.org/10.1061/(ASCE)1090-0268(2003)7:4(302))
- Di Ludovico, M.; Balsamo, A.; Prota, A.; and Manfredi, G., 2008a, "Comparative Assessment of Seismic Rehabilitation Techniques on a Full Scale 3-Story RC Moment Frame Structure," *Journal of Structural Engineering and Mechanics*, V. 28, No. 6, pp. 727-747. doi: [10.12989/sem.2008.28.6.727](https://doi.org/10.12989/sem.2008.28.6.727)
- Di Ludovico, M.; Manfredi, G.; Mola, E.; Negro, P.; and Prota, A., 2008b, "Seismic Behavior of a Full-Scale RC Structure Retrofitted Using GFRP Laminates," *Journal of Structural Engineering*, V. 134, No. 5, pp. 810-821. doi: [10.1061/\(ASCE\)0733-9445\(2008\)134:5\(810\)](https://doi.org/10.1061/(ASCE)0733-9445(2008)134:5(810))
- Dolan, C. W.; Tanner, J.; Mukai, D.; Hamilton, H. R.; and Douglas, E., 2008, "Design Guidelines for Durability of Bonded CFRP Repair/Strengthening of Concrete Beams," *NCHRP Web-Only Document 155*, http://onlinepubs.trb.org/onlinepubs/nchrp/nchrp_w155.pdf (accessed Aug. 17, 2015).
- Ehsani, M. R., 1993, "Glass-Fiber Reinforcing Bars," *Alternative Materials for the Reinforcement and Prestressing of Concrete*, J. L. Clarke, Blackie Academic & Professional, London, pp. 35-54.
- El-Maaddawy, T.; Chahrouh, A.; and Soudki, K. A., 2006, "Effect of Fiber-Reinforced Polymer Wraps on Corrosion Activity and Concrete Cracking in Chloride-Contaminated Concrete Cylinders," *Journal of Composites for Construction*, V. 10, No. 2, pp. 139-147. doi: [10.1061/\(ASCE\)1090-0268\(2006\)10:2\(139\)](https://doi.org/10.1061/(ASCE)1090-0268(2006)10:2(139))
- Elnabesy, G., and Saatcioglu, M., 2004, "Seismic Retrofit of Circular and Square Bridge Columns with CFRP Jackets," *Advanced Composite Materials in Bridges and Structures*, Calgary, AB, Canada, 8 pp. (CD-ROM)
- El-Refai, S. A.; Ashour, A. F.; and Garrity, S. W., 2003, "Sagging and Hogging Strengthening of Continuous Reinforced Concrete Beams using CFRP sheets," *ACI Structural Journal*, V. 100, No. 4, July-Aug., pp. 446-453.
- El-Tawil, S.; Ogunc, C.; Okeil, A. M.; and Shahawy, M., 2001, "Static and Fatigue Analyses of RC Beams Strengthened with CFRP Laminates," *Journal of Composites for Construction*, V. 5, No. 4, pp. 258-267. doi: [10.1061/\(ASCE\)1090-0268\(2001\)5:4\(258\)](https://doi.org/10.1061/(ASCE)1090-0268(2001)5:4(258))
- Engindeniz, M.; Kahn, L. F.; and Zureick, A. H., 2005, "Repair and Strengthening of Reinforced Concrete Beam-Column Joints: State of the Art," *ACI Structural Journal*, V. 102, No. 2, Mar.-Apr., pp. 187-197.
- Engindeniz, M.; Kahn, L. F.; and Zureick, A. H., 2008a, "Pre-1970 RC Corner-Beam Column-Slab Joints: Seismic Adequacy and Upgradability with CFRP Composites," *Proceedings of the Fourteenth World Conference on Earthquake Engineering*, Beijing, China, Oct.
- Engindeniz, M.; Kahn, L. F.; and Zureick, A. H., 2008b, "Performance of an RC Corner-Beam Column Joint Severely Damaged under Bidirectional Loading and Rehabilitated with FRP Composites," SP-258, *Seismic Strengthening of Concrete Buildings Using FRP Composites*, Farmington Hills, MI, pp. 19-36.
- Eshwar, N.; Ibell, T. J.; and Nanni, A., 2003, "CFRP Strengthening of Concrete Bridges with Curved Soffits," *International Conference Structural Faults + Repair 2003*, M. C. Forde, ed., Commonwealth Institute, London, 10 pp. (CD-ROM)
- Eshwar, N.; Nanni, A.; and Ibell, T. J., 2005, "Effectiveness of CFRP Strengthening On Curved Soffit RC Beams," *Advances in Structural Engineering*, V. 8, No. 1, pp. 55-68. doi: [10.1260/1369433053749607](https://doi.org/10.1260/1369433053749607)

Eurocode 8, 2005, "Design of Structures for Earthquake Resistance, Part 3: Strengthening and Repair of Buildings," European Standard EN 1998-3, European Committee for Standardization, Brussels, Belgium, 89 pp.

Fardis, M. N., and Khalili, H., 1981, "Concrete Encased in Fiberglass Reinforced Plastic," *ACI Journal Proceedings*, V. 78, No. 6, Nov.-Dec., pp. 440-446.

Federal Emergency Management Agency, 2006, "Techniques for the Seismic Rehabilitation of Existing Buildings," FEMA-547, Building Seismic Safety Council for the Federal Emergency Management Agency, Washington, DC, 571 pp.

Federal Emergency Management Agency, 2009, "Quantification of Building Seismic Performance Factors," FEMA-P695, Applied Technology Council FEMA P695, Washington, DC, 421 pp.

Firno, J. P.; Correia, J. R.; and França, P., 2012, "Fire Behaviour of Reinforced Concrete Beams Strengthened with CFRP Laminates: Protection Systems with Insulation of the Anchorage Zones," *Composites. Part B, Engineering*, V. 43, No. 3, pp. 1545-1556. doi: [10.1016/j.compositesb.2011.09.002](https://doi.org/10.1016/j.compositesb.2011.09.002)

Fleming, C. J., and King, G. E. M., 1967, "The Development of Structural Adhesives for Three Original Uses in South Africa," *RILEM International Symposium, Synthetic Resins in Building Construction*, Paris, pp. 75-92.

Funakawa, I.; Shimono, K.; Watanabe, T.; Asada, S.; and Ushijima, S., 1997, "Experimental Study on Shear Strengthening with Continuous Fiber Reinforcement Sheet and Methyl Methacrylate Resin," *Third International Symposium on Non-Metallic (FRP) Reinforcement for Concrete Structures (FRPRCS-3)*, V. 1, Japan Concrete Institute, Tokyo, Japan, pp. 475-482.

GangaRao, H. V. S., and Vijay, P. V., 1998, "Bending Behavior of Concrete Beams Wrapped with Carbon Fabric," *Journal of Structural Engineering*, V. 124, No. 1, pp. 3-10. doi: [10.1061/\(ASCE\)0733-9445\(1998\)124:1\(3\)](https://doi.org/10.1061/(ASCE)0733-9445(1998)124:1(3))

Gergely, J.; Pantelides, C. P.; and Reaveley, L. D., 2000, "Shear Strengthening of RC T-Joints Using CFRP Composites," *Journal of Composites for Construction*, V. 4, No. 2, pp. 56-64. doi: [10.1061/\(ASCE\)1090-0268\(2000\)4:2\(56\)](https://doi.org/10.1061/(ASCE)1090-0268(2000)4:2(56))

Ghobarah, A., and Said, A., 2002, "Shear Strengthening of Beam-Column Joints," *The Journal of Earthquake, Wind, and Ocean Engineering*, V. 24, No. 7, pp. 881-888.

Green, M.; Bisby, L.; Beaudoin, Y.; and Labossiere, P., 1998, "Effects of Freeze-Thaw Action on the Bond of FRP Sheets to Concrete," *Proceedings of the First International Conference on Durability of Composites for Construction*, Sherbrooke, QC, Canada, pp. 179-190.

Grelle, S. V., and Sneed, L. H., 2013, "Review of Anchorage Systems for Externally-Bonded FRP Laminates," *International Journal of Concrete Structures and Materials*, V. 7, No. 1, pp. 17-33. doi: [10.1007/s40069-013-0029-0](https://doi.org/10.1007/s40069-013-0029-0)

Griffin, C. T., and Hsu, R. S., 2010, "Comparing the Embodied Energy of Structural Systems in Buildings," *ICSA 2010 – 1st International Conference on Structures & Architecture*, CRC Press, 8 pp.

Hamed, E., and Rabinovitch, O., 2005, "Dynamic Behavior of Reinforced Concrete Beams Strengthened

with Composite Materials," *Journal of Composites for Construction*, V. 9, No. 5, Sept., pp. 429-440. doi: [10.1061/\(ASCE\)1090-0268\(2005\)9:5\(429\)](https://doi.org/10.1061/(ASCE)1090-0268(2005)9:5(429))

Harajli, M., and Rteil, A., 2004, "Effect of Confinement Using Fiber-Reinforced Polymer or Fiber-Reinforced Concrete on Seismic Performance of Gravity Load-Designed Columns," *ACI Structural Journal*, V. 101, No. 1, Jan.-Feb., pp. 47-56.

Haroun, M. A., and Elsanadedy, H. M., 2005, "Fiber-Reinforced Plastic Jackets for Ductility Enhancement of Reinforced Concrete Bridge Columns with Poor Lap-Splice Detailing," *Journal of Bridge Engineering*, V. 10, No. 6, pp. 749-757. doi: [10.1061/\(ASCE\)1084-0702\(2005\)10:6\(749\)](https://doi.org/10.1061/(ASCE)1084-0702(2005)10:6(749))

Haroun, M. A., and Mosallam, A., 2002, "Shear Behavior of Unreinforced Masonry Wall strengthened with FRP Composites," *Proceedings of SAMPE Conference*, Baltimore, MD, pp. 862-871.

Haroun, M. A.; Mosallam, A. S.; and Allam, K. H., 2005, "Cyclic In-Plane Shear of Concrete Masonry Walls Strengthened by FRP Laminates," SP-230, *7th International Symposium on Fiber-Reinforced Polymer FRP Reinforcement for Concrete Structures* editors: C. Shield, J. P. Busel, S. L. Walkup, and D. G. Gremel, eds., American Concrete Institute, Farmington Hills, MI, pp. 327-340.

Haroun, M. A.; Mosallam, A. S.; Feng, M. Q.; and Elsanadedy, H. M., 2003, "Experimental Investigation of Seismic Repair and Retrofit of Bridge Columns by Composite Jackets," *Journal of Reinforced Plastics and Composites*, V. 22, No. 14, Sept., pp. 1243-1268. doi: [10.1177/0731684403035573](https://doi.org/10.1177/0731684403035573)

Harries, K. A., and Carey, S. A., 2003, "Shape and 'Gap' Effects on the Behavior of Variably Confined Concrete," *Cement and Concrete Research*, V. 33, No. 6, pp. 881-890. doi: [10.1016/S0008-8846\(02\)01085-2](https://doi.org/10.1016/S0008-8846(02)01085-2)

Harries, K. A.; Ricles, J. R.; Pessiki, S.; and Sause, R., 2006, "Seismic Retrofit of Lap Splices in Nonductile Square Columns Using Carbon Fiber-Reinforced Jackets," *ACI Structural Journal*, V. 103, No. 6, Nov.-Dec., pp. 874-884.

Hassan, T., and Rizkalla, S., 2003, "Investigation of Bond in Concrete Structures Strengthened with Near Surface Mounted Carbon Fiber Reinforced Polymer Strips," *Journal of Composites for Construction*, V. 7, No. 3, pp. 248-257. doi: [10.1061/\(ASCE\)1090-0268\(2003\)7:3\(248\)](https://doi.org/10.1061/(ASCE)1090-0268(2003)7:3(248))

Hiotakis, S.; Lau, D. T.; and Londono, N. L., 2004, "Research on Seismic Retrofit and Rehabilitation of Concrete Shear Walls Using FRP Materials," *NSC-NRC Taiwan-Canada Workshop on Construction Technologies National Center for Research on Earthquake Engineering*, Taipei, Taiwan, pp. 17-26.

Hognestad, E., 1951, "A Study of Combined Bending and Axial Load in Reinforced Concrete Members," *Bulletin* 399, University of Illinois Engineering Experiment Station, Urbana, IL.

Hollings, J., 1968, "Reinforced Concrete Seismic Design," *Bulletin of the New Zealand Society for Earthquake Engineering*, V. 23, pp. 217-250.

Howarth, J.; Mareddy, S. S. R.; and Mativenga, P. T., 2014, "Energy Intensity and Environmental Analysis of

Mechanical Recycling of Carbon Fibre Composite,” *Journal of Cleaner Production*, V. 81, No. 15, pp. 50-64.

Iacobucci, R.; Sheikh, S.; and Bayrak, O., 2003, “Retrofit of Square Concrete Columns with Carbon Fiber-Reinforced Polymer for Seismic Resistance,” *ACI Structural Journal*, V. 100, No. 6, Nov.-Dec., pp. 785-794.

International Federation for Structural Concrete, 2001, *FIB 2001: Externally Bonded FRP Reinforcement for RC Structures*, fib, Lausanne, Switzerland, 138 pp.

International Federation for Structural Concrete, 2003, “Seismic Assessment and Retrofit of Reinforced Concrete Buildings” *fib Bulletin* No. 24, fib, Lausanne, Switzerland, 312 pp.

International Federation for Structural Concrete, 2006, “Retrofitting of Concrete Structures by Externally Bonded FRPs with Emphasis on Seismic Applications” *fib Bulletin* No. 35, fib, Lausanne, Switzerland, 220 pp.

Italian National Research Council, 2004, “Guide for the Design and Construction of Externally Bonded FRP Systems for Strengthening Existing Structures: Materials, RC and PC Structures, Masonry Structures,” CNR-DT 200/2004, Advisory Committee on Technical Recommendations for Construction, Rome, Italy, 154 pp.

Japan Building Disaster Prevention Association, 2005, “Recent Development of Seismic Retrofit Methods in Japan,” Technical Committee on Evaluation of Building Disaster Prevention Methods, T. Kabeyasawa, ed., 94 pp.

Japan Society of Civil Engineers, 2001, “Recommendations for Upgrading of Concrete Structures with Use of Continuous Fiber Sheet,” *Concrete Engineering Series 41*, JSCE.

Kachlakev, D., and McCurry, D., 2000, “Testing of Full-Size Reinforced Concrete Beams Strengthened with FRP Composites: Experimental Results and Design Methods Verification,” Report No. FHWA-OR-00-19, U.S. Department of Transportation Federal Highway Administration, 109 pp.

Kalfat, R.; Al-Mahaidi, R.; and Smith, S. T., 2013, “Anchorage Devices used to Improve the Performance of Reinforced Concrete Beams Retrofitted with FRP Composites: State-of-the-Art Review,” *Journal of Composites for Construction*, V. 17, No. 1, pp. 14-33. doi: [10.1061/\(ASCE\)CC.1943-5614.0000276](https://doi.org/10.1061/(ASCE)CC.1943-5614.0000276)

Karbhari, V., ed., 2007, *Durability of Composites for Civil Structural Applications*, Woodhead Publishing, 384 pp.

Katsumata, H.; Kobatake, Y.; and Takeda, T., 1987, “A Study on the Strengthening with Carbon Fiber for Earthquake-Resistant Capacity of Existing Concrete Columns,” *Proceedings from the Workshop on Repair and Retrofit of Existing Structures, U.S.-Japan Panel on Wind and Seismic Effects*, U.S.-Japan Cooperative Program in Natural Resources, Tsukuba, Japan, pp. 1816-1823.

Khalifa, A.; Gold, W.; Nanni, A.; and Abel-Aziz, M., 1998, “Contribution of Externally Bonded FRP to the Shear Capacity of RC Flexural Members,” *Journal of Composites for Construction*, V. 2, No. 4, pp. 195-203. doi: [10.1061/\(ASCE\)1090-0268\(1998\)2:4\(195\)](https://doi.org/10.1061/(ASCE)1090-0268(1998)2:4(195))

Khalifa, A.; Alkhrdaji, T.; Nanni, A.; and Lansburg, S., 1999, “Anchorage of Surface-Mounted FRP Reinforcement,” *Concrete International*, V. 21, No. 10, Oct., pp. 49-54.

Khomwan, N., and Foster, S. J., 2005, “FE Modelling of FRP-Strengthened RC Shear walls Subjected to Reverse Cyclic Loading,” *Proceedings of the International Symposium on Bond Behaviour of FRP in Structures 2005*, pp. 519-524.

Kim, I. S.; Jirsa, J. O.; and Bayrak, O., 2011, “Use of Carbon Fiber-Reinforced Polymer Anchors to Repair and Strengthen Lap Splices of Reinforced Concrete Columns,” *ACI Structural Journal*, V. 108, No. 5, Nov.-Dec., pp. 630-640.

Kim, S. J., and Smith, S. T., 2010, “Pullout Strength Models for FRP Anchors in Uncracked Concrete,” *Journal of Composites for Construction*, V. 14, No. 4, pp. 406-414. doi: [10.1061/\(ASCE\)CC.1943-5614.0000097](https://doi.org/10.1061/(ASCE)CC.1943-5614.0000097)

Kumahara, S.; Masuda, Y.; and Tanano, Y., 1993, “Tensile Strength of Continuous Fiber Bar Under High Temperature,” *International Symposium on Fiber-Reinforced Plastic Reinforcement for Concrete Structures*, SP-138, A. Nanni and C. W. Dolan, eds., American Concrete Institute, Farmington Hills, MI, pp. 731-742.

Lam, L., and Teng, J., 2003a, “Design-Oriented Stress-Strain Model for FRP-Confined Concrete,” *Construction & Building Materials*, V. 17, No. 6-7, pp. 471-489. doi: [10.1016/S0950-0618\(03\)00045-X](https://doi.org/10.1016/S0950-0618(03)00045-X)

Lam, L., and Teng, J., 2003b, “Design-Oriented Stress-Strain Model for FRP-Confined Concrete in Rectangular Columns,” *Journal of Reinforced Plastics and Composites*, V. 22, No. 13, pp. 1149-1186. doi: [10.1177/0731684403035429](https://doi.org/10.1177/0731684403035429)

Lee, J.-H.; Chacko, R. M.; and Lopez, M. M., 2010, “Use of Mixed Mode Fracture Interfaces for the Modeling of Large Scale FRP Strengthened Beams,” *Journal of Composites for Construction*, V. 14, No. 6, pp. 845-855. doi: [10.1061/\(ASCE\)CC.1943-5614.0000143](https://doi.org/10.1061/(ASCE)CC.1943-5614.0000143)

Lombard, J.; Lau, D. T.; Humar, J. L.; Foo, S.; and Cheung, G. M. S., 2000, “Seismic Strengthening and Repair of Reinforced Concrete Shear Walls,” *Proceedings of the 12th World Conference on Earthquake Engineering*, Auckland, New Zealand, 8 pp.

Luo, S., and Wong, C. P., 2002, “Thermo-Mechanical Properties of Epoxy Formulations with Low Glass Transition Temperatures,” *Proceedings of the 8th International Symposium on Advanced Packaging Materials*, pp. 226-231.

Malek, A.; Saadatmanesh, H.; and Ehsani, M., 1998, “Prediction of Failure Load of R/C Beams Strengthened with FRP Plate Due to Stress Concentrations at the Plate End,” *ACI Structural Journal*, V. 95, No. 1, Jan.-Feb., pp. 142-152.

Malvar, L., 1998, “Durability of Composites in Reinforced Concrete,” *Proceedings of the First International Conference on Durability of Composites for Construction*, Sherbrooke, QC, Canada, Aug., pp. 361-372.

Malvar, L.; Warren, G.; and Inaba, C., 1995, “Rehabilitation of Navy Pier Beams with Composite Sheets,” *Second FRP International Symposium on Non-Metallic (FRP) Reinforcement for Concrete Structures*, Ghent, Belgium, Aug., pp. 533-540.

Mandell, J. F., 1982, "Fatigue Behavior of Fibre-Resin Composites," *Developments in Reinforced Plastics*, V. 2, Applied Science Publishers, London, UK, pp. 67-107.

Mandell, J. F., and Meier, U., 1983, "Effects of Stress Ratio Frequency and Loading Time on the Tensile Fatigue of Glass-Reinforced Epoxy," *Long Term Behavior of Composites*, ASTM STP 813, ASTM International, West Conshohocken, PA, pp. 55-77.

Masoud, S. A., and Soudki, K. A., 2006, "Evaluation of Corrosion Activity in FRP Repaired RC Beams," *Cement and Concrete Composites*, V. 28, No. 10, pp. 969-977. doi: [10.1016/j.cemconcomp.2006.07.013](https://doi.org/10.1016/j.cemconcomp.2006.07.013)

Matthys, S., and Triantafyllou, T., 2001, "Shear and Torsion Strengthening with Externally Bonded FRP Reinforcement," *Proceedings of the International Workshop on: Composites in Construction: A Reality*, ASCE, Reston, VA, pp. 203-212.

Matthys, S.; Toutanji, H.; Audenaert, K.; and Taerwe, L., 2005, "Axial Load Behavior of Large-Scale Columns Confined with Fiber-Reinforced Polymer Composites," *ACI Structural Journal*, V. 102, No. 2, Mar.-Apr., pp. 258-267.

Meier, U., 1987, "Bridge Repair with High Performance Composite Materials," *Materials Technology*, V. 4, pp. 125-128. (in German)

Meier, U., and Kaiser, H., 1991, "Strengthening of Structures with CFRP Laminates," *Advanced Composite Materials in Civil Engineering Structures*, ASCE Specialty Conference, pp. 224-232.

Memon, M., and Sheikh, S., 2005, "Seismic Resistance of Square Concrete Columns Retrofitted with Glass Fiber-Reinforced Polymer," *ACI Structural Journal*, V. 102, No. 5, Sept.-Oct., pp. 774-783.

Menna, C.; Asprone, D.; Jalayer, F.; Prota, A.; and Manfredi, G., 2013, "Assessment of Ecological Sustainability of a Building Subjected to Potential Seismic Events During its Lifetime," *The International Journal of Life Cycle Assessment*, V. 18, No. 2, pp. 504-515. doi: [10.1007/s11367-012-0477-9](https://doi.org/10.1007/s11367-012-0477-9)

Moehle, J. P.; Elwood, K. J.; and Sezen, H., 2002, "Gravity Load Collapse of Building Frames during Earthquakes," SP-197, *Behavior and Design of Concrete Structures for Seismic Performance*, American Concrete Institute, Farmington Hills, MI, pp. 215-238.

Moliner Santistevé, E.; Bastida, J.; Cseh, M.; and Vidal, R., 2013, "Life Cycle Assessment of a Fibre-Reinforced Polymer Made of Glass Fibre Phenolic Resin with Brominated Flame Retardant," *1st Symposium of the Spanish LCA Network: LCA & Bioenergy*.

Motavalli, M.; Terrasi, G. P.; and Meier, U., 1997, "On the Behavior of Hybrid Aluminum/CFRP Box Beams at Low Temperatures," *Composites. Part A, Applied Science and Manufacturing*, V. 28, No. 2, pp. 121-129. doi: [10.1016/S1359-835X\(96\)00100-5](https://doi.org/10.1016/S1359-835X(96)00100-5)

Mutsuyoshi, H.; Uehara, K.; and Machida, A., 1990, "Mechanical Properties and Design Method of Concrete Beams Reinforced with Carbon Fiber Reinforced Plastics," *Transaction of the Japan Concrete Institute*, V. 12, Japan Concrete Institute, Tokyo, Japan, pp. 231-238.

Nanni, A., 1995, "Concrete Repair with Externally Bonded FRP Reinforcement," *Concrete International*, V. 17, No. 6, June, pp. 22-26.

Nanni, A., and Bradford, N., 1995, "FRP Jacketed Concrete Under Uniaxial Compression," *Construction & Building Materials*, V. 9, No. 2, pp. 115-124. doi: [10.1016/0950-0618\(95\)00004-Y](https://doi.org/10.1016/0950-0618(95)00004-Y)

Nanni, A., and Gold, W., 1998, "Strength Assessment of External FRP Reinforcement," *Concrete International*, V. 20, No. 6, June, pp. 39-42.

Nanni, A.; Bakis, C. E.; Boothby, T. E.; Lee, Y. J.; and Frigo, E. L., 1997, "Tensile Reinforcement by FRP Sheets Applied to RC," *9C/1-8, ICE 97 International Composites Exposition*, Nashville, TN, Jan., pp. 9C/1 to 8.

Napolano, L.; Menna, C.; Asprone, D.; Prota, A.; and Manfredi, G., 2015, "LCA-Based Study on Structural Retrofit Options for Masonry Buildings," *The International Journal of Life Cycle Assessment*, V. 20, No. 1, pp. 23-35. doi: [10.1007/s11367-014-0807-1](https://doi.org/10.1007/s11367-014-0807-1)

National Research Council, 1991, "Life Prediction Methodologies for Composite Materials," *Committee on Life Prediction Methodologies for Composites*, NMAB-460, National Materials Advisory Board, Washington, DC, 75 pp.

Norris, T.; Saadatmanesh, H.; and Ehsani, M., 1997, "Shear and Flexural Strengthening of R/C Beams with Carbon Fiber Sheets," *Journal of Structural Engineering*, V. 123, No. 7, pp. 903-911. doi: [10.1061/\(ASCE\)0733-9445\(1997\)123:7\(903\)](https://doi.org/10.1061/(ASCE)0733-9445(1997)123:7(903))

Nosho, K. J., 1996, "Retrofit of Rectangular Reinforced Concrete Columns using Carbon Fiber," MS thesis, University of Washington, Seattle, WA, 194 pp.

Nowak, A. S., and Szerszen, M. M., 2003, "Calibration of Design Code for Buildings (ACI 318): Part 1—Statistical Models for Resistance," *ACI Structural Journal*, V. 100, No. 3, May-June, pp. 377-382.

Odagiri, T.; Matsumoto, K.; and Nakai, H., 1997, "Fatigue and Relaxation Characteristics of Continuous Aramid Fiber Reinforced Plastic Rods," *Third International Symposium on Non-Metallic (FRP) Reinforcement for Concrete Structures (FRPRCS-3)*, V. 2, Japan Concrete Institute, Tokyo, Japan, pp. 227-234.

Okeil, A. M.; Bingol, Y.; and Alkhrdaji, T., 2007, "Analyzing Model Uncertainties for Concrete Beams Flexurally Strengthened with FRP Laminates," *Proceedings of the Transportation Research Board 86th Annual Meeting*, Washington, DC, 15 pp. (CD-ROM)

Orton, S. L.; Jirsa, J. O.; and Bayrak, O., 2008, "Design Considerations of Carbon Fiber Anchors," *Journal of Composites for Construction*, V. 12, No. 6, pp. 608-616. doi: [10.1061/\(ASCE\)1090-0268\(2008\)12:6\(608\)](https://doi.org/10.1061/(ASCE)1090-0268(2008)12:6(608))

Orton, S. L.; Jirsa, J. O.; and Bayrak, O., 2009, "CFRP for Continuity in Existing RC Buildings Vulnerable to Collapse," *ACI Structural Journal*, V. 106, No. 5, Sept.-Oct., pp. 608-616.

Palmieri, A.; Matthys, S.; and Taerwe, L., 2011, "Fire Testing of RC Beams Strengthened with NSM Reinforcement," *10th International Symposium on Fiber-Reinforced Polymer Reinforcement for Concrete Structures (FRPRCS-*

- 10), SP-275, American Concrete Institute, Farmington Hills, MI. (CD-ROM)
- Pampanin, S.; Bolognini, D.; and Pavese, A., 2007, "Performance-Based Seismic Retrofit Strategy for Existing Reinforced Concrete Frame Systems Using Fiber-Reinforced Polymer Composites," *Journal of Composites for Construction*, V. 11, No. 2, pp. 211-226. doi: [10.1061/\(ASCE\)1090-0268\(2007\)11:2\(211\)](https://doi.org/10.1061/(ASCE)1090-0268(2007)11:2(211))
- Pantelides, C. P.; Gergely, J.; Reaveley, L. D.; and Volnyy, V. A., 1999, "Retrofit of R/C Bridge Pier with CFRP Advanced Composites," *Journal of Structural Engineering*, V. 125, No. 10, pp. 1094-1099. doi: [10.1061/\(ASCE\)0733-9445\(1999\)125:10\(1094\)](https://doi.org/10.1061/(ASCE)0733-9445(1999)125:10(1094))
- Pantelides, C. P.; Clyde, C.; and Reaveley, L. D., 2000, "Rehabilitation of R/C Building Joints with FRP Composites," *12th World Conference on Earthquake Engineering*, Auckland, New Zealand. (CD-ROM)
- Pantelides, C. P.; Alameddine, F.; Sardo, T.; and Imbsen, R., 2004, "Seismic Retrofit of State Street Bridge on Interstate 80," *Journal of Bridge Engineering*, V. 9, No. 4, pp. 333-342. doi: [10.1061/\(ASCE\)1084-0702\(2004\)9:4\(333\)](https://doi.org/10.1061/(ASCE)1084-0702(2004)9:4(333))
- Pantelides, C. P.; Okahashi, Y.; and Reaveley, L. D., 2008, "Seismic Rehabilitation of Reinforced Concrete Frame Interior Beam-Column Joints with FRP Composites," *Journal of Composites for Construction*, V. 12, No. 4, pp. 435-445. doi: [10.1061/\(ASCE\)1090-0268\(2008\)12:4\(435\)](https://doi.org/10.1061/(ASCE)1090-0268(2008)12:4(435))
- Park, R., and Paulay, T., 1976, *Reinforced Concrete Structures*, Wiley, 800 pp.
- Paterson, J., and Mitchell, D., 2003, "Seismic Retrofit of Shear Walls with Headed Bars and Carbon Fiber Wrap," *Journal of Structural Engineering*, V. 129, No. 5, pp. 606-614. doi: [10.1061/\(ASCE\)0733-9445\(2003\)129:5\(606\)](https://doi.org/10.1061/(ASCE)0733-9445(2003)129:5(606))
- Prestressed/Precast Concrete Institute, 2004, *PCI Design Handbook Precast and Prestressed Concrete*, sixth edition, Prestressed/Precast Concrete Institute, Chicago, IL, 750 pp.
- Pellegrino, C., and Modena, C., 2002, "Fiber Reinforced Polymer Shear Strengthening of Reinforced Concrete Beams with Transverse Steel Reinforcement," *Journal of Composites for Construction*, V. 6, No. 2, pp. 104-111. doi: [10.1061/\(ASCE\)1090-0268\(2002\)6:2\(104\)](https://doi.org/10.1061/(ASCE)1090-0268(2002)6:2(104))
- Pessiki, S. P.; Conley, C. H.; Gergely, P.; and White, R. N., 1990, "Seismic Behavior of Lightly Reinforced Concrete Column and Beam-Column Joint Details," *NCEER Report No. 90-0014*, 184 pp.
- Pessiki, S.; Harries, K. A.; Kestner, J.; Sause, R.; and Ricles, J. M., 2001, "The Axial Behavior of Concrete Confined with FRP Jackets," *Journal of Composites for Construction*, V. 5, No. 4, pp. 237-245. doi: [10.1061/\(ASCE\)1090-0268\(2001\)5:4\(237\)](https://doi.org/10.1061/(ASCE)1090-0268(2001)5:4(237))
- Porter, M. L.; Mehus, J.; Young, K. A.; O'Neil, E. F.; and Barnes, B. A., 1997, "Aging for Fiber Reinforcement in Concrete," *Proceedings of the Third International Symposium on Non-Metallic (FRP) Reinforcement for Concrete Structures*, Japan Concrete Institute, Sapporo, Japan.
- Priestley, M.; Seible, F.; and Calvi, G., 1996, *Seismic Design and Retrofit of Bridges*, John Wiley and Sons, New York, 704 pp.
- Prota, A.; Nanni, A.; Manfredi, G.; and Cosenza, E., 2004, "Selective Upgrade of Underdesigned Reinforced Concrete Beam-Column Joints Using Carbon Fiber-Reinforced Polymers," *ACI Structural Journal*, V. 101, No. 5, Sept.-Oct., pp. 699-707.
- Reed, C. E.; Peterman, R. J.; and Rasheed, H. A., 2005, "Evaluating FRP Repair Method for Cracked Prestressed Concrete Bridge Members Subjected to Repeated Loadings (Phase 1)," *KTRAN Report No. K-TRAN: KSU-01-2*, Kansas Department of Transportation, Topeka, KS, 106 pp.
- Ritchie, P.; Thomas, D.; Lu, L.; and Conneley, G., 1991, "External Reinforcement of Concrete Beams Using Fiber Reinforced Plastics," *ACI Structural Journal*, V. 88, No. 4, July-Aug., pp. 490-500.
- Roberts, T. M., and Haji-Kazemi, H., 1989, "Theoretical Study of the Behavior of Reinforced Concrete Beams Strengthened by Externally Bonded Steel Plates," *Proceedings of the Institute of Civil Engineers*, Part 2, V. 87, No. 9344, pp. 39-55.
- Rocca, S.; Galati, N.; and Nanni, A., 2006, "Experimental Evaluation of FRP Strengthening of Large-Size Reinforced Concrete Columns," *Report No. UTC-142*, University of Missouri-Rolla, MO.
- Rocca, S.; Galati, N.; and Nanni, A., 2008, "Review of Design Guidelines for FRP Confinement of Reinforced Concrete Columns of Noncircular Cross Sections," *Journal of Composites for Construction*, V. 12, No. 1, Jan.-Feb., pp. 80-92. doi: [10.1061/\(ASCE\)1090-0268\(2008\)12:1\(80\)](https://doi.org/10.1061/(ASCE)1090-0268(2008)12:1(80))
- Rosenboom, O. A., and Rizkalla, S. H., 2006, "Behavior of Prestressed Concrete Strengthened with Various CFRP Systems Subjected to Fatigue Loading," *Journal of Composites for Construction*, V. 10, No. 6, Nov.-Dec., pp. 492-502. doi: [10.1061/\(ASCE\)1090-0268\(2006\)10:6\(492\)](https://doi.org/10.1061/(ASCE)1090-0268(2006)10:6(492))
- Rostasy, F. S., 1987, "Bonding of Steel and GFRP Plates in the Area of Coupling Joints. Talbrucke Kattenbusch," *Research Report No. 3126/1429*, Federal Institute for Materials Testing, Braunschweig, Germany. (in German)
- Rostasy, F. S., 1997, "On Durability of FRP in Aggressive Environments," *Third International Symposium on Non-Metallic (FRP) Reinforcement for Concrete Structures (FRPRCS-3)*, V. 2, Japan Concrete Institute, Tokyo, Japan, pp. 107-114.
- Roylance, M., and Roylance, O., 1981, "Effect of Moisture on the Fatigue Resistance of an Aramid-Epoxy Composite," *Organic Coatings and Plastics Chemistry*, V. 45, American Chemical Society, Washington, DC, pp. 784-788.
- Saadatmanesh, H.; Ehsani, M. R.; and Jin, L., 1996, "Seismic Strengthening of Circular Bridge Pier Models with Fiber Composites," *ACI Structural Journal*, V. 93, No. 6, Nov.-Dec., pp. 639-647.
- Sabnis, G. M.; Shroff, A. C.; and Kahn, L. F., eds., 1996, "Seismic Rehabilitation of Concrete Structures," SP-160, American Concrete Institute, Farmington Hills, MI, 318 pp.
- Sato, Y.; Ueda, T.; Kakuta, Y.; and Tanaka, T., 1996, "Shear Reinforcing Effect of Carbon Fiber Sheet Attached to Side of Reinforced Concrete Beams," *Advanced Composite Materials in Bridges and Structures*, M. M. El-Badry, ed., pp. 621-627.

Sause, R.; Harries, K. A.; Walkup, S. L.; Pessiki, S.; and Ricles, J. M., 2004, "Flexural Behavior of Concrete Columns with Carbon Fiber Composite Jackets," *ACI Structural Journal*, V. 101, No. 5, Sept.-Oct., pp. 708-716.

Seible, F.; Priestley, M. J. N.; Hegemier, G. A.; and Innamorato, D., 1997, "Seismic Retrofit of RC Columns with Continuous Carbon Fiber Jackets," *Journal of Composites for Construction*, V. 1, No. 2, pp. 52-62. doi: [10.1061/\(ASCE\)1090-0268\(1997\)1:2\(52\)](https://doi.org/10.1061/(ASCE)1090-0268(1997)1:2(52))

Sezen, H.; Whittaker, A. S.; Elwood, K. J.; and Mosalam, K. M., 2003, "Performance of Reinforced Concrete Buildings during the August 17, 1999 Kocaeli, Turkey Earthquake, and Seismic Design and Construction Practice in Turkey," *Journal of Engineering Structures*, V. 25, No. 1, pp. 103-114. doi: [10.1016/S0141-0296\(02\)00121-9](https://doi.org/10.1016/S0141-0296(02)00121-9)

Sharaf, M. H.; Soudki, K. A.; and Van Dusen, M., 2006, "CFRP Strengthening for Punching Shear of Interior Slab-Column Connections," *Journal of Composites for Construction*, V. 10, No. 5, pp. 410-418. doi: [10.1061/\(ASCE\)1090-0268\(2006\)10:5\(410\)](https://doi.org/10.1061/(ASCE)1090-0268(2006)10:5(410))

Sharif, A.; Al-Sulaimani, G.; Basunbul, I.; Baluch, M.; and Ghaleb, B., 1994, "Strengthening of Initially Loaded Reinforced Concrete Beams Using FRP Plates," *ACI Structural Journal*, V. 91, No. 2, Mar.-Apr., pp. 160-168.

Sheikh, S., and Yau, G., 2002, "Seismic Behavior of Concrete Columns Confined with Steel and Fiber-Reinforced Polymers," *ACI Structural Journal*, V. 99, No. 1, Jan.-Feb., pp. 72-80.

Silva, P. F., and Ibell, T. J., 2008, "Evaluation of Moment Redistribution in Continuous FRP-Strengthened Concrete Structures," *ACI Structural Journal*, V. 105, No. 6, Nov.-Dec., pp. 729-739.

Silva, P. F.; Ereckson, N. J.; and Chen, G., 2007, "Seismic Retrofit of Bridge Joints in the Central U.S. with CFRP Composites," *ACI Structural Journal*, V. 104, No. 2, Mar.-Apr., pp. 207-217.

Soudki, K. A., and Green, M. F., 1997, "Freeze-Thaw Response of CFRP Wrapped Concrete," *Concrete International*, V. 19, No. 8, Aug., pp. 64-67.

Spoelstra, M. R., and Monti, G., 1999, "FRP-Confined Concrete Model," *Journal of Composites for Construction*, V. 3, No. 3, pp. 143-150. doi: [10.1061/\(ASCE\)1090-0268\(1999\)3:3\(143\)](https://doi.org/10.1061/(ASCE)1090-0268(1999)3:3(143))

Suppliers of Advanced Composite Materials Association, 1994, *SACMA Recommended Methods (SRM) Manual*, Suppliers of Advanced Composite Materials Association, Arlington, VA.

Szerszen, M. M., and Nowak, A. S., 2003, "Calibration of Design Code for Buildings (ACI 318): Part 2—Reliability Analysis and Resistance Factors," *ACI Structural Journal*, V. 100, No. 3, May-June, pp. 383-391.

Teng, J. G.; Chen, J. F.; Smith, S. T.; and Lam, L., 2002, *FRP Strengthened RC Structures*, John Wiley & Sons, West Sussex, UK, 266 pp.

Teng, J. G.; Smith, S. T.; Yao, J.; and Chen, J. F., 2003, "Intermediate Crack Induced Debonding in RC Beams and Slabs," *Construction & Building Materials*, V. 17, No. 6-7, pp. 447-462. doi: [10.1016/S0950-0618\(03\)00043-6](https://doi.org/10.1016/S0950-0618(03)00043-6)

Teng, J. G.; Lu, X. Z.; Ye, L. P.; and Jiang, J. J., 2004, "Recent Research on Intermediate Crack Induced Debonding in FRP Strengthened Beams," *Proceedings of the 4th International Conference on Advanced Composite Materials for Bridges and Structures*, Calgary, AB, Canada.

Toutanji, H., 1999, "Stress-Strain Characteristics of Concrete Columns Externally Confined with Advanced Fiber Composite Sheets," *ACI Materials Journal*, V. 96, No. 3, May-June, pp. 397-404.

Triantafillou, T. C., 1998, "Shear Strengthening of Reinforced Concrete Beams Using Epoxy-Bonded FRP Composites," *ACI Structural Journal*, V. 95, No. 2, Mar.-Apr., pp. 107-115.

Wallace, J. W., 1995, "Seismic Design of RC Structural Walls; Part I: New Code Format," *Journal of Structural Engineering*, V. 121, No. 1, pp. 75-87. doi: [10.1061/\(ASCE\)0733-9445\(1995\)121:1\(75\)](https://doi.org/10.1061/(ASCE)0733-9445(1995)121:1(75))

Wang, N., and Evans, J. T., 1995, "Collapse of Continuous Fiber Composite Beam at Elevated Temperatures," *Composites*, V. 26, No. 1, pp. 56-61. doi: [10.1016/0010-4361\(94\)P3630-J](https://doi.org/10.1016/0010-4361(94)P3630-J)

Wang, Y. C., and Restrepo, J. I., 2001, "Investigation of Concentrically Loaded Reinforced Concrete Columns Confined with Glass Fiber-Reinforced Polymer Jackets," *ACI Structural Journal*, V. 98, No. 3, May-June, pp. 377-385.

Williams, B. K.; Bisby, L. A.; Kodur, V. K. R.; Green, M. F.; and Chowdhury, E., 2006, "Fire Insulation Schemes for FRP-Strengthened Concrete Slabs," *Composites. Part A, Applied Science and Manufacturing*, V. 37, No. 8, pp. 1151-1160. doi: [10.1016/j.compositesa.2005.05.028](https://doi.org/10.1016/j.compositesa.2005.05.028)

Wolf, R., and Miessler, H. J., 1989, "HLV-Spannglieder in der Praxis," *Erfahrungen Mit Glasfaserverbundstaben Beton*, V. 2, pp. 47-51.

Wu, W., 1990, "Thermomechanical Properties of Fiber Reinforced Plastics (FRP) Bars," PhD dissertation, West Virginia University, Morgantown, WV, 292 pp.

Xian, G., and Karbhari, V. M., 2007, "Segmental Relaxation of Water-Aged Ambient Cured Epoxy," *Journal of Polymer Degradation and Stability*, V. 92, No. 9, pp. 1650-1659. doi: [10.1016/j.polymdegradstab.2007.06.015](https://doi.org/10.1016/j.polymdegradstab.2007.06.015)

Yamaguchi, T.; Kato, Y.; Nishimura, T.; and Uomoto, T., 1997, "Creep Rupture of FRP Rods Made of Aramid, Carbon and Glass Fibers," *Third International Symposium on Non-Metallic (FRP) Reinforcement for Concrete Structures (FRPRCS-3)*, V. 2, Japan Concrete Institute, Tokyo, Japan, pp. 179-186.

Youssef, M. N., 2003, "Stress Strain Model for Concrete Confined by FRP Composites," PhD dissertation, University of California-Irvine, Irvine, CA, 310 pp.

Zhang, C.; Lin, W. X.; Abududdin, M.; and Canning, L., 2012, "Environmental Evaluation of FRP in UK Highway Bridge Deck Replacement Applications Based on a Comparative LCA Study," *Advanced Materials Research*, V. 374, pp. 43-48.

Zureick, A.-H.; Ellingwood, B. R.; Nowak, A. S.; Mertz, D. R.; and Triantafillou, T. C., 2010, "Recommended Guide Specification for the Design of Externally Bonded FRP Systems for Repair and Strengthening of Concrete Bridge Elements," *NCHRP Report 655*, Transportation Research Board, Washington, DC, 49 pp.

APPENDIX A—MATERIAL PROPERTIES OF CARBON, GLASS, AND ARAMID FIBERS

Table A.1 presents ranges of values for the tensile properties of carbon, glass, and aramid fibers. The tabulated values are based on the testing of impregnated fiber yarns or strands in accordance with suppliers of SACMA Recommended Method 16R-1994 (Suppliers of Advanced Composite Materials Association 1994). The strands or fiber yarns are impregnated with resin, cured, and then tested in tension. The tabulated properties are calculated using the area of the fibers; the resin area is ignored. Hence, the properties listed in Table A.1 are representative of unidirectional FRP systems whose properties are reported using net-fiber area (4.3.1).

Table A.2 presents ranges of tensile properties for carbon FRP (CFRP), glass FRP (GFRP), and aramid FRP (AFRP)

bars with fiber volumes of approximately 50 to 70 percent. Properties are based on gross-laminate area (4.3.1).

Table A.3 presents ranges of tensile properties for CFRP, GFRP, and AFRP laminates with fiber volumes of approximately 40 to 60 percent. Properties are based on gross-laminate area (4.3.1). The properties are shown for unidirectional, bidirectional, and +45/–45-degree fabrics. Table A.3 also shows the effect of varying the fiber orientation on the 0-degree strength of the laminate.

Table A.4 gives the tensile strengths of some commercially available FRP systems. The strength of unidirectional laminates is dependent on fiber type and dry fabric weight.

These tables are not intended to provide ultimate strength values for design purposes.

Table A.1—Typical tensile properties of fibers used in FRP systems

Fiber type	Elastic modulus		Ultimate strength		Rupture strain, minimum, %
	10 ³ ksi	GPa	ksi	MPa	
Carbon					
General purpose	32 to 34	220 to 240	300 to 550	2050 to 3790	1.2
High-strength	32 to 34	220 to 240	550 to 700	3790 to 4820	1.4
Ultra-high-strength	32 to 34	220 to 240	700 to 900	4820 to 6200	1.5
High-modulus	50 to 75	340 to 520	250 to 450	1720 to 3100	0.5
Ultra-high-modulus	75 to 100	520 to 690	200 to 350	1380 to 2400	0.2
Glass					
E-glass	10 to 10.5	69 to 72	270 to 390	1860 to 2680	4.5
S-glass	12.5 to 13	86 to 90	500 to 700	3440 to 4140	5.4
Aramid					
General purpose	10 to 12	69 to 83	500 to 600	3440 to 4140	2.5
High-performance	16 to 18	110 to 124	500 to 600	3440 to 4140	1.6

Table A.2—Tensile properties of FRP bars with fiber volumes of 50 to 70 percent

FRP system description	Elastic modulus, 10 ³ ksi (GPa)	Ultimate tensile strength, ksi (MPa)	Rupture strain, %
High-strength carbon/epoxy	17 to 24 (115 to 165)	180 to 400 (1240 to 2760)	1.2 to 1.8
E-glass/epoxy	4 to 7 (27 to 48)	70 to 230 (480 to 1580)	1.6 to 3.0
High-performance aramid	8 to 11 (55 to 76)	130 to 280 (900 to 11,930)	2.0 to 3.0

Table A.3—Tensile properties of FRP laminates with fiber volumes of 40 to 60 percent

FRP system description (fiber orientation)	Elastic modulus		Ultimate tensile strength		Rupture strain at 0 degrees, %
	Property at 0 degrees	Property at 90 degrees	Property at 0 degrees	Property at 90 degrees	
	10 ³ ksi (GPa)	10 ³ ksi (GPa)	ksi (MPa)	ksi (MPa)	
High-strength carbon/epoxy, degrees					
0	15 to 21 (100 to 140)	0.3 to 1 (2 to 7)	150 to 350 (1020 to 2080)	5 to 10 (35 to 70)	1.0 to 1.5
0/90	8 to 11 (55 to 76)	8 to 11 (55 to 75)	100 to 150 (700 to 1020)	100 to 150 (700 to 1020)	1.0 to 1.5
+45/-45	2 to 4 (14 to 28)	2 to 4 (14 to 28)	25 to 40 (180 to 280)	25 to 40 (180 to 280)	1.5 to 2.5
E-glass/epoxy, degrees					
0	3 to 6 (20 to 40)	0.3 to 1 (2 to 7)	75 to 200 (520 to 1400)	5 to 10 (35 to 70)	1.5 to 3.0
0/90	2 to 5 (14 to 34)	2 to 5 (14 to 35)	75 to 150 (520 to 1020)	75 to 150 (520 to 1020)	2.0 to 3.0
+45/-45	2 to 3 (14 to 21)	2 to 3 (14 to 20)	25 to 40 (180 to 280)	25 to 40 (180 to 280)	2.5 to 3.5
High-performance aramid/epoxy, degrees					
0	7 to 10 (48 to 68)	0.3 to 1 (2 to 7)	100 to 250 (700 to 1720)	5 to 10 (35 to 70)	2.0 to 3.0
0/90	4 to 5 (28 to 34)	4 to 5 (28 to 35)	40 to 80 (280 to 550)	40 to 80 (280 to 550)	2.0 to 3.0
+45/-45	1 to 2 (7 to 14)	1 to 2 (7 to 14)	20 to 30 (140 to 210)	20 to 30 (140 to 210)	2.0 to 3.0

Notes:
FRP composite properties are based on FRP systems having an approximate fiber volume of 50 percent and a composite thickness of 0.1 in. (2.5 mm). In general, FRP bars have fiber volumes of 50 to 70 percent, precured systems have fiber volumes of 40 to 60 percent, and wet layup systems have fiber volumes of 25 to 40 percent. Because the fiber volume influences the gross-laminate properties, precured laminates usually have higher mechanical properties than laminates created using the wet layup technique.
Zero degrees represents unidirectional fiber orientation.
Zero/90 degrees (or +45/-45 degrees) represents fiber balanced in two orthogonal directions, where 0 degrees is the direction of loading, and 90 degrees is normal to the direction of loading.
Tension is applied to 0-degree direction. All FRP bar properties are in the 0-degree direction.

Table A.4—Ultimate tensile strength* of some commercially available FRP systems

FRP system description (fiber type/saturating resin/fabric type)	Fabric weight		Ultimate strength [†]	
	oz/yd ³	g/m ³	lb/in.	kN/mm
General purpose carbon/resin unidirectional sheet	6	200	2600	500
	12	400	3550	620
High-strength carbon/resin unidirectional sheet	7	230	1800	320
	9	300	4000	700
	18	620	5500	960
High-modulus carbon/resin unidirectional sheet	9	300	3400	600
General-purpose carbon/resin balanced sheet	9	300	1000	180
E-glass/resin unidirectional sheet	27	900	4100	720
	10	350	1300	230
E-glass/balanced fabric	9	300	680	120
Aramid/resin unidirectional sheet	12	420	4000	700
High-strength carbon/resin precured, unidirectional laminate	70 [‡]	2380 [‡]	19,000	3300
E-glass/vinyl ester precured, unidirectional shell	50 [‡]	1700 [‡]	9000	1580

*Values shown should not be used for design.
[†]Ultimate tensile strength per unit width of sheet or fabric.
[‡]Precured laminate weight.

APPENDIX B—SUMMARY OF STANDARD TEST METHODS

Table B provides a summary of test methods for the short- and long-term mechanical and durability testing of FRP rods and sheets. The recommended test methods are based on the knowledge gained from research results and literature worldwide and include those methods described in ACI 440.3R that have not yet been adopted by ASTM.

Durability-related tests use the same test methods but require application-specific preconditioning of specimens. Acceptance of the data generated by the listed test methods can be the basis for FRP material system qualification and acceptance (for example, ACI 440.8).

Table B—Test methods for FRP material systems

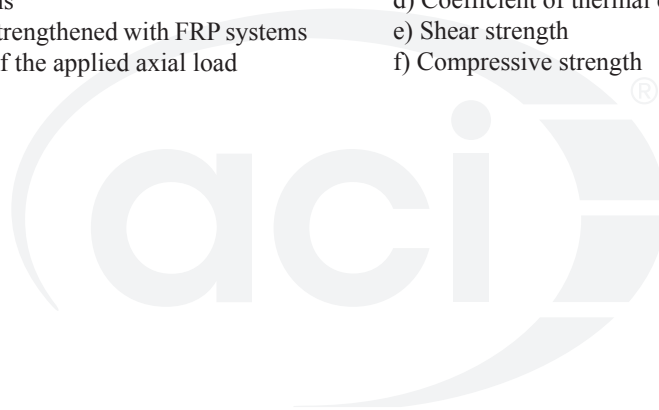
Property	ASTM test method(s)	ACI 440.3R test method	Summary of differences
Test methods for sheets, prepreg, and laminates			
Surface hardness	D2538	—	No ACI methods developed
	D2240		
	D3418		
Coefficient of thermal expansion	D696	—	No ACI methods developed
Glass-transition temperature	E1640	—	No ACI methods developed
Volume fraction	D3171	—	No ACI methods developed
	D2584		
Sheet to concrete adhesion (direct tension pulloff)	D7522/D7522M	L.1*	ACI method provides specific requirements for specimen preparation not found in the ASTM method
Tensile strength and modulus	D3039/D3039M or D7565/D7565M, as appropriate	L.2*	ACI method provides methods for calculating tensile strength and modulus on gross cross-sectional and effective fiber area basis. Section 3.3.1 is used to calculate design values.
Lap shear strength	D7616/D7616M	L.3*	ACI method provides specific requirements for specimen preparation.
Test methods for FRP bars			
Cross-sectional area	D7205/D7207M	B.1*	Two options for bar area are provided in ASTM D7205/D7205M (nominal and actual) whereas only nominal area is used in ACI 440.3R Method B.1
Longitudinal tensile strength and modulus	D7205/D7205M	B.2*	Strain limits for calculation of modulus are different in the two methods.
Shear strength	D7617/D7617M	B.4*	The ACI method focuses on dowel action of bars and does not overlap with existing ASTM methods that focus mainly on beam shearing failure modes. Bar shear strength is of specific concern for applications where FRP rods are used to cross construction joints in concrete pavements.
Durability properties	—	B.6	No existing ASTM test methods available.
Fatigue properties	D3479/D3479M	B.7	ACI methods provide specific information on anchoring bars in the test fixtures and on attaching elongation measuring devices to the bar. The ACI methods also require specific calculations that are not provided in the ASTM methods.
Creep properties	D7337/D7337M	B.8*	
Relaxation properties	D2990	B.9	
	E328		
Flexural tensile properties	—	B.11	No existing ASTM test methods available.
Flexural properties	D790	—	No ACI methods developed.
	D4476/D4476M		
Coefficient of thermal expansion	E831	—	No ACI methods developed.
	D696		
Glass-transition temperature	E1356	—	No ACI methods developed.
	E1640		
	D648		
	E2092		
Volume fraction	D3171	—	No ACI methods developed.

*Test method in ACI 440.3R is replaced by reference to appropriate ASTM method.

APPENDIX C—AREAS OF FUTURE RESEARCH

Future research is needed to provide information in areas that are still unclear or are in need of additional evidence to validate performance. The list of topics presented in this appendix provides a summary.

- a) Materials
 - i. Methods of fireproofing FRP strengthening systems
 - ii. Behavior of FRP-strengthened members under elevated temperatures
 - iii. Behavior of FRP-strengthened members under cold temperatures
 - iv. Fire rating of concrete members strengthened with FRP systems
 - v. Effect of different coefficients of thermal expansion between FRP systems and member substrates
 - vi. Creep-rupture behavior and endurance times of FRP systems
 - vii. Strength and stiffness degradation of FRP systems in harsh environments
 - b) Flexure/axial force
 - i. Compression behavior of noncircular members wrapped with FRP systems
 - ii. Behavior of members strengthened with FRP systems oriented in the direction of the applied axial load
 - iii. Effects of high concrete strength on behavior of FRP-strengthened members
 - iv. Effects of lightweight concrete on behavior of FRP-strengthened members
 - v. Maximum crack width and deflection prediction and control of concrete reinforced with FRP systems
 - vi. Long-term deflection behavior of concrete flexural members strengthened with FRP systems
 - c) Shear
 - i. Effective strain of FRP systems that do not completely wrap around the section
 - ii. Use of FRP systems for punching shear reinforcement in two-way systems
 - d) Detailing
 - i. Anchoring of FRP systems
- The design guide specifically indicates that test methods are needed to determine the following properties of FRP:
- a) Bond characteristics and related bond-dependent coefficients
 - b) Creep rupture and endurance times
 - c) Fatigue characteristics
 - d) Coefficient of thermal expansion
 - e) Shear strength
 - f) Compressive strength



APPENDIX D—METHODOLOGY FOR COMPUTATION OF SIMPLIFIED P-M INTERACTION DIAGRAM FOR NONCIRCULAR COLUMNS

Axial load-moment (*P-M*) interaction diagrams may be developed by satisfying strain compatibility and force equilibrium using the model for the stress strain behavior for FRP-confined concrete presented in Eq. (12.1c) through (12.1e). For simplicity, the portion of the unconfined and confined P-M diagrams corresponding to compression-controlled failure can be reduced to two bilinear curves passing through the following points (Fig 12.2). (The following only makes reference to the confined case because the unconfined case is analogous):

a) Point A (pure compression) at a uniform axial compressive strain of confined concrete ϵ_{ccu}

b) Point B with a strain distribution corresponding to zero strain at the layer of longitudinal steel reinforcement nearest to the tensile face, and a compressive strain ϵ_{ccu} on the compression face

c) Point C with a strain distribution corresponding to balanced failure with a maximum compressive strain ϵ_{ccu} and a yielding tensile strain ϵ_{sy} at the layer of longitudinal steel reinforcement nearest to the tensile face

For confined concrete, the value of ϕP_n corresponding to Point A (ϕM_n equals zero) is given in Eq. (12.1a) and (21.1b), while the coordinates of Points B and C can be computed as:

$$\phi P_{n(B,C)} = \phi \left[\begin{array}{l} A(y_i)^3 + B(y_i)^2 + C(y_i) \\ + D + \sum A_{si} f_{si} \end{array} \right] \quad (D-1)$$

$$\phi M_{n(B,C)} = \phi \left[\begin{array}{l} E(y_i)^4 + F(y_i)^3 + G(y_i)^2 \\ + H(y_i) + I + \sum A_{si} f_{si} d_i \end{array} \right] \quad (D-2)$$

where

$$A = \frac{-b(E_c - E_2)^2}{12f'_c} \left(\frac{\epsilon_{ccu}}{c} \right)^2 \quad (D-3a)$$

$$B = \frac{b(E_c - E_2)}{2} \left(\frac{\epsilon_{ccu}}{c} \right) \quad (D-3b)$$

$$C = -bf'_c \quad (D-3c)$$

$$D = bcf'_c + \frac{bcE_2}{2} (\epsilon_{ccu}) \quad (D-3d)$$

$$E = \frac{-b(E_c - E_2)^2}{16f'_c} \left(\frac{\epsilon_{ccu}}{c} \right)^2 \quad (D-3e)$$

$$F = \left[\begin{array}{l} b \left(c - \frac{h}{2} \right) \frac{(E_c - E_2)^2}{12f'_c} \left(\frac{\epsilon_{ccu}}{c} \right)^2 \\ + \frac{b(E_c - E_2)}{3} \left(\frac{\epsilon_{ccu}}{c} \right) \end{array} \right] \quad (D-3f)$$

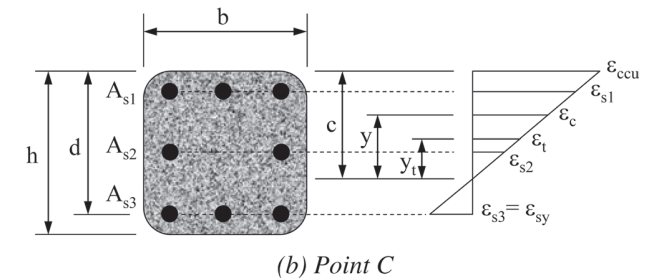
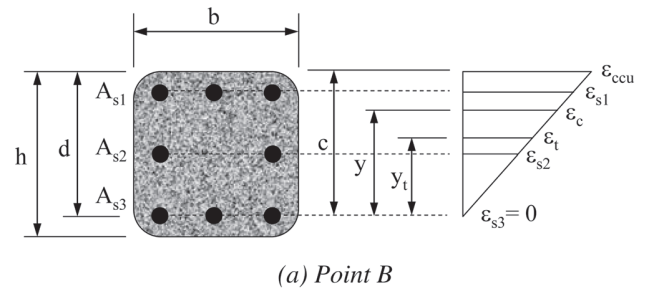


Fig. D.1—Strain distributions for Points B and C for simplified interaction diagram.

$$G = \left(\frac{b}{2} f'_c + b \left(c - \frac{h}{2} \right) \frac{(E_c - E_2)}{2} \left(\frac{\epsilon_{ccu}}{c} \right) \right) \quad (D-3g)$$

$$H = bf'_c \left(c - \frac{h}{2} \right) \quad (D-3h)$$

$$I = \left[\begin{array}{l} \frac{bc^2}{2} f'_c - bcf'_c \left(c - \frac{h}{2} \right) + \frac{bc^2 E_2}{3} (\epsilon_{ccu}) \\ - \frac{bcE_2}{2} \left(c - \frac{h}{2} \right) (\epsilon_{ccu}) \end{array} \right] \quad (D-3i)$$

In Eq. (D-3a) through (D-3i), *c* is the distance from the extreme compression fiber to the neutral axis (Fig D.1) and it is given by Eq. (D-4). The parameter *y_i* represents the vertical coordinate within the compression region measured from the neutral axis position and corresponds to the transition strain ϵ'_t (Eq. (D-5) [refer to Fig. D.1]).

$$c = \begin{cases} d & \text{for Point B} \\ d \frac{\epsilon_{ccu}}{\epsilon_{sy} + \epsilon_{ccu}} & \text{for Point C} \end{cases} \quad (D-4)$$

$$y_i = c \frac{\epsilon'_t}{\epsilon_{ccu}} \quad (D-5)$$

where *f_{si}* is the stress in the *i*-th layer of longitudinal steel reinforcement. The values are calculated by similar triangles from the strain distribution corresponding to Points B and C. Depending on the neutral axis position *c*, the sign of *f_{si}* will be positive for compression and negative for tension. A flowchart illustrating the application of the proposed methodology is shown in Fig. D.2.

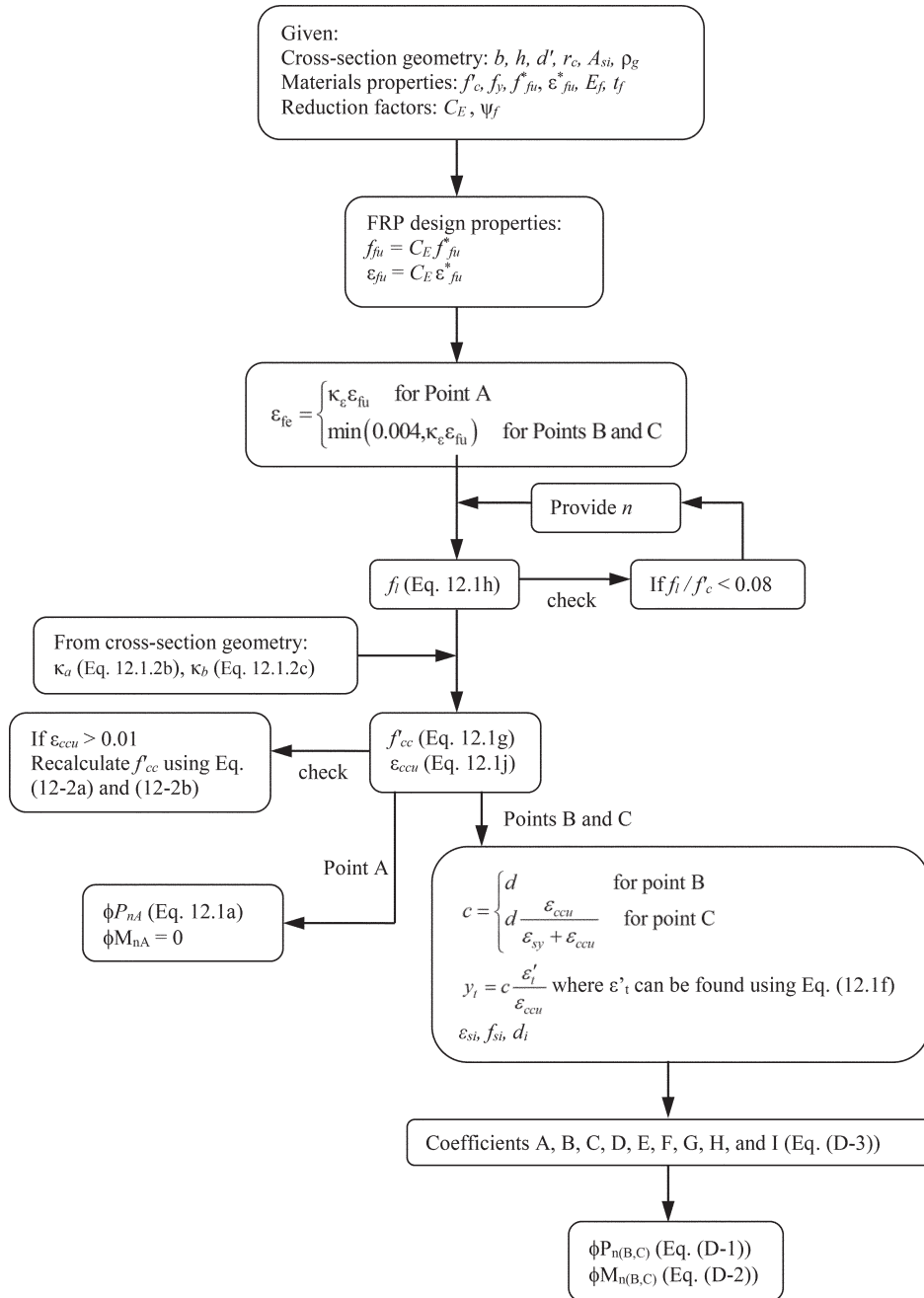


Fig. D.2—Flowchart for application of methodology.







American Concrete Institute
Always advancing

As ACI begins its second century of advancing concrete knowledge, its original chartered purpose remains “to provide a comradeship in finding the best ways to do concrete work of all kinds and in spreading knowledge.” In keeping with this purpose, ACI supports the following activities:

- Technical committees that produce consensus reports, guides, specifications, and codes.
- Spring and fall conventions to facilitate the work of its committees.
- Educational seminars that disseminate reliable information on concrete.
- Certification programs for personnel employed within the concrete industry.
- Student programs such as scholarships, internships, and competitions.
- Sponsoring and co-sponsoring international conferences and symposia.
- Formal coordination with several international concrete related societies.
- Periodicals: the ACI Structural Journal, Materials Journal, and Concrete International.

Benefits of membership include a subscription to Concrete International and to an ACI Journal. ACI members receive discounts of up to 40% on all ACI products and services, including documents, seminars and convention registration fees.

As a member of ACI, you join thousands of practitioners and professionals worldwide who share a commitment to maintain the highest industry standards for concrete technology, construction, and practices. In addition, ACI chapters provide opportunities for interaction of professionals and practitioners at a local level to discuss and share concrete knowledge and fellowship.

American Concrete Institute
38800 Country Club Drive
Farmington Hills, MI 48331
Phone: +1.248.848.3700
Fax: +1.248.848.3701

www.concrete.org



American Concrete Institute
Always advancing

38800 Country Club Drive
Farmington Hills, MI 48331 USA
+1.248.848.3700
www.concrete.org

The American Concrete Institute (ACI) is a leading authority and resource worldwide for the development and distribution of consensus-based standards and technical resources, educational programs, and certifications for individuals and organizations involved in concrete design, construction, and materials, who share a commitment to pursuing the best use of concrete.

Individuals interested in the activities of ACI are encouraged to explore the ACI website for membership opportunities, committee activities, and a wide variety of concrete resources. As a volunteer member-driven organization, ACI invites partnerships and welcomes all concrete professionals who wish to be part of a respected, connected, social group that provides an opportunity for professional growth, networking and enjoyment.

